BEHAVIOUR OF A TWO-CELL PRESTRESSED CONCRETE BOX GIRDER BRIDGE: EXPERIMENTAL STUDY

by

Karim Joucdar

A thesis submitted to the Faculty of Graduate Studies and Research in partial fulfilment of the requirements for the degree of Master of Engineering

Department of Civil Engineering
and Applied Mechanics
McGill University
Montreal, Quebec,
Canada.

January 1988

To my PARENTS

ABSTRACT

This thesis reports an extension of the work undertaken by Ferdjani and Hadj-Arab. It consists of an experimental study of the behaviour of a 1:7.0-scale direct physical model of a simply supported single span, two-cell, prestressed concrete box girder. The experimental techniques developed for construction and instrumentation required during testing of the bridge model are summarized.

Variation of the flexural stiffness and the dynamic characteristics, such as the fundamental natural frequency and the damping ratio, of the bridge model at different level of damage is presented.

The experimental results for the bridge responses at the working load, overload and failure load level are discussed, and compared with the corresponding analytical results obtained using the SAP IV and the nonlinear NONLACS programs. In general, a reasonable agreement was found between the experimental and the analytical results.

The physical model proved to be an adequate tool for the study of the static and dynamic responses of the box girder bridge at all load levels.

RÉSUMÉ

Cette étude représente une extension du travail accompli par Ferdjani, O. et Hadj-Arab, A. Elle consiste en l'étude du comportement d'un modèle à échelle réduite 1:7.0 d'un pont à poutres-caisson, simplement appuyé, en béton précontraint. Les techniques expérimentales développées pour la construction du modèle et l'instrumentation nécessaire pour les tests sont résumées.

La variation de la rigidité en flexion et les caractéristiques dynamiques, comme le coefficient d'amortissement et la fréquence naturelle fondamentale, du pont modèle à différent niveau de détérioration sont présentées.

Les résultats expérimentaux obtenus pour les différentes réponses du pont soumis à des charges normales, des surcharges, et à la charge de rupture sont discutés, et comparés avec les correspondants résultats analytiques obtenus par : le programme SAP IV et le programme non-lineaire NONLACS. En général, une concordance appréciable a été trouvée entre les résultats expérimentaux et analytiques.

Le modèle physique a prouvé être un moyen adéquat pour l'étude des réponses statiques et dynamiques des ponts à poutres-caisson à tous les niveaux de charge.

ACKNOWLECEMENTS

The author wishes to express his deepest gratitude to his research director, Professor M. S. Mirza, for his guidance, valuable suggestions, constant encouragement and precious advice during the course of this thesis.

Thanks are also due to Professor A. G. Razaqpur of the Department of Civil Engineering at Carleton University, for the use of his finite element computer program (NONLACS), and to Mr. M. NOFAL, graduate student at Carleton University, for spending several hours running the program.

The author would also like to thank Mr. Amar Khaled for his cooperation in this joint project, as well as the technicians of the Structures Laboratory of McGill University, Mr. Brian Cockayne and Mr. Ron Sheppard, who actively helped with the vast amount of skilled work necessary to complete this project.

The support of the Ministry of Education and Research of the Democratic and Popular Republic of Algeria in granting the author a study leave for M. Eng. studies at McGill University is gratefully acknowledged. The support of the Natural Sciences and Engineering Research Council to the continuing research program in this area is also gratefully acknowledged.

The helpful suggestions of fellow graduate students have contributed significantly to this thesis.

TABLE OF CONTENTS

LIST OF FIGURES

LIST OF TABLES

LIST OF NOTATIONS

A_m :	Model Cross-Sectional Area, mm^2
A_p :	Prototype Cross-Sectional Area, mm^2
L_m :	Length of the Model, mm
L_p :	Length of the Prototype, mm
S_l :	Length Scale for the Model
ρ_m :	Mass Density of the Model, kg/m^3
E_c :	Modulus of Elasticity of Concrete, MPa
E_s :	Modulus of Elasticity of Steel, MPa
β :	Shear Reduction Factor
ζ :	Damping Ratio

CHAPTER 1

INTRODUCTION

1.1 GENERAL

In Europe and North America, reinforced and prestressed concrete bridges have become a very important part of the modern transportation system. Since World War II, box girder bridges have become the most popular form of modern highway bridges, because these are more economical and aesthetically attractive compared with other types of concrete bridges. It has also been observed that this type of bridges has a high torsional stiffness and superior load distribution properties [23,39]. A large number of model tests have been performed in different industrialized countries to study the behaviour of box girder bridges. Because of their geometry, these type of bridges is able to carry utilities within the hollow boxes. Also, investigators have found a solution to the problem of large deflections due to the dead load in long span bridges in the stiffer box girder bridges. The introduction of the prestressing has helped this development. Nevertheless, the improvement in design and construction techniques has made the box girder bridges adaptable to a complex geometry and become suitable for an urban environment.

1.2 PREVIOUS WORK

Over the past four decades, several analytical and experimental studies have been undertaken into the behaviour of reinforced and prestressed concrete box girder bridges under various types of loadings with the objective of improving the present design methods. Improvements in the modeling techniques have made the structural model one of the most important tools in studying the response of box girder sections [33]. Scordelis, Bouwkamp, and Wasti [35] conducted tests on a 1:2.82 large scale model of a two span, four cell reinforced concrete box girder bridge subjected to the current AASHTO loadings [1]. The results showed that the box girder bridge has excellent load distribution characteristics. Nevertheless, they found that the AASHTO empirical formula overestimated the actual value of the girder bending moment for two lanes of trucks, and underestimated it for three lanes of trucks.

Soliman [38] tested a 1:2.82-scale direct model of an intermediate span of a continuous box girder bridge. An analytical-experimental program was undertaken to study the general behavior of the model bridge through all loading ranges. The principal objective was to study the effects of formation and propagation of cracks on the flexural and torsional response of the system and on the shear transfer across the cracks and on the stiffness perpendicular to the cracks. He concluded that a reduction in the shear modulus with the widening of the cracks did not have a significant influence on stress distribution in the bridge section except at the ultimate load level . Also, a non-zero concrete modulus value perpendicular to the cracks had a significant influence on bridge behaviour as compared with a zero value for this modulus. However, at the ultimate load stage, the computed stresses were insensitive to this value.

Cordoba and Tschanz [12,41] performed an experimental-analytical study on a 1:3.76-scale direct model of a single span, two cell, precast, pretensioned box girder bridge. The scope of this investigation was to study the structure with emphasis on the load distribution characteristics . The analysis was concerned with the elastic response only. They found that the transverse distribution of the concentrated load through the thin top slab was adequate. The results of the behaviour of the bridge model under working load were compared with an analysis by the finite element method. Good agreement was found between the computed and experimental results.

Scordelis [34] developed a general method of analysis for simply supported box girder bridges, using the folded plate method and harmonic representation of the loadings. A number of bridges with different spans and number of box cells was analyzed.

Maisel, Rowe, and Swan [23] summarized the different methods of elastic analysis which can be used efficiently by the designer for different type of box girder structures. The analysis uses a grillage model which is designed to consider the effects of longitudinal bending, St-Venant torsion, distortional, and torsional and distorsional warping due to inplane flexure of the webs. The shear-flexible grillage can be used to reproduce the stuctural behaviour of a box girder deck with the accuracy of a more sophisticated technique. It can, also, accommodate variations of geometry in plan and section.

Tabba [40] conducted an experimental study on the free vibration response of one-and two-cell curved box girder Plexiglas models. He evaluated the simplifying assumptions made in the thin walled beam theory. He compared the experimental and the theoretical results. Good agreement was obtained between the computed and the experimental modal shapes and frequencies.

The above research programs were mostly concerned with the elastic response only. A relatively few investigations have been undertaken to study the dynamic behaviour of box girder bridges. The behaviour of the structure becomes complex and different from the elastic behaviour when the reinforced concrete elements crack and/or the reinforcement starts to yield. The recent development of techniques in structural modeling and the introduction of a number of finite element analysis programs which take into account the nonlinear material properties and geometric non-linearities of the structure have led the researchers to deal with the nonlinear behavior of these structures. Some of these recent investigations are summarized below.

Ferdjani [16] and Hadj-Arab [18] completed an experimental-analytical study on a 1:7.1-scale direct model of a one-cell prestressed concrete box girder bridge. The objectives of this investigation were to study the behaviour of the bridge model under static and dynamic loadings. They found that the physical model proved to be an adequate tool to predict the linear and non-linear static and dynamic response of reinforced and prestressed concrete box girder bridge. The physical model was able to resist an ultimate load equal to six times the Ontario Highway Bridge Design Code truck. Also, the longitudinal and transverse stress distributions obtained across the width of the top and bottom slabs of the box section were not uniform under concentrated and truck loadings. They concluded that a single-cell box section subjected to concentrated and truck loadings was unable to redistribute the applied loads uniformly across the width, at the same location.

Spiller, Danghidis, and Kromolicki [39] conducted an experimental-analytical study on the effect of lateral forces due to longitudinal prestressing of concrete box spine-beam bridges with inclined webs. A method was derived and verified for the analysis of transverse stresses induced by the longitudinal prestressing with tendon profile parallel to inclined webs.

Mirza et al [25] performed a study on a 1:10.45 scale direct physical model of a composite concrete deck-steel box girder bridge. The direct physical model consisted of box girders made from 13, 17 and 21 gauge steel plates and a 21 mm thick concrete deck was used for the experimental study. Bracings were provided in different configurations in this model. The main investigation on this model was concerned with the elastic free vibration response and the complex nonlinear static response at higher load levels. The study was also concerned with establishing a framework for the limit states design of composite concrete deck-steel box girder bridges. They concluded that the influence of these bracings was not significant on the static and dynamic response of the composite box girder bridge.

Perry, Pinkney and Waldron [31] studied the behaviour of one- and two-cell box girder bridges using a 1/12-scale prestressed concrete elevated road junction model which consisted of box beam sections with large side cantilevers. This structure with a very complex geometry was highly curved in plan and was continuous over three central supports and torsionally restrained at three outer supports.

Billing [4] completed dynamic tests on 27 bridges with different configurations, of steel, timber and concrete construction and with spans varying from 5 m to 122 m. The results of this comprehensive study were used to support the Ontario Highway Bridge Design Code provisions for dynamic loadings and dynamic response of bridges [29]. Also, the data generally comfirmed that the form and values for dynamic load and serviceability provisions of the code were adeqmate. Good agreement was noted between the analytical and experimental results.

Cheung, Gardner and Ng [7] completed an analytical-experimetal study on a slab-on-girder bridges concerning the load distribution characteristics at the ultimate load. The tests were performed on 1/4-scale model of a simply supported three-lane, composite steel beam-concrete deck bridge. They developed the load distribution factors for the ultimate limit state including the influence of load redistribution, non-linear behaviour, residual stresses, and accounted for the effect of intermediate diaphragms on load distribution characteristics. The experimental results were compared with the results obtained from a finite element model and good agreement was observed. They concluded that there was a considerable reduction of load distribution factors between linear elastic and post yielding stages. This reduction was at least equal to the shape factor of the girder section. For wide flange and I sections, the shape factors vary within the small range of 1.15 to 1.17.

Conrad, Heins and Sahin [10] developed a series of empirical equations used for the evaluation of the natural frequencies of curved and straight box section bridges. Experimental studies on a series of two and three span continuous curved bridges were performed. Good agreement was obtained between approximate and "exact" natural frequencies, calculated using Stodola and thin-walled theory methods, respectively, and experimental results.

Seible and Scordelis [37] developed an analytical model which can give the complete nonlinear behaviour of a reinforced concrete multi-cell box girder bridge under increasing loads up to the ultimate load and collapse of the structure. For linear elastic analysis, the displacement model was used on transforming the box section system into a three-dimensional grillage, formed by longitudinal beam elements, transverse bending frames at discrete intervals and shear panels. However, the nonlinear analytical model was based on introducing the flexural and shear hinges in the model. The analytical scheme was demonstrated and tested on two numerical examples. Analytical results were derived and were compared with the experimental results obtained from tests on a large scale model of a reinforced concrete box girder bridge. The above research programs provided significant useful information on the linear deformational behaviour of box girder bridges, however, only a few of these investigators dealt with the nonlinear deformational behaviour of the box girder bridge at higher load levels up to the ultimate load. At this stage, more experimental and analytical data are needed. Also, the dynamic response of bridges after cracking of the section needs to be examined.

1.3 VIBRATION OF BRIDGES

A comprehensive review of vibration response of bridges was undertaken by Huang [19]. Bridge engineers and bridge designers are primarily concerned with vibrations caused by moving vehicles. The objectives of bridge engineers are to provide sufficient stiffness, to prevent excessive bridge deflections to cater for the psychological comfort of the individuals crossing the bridge. Also, wind effects are more prominent in the response of suspension bridges than in any other types of bridges causing aerodynamic instability of the bridge. Furthermore, the dynamic response of bridges due to seismic excitations is more complex. The extent of seismic damage depends on the dynamic behaviour of the soil, seismic intensity and the type of the structure.

Over the past few decades, the use of high strength materials has led to the construction of slender bridge sections which has resulted in considerable vibration problems due to the passage of heavy vehicles. Some analytical and experimental investigations have been undertaken to study the dynamic response of highway bridges at different levels of damage to determine the damage level up to which a bridge can be considered functional for safety of users.

1.4 SCOPE AND OBJECT OF MODEL INVESTIGATIONS

A direct physical model of a prototype structure is a powerful design aid which can be loaded in the same way as the prototype. These models can simulate the behaviour of the structure through all loading stages from zero load up to the ultimate load and the final collapse of the structure and would in general be required to account for such characteristic phenomena in structural concrete as cracking, stress redistribution, nonlinear response,etc. Therefore, the use of suitable model materials and the correct choice of scales are of paramount importance.

The main advantage of the model investigation is that it enables the designer to concentrate on the structure itself. The experimental results provide a first hand knowledge of the structural behaviour when theories to predict its behaviour are not available. The greatest advantage of the model study is the low cost of fabrication, relative ease of handling the specimen and the small testing and storage space. Model testing does not usually require elaborate expensive testing equipment. Furthermore, the casting and curing of structural concrete models can usually be conducted in the laboratory under more closely controlled conditions than the prototype structures.

1.5 AIMS OF THE PRESENT STUDY

This study is an extension of the research program undertaken by Ferdjani and Hadj-Arab, who performed an analytical-experimental study on a 1/7.1-scale direct physical model of a simply supported single span single, one-cell, prestressed concrete box section bridge.

The present study is aimed at investigating the general behaviour of a box girder bridge structure using tests on a 1/7.-scale direct physical model of a simply supported single span, two-cell, prestressed concrete box section bridge. The objectives of the study were:

(i) To study the overall static and dynamic responses of the bridge model at different levels of damage up to the ultimate load level.

(ii) To examine the load distribution characteristics of the structure in both the linear and nonlinear ranges under concentrated and the Ontario Highway Bridge Design Code truck loading.

(iii) To study the effect of cracking of the concrete at different levels of damage on the flexural and torsional response of the model bridge and the shear transfer across the cracks.

(iv) To determine the dynamic characteristics of the structure such as the natural frequencies of vibration and the damping ratio at different levels of damage.

(v) To analyse the bridge using the SAP IV program and the non-linear NONLACS program at Carleton University .

CHAPTER 2

PHYSICAL MODEL

2.1 ADVANTAGES OF MODEL TESTING

Model testing of structures in the laboratory has gained wide acceptance among both structural researchers and design engineers over the past three decades. Several experimental investigations have been conducted in recent years to study the behaviour of structures under static and dynamic loadings. The behaviour of physical models can duplicate the complete prototype behaviour to a high degree of accuracy better than any analytical model.

The errors in measurements magnify as the size of the model decreases. In addition, the engineer is unable to simulate more accurately the complex boundary conditions and the internal force distribution in the physical model.

Advantages of model testing include the low cost of fabrication, saving of space in the laboratory, small live loads which can produce large stresses in models until failure, control of humidity and temperature conditions in the laboratory, and no interruption from traffic or other sources. These have made the use of small-scale direct models of reinforced and prestressed concrete bridge structures popular and useful.

The only disadvantage in the use of small scale model is the simulation of the prototype dead weight. Compensation of the dead load was achieved in the model by distributing concrete blocks and/or steel billets in the model. Special care is needed during all modeling stages. The accuracy of the results from a given physical model test depends on the construction accuracy, the material properties , loading techniques, measurement methods and the interpretation of the results.

Over the past few years, intensive development of analytical methods due to the introduction of powerful computers and finite element programs has changed the application of physical models. Nevertheless, the accuracy of these analytical methods must be established by comparing the analysis results with appropriate experimental data from tests done on carefully chosen physical models.

Physical models are being accepted by the various building codes [2,8] as alternate design tools. Many researchers [24,33] have proved that models constructed to scales as small as 1/5 to 1/8, can be reliable, time-saving and inexpensive tools to investigate the behaviour of a structure under any type of monotonically increasing loading until the collapse of the structure. Also, recent studies have shown that 1/2 - 1/4 scale direct models of reinforced and prestressed concrete stuctures can predict the prototype behaviour and strength with a reasonable degree of reliability [26].

2.2 DIMENSIONAL ANALYSIS

Dimensional analysis has been used to develop the similitude requirements which relate the model to the prototype structure. The physical model must be designed, tested under combined loadings and interpreted according to the laws of similitude in order to to be able to predict the prototype response from the model response.

For dimensional analysis of a structure, the independent or basic dimensions must first be selected. All significant variables are then expressed in terms of these dimensions by combining the physical variables, which are related to the phenomena involved in the behaviour of the structure, into convenient groupings. Therefore, these similitude equations define the relationship for the various physical equations between the model and the prototype.

For a problem involving a structure subjected to static and dynamic loadings, the fundamental quantities are usually chosen as force (F), length (L), and time (T). Other variables related to the phenomena under study such as ultimate strength of the structure, elastic or inelastic deformations, elastic or inelastic vibrations are defined in terms of the governing dimensions (Table 2.1). According to the Buckingham's Pi-theorem, a complete independent set of dimensionless Pi-terms can be assembled for the different physical quantities and these are made equal for both the model and the prototype. The resulting equations can then be solved to derive the scale factors. The condition of true representation of a given prototype by a scale model can therefore be stated in the form: $\Pi_{im} = \Pi_{ip}$ where $i = 1,2,3,4...n$. A summary of the scale factors used for this investigation is given in Table 2.2.

2.3 SELECTION OF SCALE

Direct physical models have been shown to be suitable to investigate the complete behaviour of the prototype structure both in the elastic and the post-elastic range and also to determine the ultimate capacity and the failure mode of the prototype structure. The direct model used in the study of this box girder bridge was constructed using a length scale factor of 1/7.0. The selected linear scale factor of 1/7.0 for the box girder bridge was based on the smallest size of prestressing wire that could be supplied by the manufacturer. The 12.7 mm nominal diameter seven wire strands having an ultimate tensile strength (UTS) of 1860 MPA was simulated by a 5.0 mm nominal diameter prestressing wires having an ultimate tensile strength of 1550 MPa, as recommanded by the manufacturer. This leads to the relationship :

$$S_l = \frac{Lm}{Lp} = \sqrt{\frac{Am}{Ap}} = 1/7.0$$

Physical quantity	Description	Dimension
l	Length	L
δ	Displacement	L
F	Force	F
σ_c	Concrete stress	$F\ L^{-2}$
σ_s	Steel stress	$F\ L^{-2}$
E_c	Modulus of elasticity of concrete	$F\ L^{-2}$
E_s	Modulus of elasticity of steel	$F\ L^{-2}$
t	Time	T
v	Velocity	$L\ T^{-1}$
a	Acceleration	$L\ T^{-2}$
g	Gravitational acceleration	$L\ T^{-2}$
f	Frequency	T^{-1}
ρ_c	Mass density of concrete	$F\ L^{-4}\ T^2$
ρ_s	Mass density of steel	$F\ L^{-4}\ T^2$
ϵ	Strain	----
ν	Poisson's ratio	----

TABLE 2.1 DIMENSIONS OF THE GOVERNING PHYSICAL QUANTITIES

Group	Physical Quantities	Scale Factor	Scale Factor (S_E = 1)
Loading	Force, F	$S_E S_l^2$	S_l^2
	Gravitational acceleration, g	1	1
	Acceleration, a	1	1
	Time, t	$S_l^{1/2}$	$S_l^{1/2}$
	Velocity, V	$S_l^{1/2}$	$S_l^{1/2}$
Geometry	Linear dimension, l	S_l	S_l
	Displacemnet, δ	S_l	S_l
	Frequency, f	$S_l^{-1/2}$	$S_l^{-1/2}$
Material	Young's modulus, E_c, E_s	S_E	1
properties	Stress, σ	S_E	1
	Mass density, ρ	$S_E S_l^{-1}$	S_l^{-1}
	Poisson's ratio, ν	1	1
	Strain, ϵ	1	1

TABLE 2.2 SUMMARY OF SCALE FACTORS

where the subscripts m and p stand for the model and the prototype, respectively. Following the provisions of the Ontario Highway Bridge Design Code, a prototype bridge was designed as single span, simply supported structure, 25.0 m long, 8.0 m wide, 1.8 m deep and consisting of a two rectangular cells. The geometry and the details of the reinforcing and the prestressing steel for the model were then selected. The dimensions of a typical cross section of the prototype and the model are shown in Fig.2.1 and Fig.2.2, respectively. Also, the dimensions of the model in plan are shown in Fig.2.3. Since the same materials, concrete, reinforcing and prestressing steel are used for both the prototype and the model, the principles of similitude are applicable in the elastic and the inelastic ranges up to the ultimate load.

2.4 DESIGN OF THE MODEL

Two types of reinforcement were used for the box girder bridge model, a 5.0 mm nominal diameter prestressing wire having an ultimate tensile strength of 1550 MPa, and a normal reinforcement, 4.0 mm nominal diameter and a yield strength of 298 MPa. Typical stress-strain curves for the prestressing wire and normal reinforcement are shown in Figures 3.3 and 3.4, respectively. The main reinforcement

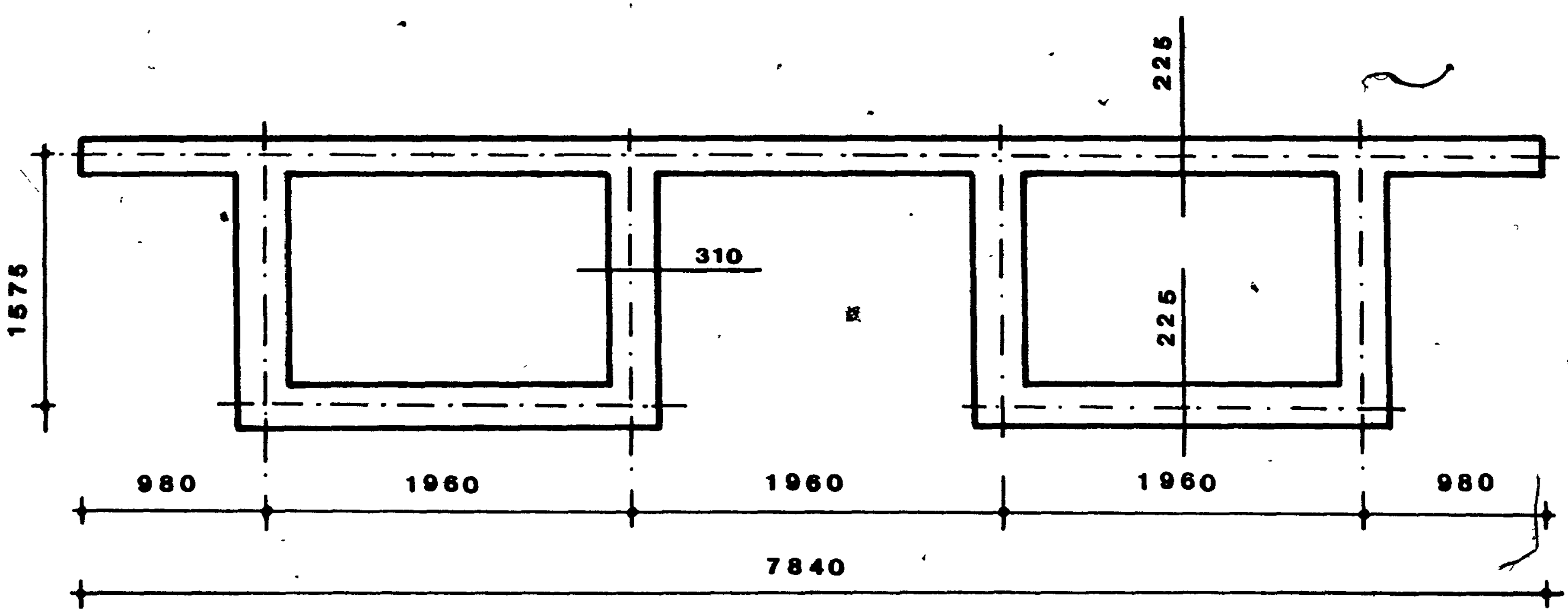

Figure 2.1 DIMENSIONS OF THE PROTOTYPE CROSS-SECTION

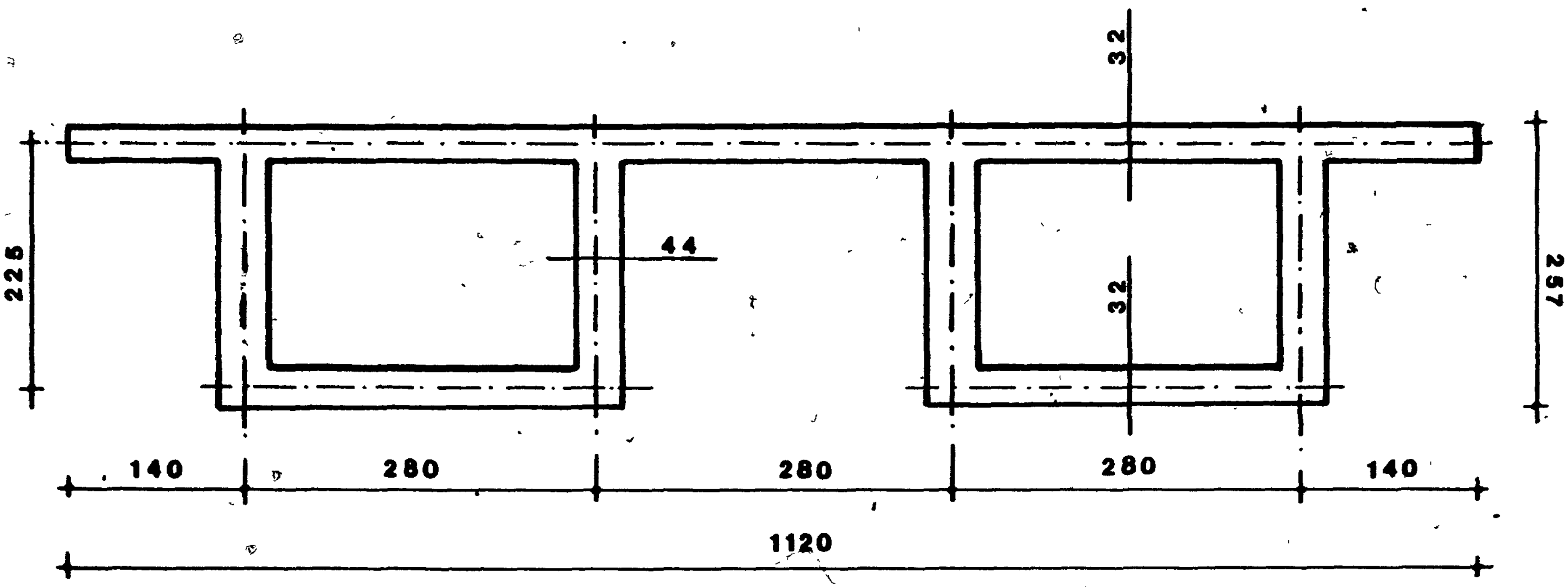

Figure 2.2 DIMENSIONS OF THE MODEL CROSS-SECTION

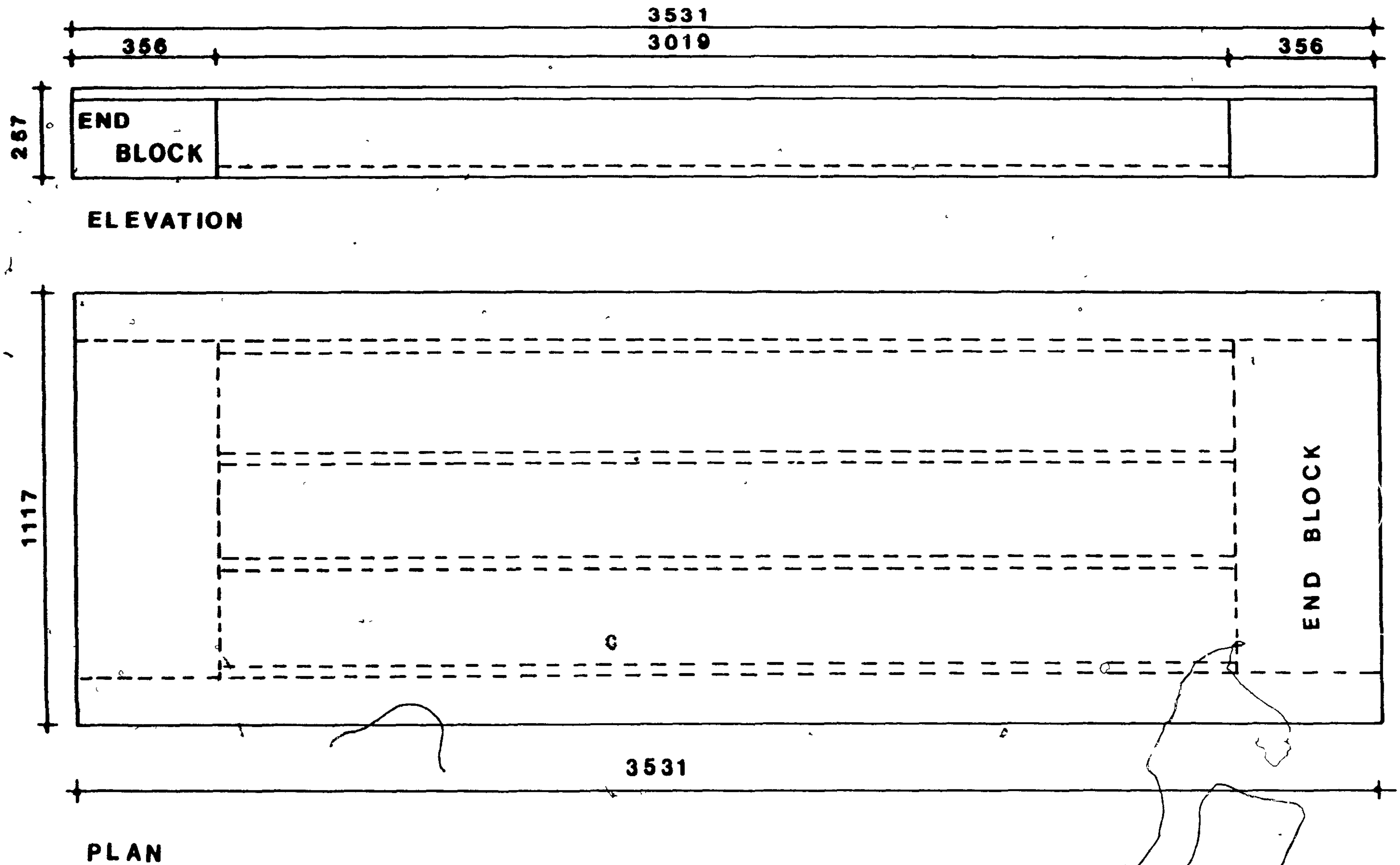

Figure 2.3 DETAILS OF DIMENSIONS OF THE BRIDGE MODEL

consisted of ten prestressing wires. These were located as four wires for each box and one wire at the middle of each bottom slab. These wires were tensioned initially to 1080 MPa which is approximately 0.7 of the wire ultimate strength. At the midspan section, a system was provided for harping the prestressing wires in the webs. Figure 2.3 shows the locations of the prestressing wires and the normal reinforcement at the support and at the midspan section.

The longitudinal and transverse reinforcement for webs, bottom and top slabs consisted of two layers of continuous wire meshes of 4.0 mm nominal diameter steel reinforcement. These meshes were placed along the length of the bridge. The details of the reinforcements for the model with spacings of the wire meshes and their locations are shown in Figures 2.4 and 2.5. The end blocks provided a suitable rigid end to simulate warping restraint conditions. Figure 2.6 shows the details of reinforcing for the end blocks. According to the Canadian Standard CAN3-A23.3-M84, the fundamental requirements of strength, limited cracking, ductility and simplicity of construction were satisfied by the reinforcement details adopted.

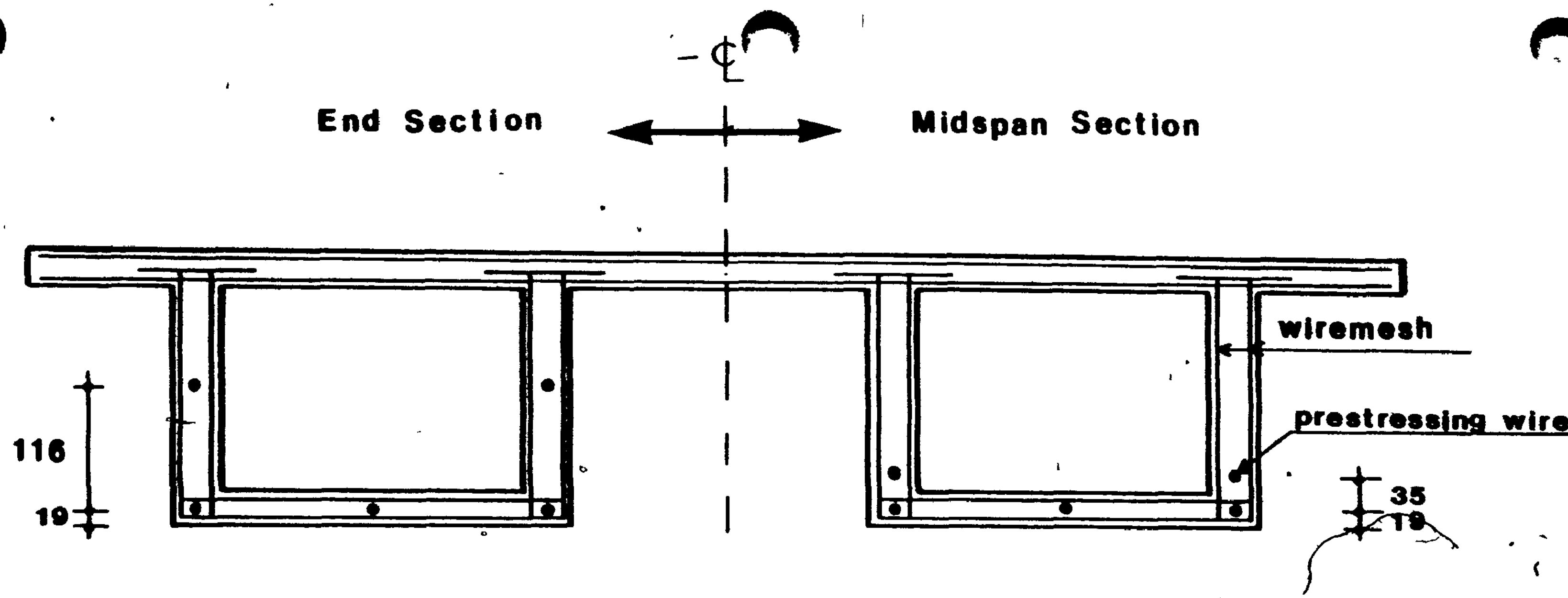

DIMENSIONS	
1050	Top and Bottom Transverse,Reinforcement Top Slab
280	Top and Bottom Transverse Reinforcement Bottom Slab
50 50 225 35	Stirrups for Reinforcement of Webs

Figure 2.4 REINFORCEMENT DETAILS FOR THE MODEL CROSS-SECTION

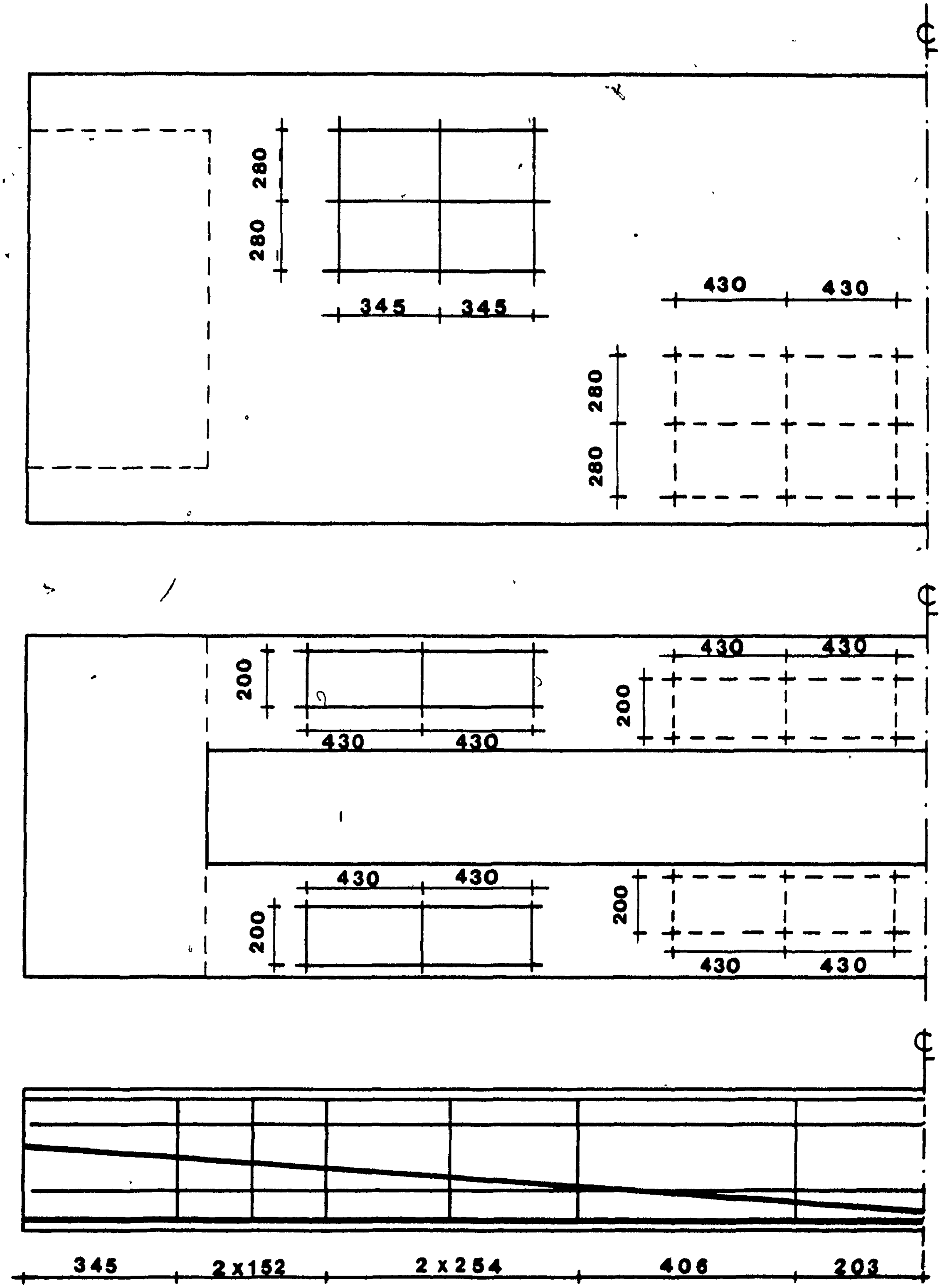

Figure 2.5 REINFORCEMENT DETAILS OF THE MODEL.

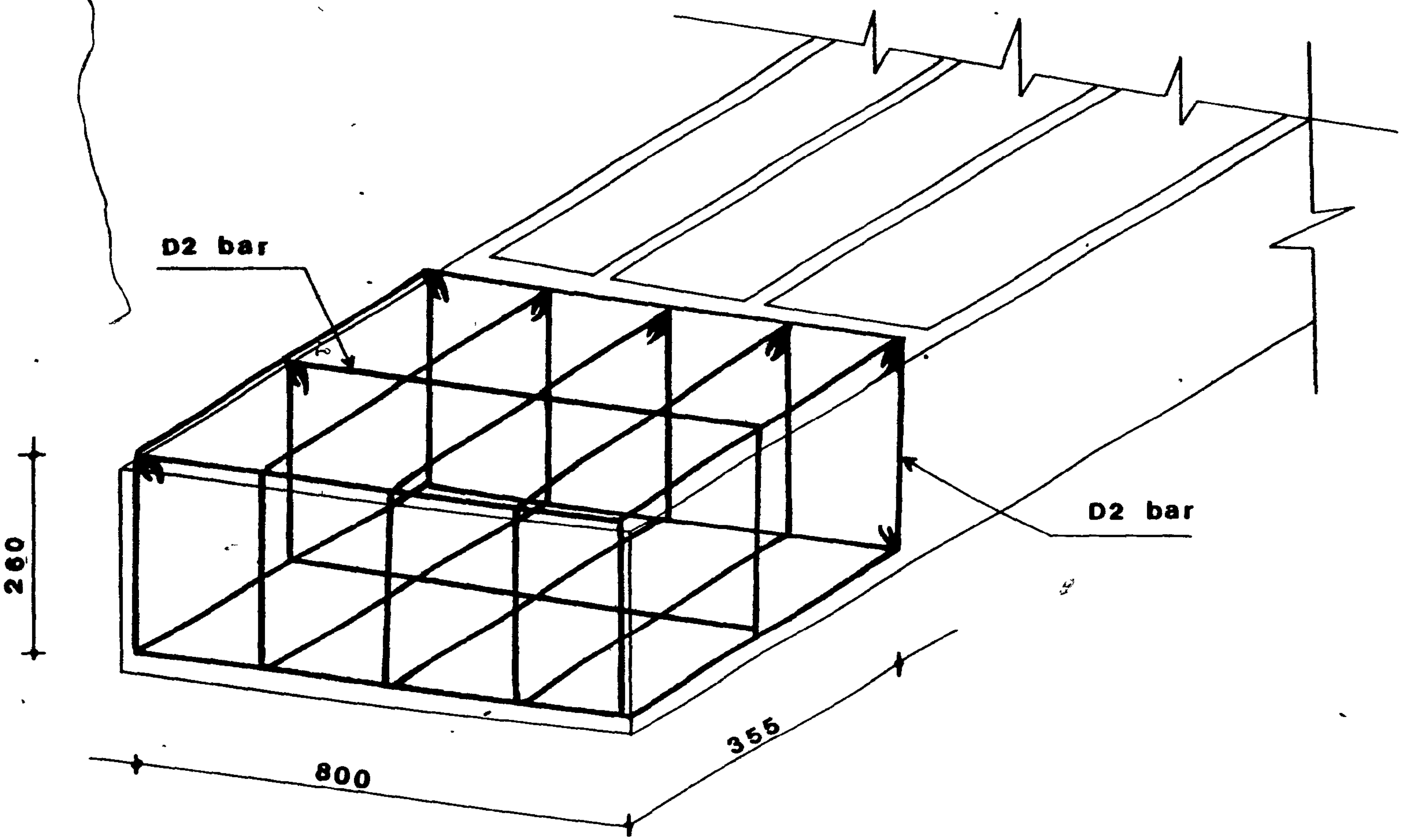

Figure 2.6 REINFORCEMENT DETAILS OF THE END BLOCK

CHAPTER 3

EXPERIMENTAL PROGRAM

The structural design of the bridge model was conducted in a manner identical to that of the prototype. Strict specifications dealing in detail with the design of the concrete mix, formwork requirements and the stringent tolerences in constructional dimensions were required for the scale model. All of the instrumentation was calibrated prior to the tests. The tests on scale model bridge were performed on the strong floor of the Strength of Materials Laboratory at McGill University.

3.1 MATERIAL PROPERTIES

3.1.1 CONCRETE

The model concrete mix used for the box girder bridge model was designed according to Mirza's recommendations [24]. The selection of a model material to simulate concrete requires a cementitious material whose stress-strain curve up to failure is similar to that of the prototype concrete, and whose Poisson's ratio, tensile strength-compressive strength ratio, shrinkage and creep characteristics are identical to the counterpart prototype properties [24]. After several trials for workability of the model concrete, a higher water content was used.

The model concrete mix was designed for a nominal compressive strength of 30 MPa. It consisted of a blended mixture of coarse aggregates, narrowly graded crushed quartz sands, high early strength Portland Cement (Type III) and water. The aggregate proportions by weight were:

1.6 mm - 3.2 mm limestone aggregates	15%
No. 10 crushed quartz sand	15%
No. 16 crushed quartz sand	15%
No. 24 crushed quartz sand	25%
No. 40 crushed quartz sand	20%
No. 70 crushed quartz sand	10%

The grading used is based on the sieve analysis results for the model concrete mix. The particle size distribution curve for the mix is shown in Figure 3.2. The water-cement-aggregate proportions in the mix were: 0.55-1.0-2.75 by weight.

Compression and tension tests were performed on 56 concrete cylinders of size 50 mm x 100 mm. Some of the cylinders were equipped with electrical resistance strain gauges. Twenty cylinders was tested at an age of 28 days, while 26 cylinders were tested the day corresponding to the day of testing the model, to estimate the strength characteristics of the model. A typical stress-strain curve of the concrete mix is shown in Figure 3.3.

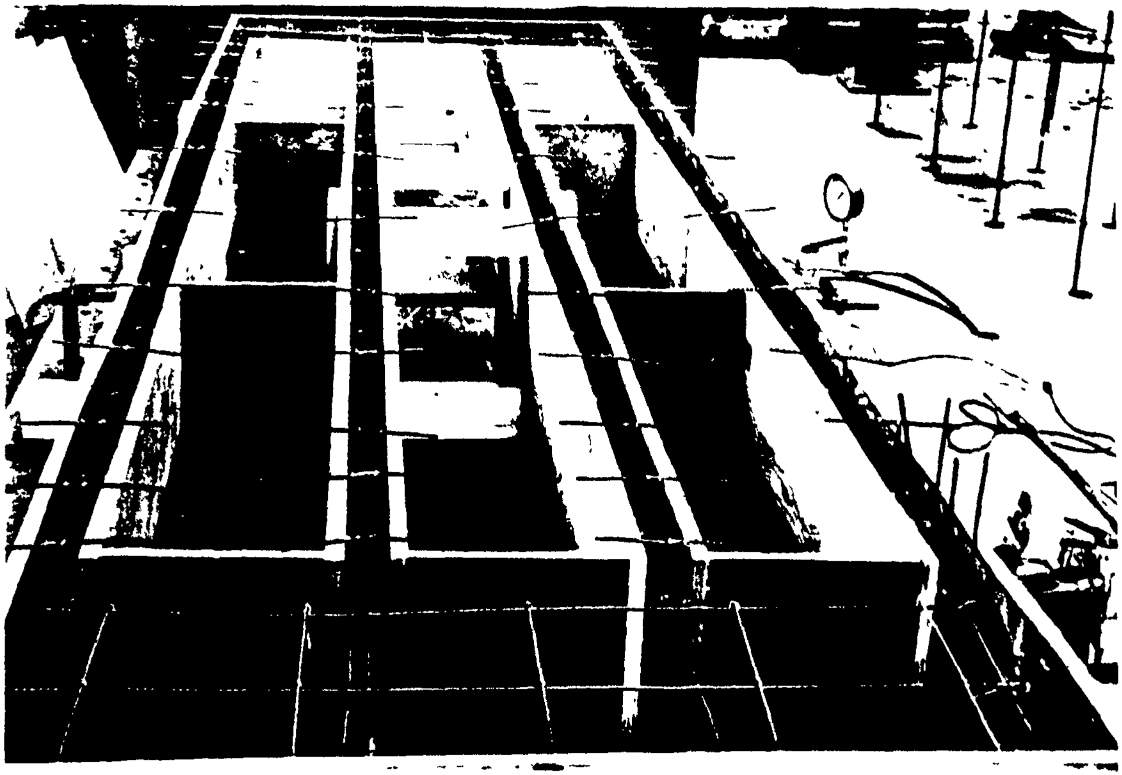

(a) Reinforcement Details For Webs, Bottom Slabs, End Blocks

(b) Bridge under Static Load

Figure 3.1 BRIDGE MODEL

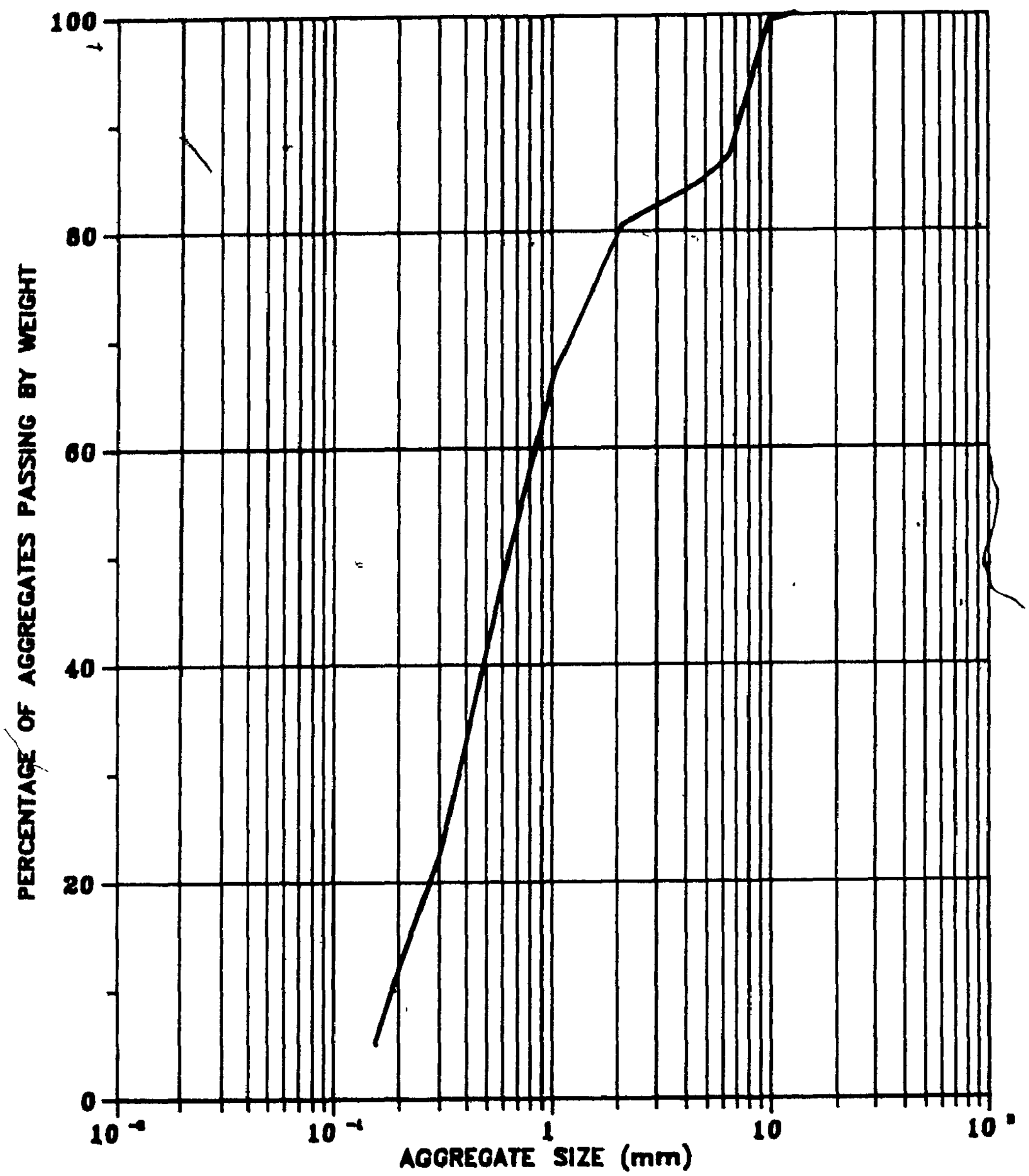

Figure 3.2 GRADING THE MODEL AGGREGATES USED FOR THE CONCRETE MIX.

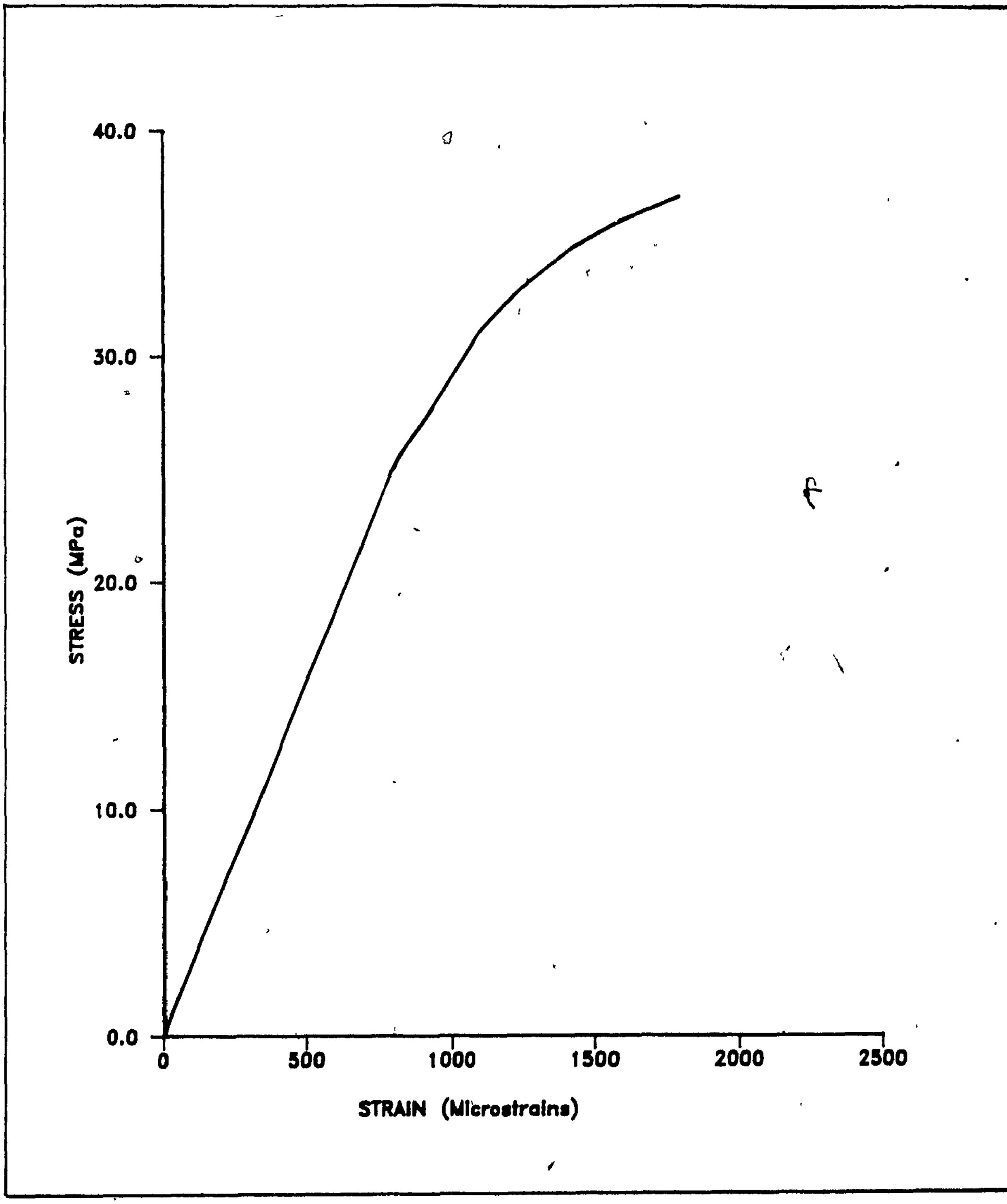

Figure 3.3 TYPICAL STRESS-STRAIN CURVE
OF THE CONCRETE.

The results from the tests performed on 50 mm x 100 mm cylinders to evaluate the compressive and the tensile strengths are tabulated in Tables 3.1 and 3.2, respectively. For design purposes, the compressive strength was taken equal to 37 MPa and the tensile strength equal to 2.25 MPa.

3.1.2 STEEL REINFORCEMENT

During the design and the construction of the bridge model, several characteristic properties of the reinforcing steel were considered in the selection of suitable reinforcement. Among these properties, emphasis was placed on the following:

- Shape of the stress-strain curve.
- Yield and ultimate strengths in tension and in compression.
- Bond characteristics at the steel-concrete interface.
- Ductility.

Five pull-out tests were conducted to study the bond characteristics of the prestressing wire to establish the bond characteristics at the steel-concrete interface.

3.1.2.1 PRESTRESSING STEEL

The 5.0 mm nominal diameter prestressing wire was supplied by a local manufacturer, who indicated an ultimate tensile strength of 1550 MPa for the wire.

Structural Element	Number of Cylinders Tested 50 mm x 100 mm	Age (days)	Average Compressive Strength (MPa)	Standard Deviation (MPa)	Coefficient of Variation (%)	Modulus of Elasticity (MPa)
Bottom Slab and Webs	5	28	34.10	1.20	2.90	28500.
	8	day of testing	37.0	1.10	2.90	28700.
Top Slab	5	28	34.2	1.25	3.20	28600.
	8	day of testing	36.9	1.18	2.60	29000.

TABLE 3.1 COMPRESSIVE STRENGTH OF THE MODEL CONCRETE

Structural Element	Number of Cylinders Tested 50 mm x 100 mm	Age (days)	Average Tensile Strength (MPa)	Standard Deviation (MPa)	Coefficient of Variation (%)	Modulus of Elasticity (MPa)
Bottom Slab and Webs	5	28	2.06	0.11	5.34	28500.
	8	day of testing	2.25	0.11	4.88	28700.
Top Slab	5	28	2.07	0.11	5.31	28600.
	8	day of testing	2.24	0.09	4.00	29000.

TABLE 3.2 TENSILE STRENGTH OF THE MODEL CONCRETE

This wire had a rough surface which allowed for a good bond with the concrete. Six prestressing wire specimens were tested using the Instron Universal Testing Machine and the results are summarized in Table 3.3. A typical stress-strain curve for the prestressing wire is shown in Figure 3.4. The average ultimate tensile strength was found to be equal to 1550 MPa.

3.1.2.2 STEEL WIRE REINFORCEMENT

A 4.0 mm nominal diameter steel reinforcement wire with a yield strength of 580 MPa was selected. According to Mirza's recommendations [24] and in order to improve the ultimate strain capacity and to lower the yield strength of this steel reinforcement, the following heat treatment was conducted. The steel was first heated to a temperature of 315 C and then the temperature was increased at a rate of 95 C per hour for another 3 hours. This temperature was then maintained at 610 C for 2 hours. The cooling process started by decreasing the temperature from 610 C to 315 C at 95 C per hour. The steel was then removed from the oven and cooled in the air.

After this process, the steel reinforcement become considerably ductile with a yield strength of 298 MPa. The steel was cleaned carefully after the above operation. A typical stress-strain curve, obtained from the tension tests

Number of Specimens Tested	Ultimate Tensile Strength (MPa)	Average Strength (MPa)	Standart Deviation (MPa)	Coefficient of Variation (%)	Modulus of Elasticity (MPA)
1	1562				
2	1592				
3	1525	1550	22.48	1.45	175000
4	1548				
5	1543				
6	1559				

TABLE 3.3 TENSILE STRENGTH OF 5.0 mm PRESTRESSING WIRE

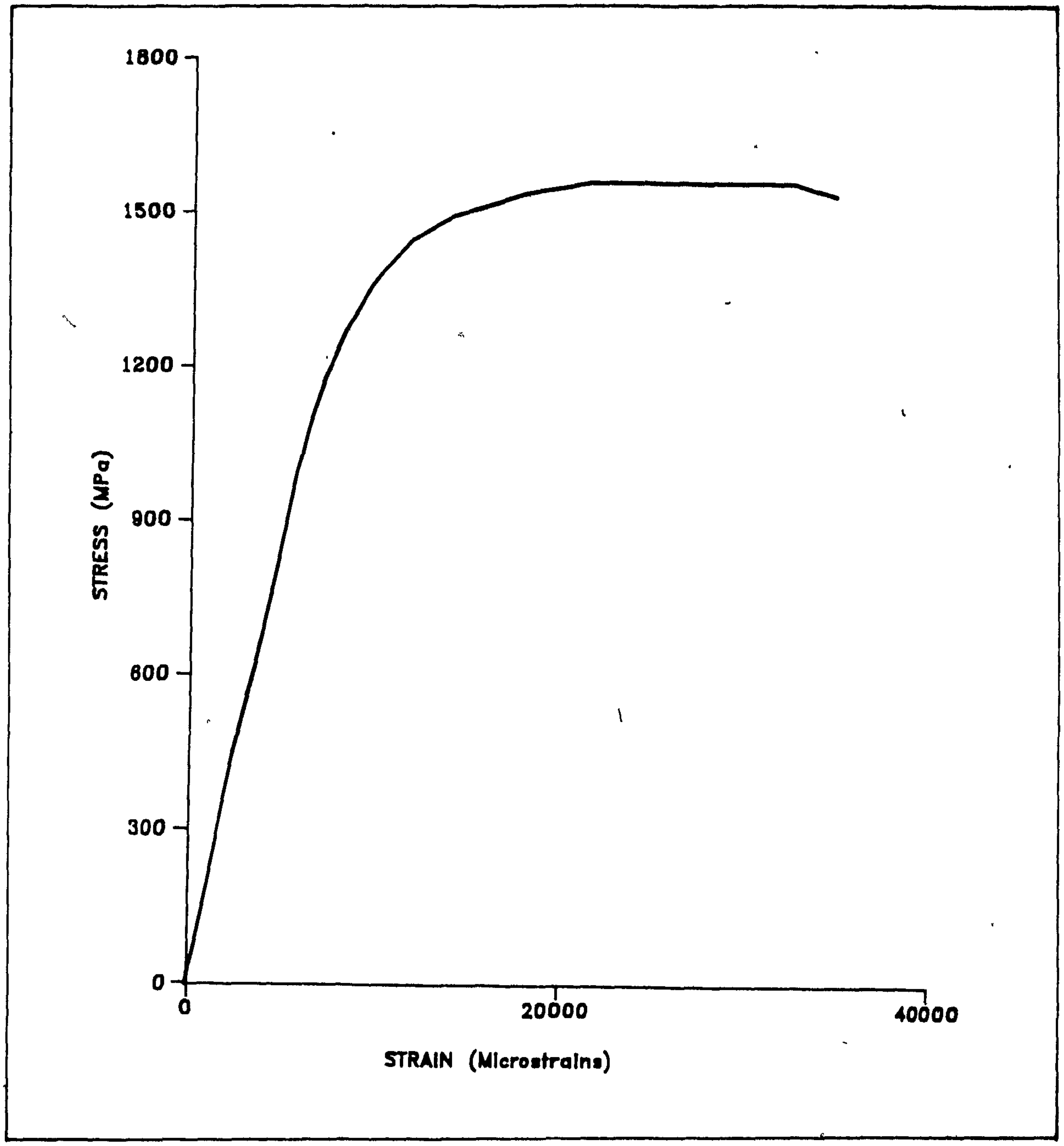

Figure 3.4 TYPICAL STRESS-STRAIN CURVE OF
5 mm PRESTRESSING WIRE.

on ten specimens, is shown in Figure 3.5.

3.2 PRETENSIONING TECHNIQUES

Three tensioning methods were tested by Ferdjani [16] and Hadj-Arab [18] . The methods consisted of a single prestressing wire, equipped with electrical resistance strain gauges, pretensioned using a pump and a hydraulic jack. The strain readings were taken every day during the subsequent week to evaluate the losses.

Method I : The pump and the hydraulic jack were not removed after prestressing the wire. The losses were significant (approximately 20 %) before releasing the wire, mainly due to the permanent presence of the pump and the hydraulic jack.

Method II : The operation was to fix the chuck on the hollow load cell after releasing the pump and the hydraulic jack. Control of losses was not possible.

Method III : The operation was to set the chuck before jacking and to close the chuck before releasing the wire. After releasing the force applied by the hydraulic jack, the losses were negligible (approximately 4 %). After releasing the wire itself, a prestressing loss of about 15 % was noted. The losses noted were considered acceptable. Method III was selected and the details of the set-up are shown in Figure 3.6.

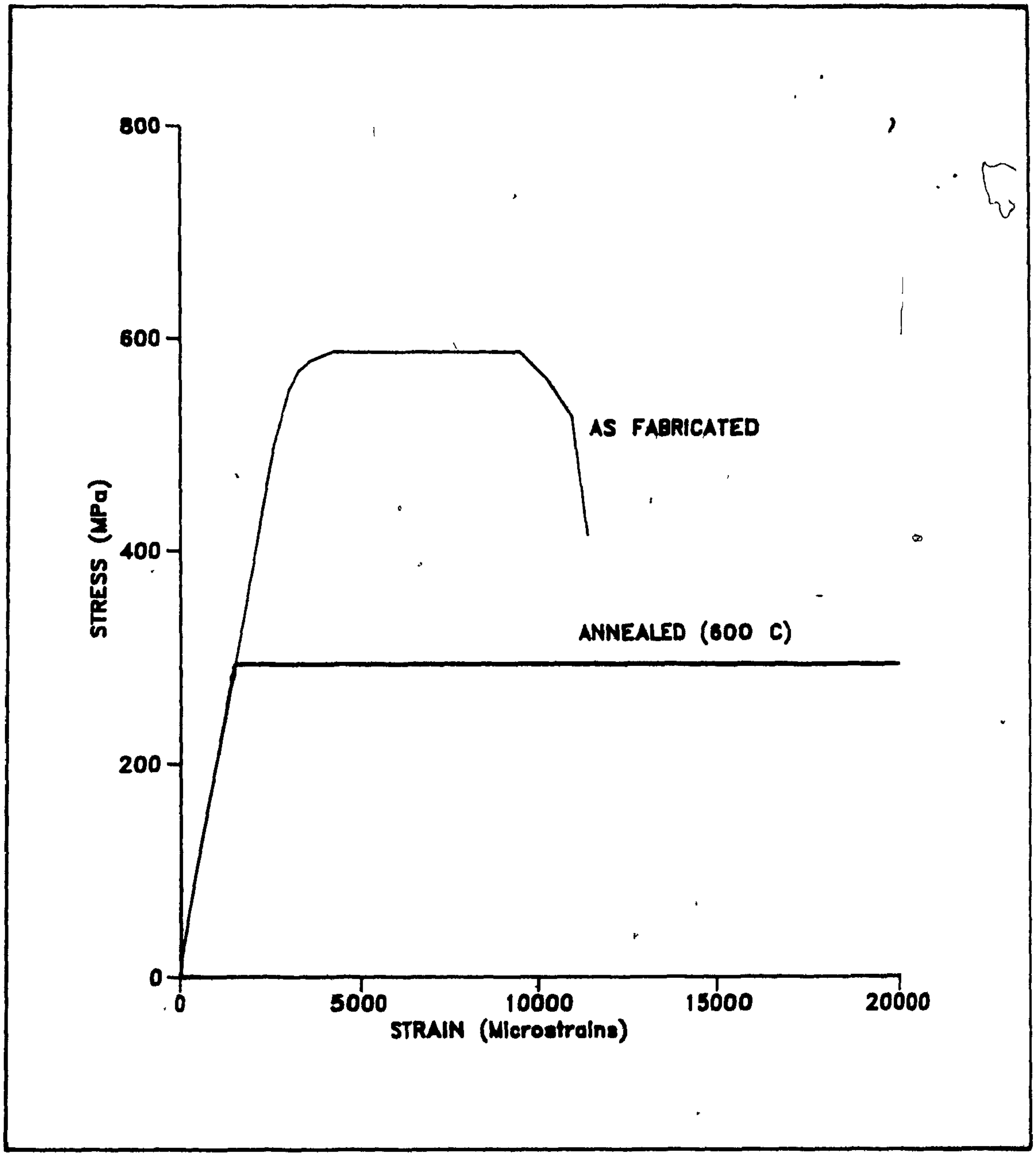

Figure 3.5 STRESS-STRAIN CURVE OF D2 WIRE.

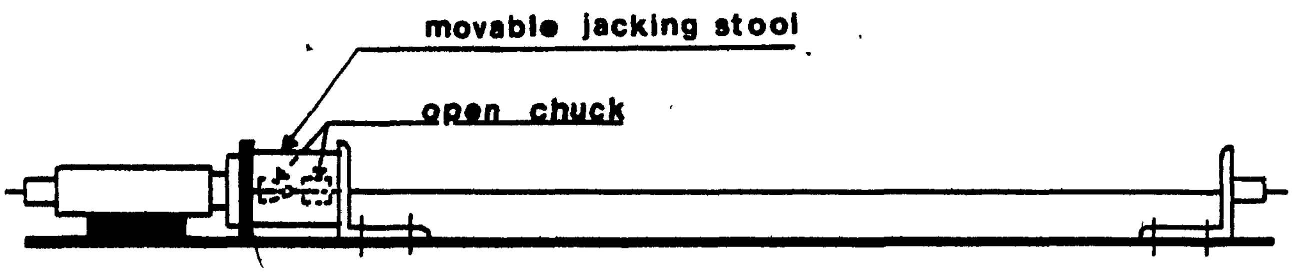

a. Before Release

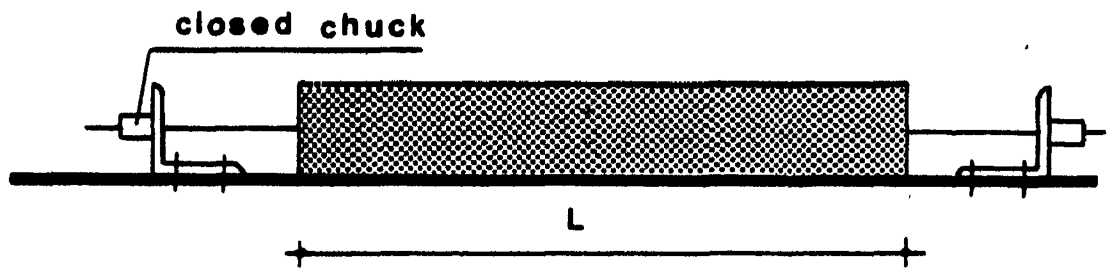

b. After Release

Figure 3.6 SET-UP FOR THE TENSIONING METHOD.

3.2.1 HARPING OF PRESTRESSING WIRES

With the collaboration of the Structural Laboratory technicians, a system was designed to obtain a harping point for the prestressing wire at midspan. The system consisted of two harping point supports bolted to the beams of the prestressing bed with M20 high strength bolts. Also, a 25 mm rod, covered with a plastic tube at the level of the girders, was connected to the two supports. The details of the prestressing bed and the harping point system are shown in Figure 3.7.

3.2.2 PULL-OUT TEST

Five pull-out tests were conducted on five samples of prestressing wire of 5.0 mm diameter to check the adequacy of the bond at the steel-concrete interface and to verify if the slip occurred before or after that the prestressing wire had developed its yield strength. A series of tests was completed on specimens with five different embedment lengths of 300 mm, 400 mm, 500 mm, 600 mm and 900 mm. The cross-sectional area of the pull-out specimens was 44 mm x 86 mm. The set-up for a pull-out test is shown in Figure 3.8. The results are summarized in Table 3.4. It was observed that the wire developed its yield strength for an embedment length equal to or greater than 600 mm. The results were plotted and shown in Figure 3.9.

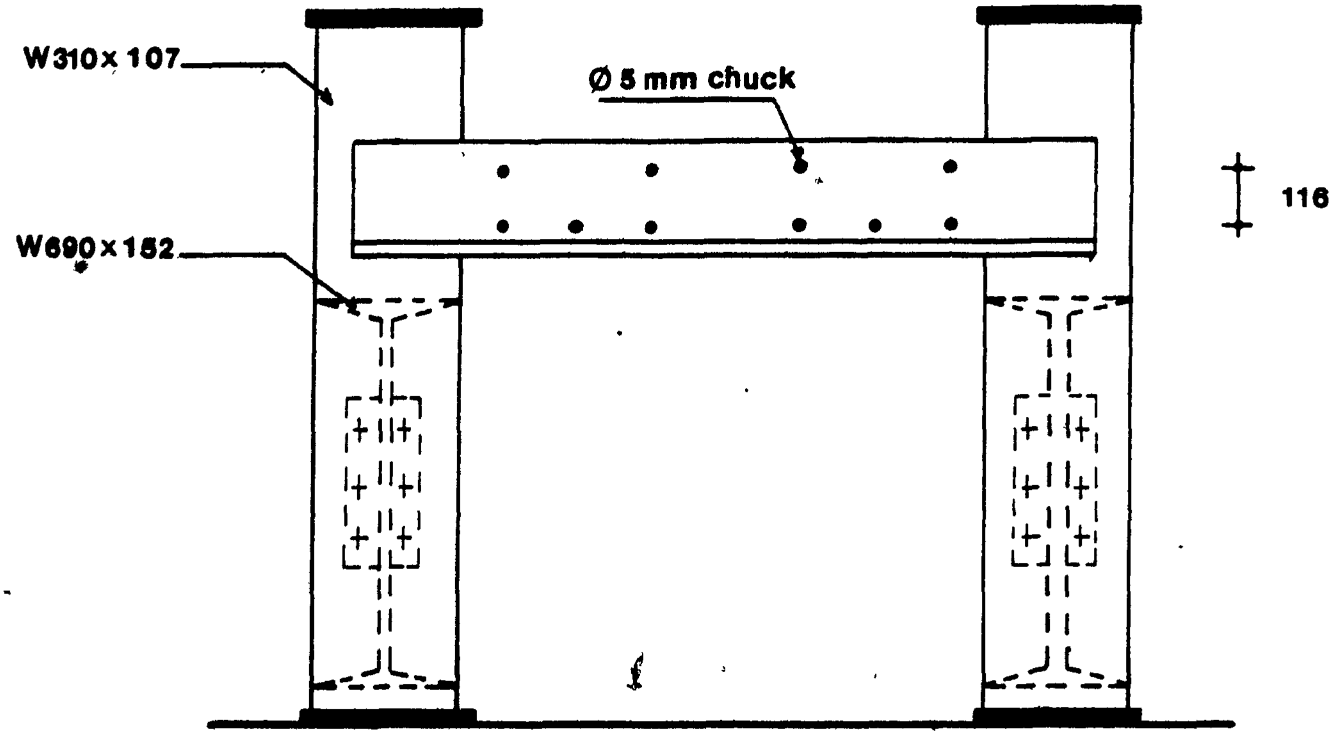

a) Prestressing Abutment Details.

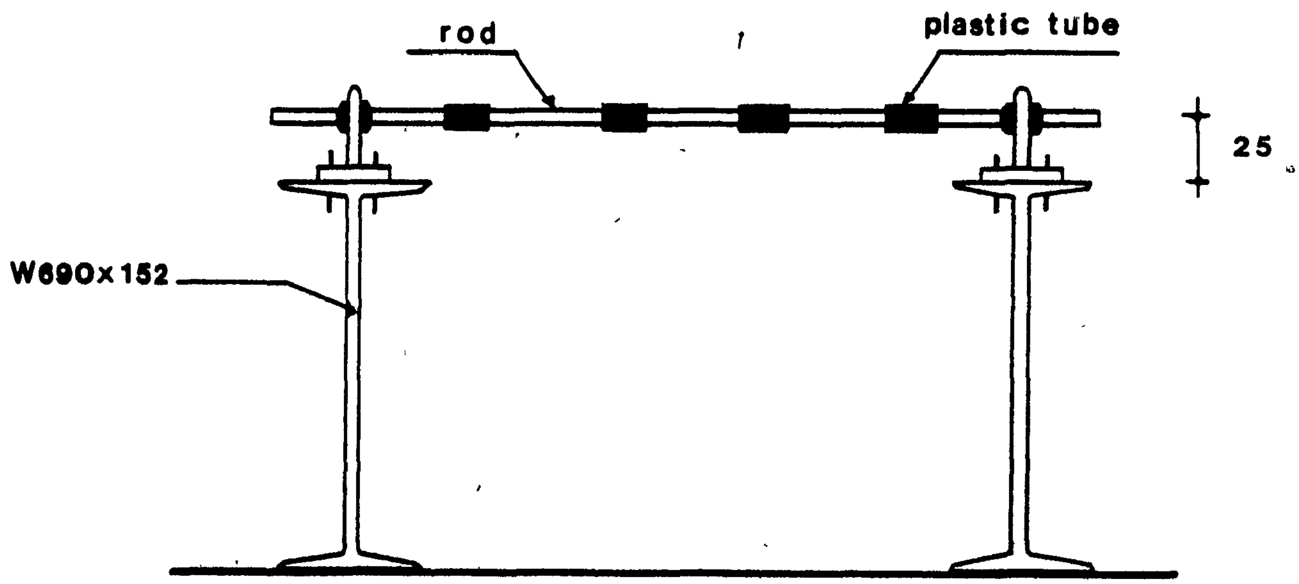

b) Harping Point Details.

Figure 3.7 DETAILS OF SET-UP FOR HARPING THE PRESTRESSING WIRES.

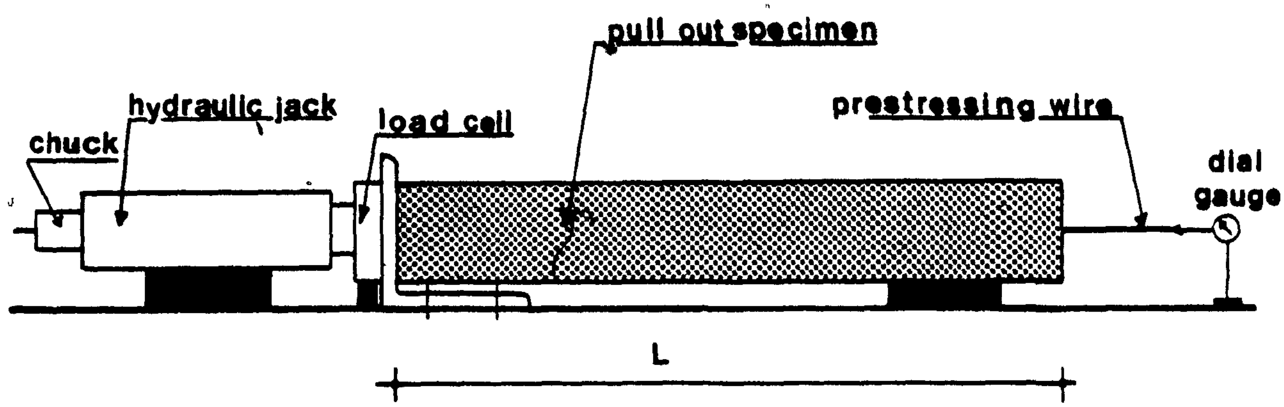

Figure 3.8 PULL-OUT TEST SET-UP.

Embedment Length L (mm)	Axial Load P (kN)	Comments
300.	-	Crack appeared shortly after pulling out
400.	12.30	Wire slipped - No cracks
500.	24.90	Wire slipped - Longitudinal cracks
600.	29.70	No cracks - Wire yielded
900.	29.8	Wire yielded

TABLE 3.4 PULL-OUT TEST RESULTS.

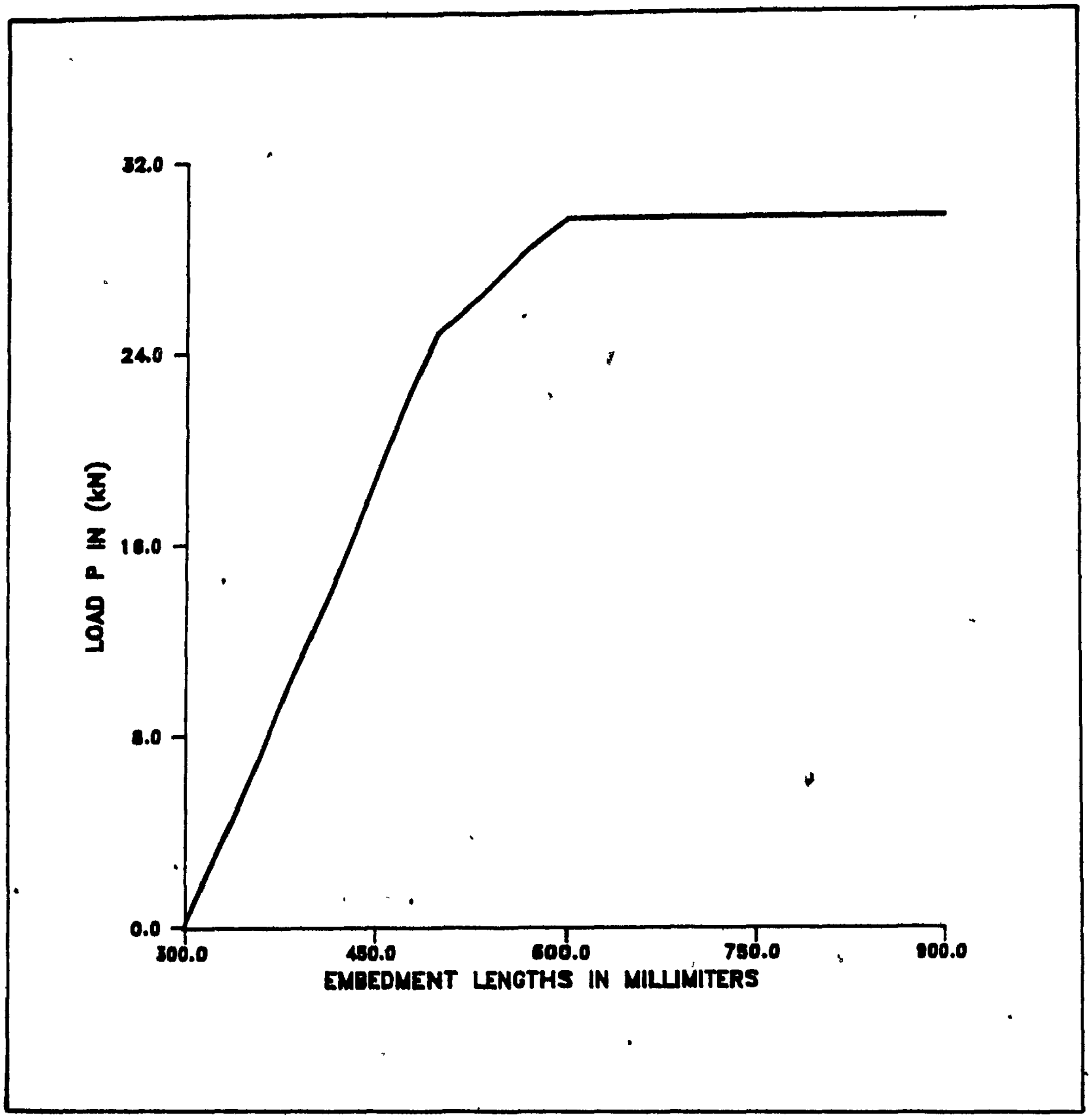

Figure 3.9 PULL-OUT TEST RESULTS FOR 5 mm PRESTRESSING WIRE.

CHAPTER 4

CONSTRUCTION OF THE BOX GIRDER BRIDGE

The construction of the box girder bridge model required adherence to strict specifications including those for the preparation of the formwork, the design of the concrete mix and the stringent tolerances in construction dimensions required for the physical model.

4.1 CONSTRUCTION PROCEDURE

The construction of the box girder bridge model consisted of the following operations:

1. Construction of the outer channel formwork and the support of the bottom slab.
2. Placing of the bottom slab and channel reinforcing wire meshes after installation of the electrical strain gauges.
3. Tensioning of the prestressing wires after installation of the electrical resistance strain gauges.
4. Construction of the inner channel formwork.
5. Casting and curing of the bottom slab and the channel; removal of the inner channel formwork.
6. Filling the box with steel billets as partial compensation for dead weight.
7. Covering the filled boxes with styrofoam, construction

of the top slab formwork and placing of the reinforcing wire meshes.

8. Casting and curing of the top slab; removal of forms.

9. Placing of concrete blocks on the deck and cutting of the prestressing wires.

10. Removal of the prestressing bed and placing the box girder model on supports.

11. Installation of strain gauges on the concrete surface; painting the bridge model with white paint.

4.2. CONSTRUCTION DETAILS

4.2.1 PRESTRESSING BED

The prestressing bed consisted of two W690 X 152 sections, 4.27 m long, four W310 X 107 vertical sections, 1.80 m high, and two 200 X 200 X 20 mm angles, 1.50 m long used as prestressing abutment. The two beams were bolted to the four vertical sections by M20 high strength bolts. Also, the vertical sections were welded to these angles where holes were provided to allow for the correct positioning of the prestressing wire. Details of the reaction frame with the harping point supports bolted to the beams at midspan are shown in Figure 4.1.

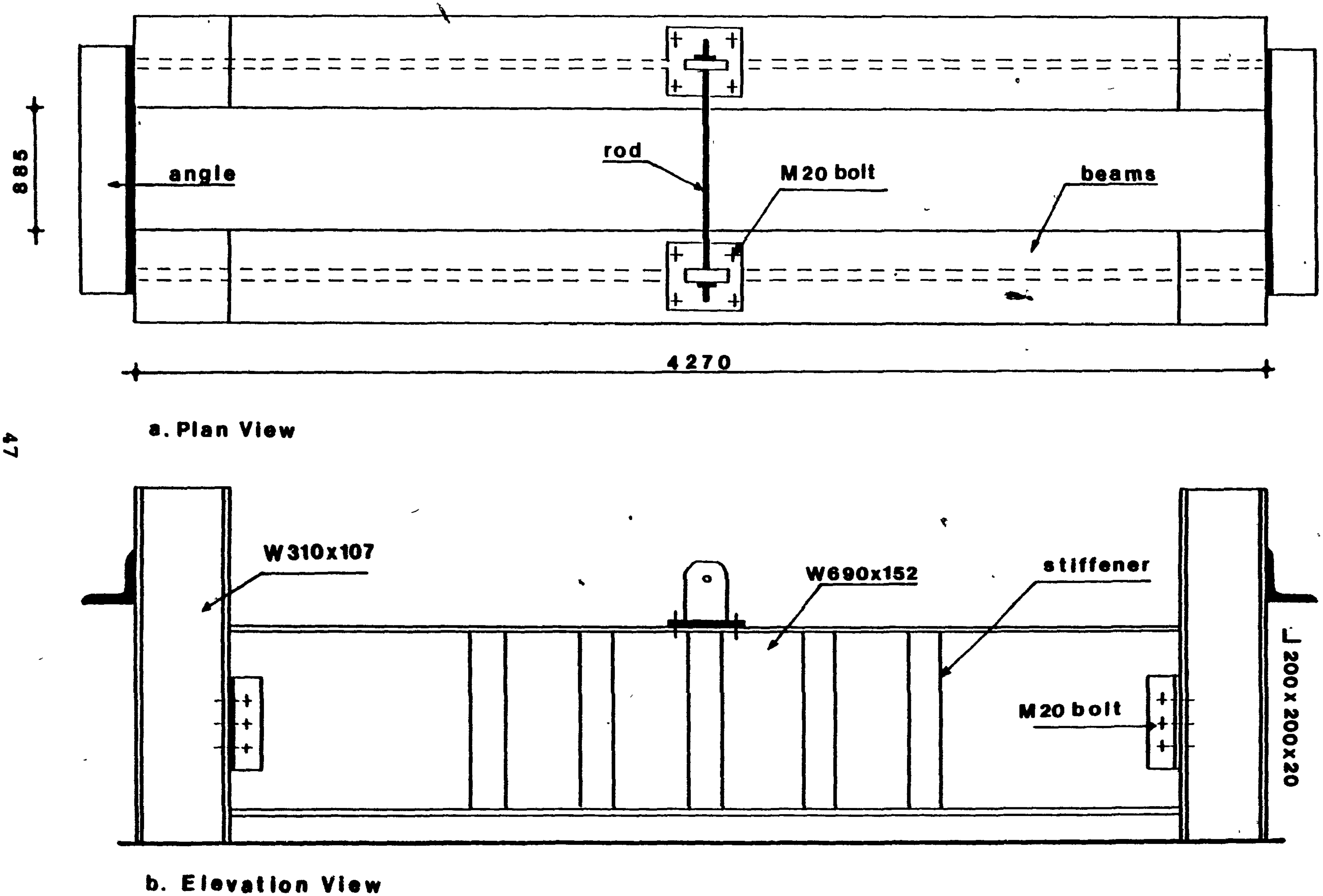

Figure 4.1 PRESTRESSING BED DETAILS

4.2.2 PREPARATION OF FORMWORK

The box girder bridge model was constructed using two types of formwork. All formwork was made using 19 mm thick plywood sheets with a polyuerethene varnish and was removed when the concrete cured. A minimum amount of light form oil was used on the forms to facilitate stripping. Also, a 20 mm thick styroform was used to support the slab over the boxes, to cover the steel billets and not to allow the concrete to fill the inside of the boxes. It had a negligible stiffness and did not influence the model response and its behaviour.

4.2.3 STEEL REINFORCEMENT

The webs, top and bottom slab reinforcements consisted of wire meshes. The wire meshes consisted of annealed D2 bars placed in two orthogonal directions.

4.2.4 TENSIONING OF PRESTRESSING WIRES

For this purpose, the same method as used by Ferdjani [16] and Hadj-Arab [18] was adopted for this project. But instead of having three angles, one extreme angle was replaced by three movable jacking abutments. The tensioning of the prestressing wire for the box girder bridge model consisted of the following steps:

1. Tensioning of the prestressing wire by means of the hydraulic jack. The two extreme chucks were closed while the intermediate one was open.

2. Closing the intermediate chuck on the respective abutment.

3. Releasing of the tensioning force applied by the hydraulic jack. The prestressing wire was attached to the abutment using 5.0 mm diameter chucks.

All of the ten wires were equipped with linear electrical resistance strain gauges. They were tensioned sequentially by the hydraulic jack and a calibrated hollow load cell was used to evaluate the applied force. The strain measurements given by the linear electrical strain gauges were used to check the force applied to each wire. The measured prestressing forces are summarized in Table 4.1. The average total loss of the prestressing wires was found to be equal to 15 %.

4.2.5 CONCRETING OF BOX GIRDER BRIDGE MODEL

The concreting process of the box girder bridge model was completed in two steps . The first step consisted of concreting the bottom slab and the webs. The concreting commenced at one end of the bridge and continued to the other end in short lengths to avoid air pockets in the concrete. During this process, the concrete was vibrated by a needle vibrator to consolidate it and to eliminate any

Wire No	Initial Values Strain (Microstrain)	Values After Release Strain (Microstrain)	Losses %	At Transfer Strain (Microstrain)	Total Losses %
1	6175	5815	5.85	5257	14 85
2	6452	6420	0 5	6373	1 2
3	6023	5866	2.6	5498	8.7
4	6020	5954	1.1	4230	29.7
5	6955	6905	0.7	5915	14.9
6	6290	6041	3 96	5066	16.6
7	6200	6033	2.7	5606	9 6
8	6012	5860	3.6	4643	22.8
9	6002	5890	2 9	4461	25.7
10	6154	5795	5.9	5248	14.7

TABLE 4.1 PRESTRESS LOSSES

air pockets. Extreme care was required during the pouring of concrete where small aggregate spacers were placed under the meshes to provide a proper cover thickness to the steel reinforcement.

After casting the channels, and in order to prevent any possible loss of moisture and to cure the concrete, the structure was covered by a plastic sheet for a period of one week. Then, the inner formwork was removed and the boxes were filled with steel billets.

The second step consisted of concreting the top slab. Before that, the seven days old concrete of the webs was cleaned by a steel brush and water in order to improve the bond between the old and the new concrete. The pouring of the concrete was done with extreme care to insure a proper cover thickness by placing small aggregate spacers under the top slab reinforcement. Three holes were provided at midspan, two at the edge and one at the middle for the threaded rods. When the casting of the structure was finished, the final operation was to cover the structure with a wet plastic sheet and water was sprinkled on it at regular intervals to cure the concrete.

4.2.6 <u>DEAD WEIGHT COMPENSATION</u>

From similitude analysis requirements, the model concrete is required to be seven times as heavy as the prototype concrete in order to obtain a true model. Since this similitude conditions can obviously not be achieved, dead weight compensation was necessary. Concrete blocks were placed on the model bridge deck and steel billets were filled into the boxes to simulate the prototype dead weight. The positions of the concrete blocks are shown in Figure 4.2. Also, two boxes of steel plates were placed at the edges of the bridge model. More details of the dead weight compensation analysis are given in Appendix A. The dimensions, weights and the location of steel billets and steel plates are shown in Table 4.2.

4.2.7 CUTTING OF PRESTRESSING WIRES AND FORMWORK REMOVAL

At this stage, the structure was placed on the supports and all of the concrete blocks were placed. After cutting the prestressing wires, the removal of the formwork started. The outer formwork for the boxes and the forms on the sides of the structure were stripped easily. But a problem was encountered while trying to strip the form between the end block and the supports. The structure was carefully lifted up from one end by using two hydraulic jacks and steel plates under the end block. The formwork was then removed and rubber pads were placed at the supports. The same operation was repeated at the other end block. Finally, the preparations for the test on the bridge model were commenced.

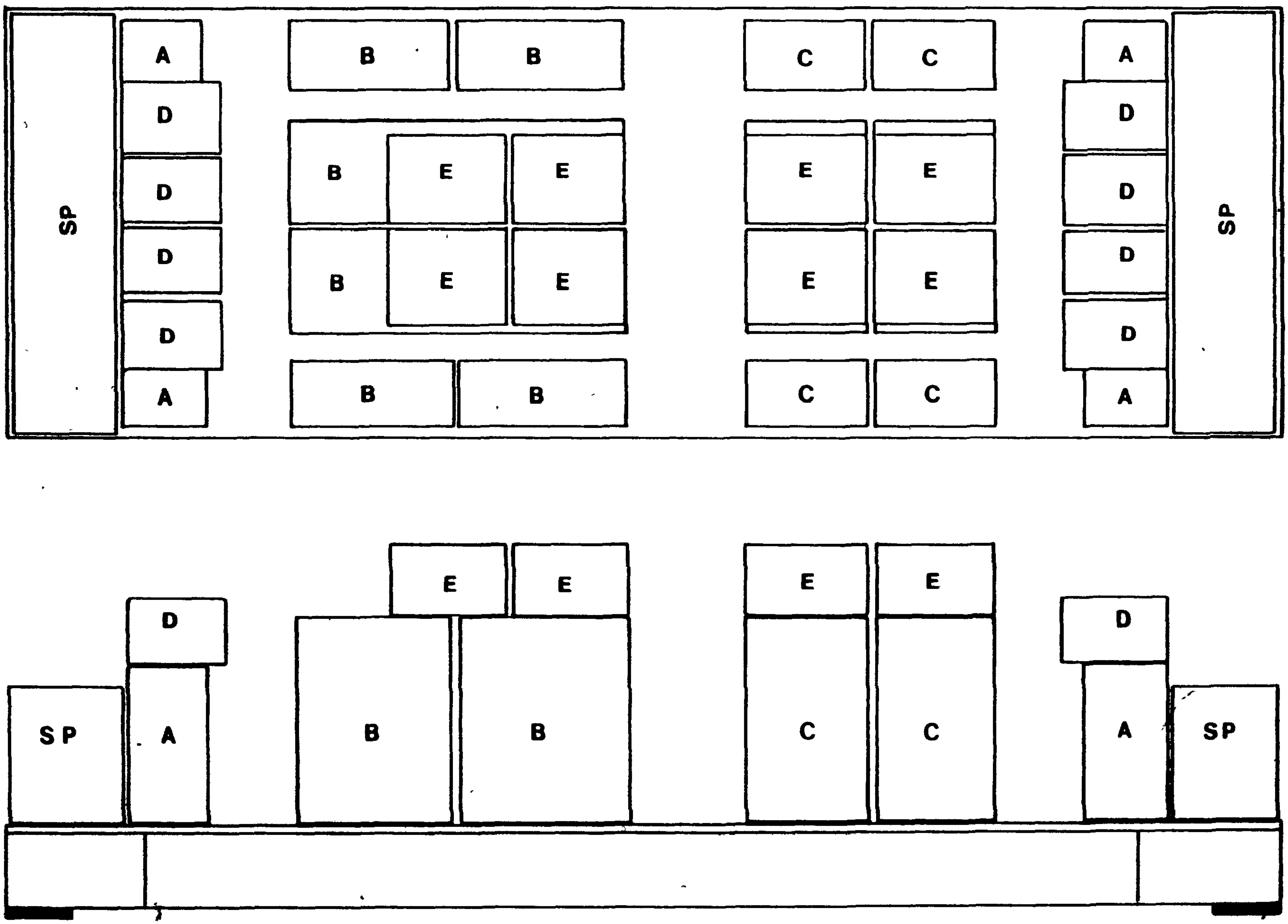

Figure 4.2 POSITION OF THE CONCRETE BLOCKS ON THE MODEL BRIDGE

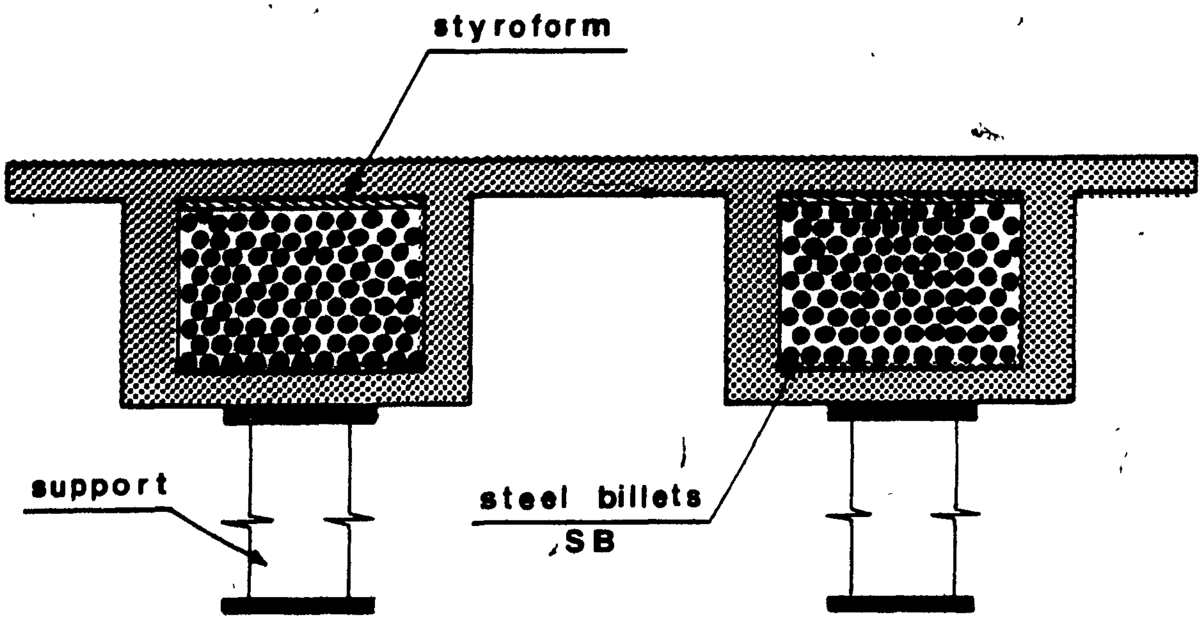

CONCRETE BLOCKS	NUMBER	DIMENSONS (mm)
A	8	0.24 x 0.28 x 0.46
B	8	0.20 x 0.42 x 0.50
C	8	0.20 x 0.32-x 0.50
D	8	0.17 x 0.20 x 0.34
E	8	0.24 x 0.34 x 0.26
STEEL	**NUMBER**	**WEIGHT (Kg)**
SP	2	1029
SB	2	980

TABLE 4.2 DETAILS OF DEAD WEIGHT COMPENSATION

4.3 INSTRUMENTATION

4.3.1 GENERAL

Proper instrumentation is required to measure the quantities related to the behaviour of the structure. The response of a structural model under any loading conditions can be determined from the model tests results. These results can be achieved with a desired level of accuracy if, before starting any test, a calibration of the different instruments and an adequate check of the equipments is undertaken.

Data for loads, strains and deformations was obtained using instruments such as load cells, L.V.D.T's (Linear Variable Differential Transformer), strain gauges, and dial gauges.

During the testing of the box girder bridge, measurements such as steel and concrete strains, loads displacements of the structure under all static and dynamic loading conditions were made.

4.3.2 STRAIN MEASUREMENTS

Strains on the concrete and the steel were obtained using electrical resistance strain gauges. A total of 22 linear electrical resistance strain gauges were installed on the prestressing wires at three different locations as shown in Figure 4.3 for girder 1 and Figure 4.4 for girder 2. The data obtained from these strain gauges was used to determine the prestressing losses and also to determine the corresponding stresses acting on the wires under the various loading conditions. Following the recommendations of the manufacturer, the gauges were waterproofed to protect them from getting damaged during the concreting operation, and to prevent bonding of the gauges to the concrete.

The concrete surface of the webs, top and bottom slabs, were equipped with eight rosettes and fifty-eight linear strain gauges, respectively, placed at three different locations. The locations of these gauges are shown in Figure 4.5 for the top slab and Figure 4.6 for webs and bottom slab.

For both steel and concrete, the strain measurements were recorded and printed using the OPTILOG data acquisition and control system connected to an IBM personal computer.

4.3.3 DISPLACEMENT MEASUREMENT

Two different instrumentations were used for static and dynamic tests; dial gauges with an accuracy of 2.54×10^{-3} mm to 2.52×10^{-2} mm per division and linear variable differential transformer (L.V.D.T's) were used for deflection measurements which are required to define the load-deflection characteristics of the structure and the

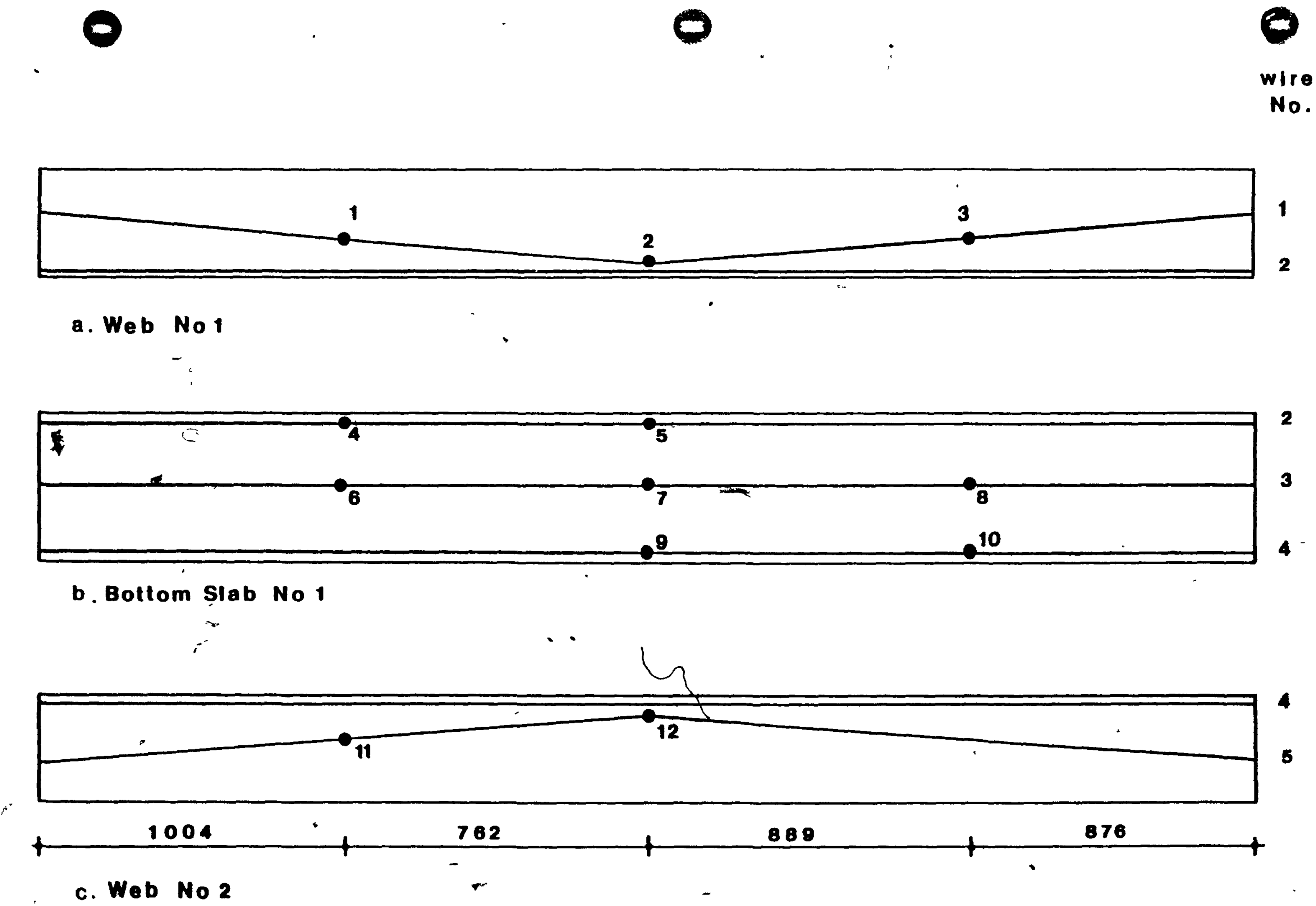

Figure 4.3 STRAIN-GAUGE LOCATIONS ON THE PRESTRESSING WIRES FOR GIRDER 1

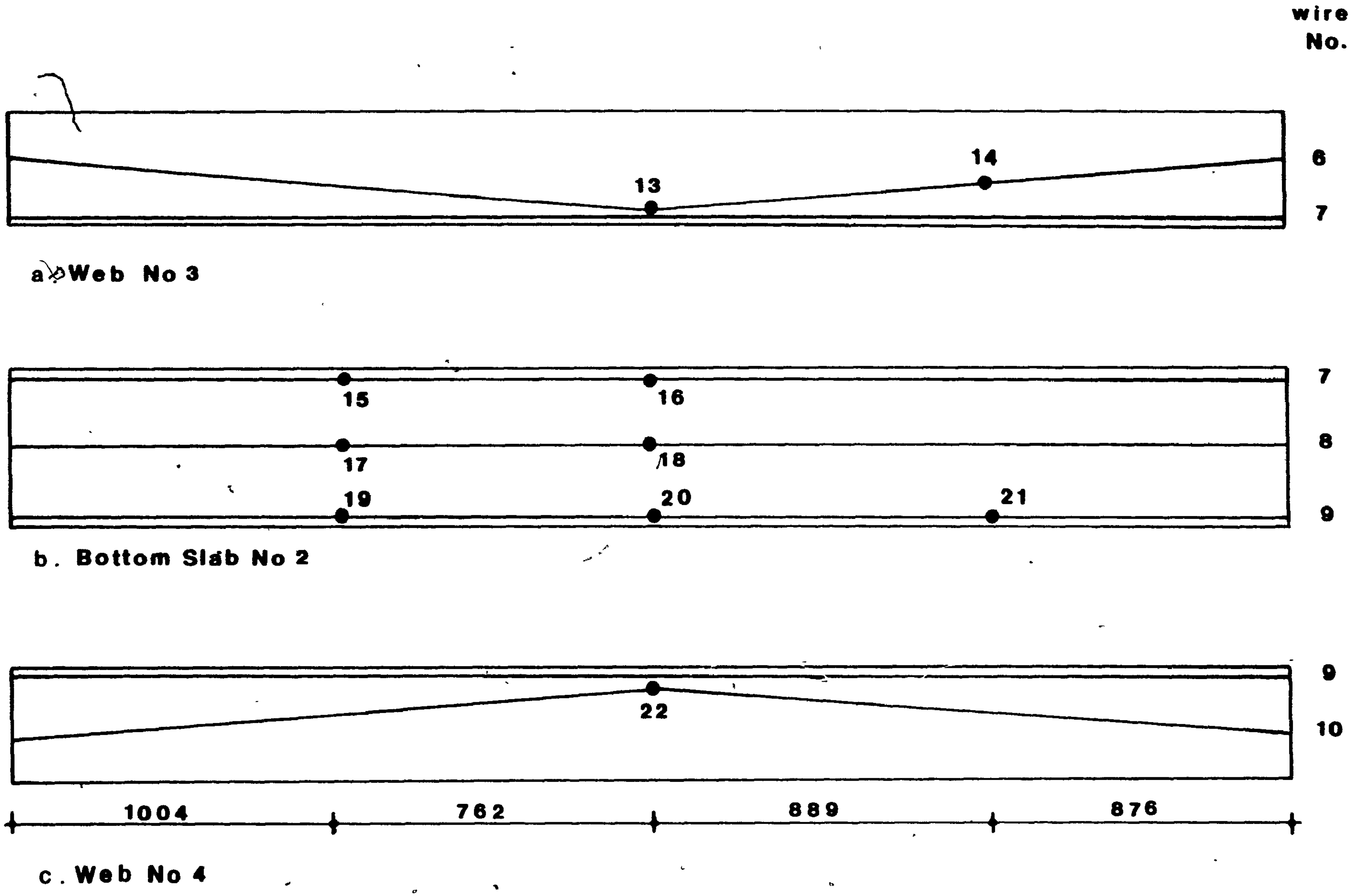

Figure 4.4 STRAIN-GAUGE LOCATIONS ON THE PRESTRESSING WIRES FOR GIRDER 2

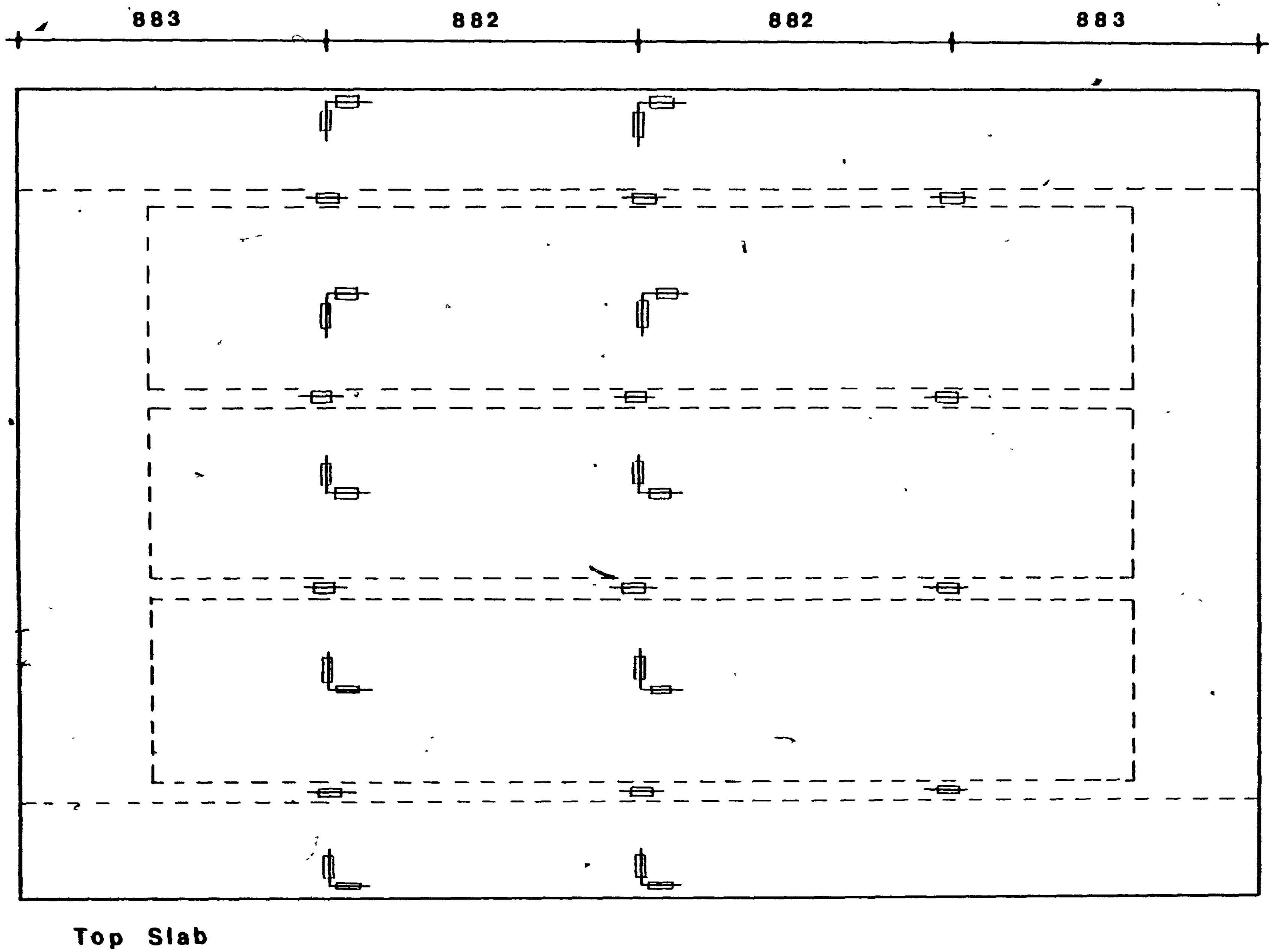

Figure 4.5 POSITION OF THE CONCRETE STRAIN-GAUGES ON THE TOP SLAB

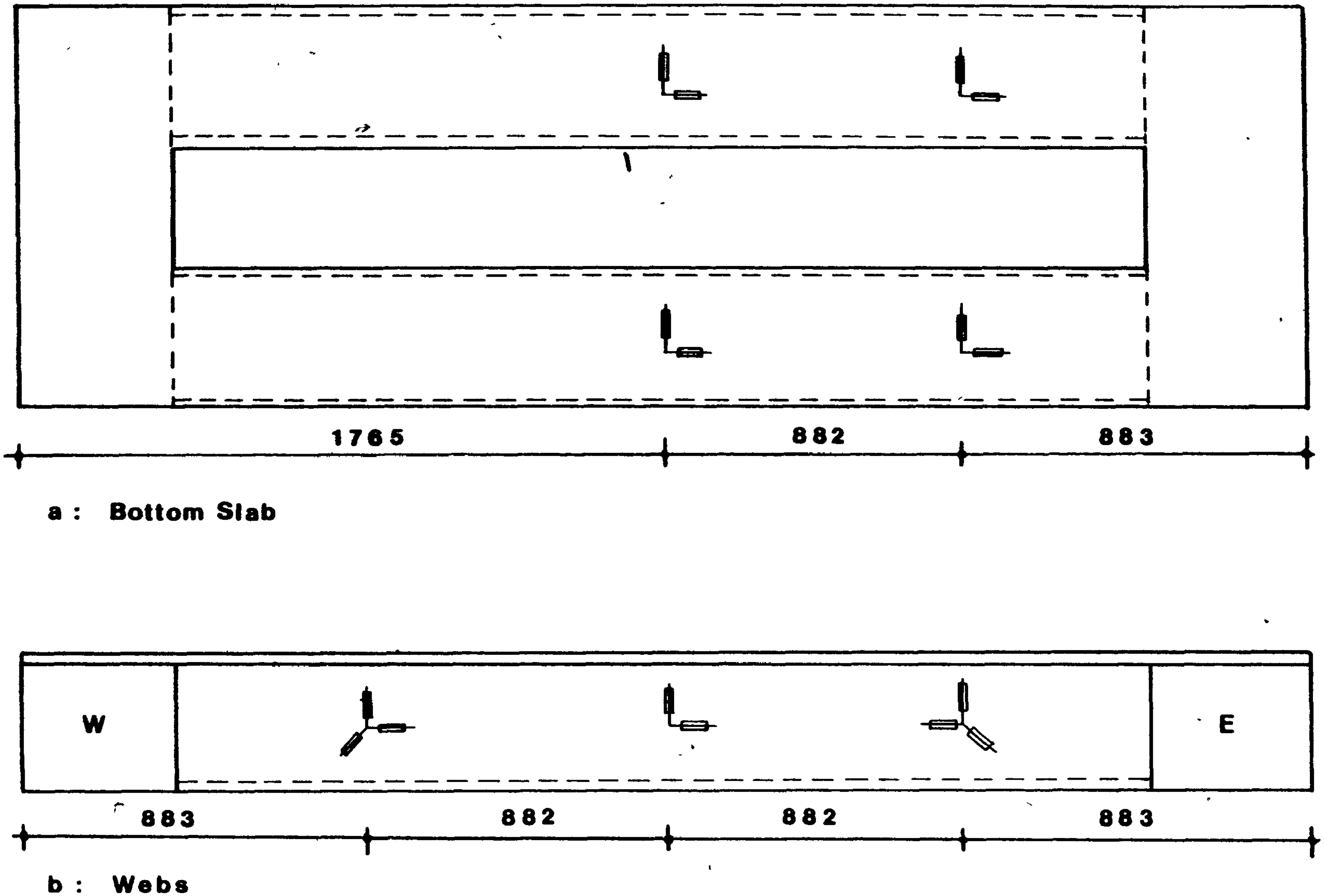

Figure 4.6 POSITION OF THE CONCRETE STRAIN-GAUGES ON THE BOTTOM SLAB AND THE WEBS

limits of linear and nonlinear behaviour of the structural model for static tests. Dial gauges were clamped on a stiff independent frame to make theses readings independent of the displacements in the structural model and the testing frame. These gauges were placed at selected locations for the various stages of the test program as shown in Figure 4.7.

For dynamic tests, the model was equipped with nine L.V.D.T's. Groups of three L.V.D.T's were located at three different sections along the bridge model as shown in Figure 4.8. These instrumentation readings were recorded and printed using the MINC computer which sampled data at a rate of 400 readings per second for each L.V.D.T.

4.3.4 LOAD APPLICATION

All of the loads were applied through a hydraulic jack and measured directly using a calibrated hollow load cell. For the tensioning of the wire, a 10-kip calibrated hollow load cell was used. But during the static tests, the load on the bridge model was applied through two hydraulic jacks and was measured using two 10-kip calibrated hollow load cells placed on the loading arm.

The digital data processor (OPTILOG), connected to the IBM personal computer, was used to record and print the load cell readings.

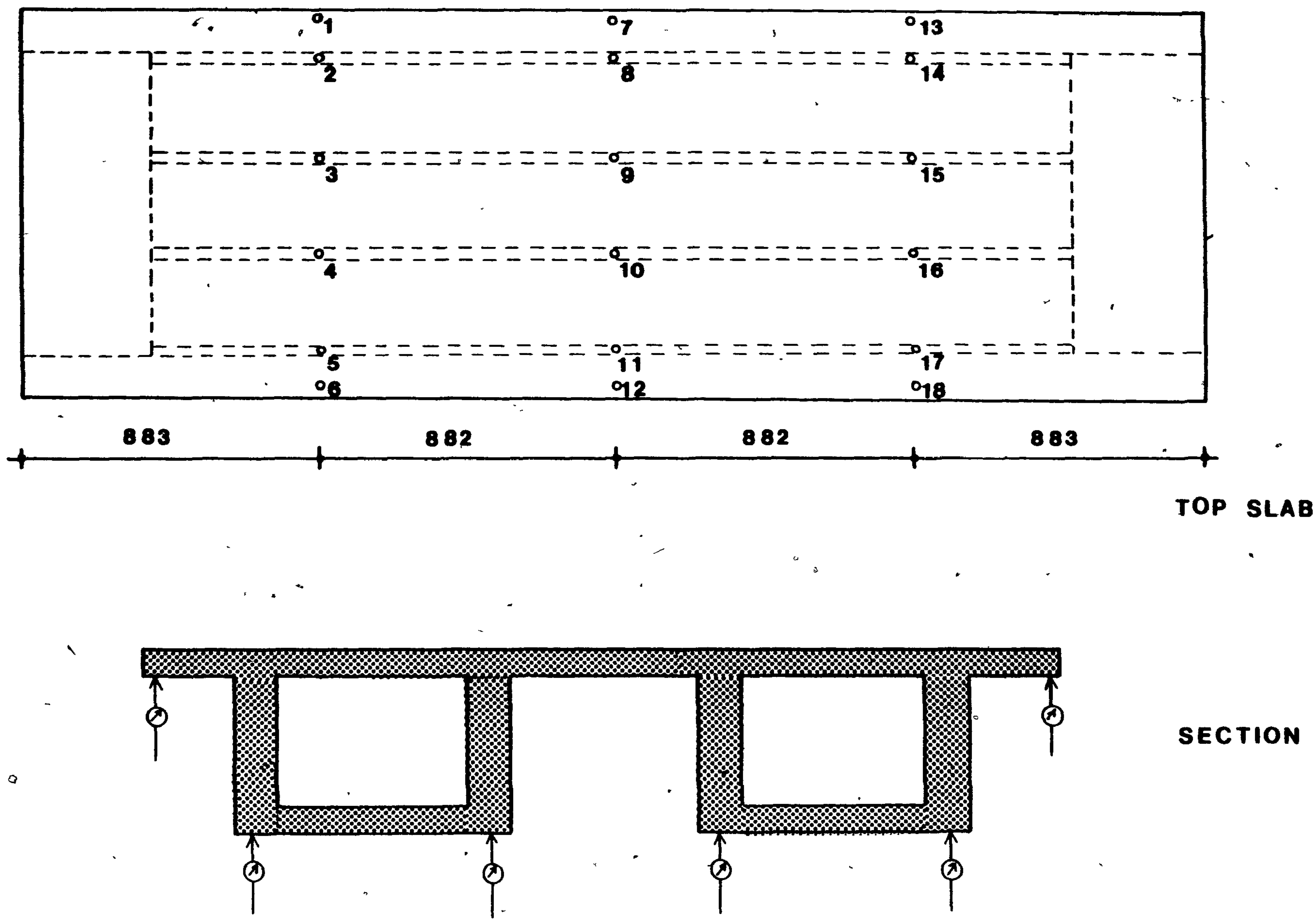

Figure 4.7 LOCATION OF DIAL GAUGES

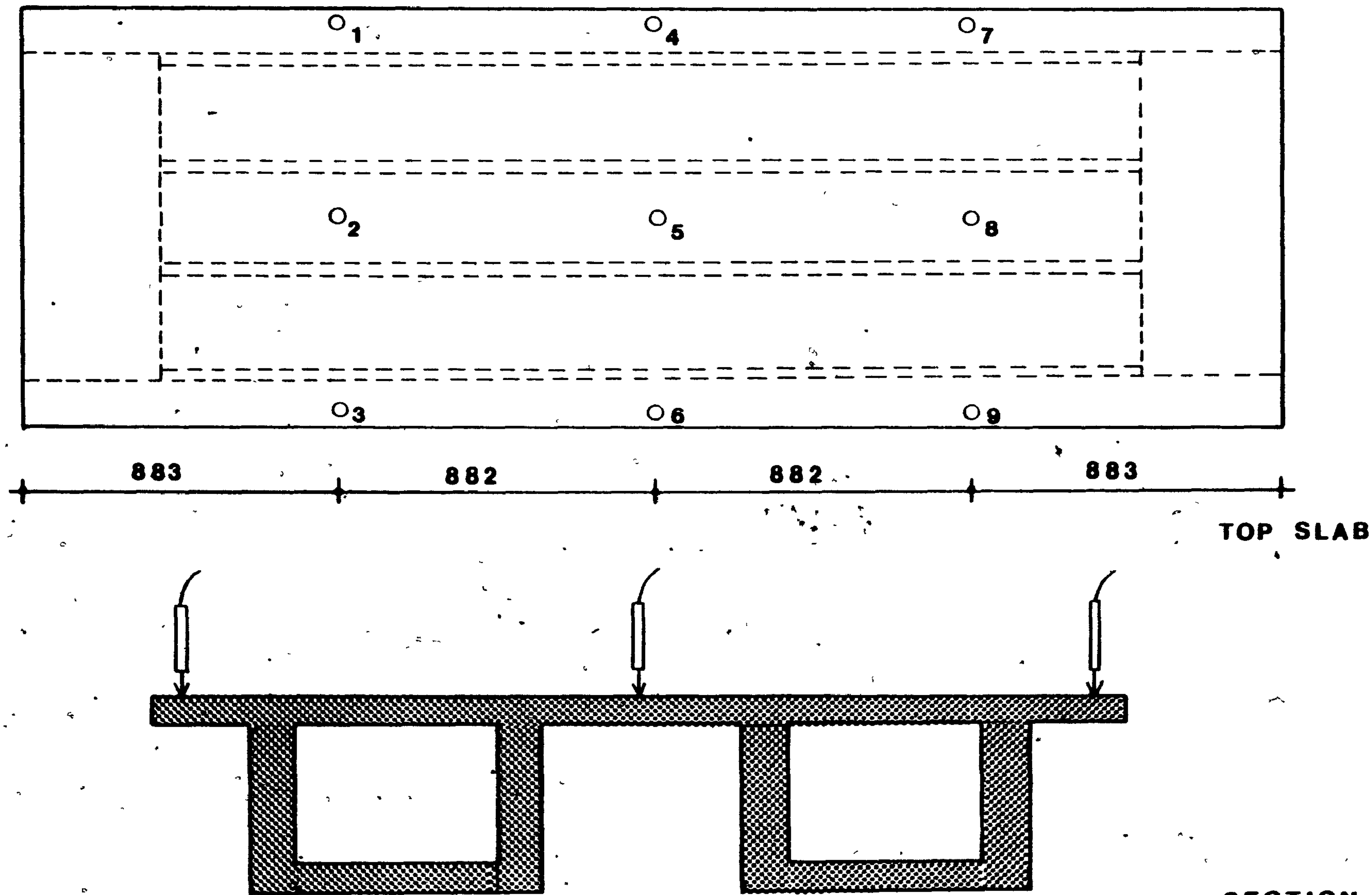

Figure 4.8 LOCATION OF L.V.D.T'S

4.3.5 DETECTION OF CRACKS

The bridge model was painted with a diluted white wash. The detection of cracks, which was conducted manually, was easy since the paint was brittle enough to show even very small cracks. After the detection of all the cracks which occurred, these were traced by a black felt pen and then photographed.

4.4 LOADING SYSTEM

The bridge model was located in the Structures Laboratory at McGill University.

4.4.1 MODEL TRUCK

In order to get a simple articulated loading system, the front axle of the OHBDC truck was not considered. This axle is relatively lighter than the other axles and does not have a significant effect on the structure due to the small contact area. Details of the OHBDC truck and model truck are shown in Figures 4.9 and 4.10, respectively.

The design of the articulated loading system was based on a system of statically determinate beams in order to achieve the exact model loads. It was fabricated from hollow square sections and connected to each other by loose

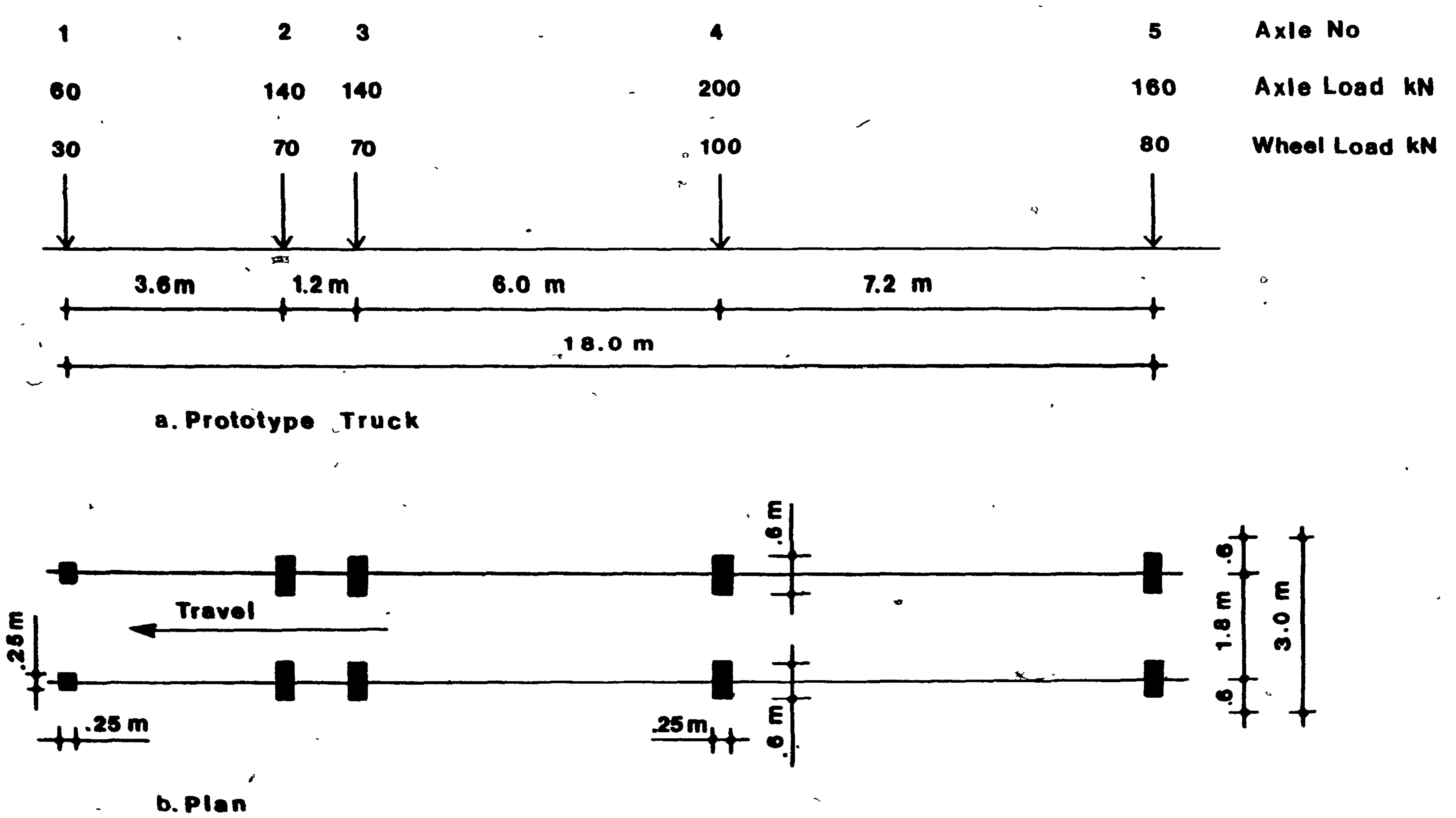

Figure 4.9 ONTARIO HIGHWAY BRIDGE DESIGN CODE TRUCK DETAILS

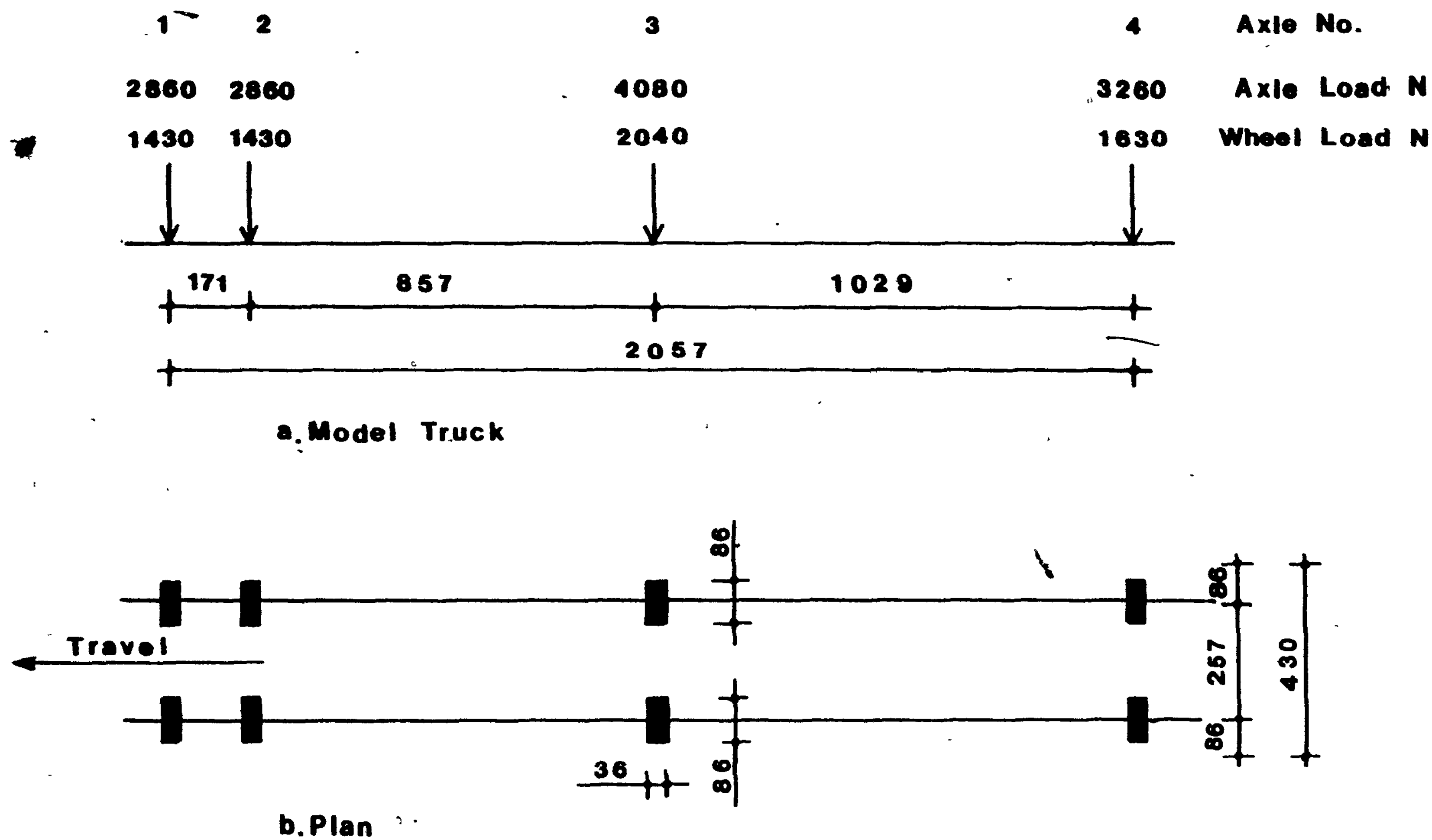

Figure 4.10 MODEL TRUCK DETAILS

pins. To simulate the model truck wheels, rubber pads with a model wheel dimensions were fixed to the free edge of each axle of the truck model acting as concentrated loads on the top slab. The articulated loading system consisted of two model trucks; the elevation and front view of the truck loads are shown in Fig. 4.11 and the plan view is shown in Fig. 4.12.

4.4.2 STATIC TEST SET-UP FOR FLEXURE

The static test set-up consisted of two model trucks loaded by a loading arm and two threaded rods. These threaded rods, 19 mm in diameter and with an ultimate tensile resistance of 100 kN each, were extended at the top of the loading arm by two 10-kips calibrated load cells and bolted. The loading arm consisted of a horizontal double channel beams with two steel plates welded on the top and the bottom along the length. The loads were applied using two hydraulic jacks through the two threaded rods reacting against the strong floor. The position of the model trucks on the bridge model and the loads acting on each one are shown in Fig. 4.13. The details of the static test set-up for flexure are shown in Fig. 4.14.

4.4.3 STATIC TEST SET-UP FOR TORSION

Concerning the static test set-up for torsion, only

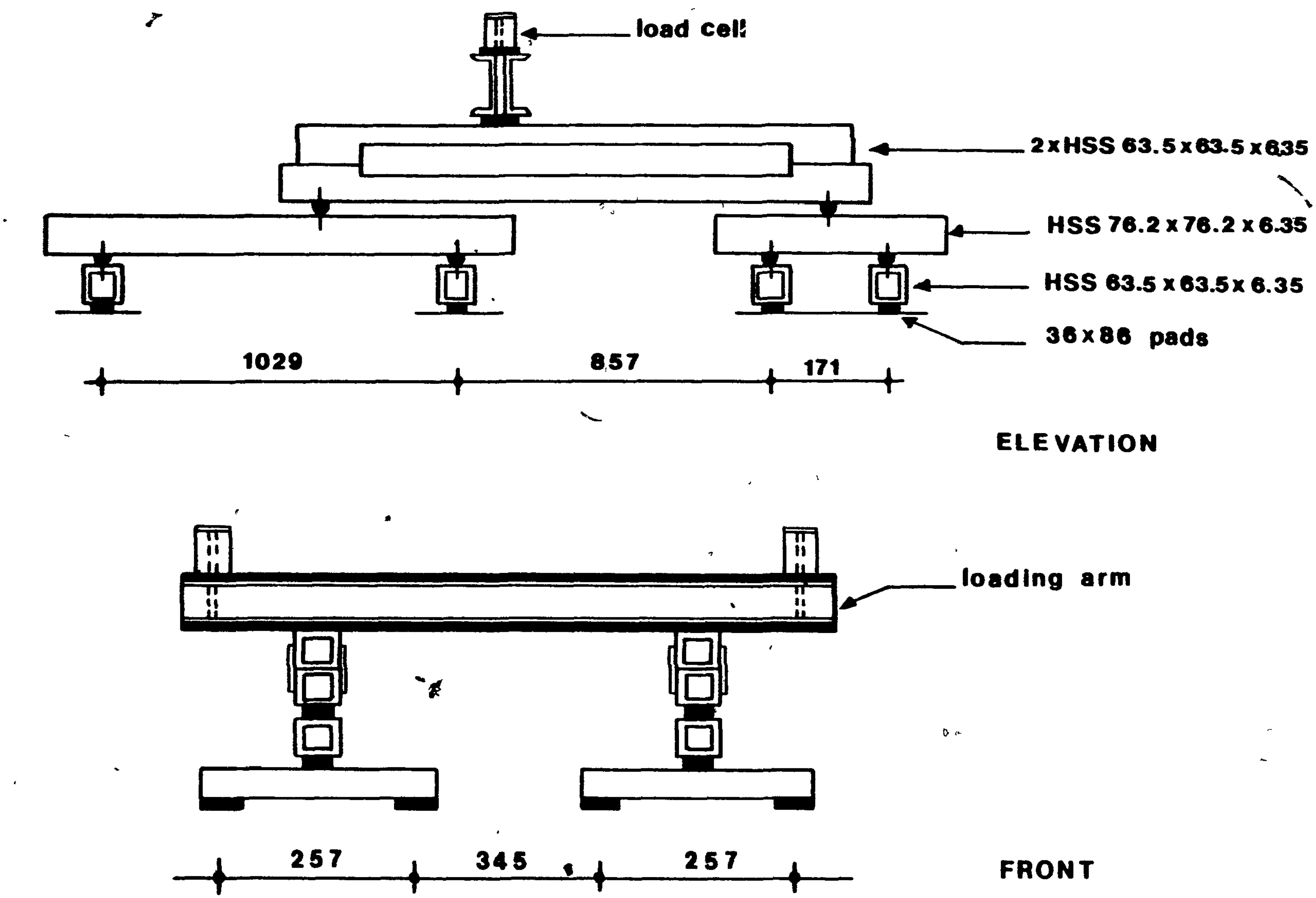

Figure 4.11 ARTICULATED LOADING SYSTEM. ELEVATION AND FRONT VIEW

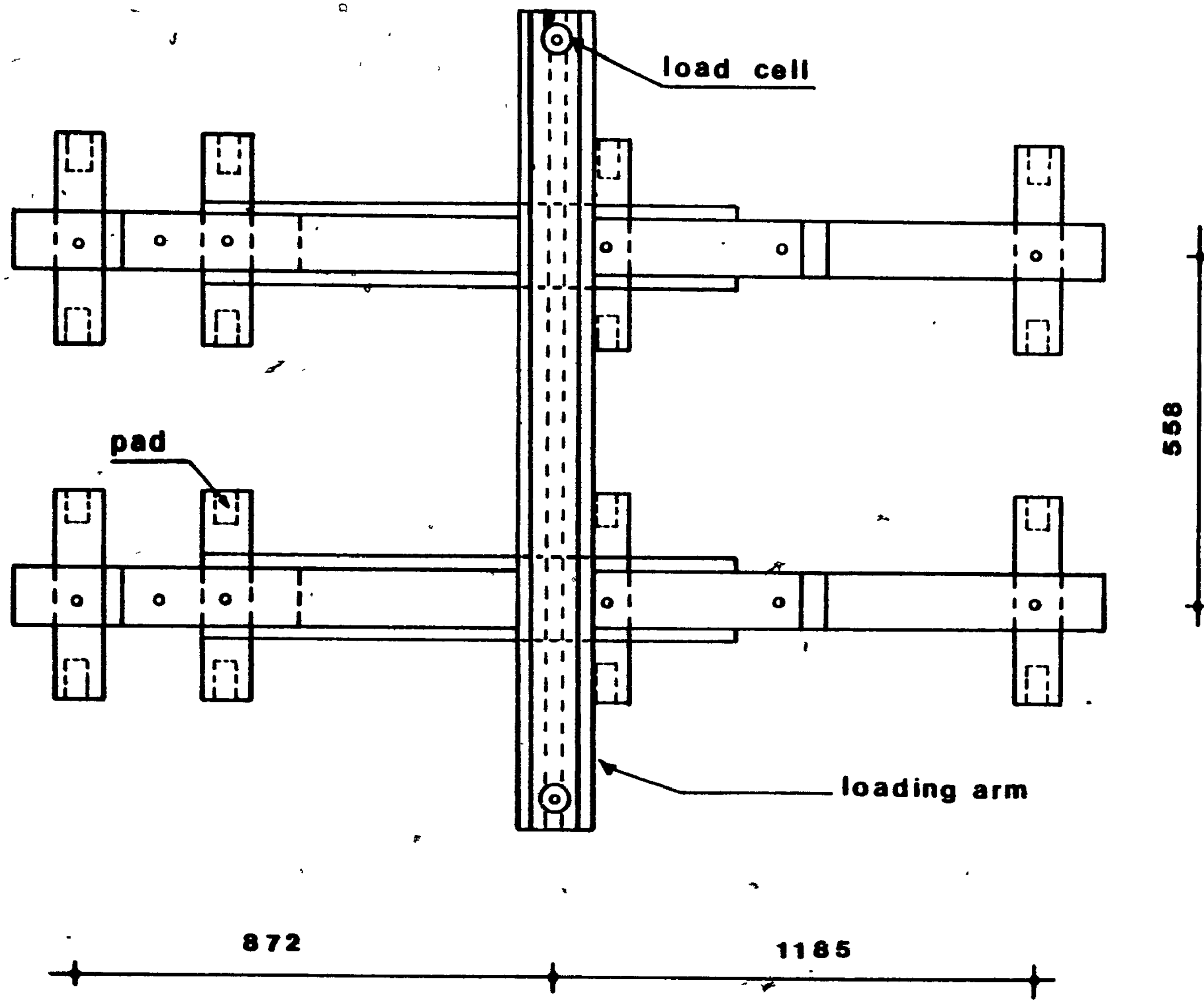

Figure 4.12 ARTICULATED LOADING SYSTEM. PLAN VIEW.

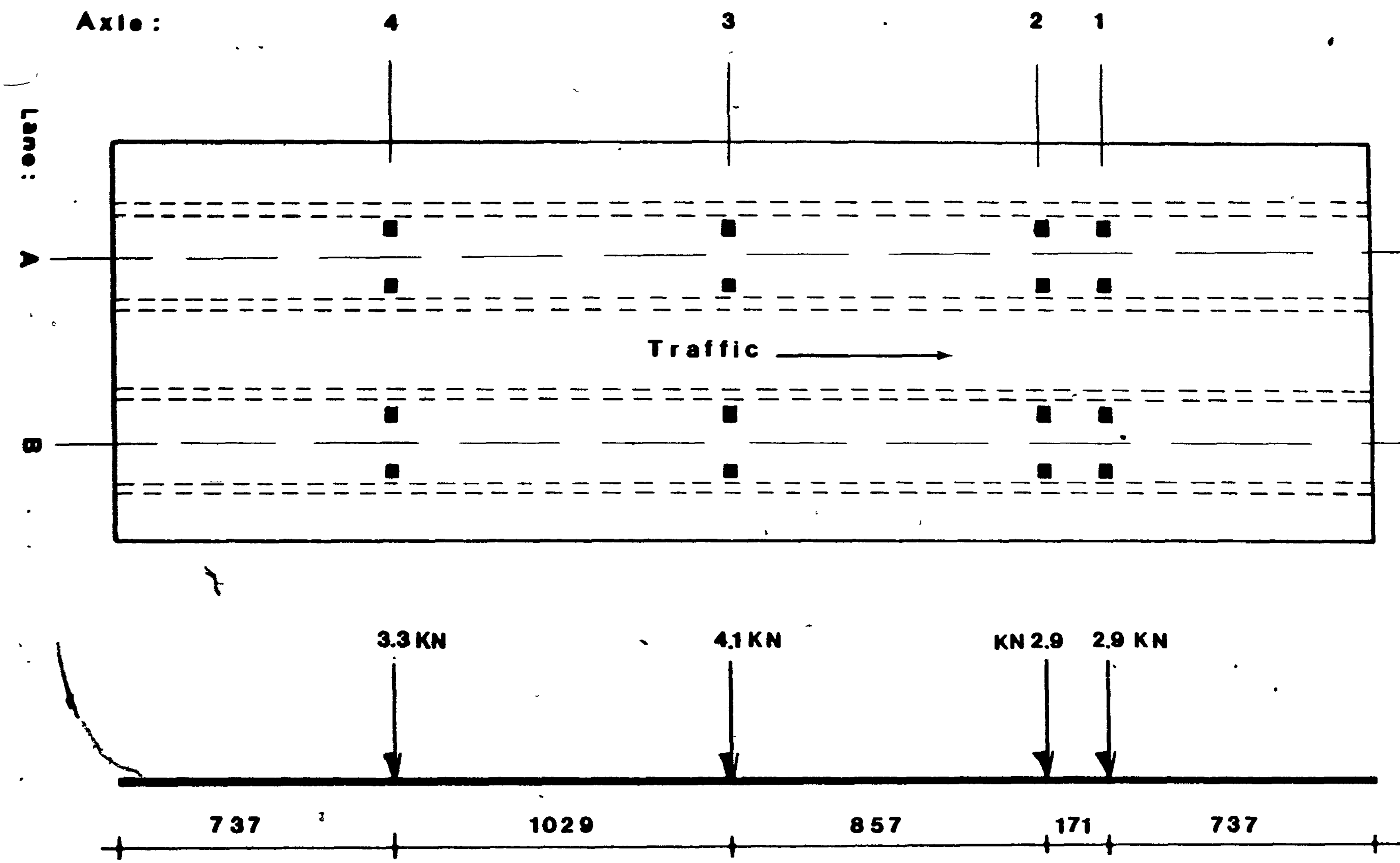

Figure 4.13 POSITION OF THE MODEL TRUCKS ON THE BRIDGE MODEL

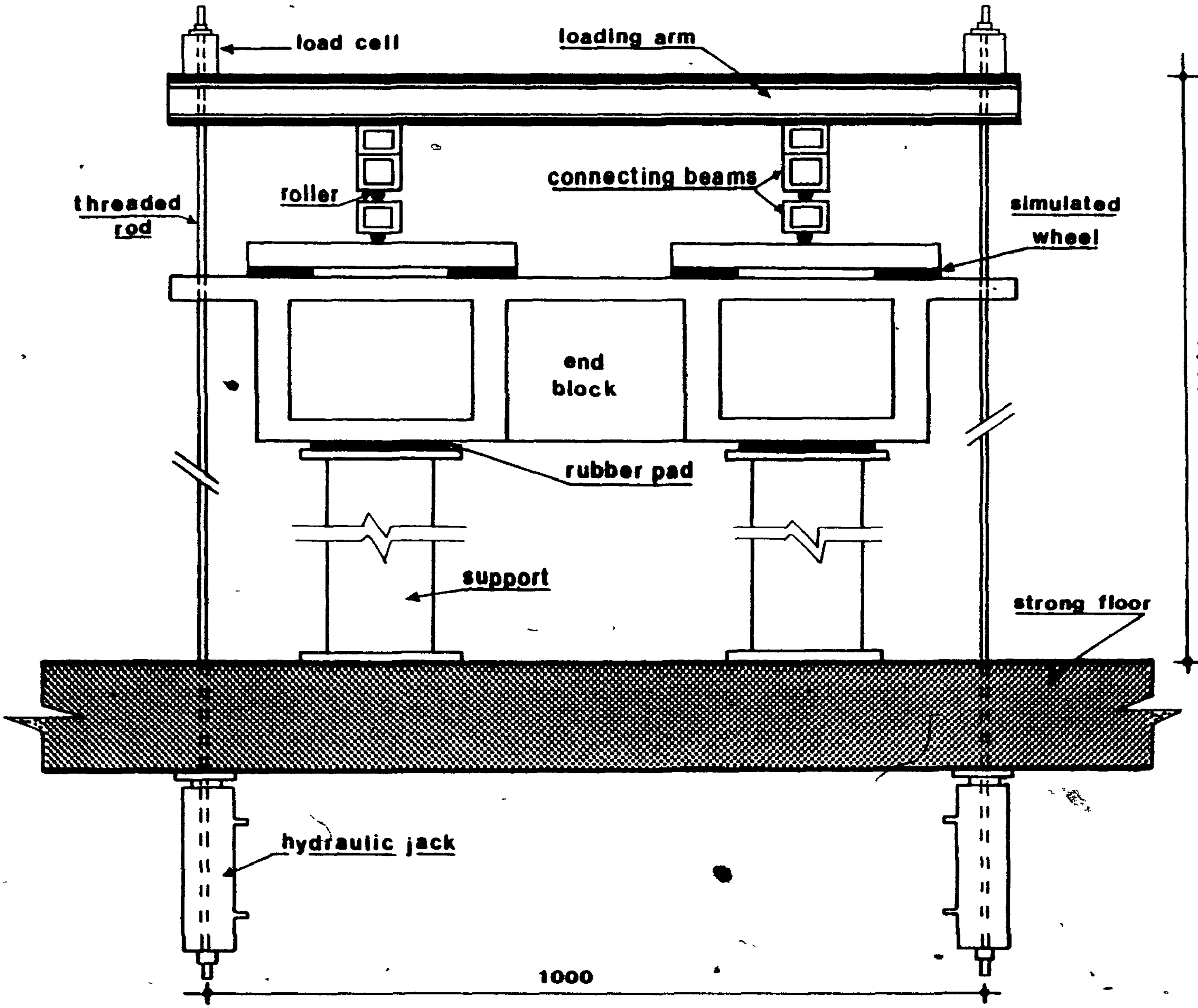

Figure 4.14 STATIC LOADING SYSTEM FOR FLEXURE

one model truck was used with two threaded rods passing through holes one at the edge of the slab and the other at the middle of the midspan. The loading arm of 560 mm length was one used for static set-up for flexure. Details of this set-up are shown in Fig. 4.15.

4.4.4 FREE VIBRATION SET-UP FOR FLEXURE

The 25 mm rod which was used for harping the prestressing wires was not removed from the structure. A mass of 230 kg, located at the midspan of the bridge model, was attached to this rod by means of a wire, which was cut by a pair of pliers to set the structure into free vibrations. Details of this process are shown in Figure 4.16.

4.4.5 FREE VIBRATION SET-UP FOR TORSION

For the free vibration set-up for torsion, the same weight of 230 kg was attached to the rod at midspan at a distance of 560 mm from the centerline of the bridge model. Details of the set-up are shown in Fig. 4.17. The loading system detailed in Section 4.4 was set up carefully and the load cells were calibrated before each test.

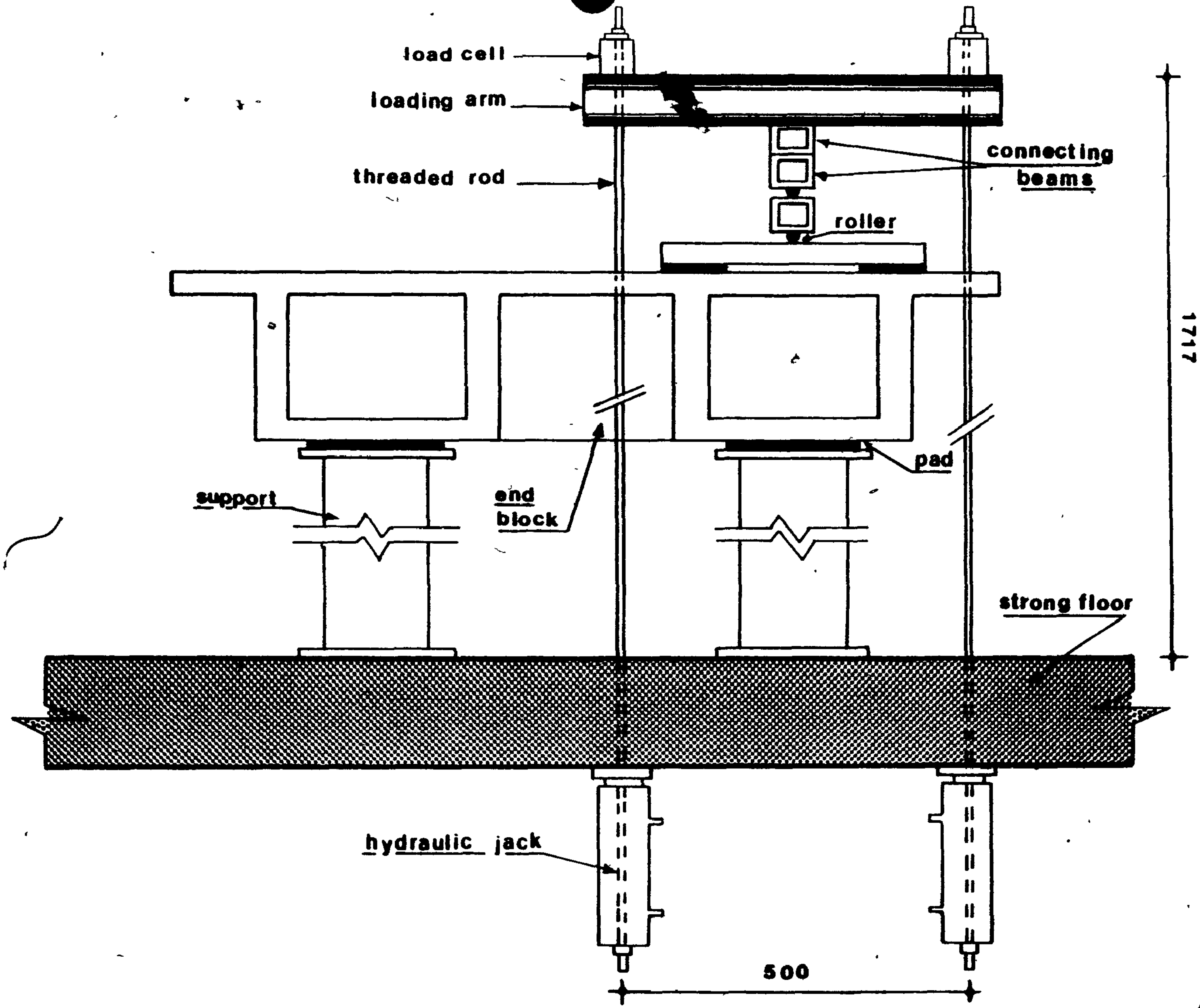

Figure 4.15 STATIC LOADING SYSTEM FOR TORSION

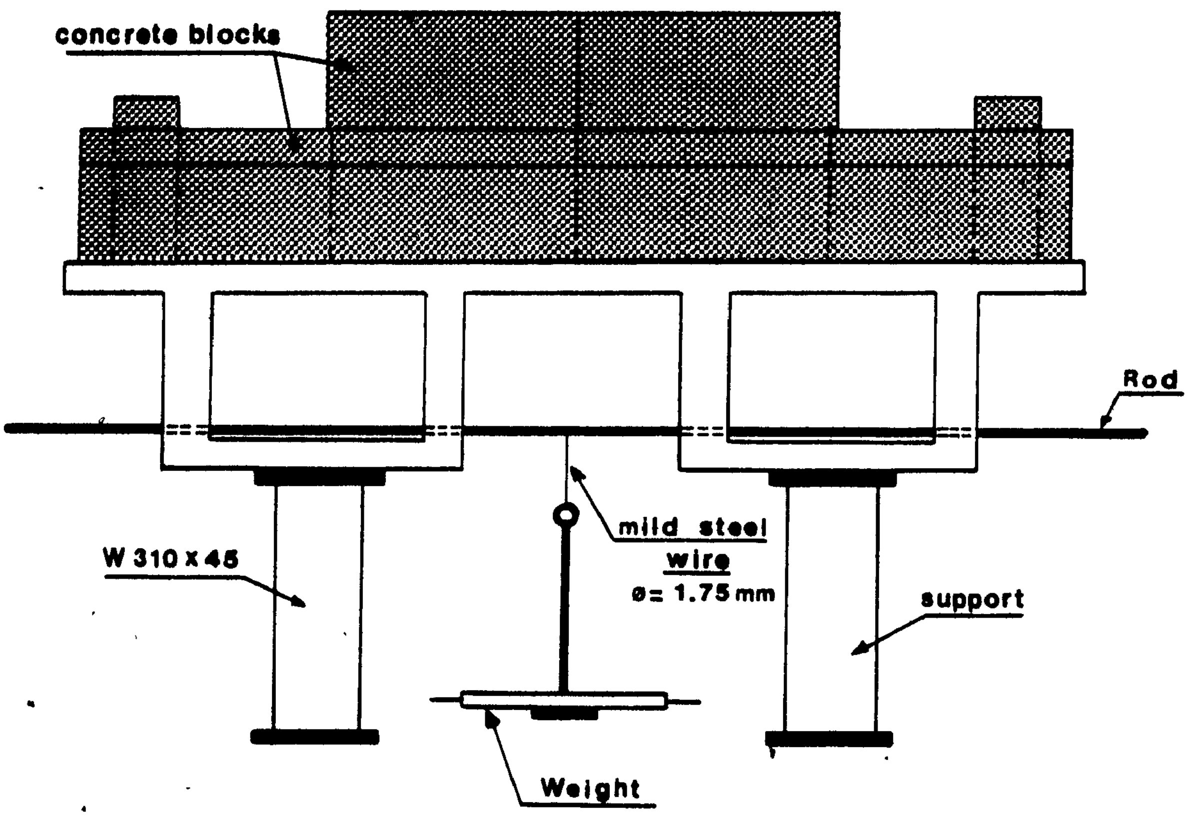

Figure 4.16 DYNAMIC LOADING SYSTEM FOR FLEXURE.

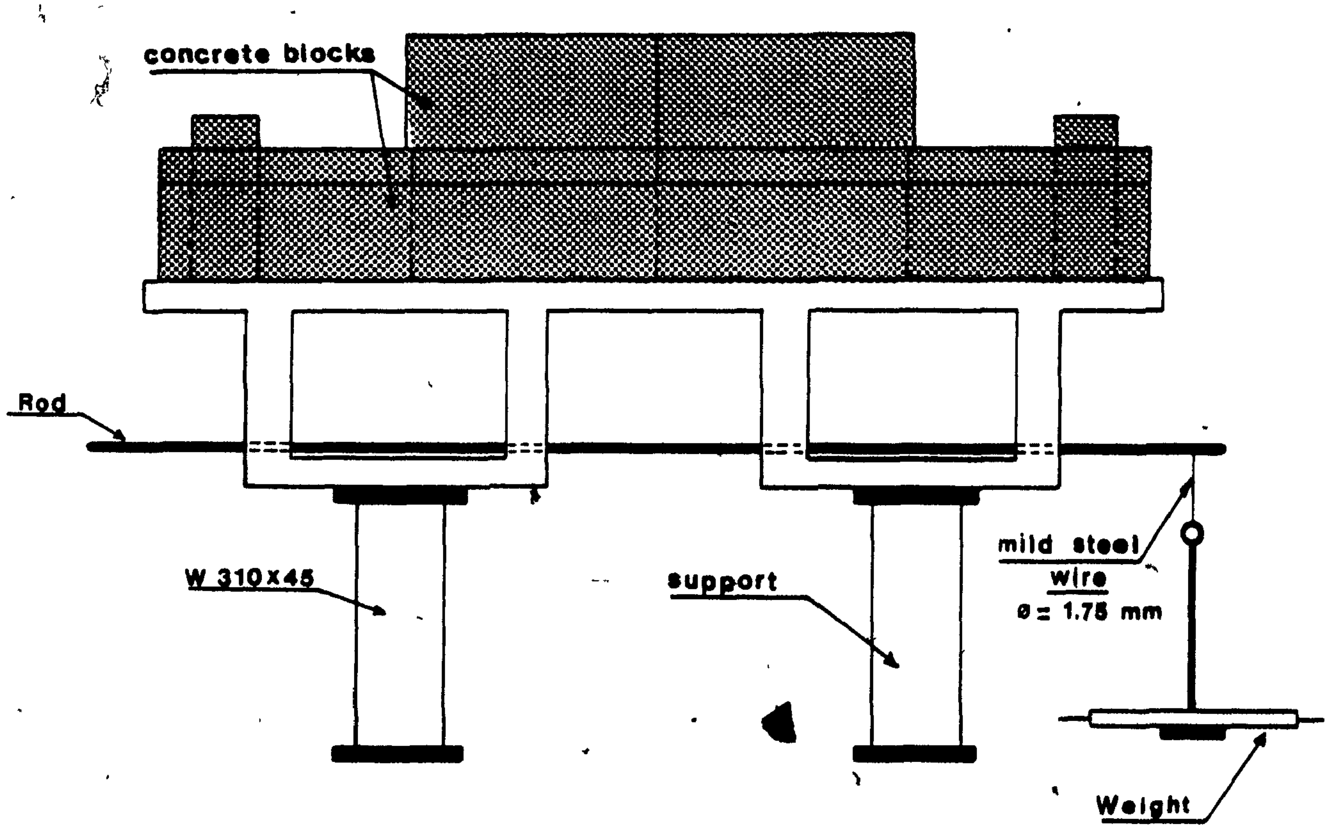

Figure 4.17 DYNAMIC LOADING SYSTEM FOR TORSION.

4.5 TESTING PROCEDURE

Static and dynamic tests were performed on the bridge model. Three different types of loads were used to study the behaviour of the structure and to trace the variation of the physical characteristics of the model bridge. The model bridge was tested under the following types of loadings:

- Concentrated load at the working load level
- Truck loading at the working load level
- Truck loading at the overload level

4.5.1 CONCENTRATED LOAD

4.5.1.1 STATIC TESTS

(1). Flexure Test: To determine the flexural stiffness of the bridge model, a concentrated load was applied at midspan at the centerline of the bridge using the loading arm and a steel plate simulating a concentrated load. The load was applied in increments of 2 kN up to a total load of 12.0 kN.

(2). Torsion Test: A load of 10.0 kN was applied at midspan at an eccentricity of 280 mm from the centerline of the model bridge in increments of 2 kN. The loading system was half the length of the one used in flexure.

The torsional stiffness of the bridge was determined from the torque-twist curve plotted using the above data.

4.5.1.2 DYNAMIC TESTS

The following tests were performed before the static tests in order to obtain the dynamic characteristics of the uncracked model bridge systme. The MINC computer was used to record the response of the L.V.D.T's.

(1) A 230 kg mass was attached to the rod at midspan at the centerline of the model bridge by a wire. To set the bridge into free vibrations, the wire are cut by a pair of pliers. The vibrations dampened rapidly.

(2) The same mass of 230 kg was suspended to the rod at midspan at an eccentricity of 560 mm from the centerline of the bridge model by a wire. To set the model into free vibrations, the wire was cut by a pair of pliers. The vibrations were dampened rapidly.

4.5.2 TRUCK LOADING AT WORKING LOAD LEVEL

4.5.2.1 STATIC TESTS

(1) Flexure Test: The two simulated OHBDC trucks were placed symmetrically on the top slab in a position to obtain the maximum bending moment. The load was applied

through the loading arm and increased in increments of 4.0 kN up to a load value of 26.4 kN corresponding to the two model truck loads. The deflection and strain measurements were recorded for each increment.

(2) Torsion Test: Only one model truck was used for this test and was placed on one box girder at a distance of 280 mm between its axis of symmetry and the centerline of the structure. The load was applied through the loading arm in increments of 2.0 kN up to a load value of 13.2 kN corresponding to one model truck load. Deflection and strain measurements were recorded after each increment.

4.5.2.2 DYNAMIC TESTS

Free vibration flexure and torsion tests were performed after the static tests. The loading procedure was similar to that presented in Section 4.5.1.2 .

4.5.3 TRUCK LOADING AT THE OVERLOAD LEVEL

4.5.3.1 STATIC TEST

Flexure tests similar to those in Section 4.5.2.1 (1) were performed with total load equal to 2, 3, 4, 5 times the two model truck loads in increments of 7 kN up to a load value of 52.8 kN, 79.2 kN, 105.6 kN, and 132.0 kN respectively. Torsion tests similar to those in Section 4.5.2.1 (2) were conducted after each flexure test mentioned above.

4.5.3.2 DYNAMIC TESTS

After each static test in Section 4.5.3.1 corresponding to 2, 3, 4, 5 times the two model truck loads, free vibration tests were performed similar to those in Section 4.5.1.2 (1) and (2).

After all of the tests in Section 4.5.3.1 and Section 4.5.3.2 were completed, the bridge model was loaded to obtain the ultimate load and the failure mode. The load was applied through the hydraulic jack in increments of 10.0 kN up to a load value of 140.0 kN corresponding to the failure laod and to 5.4 times the value of two model truck loads.

CHAPTER 5

THEORETICAL ANALYSIS

5.1 INTRODUCTION

The behaviour of prestressed concrete box girder bridges has received considerable attention over the past three decades. In particular, some governing parameters such as the torsional rigidity, warping and distortion phenomena which make the prediction of its response by the classical methods very difficult, have been examined by some investigators. However, with the present tendency to more slender sections because of the use of high strength materials and to reduce the self-weight and the use the prestressing force more efficiently, the warping and distortion effects become significant. Three different methods such as the three dimensional grillage method, the folded plate method and the finite element are commonly used to analyze the box girder systems.

The three-dimensional grillage or space frame model [14] consists of dividing the structure into longitudinal beam elements along the girder lines and transverse bending frames at discrete intervals. The accuracy of the method improves with the number of members in frame.

The folded plate method [34] consists of dividing the structure into a series of rectangular plates interconnected along their longitudinal joints. The loads applied to the structure are divided into a series of harmonic loads along the joints. The response of the bridge is obtained by superposition of the individual harmonic loading cases. The folded plate model is particularly adequate for investigaton of linear behaviour of straight or curved box girder bridges with simple end supports.

The finite element method is perhaps the most versatile method for solving the problem in its more general and complex form. It can be used for arbitrary loadings and boundary conditions. The accuracy of the analytical results compared with the experimental results improves considerably if the analytical model, the element type, and the fineness of the mesh are chosen properly.

With the development of high speed computers, a number of finite element analysis programs have been developed making the analytical model more powerful. Two programs were used in this investigation to determine the static and dynamic response of the box girder bridge : the quasi-nonlinear analysis using the commercially available SAP IV program and the nonlinear analysis using the NonLinear Analysis of Concrete and Steel structure program (NONLACS). A brief outline of analytical model is presented in this thesis with more details presented in Reference [21].

5.2 FINITE ELEMENT ANALYSIS

The finite element method is perhaps the most versatile method of solution available for the analysis of single or multi-cell box girder bridges of arbitrary plan geometry [37]. It can be used for any given geometry, loading and boundary conditions. The finite element method involves the discretization of the structure into finite shell or plate elements which retain the properties of the entire system representing the structure. Properties of these elements are determined and finally all separate elements are reassembled, interconnected at discrete nodal points to represent the original structure. The method is approximate and its accuracy is dependent on the fineness of the subdivision used in dividing the structure into finite elements.

Bathe, Wilson and Peterson developed the SAP IV program at the University of California [3] to run on mainframe computers. The SAP IV program is a structural analysis program for linear systems to obtain the static and dynamic responses of different kinds of structures.

The NONLACS (NonLinear Analysis of Concrete and Steel structures) program was developed by Razaqpur and Nofal at Carleton University [32]. It is an improved version of the FELARC (Finite Element Layered Analysis of Reinforced Concrete) program developed by Ghali and Ghoneim at University of Calgary [17]. The NONLACS program can analyse reinforced and prestressed concrete, steel and composite structures. The program uses the tangent stiffness approach through a series of incremental linear analyses. It can be used to trace the complete response of a reinforced or prestressed concrete structure up to failure. Experimental and analytical studies were conducted for the box girder bridge model.

5.2.1 LINEAR ANALYSIS

The SAP IV program was used for linear analysis of the following two loading cases: a concentrated load and a model truck load. The box girder bridge was idealized by two types finite elements : the thin shell and the three-dimensional truss elements provided in the SAP IV program. The thin shell element is a quadrilateral element of arbitrary geometry formed from four compatible triangles and has six interior degrees of freedom at each node. The three-dimensional truss element was used to represent the prestressing wire and consisted of a one-dimensional member possessing only axial stiffness. The finite element idealization of the box gider bridge model is shown in Figure 5.1.

5.2.1.1 RESPONSE UNDER STATIC LOADING

Finite element analysis was conducted for the self

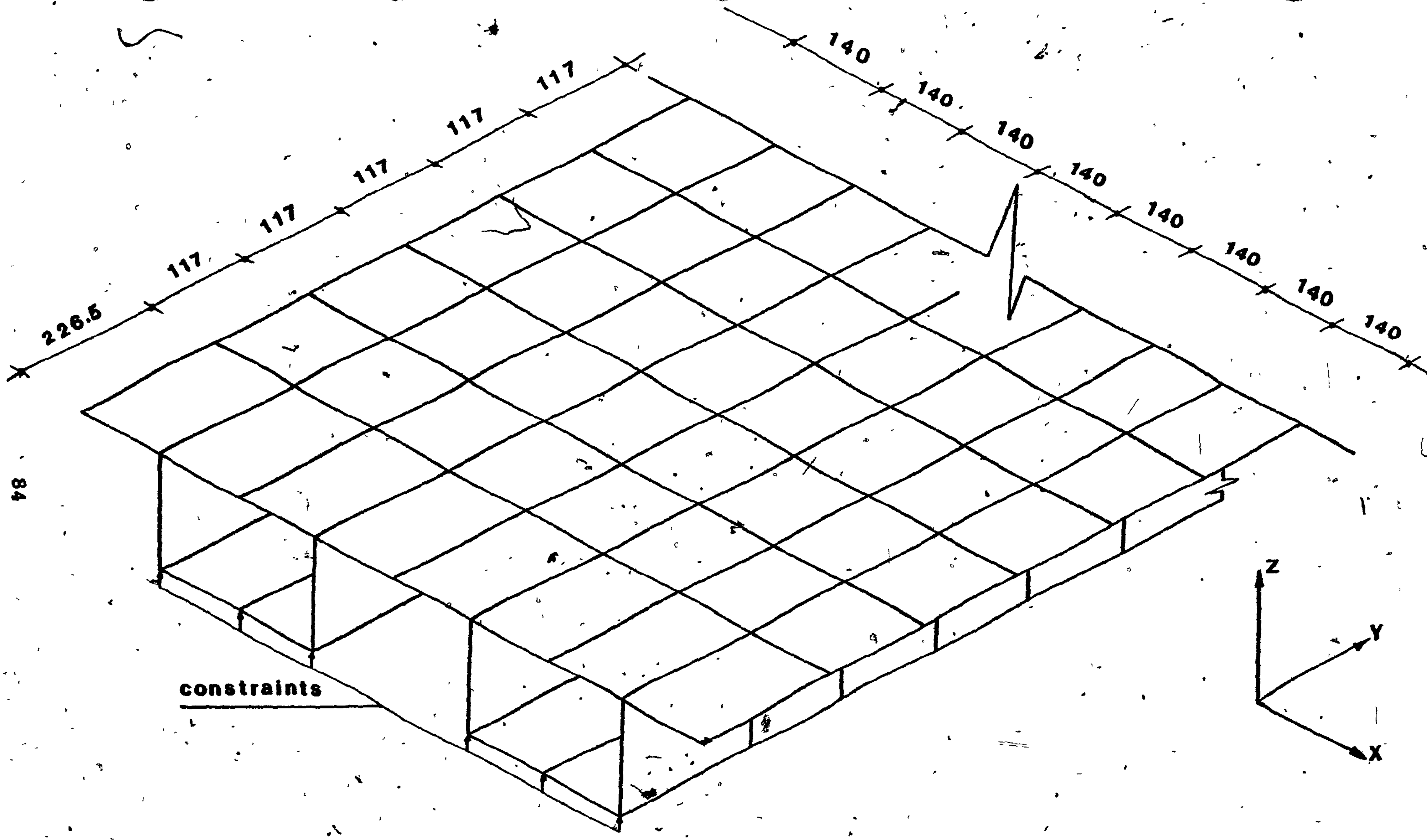

Figure 5.1 FINITE ELEMENT IDEALIZATION OF THE MODEL BRIDGE FOR THE SAP IV PROGAM

weight of the bridge model and the extra dead load used to simulate the dead weight of the prototype, in addition to the following loading conditions:

(i) Flexure tests: (a). A concentrated load placed at midspan at the centerline of the bridge model.

(b). Two scaled OHBDC truck loads placed in order to cause the maximum deflection.

(ii) Torsion tests: (a). A concentrated load at midspan at an eccentricity of 280 mm from the centerline of the bridge model.

(b). One scaled OHBDC truck load was placed on one box girder at a distance of 280 mm between its axe of symmetry and the centerline of the structure.

5.2.1.2 RESPONSE UNDER DYNAMIC LOADING

Dynamic analysis was conducted for the uncracked structure in order to determine the natural frequencies and the system modal shapes.

5.2.2 QUASI-NONLINEAR ANALYSIS

The quasi-nonlinear analysis was conducted using the SAP IV program. The quasi-nonlinear analysis introduced by Soliman [38], provides a suitable inexpensive tool for analysing bridges in the post-cracking range. The analysis was conducted by incorporating the experimental data on the number, length and orientation of cracks in developing the elasticity matrix for each element. This elasticity matrix, attributed to an uncracked element in the SAP IV program, was modified for the cracked condition to take into account the non-linearities inherent in the materials. For a cracked element in its local axis, the modified elasticity matrix was obtained from the uncracked element matrix by reducing the modulus of elasticity perpendicular to the crack, neglecting the Poisson's ratio and also by lowering the shear modulus using a reduction factor β which accounted for the crack width. The modified elasticity matrix was then transformed to the global axes. The idealization of the box girder bridge is similar to the one used for the linear analysis in Section 5.2.1. More details of the quasi-nonlinear analysis are given in Reference [21]. In order to obtain the static and dynamic responses, the SAP IV program, including the modified matrix was run for two loading cases:

5.2.2.1 RESPONSE UNDER STATIC LOADING

Analyses for flexural tests were performed at different loading levels corresponding to 2, 3, 4, and 5 times the two scaled OHBDC truck loads. The analysis for torsional tests was conducted after each loading case in the analysis for flexural tests.

5.2.2.2 RESPONSE UNDER DYNAMIC LOADING

Dynamic analyses were also performed to determine the natural frequencies and the mode shapes of the structure after each flexural test mentioned in Section 5.2.2.1.

5.2.3 NONLINEAR ANALYSIS

The NONLACS (NonLinear Analysis of Concrete and Steel structures) program was used to trace the complete response of the structure up to failure. Using the tangent stiffness approch through a series of incremental linear analysis, each finite element is divided into a number of concrete and smeared steel layers. Individual layers are assumed to respond as an orthotropic material that can assume any state : elastic, yielded, cracked or crushed, depending on the stress level in the layer. The element stiffness is obtained by assuming the stiffness contributions of the various layers. Prestressing wires or heavy reinforced bars are idealized as fully bonded truss elements. The stiffness matrix is calculated using numerical integration which permits partial degradation of the stiffnesss of an element due to cracking, yielding or crushing. For the flexural truck loadings, only one half of the bridge was modelled for the analysis because of the symmetry of both the geometry and the external loads. This resulted in considerable time savings. The finite element idealization was achieved by using four nodes facet quadrilateral sheel element. The idealization of the box girder bridge model is shown in Figure 5.2. The analysis for the flexural loading was conducted using the NONLACS program at Carleton University. In this analysis, the load was increased monotonically from zero load corresponding to no live load to 139.0 kN corresponding to 10.5 times the truck model loads in 20 load steps. Each load step required 10 iterations. At the load step corresponding to 5 times the two scaled OHBDC truck loads, the structure was severely damaged and the steel had yielded. The analysis was terminated at this stage.

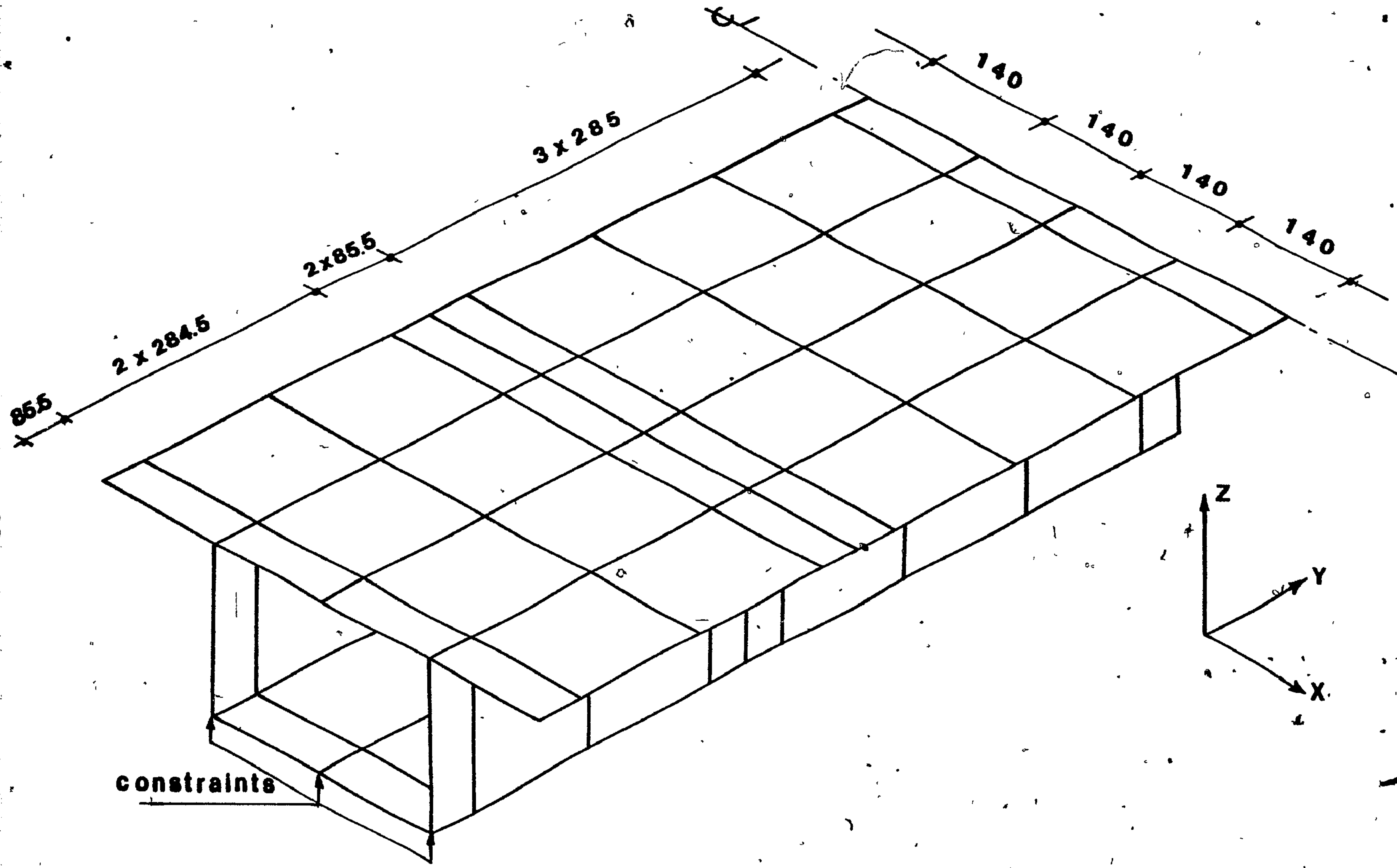

Figure 5.2 FINITE ELEMENT IDEALIZATION OF THE MODEL BRIDGE FOR THE NONLACS PROGRAM

CHAPTER 6

DISCUSSION OF TEST RESULTS

6.1 INTRODUCTION

This chapter presents discussion of the experimental data obtained from the tests on the box girder bridge model. The experimental data have been compared at the various load levels with the analytical results computed using the finite element programs (SAP IV, NONLACS) which are presented in detail in Reference [21].

This chapter consists of two parts: static tests and dynamic tests presented in Sections 6.2 and 6.3, respectively. The static tests on the bridge model was conducted under concentrated load at midspan where only vertical deflections were recorded and under the OHBD Code truck loading at the working and the overload levels and deflections and strains in steel and concrete were recorded. The dynamic tests consisted of flexural and torsional free vibration tests at the working and the overload levels. The period of vibration and the damping ratio were determined from each L.V.D.T data and were compared with the analytical results obtained from the finite element programs.

a) Bridge Model Ready for Test.

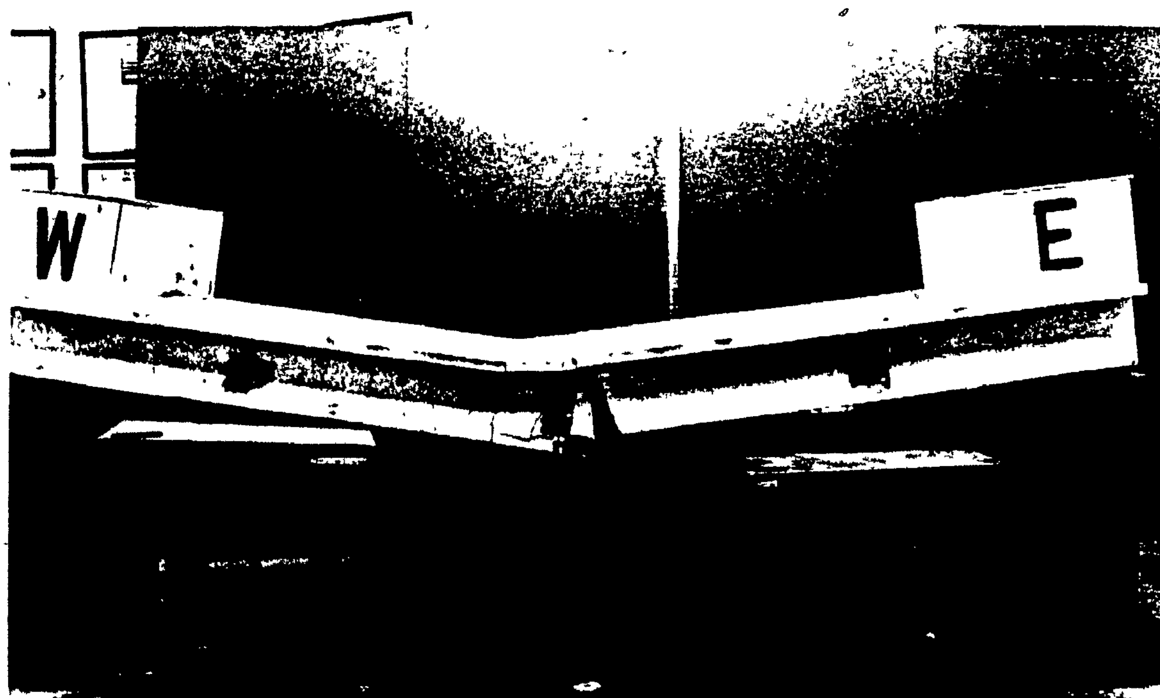

b) Bridge Model After Failure (Ultimate Load Test)

Figure 6.1 BRIDGE MODEL.

6.2 STATIC TESTS

After releasing the prestressing wires, the central camber of the model bridge was observed to be 1 mm as shown in Fig.6.1 (a). This was due to the upward force exerted by the prestressing wire on the structure at the harping point located at midspan. Also, from the initial concrete strain readings, it was noted that the bridge model was entirely in compression.

6.2.1 CONCENTRATED LOAD AT MIDSPAN

The model bridge was tested under a concentrated load at midspan in order to determine the flexural and torsional stiffness.

6.2.1.1 FLEXURE TEST

The concentrated load was located at midspan at the centerline of the bridge model. It was applied in increments of 2.0 kN up to a total load of 12.0 kN. Deflections were recorded and the resulting load-deflection curve is shown in Figure 6.2. The behaviour of the bridge model was linear. The flexural stiffness worked out to be 23.53 kN/mm. Using the linear SAP IV program, a load-deflection curve for a concentrated load at midspan was determined. The analytical flexural stiffness was found equal to 24.05 kN/mm. The two results show excellent agreement.

6.2.1.2 TORSION TEST

For the torsion test, a concentrated load was located at midspan of the bridge model at an eccentricity of 280 mm from the centerline of the bridge. The load was applied in increments of 2.0 kN up to a total load of 10.0 kN. The torque-midspan twist curve resulting from the test is shown in Fig.6.3. The torsional stiffness of the bridge model obtained from the experimental results worked out to be 17430 kN.m/rad and the analytical torsional stiffness was found equal to 22683 kN.m/rad. The linear SAP IV program overestimated the torsional stiffness by about 23 % . This difference is due to the underestimate of the stiffness of the bridge model in the computer analysis based on a Young's modulus of elasticity as obtained from the ~~standard~~ cylinder tests.

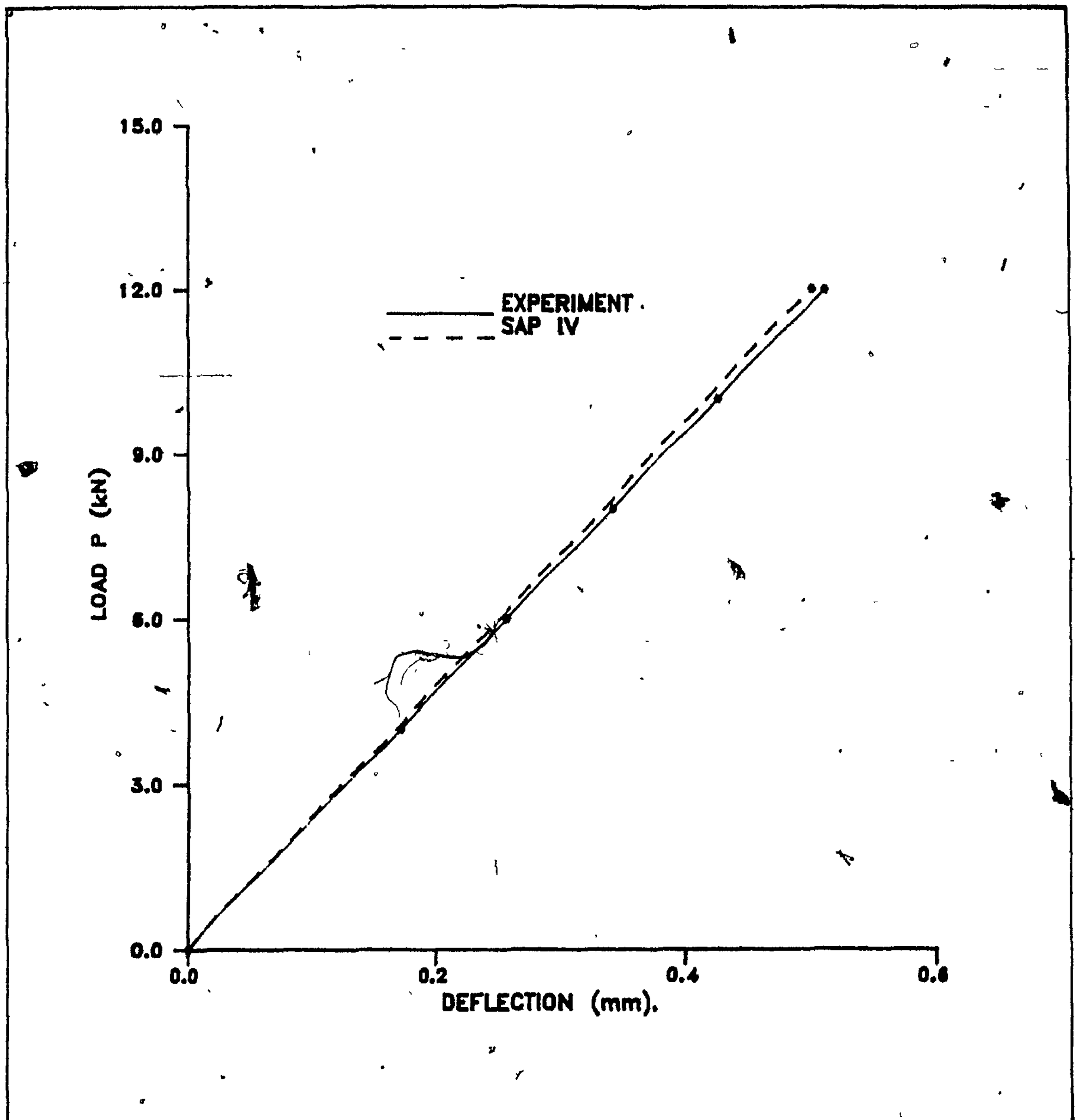

Figure 6.2 LOAD-MIDSPAN DEFLECTION CURVE (CONCENTRATED LOAD AT MIDSPAN).

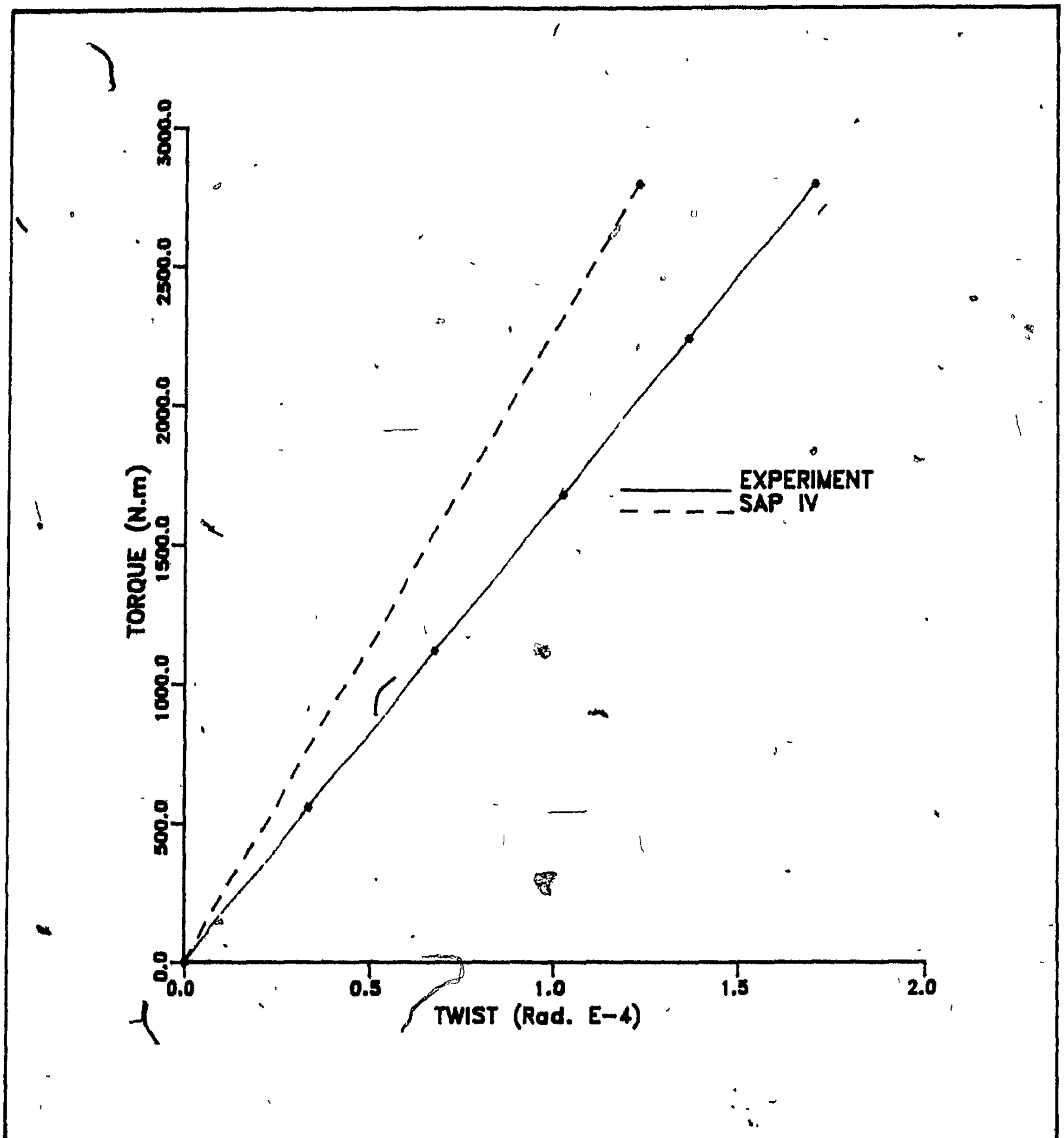

Figure 6.3 TORQUE MIDSPAN TWIST CURVE
(ECCENTRIC LOAD AT MIDSPAN)

6.2.2 TRUCK LOADING AT WORKING AND OVERLOAD LEVEL

Flexural tests were performed using the simulated model trucks placed on the bridge model in such a way as to create the maximum deflection. The flexural tests corresponded to 2, 3, 4 and 5 times two scaled Ontario Highway Bridge Design Code truck loads. The load was applied in average increments of 6.0 kN up to the desired load value . However, after each flexural test mentioned in Section 6.2.2, a torsional test was conducted using only one model truck in increments of 2.0 kN up to a total load value of 10.0 kN. To determine the failure mode, a flexural test was performed on the bridge model up to a load equal to 5.5 times the two scaled OHBDC trucks until failure.

6.2.2.1 DEFLECTIONS

Deflections were recorded for each loading case and the load-deflection curves were plotted. These load-deflection curves represent the average deflections of the bottom slab. The resulting data are shown in Figures 6.4 through 6.9. From the initial slope of these curves, the flexural stiffness of the bridge was determined for each specific loading case mentioned above. The variation of the flexural stiffness of the bridge model is tabulated in Table 6.1.

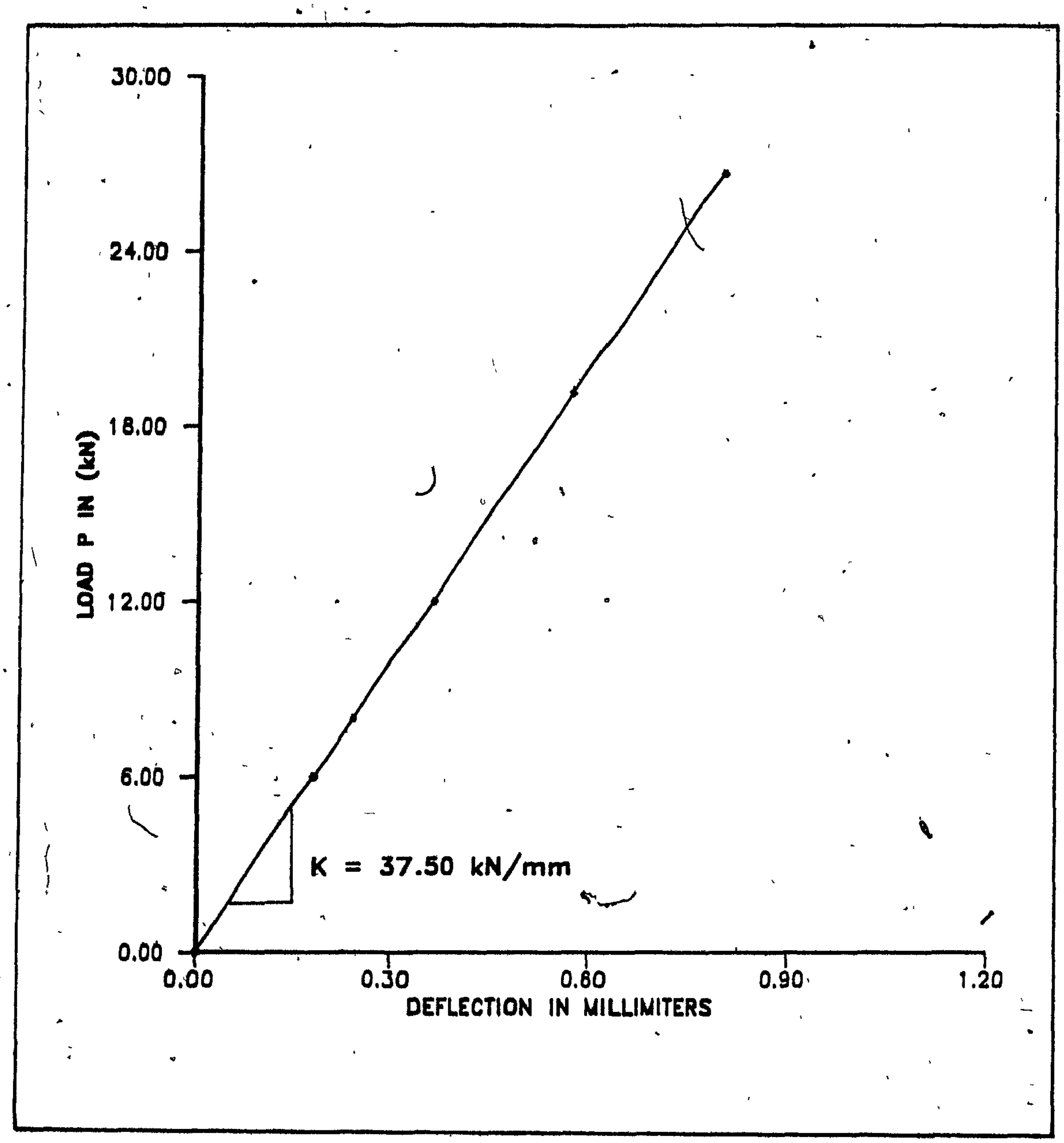

Figure 6.4 LOAD-DEFLECTION CURVE UNDER TWO TRUCK LOADS.

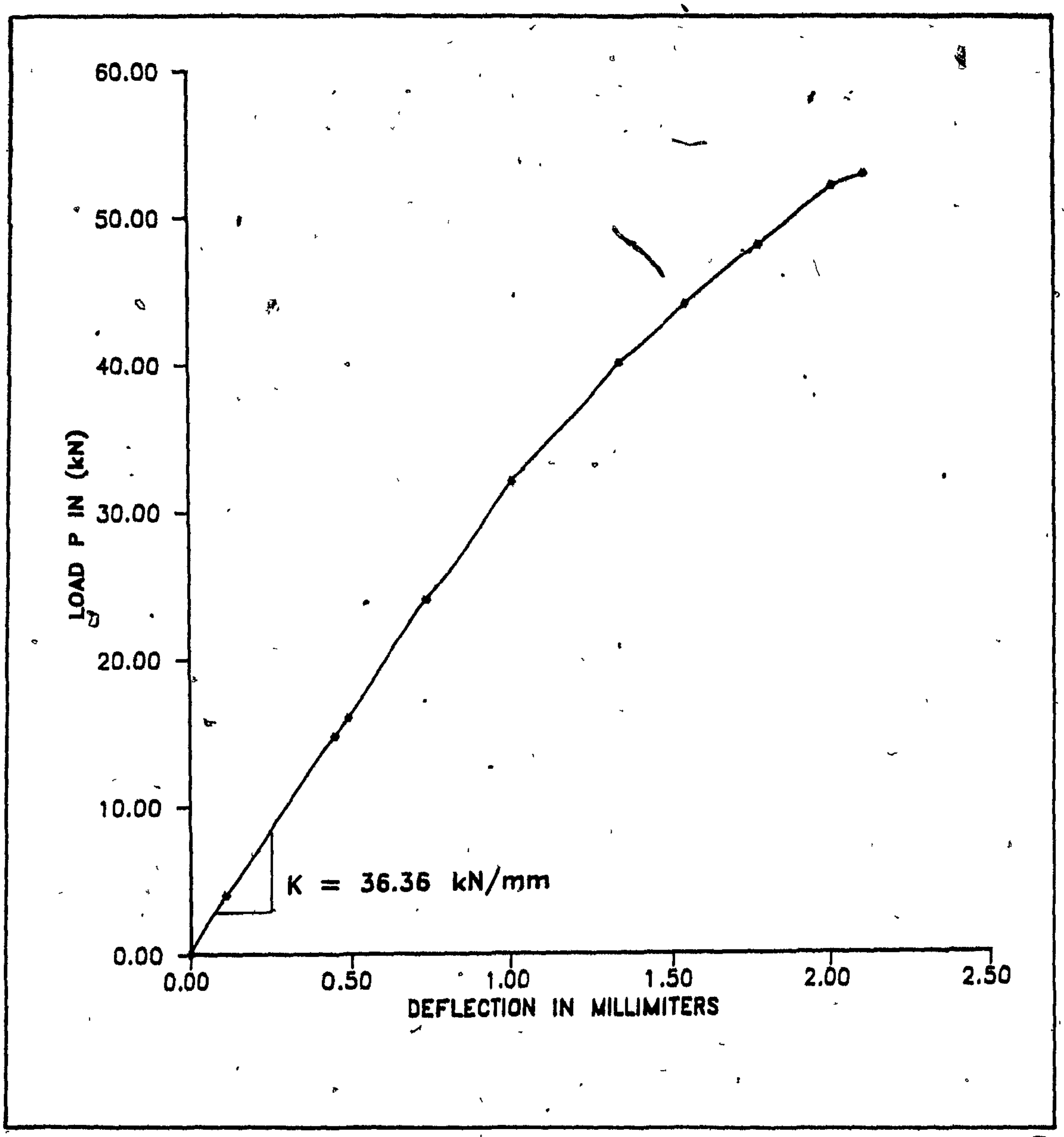

Figure 6.5 LOAD-DEFLECTION CURVE UNDER FOUR TRUCK LOADS.

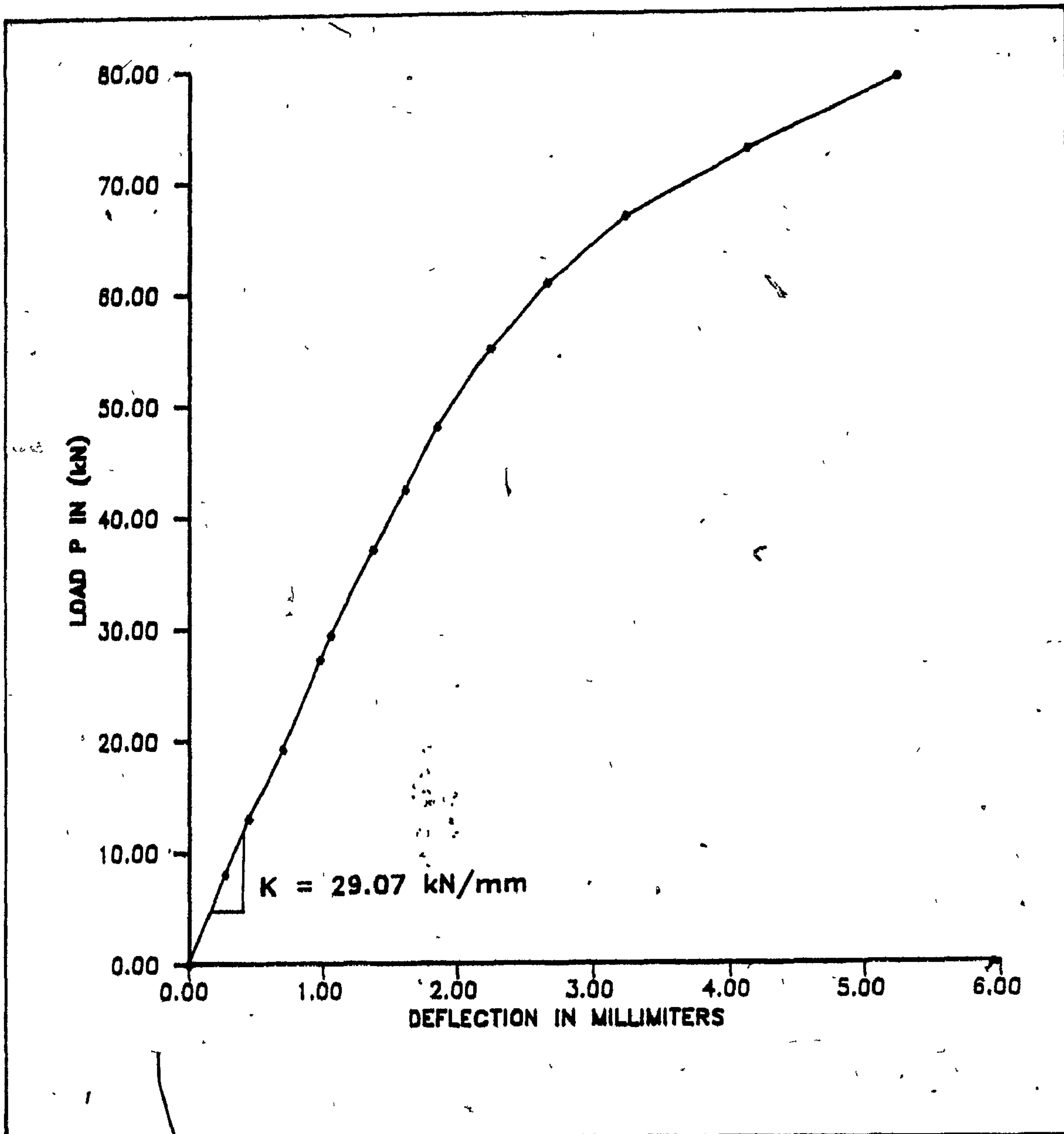

Figure 6.6 LOAD-DEFLECTION CURVE UNDER SIX TRUCK LOADS.

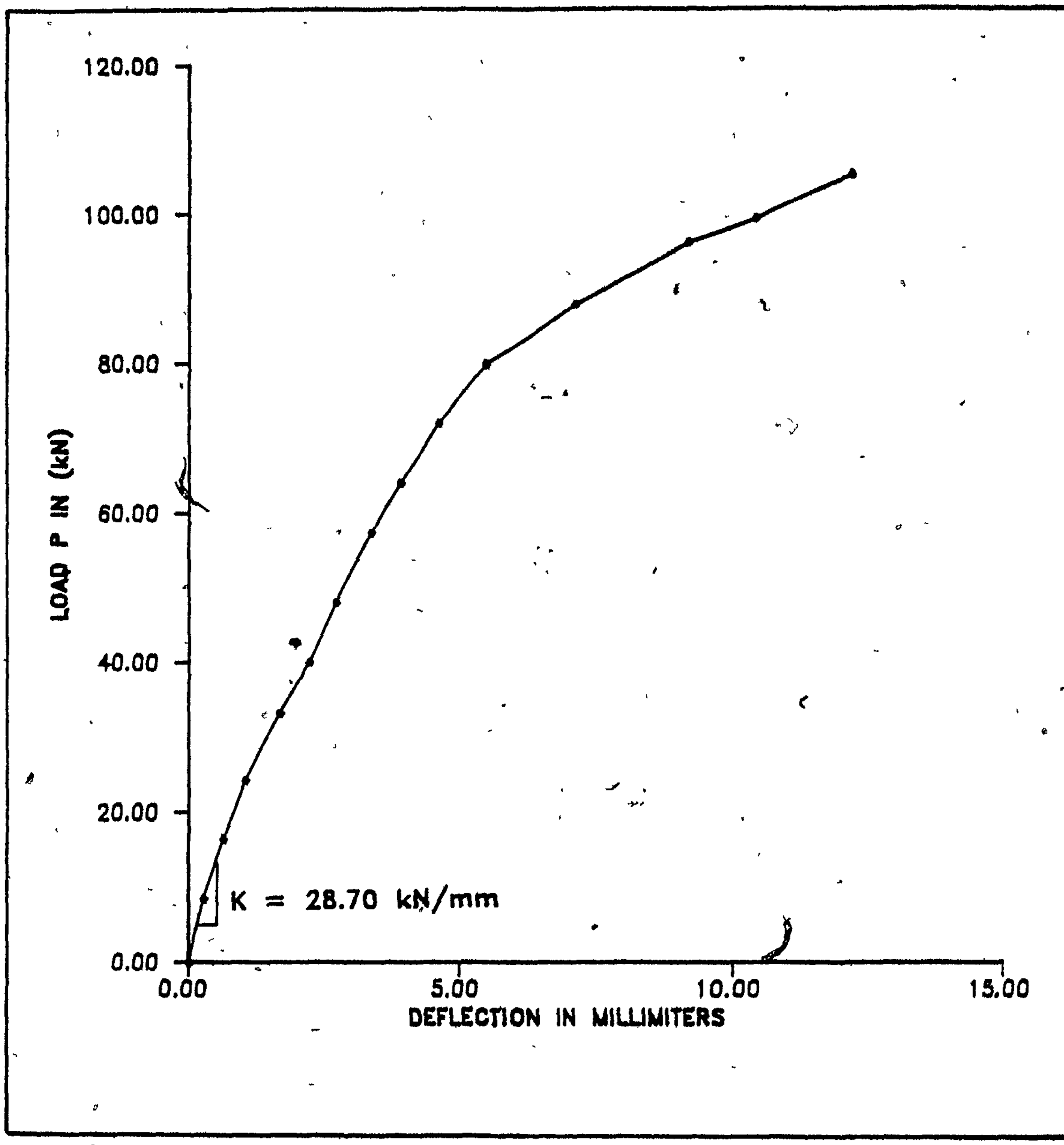

Figure 6.7 LOAD-DEFLECTION CURVE UNDER EIGHT TRUCK LOADS.

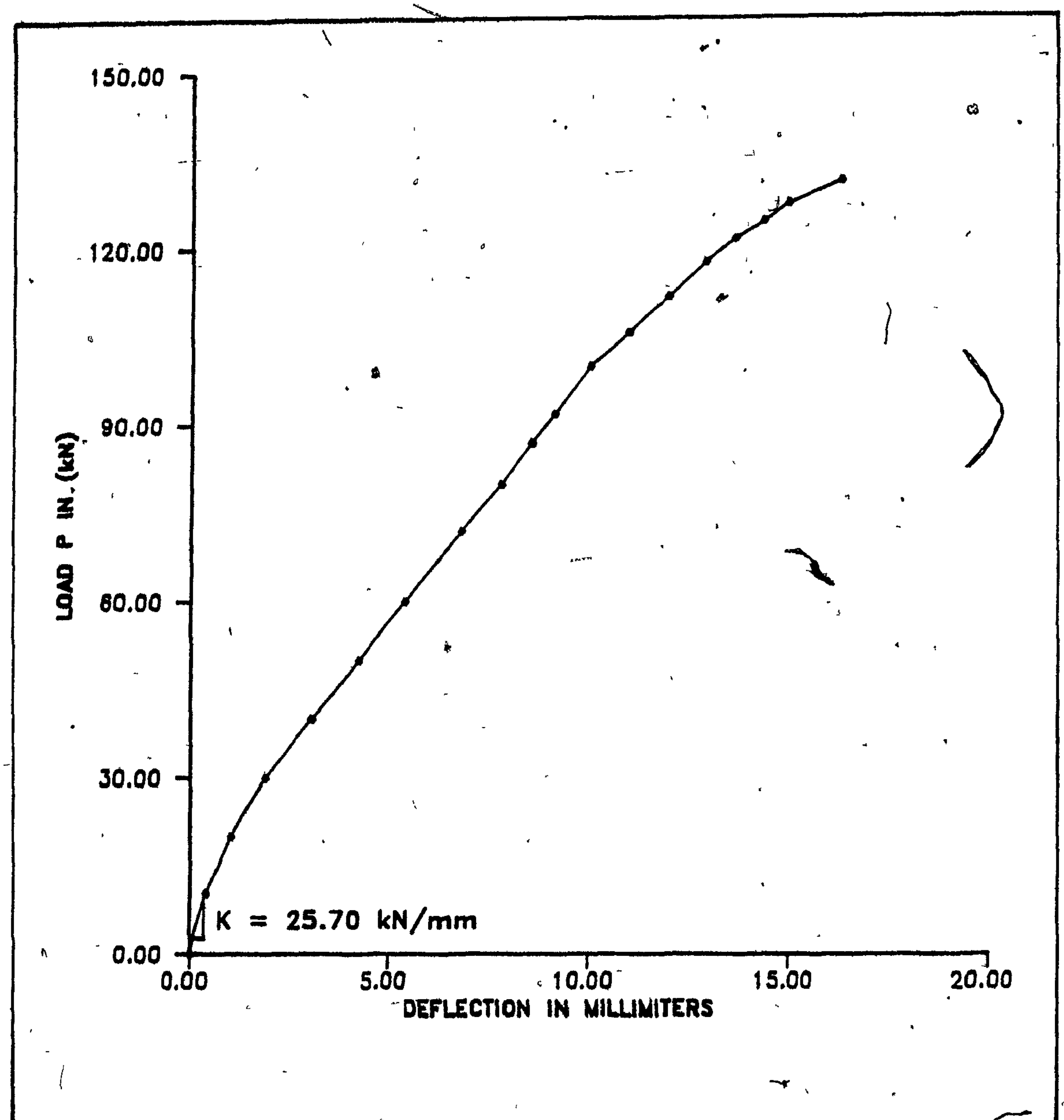

Figure 6.8 LOAD-DEFLECTION CURVE UNDER TEN TRUCK LOADS.

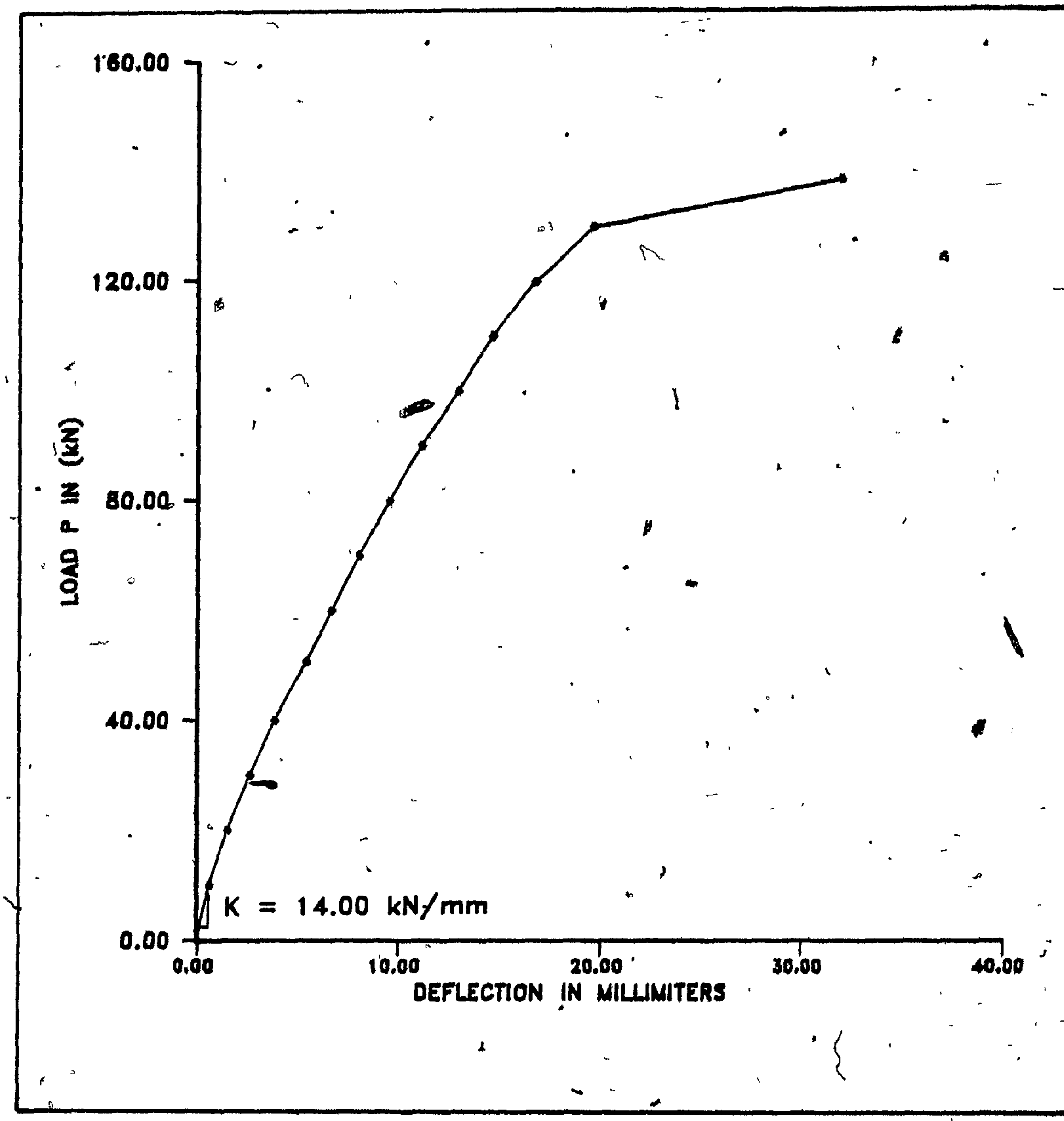

Figure 6.9 LOAD-DEFLECTION CURVE UNTIL FAILURE.

During the last test corresponding to a load level of 10.5 times the OHBDC truck load, the bridge model failed and the flexural stiffness of the structure decreased considerably. A large crack appeared at midspan along the width of the structure which can explain the cause of the sudden drop of the flexural stiffness of the bridge model. At this stage, the structure was severely damage, with a large number of cracks in the bridge model. According to the strain readings, the prestressing wires had yielded. The midspan deflection was equal to 32.10 mm which represented a deflection/span ratio of 1/110. The failure mode of the bridge model was flexural as shown in Fig.6.1 b).

The experimental and the analytical results were compared for the torsion tests performed after each flexural test. The SAP IV program was used for the analysis. The torque-twist midspan curves for the uncracked structure, after 6 truck loads, after 10 truck loads are shown in Figures 6.10, 6.11 and 6.12, respectively. Also, the variation of the experimental and analytical torsional stiffness is summarized in Table 6.2. The difference between the experimental and the analytical torsional stiffnesses decreases while the number of the flexural truck loadings increases. This is basically due to the quasi-nonlinear analysis using the SAP IV program which take into account, the number, the length and the width of the cracks in the structure after each flexural test for each analysis.

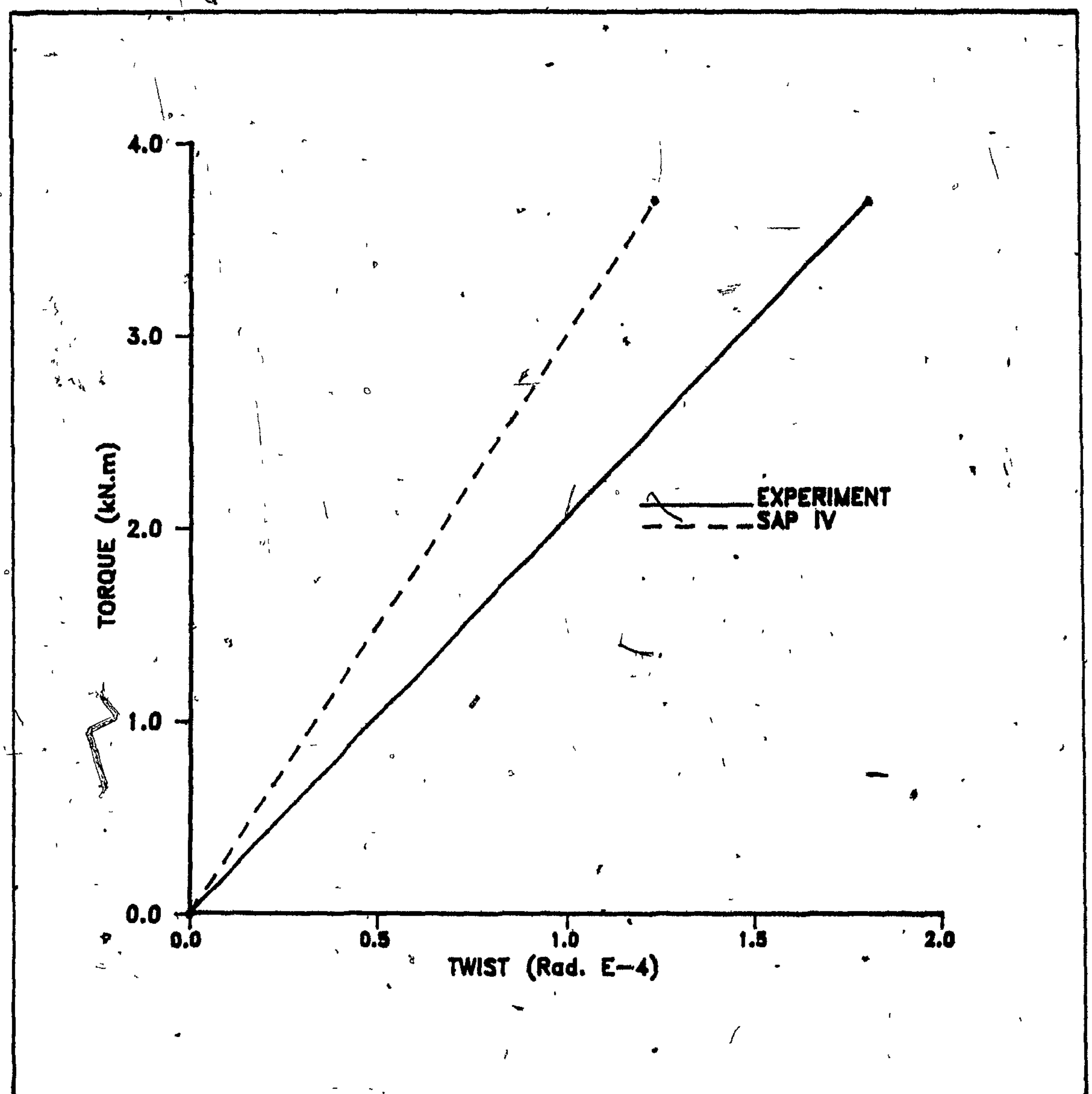

Figure 6.10 TORQUE- MIDSPAN TWIST CURVE
(UNCRACKED STRUCTURE)

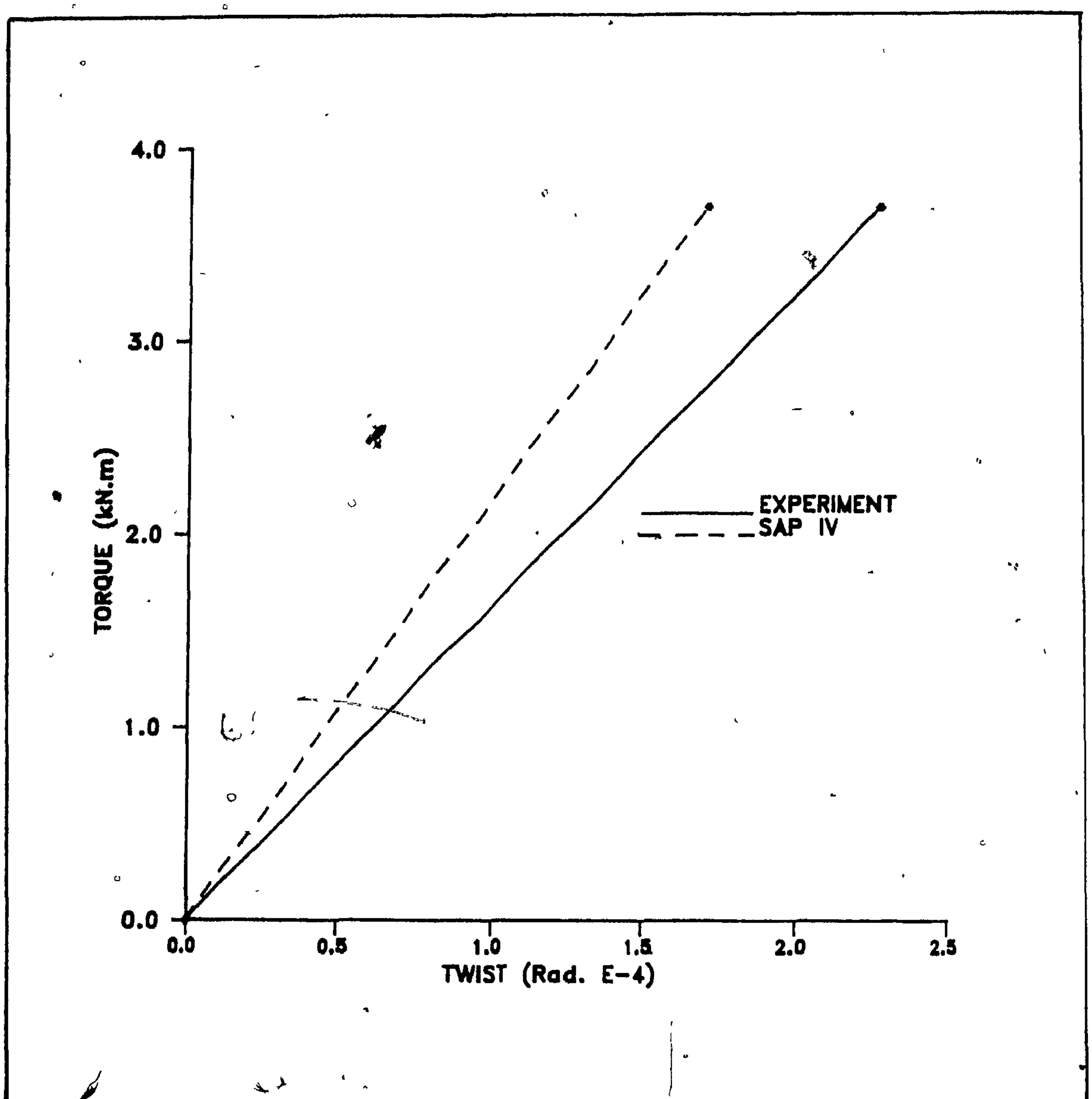

Figure 6.11 TORQUE MIDSPAN TWIST CURVE
AFTER SIX TRUCK LOADS.

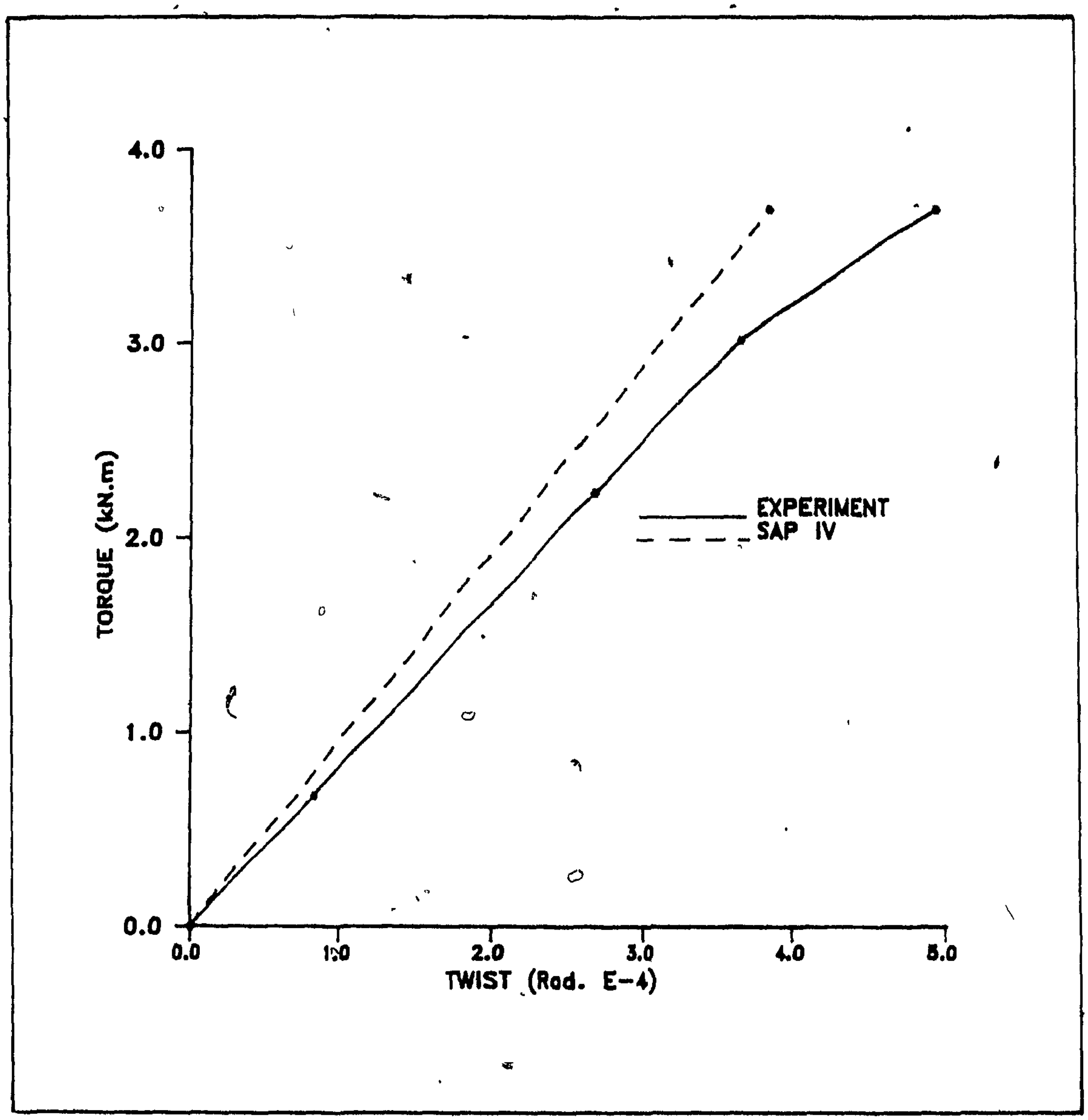

Figure 6.12 TORQUE MIDSPAN TWIST CURVE
AFTER TEN TRUCK LOADS.

NUMBER OF TRUCKS	FLEXURAL STIFFNESS (kN/mm)	PERCENTAGE OF THE STIFFNESS OF THE UNCRACKED SECTION
0	37.50	100.00
2	36.40	97.10
4	29.10	77.60
6	28.70	76.50
8	25.50	68.00
10	14.20	37.90

TABLE 6.1 VARIATION OF THE FLEXURAL STIFFNESS.

NUMBER OF TRUCKS	EXPERIMENTAL TORSIONAL STIFFNESS (kN.m/rad)	SAP IV TORSIONAL STIFFNESS (kN.m/rad)	DIFFERENCE (%)
UNCRACKED	20555	30081	31
4	18317	25874	29
6	16300	21765	25
8	10098	11821	14
10	8297	9610	13

TABLE 6.2 VARIATION OF TORSIONAL STIFFNESS.

The SAP IV program gave a difference of 30 % in the torsional stiffness for the uncracked structure program compared with the experimental data. At this stage, some microcracks had appeared in the structure, however, they could not be detected and taken into account in the analysis.

Comparison of the experimental results and the analytical results are showned in Figures 6.13 and 6.14. Under two truck loadings, the experimental deflection values were noted to be in good agreement with both finite element analyses (difference of approximately 7 %).

Figure 6.13 shows that both analytical models are stiffer than the physical model below a load value of 48.0 kN corresponding to the 1.82 two truck loadings. Above this value, the analytical model (NONLACS) was stiffer than both the experimental model and the SAP IV program model.

Figure 6.14 shows that under eight truck loadings, corresponding to a load value of 105.60 kN, the resulting deflection of the NONLACS model was 25 % lower that the experimental value. At an applied load equal to 132.0 kN corresponding to 5 times the two truck loads, the NONLACS model resulted in a deflection approximately 30 % lower than the experimental value while the SAP IV program value was 25 % higher than the experimental one.

Figures 6.15 and 6.16 show comparison of vertical deflections of the bridge model under 2 and 8 truck loadings and reasonable agreement was obtained between the NONLACS

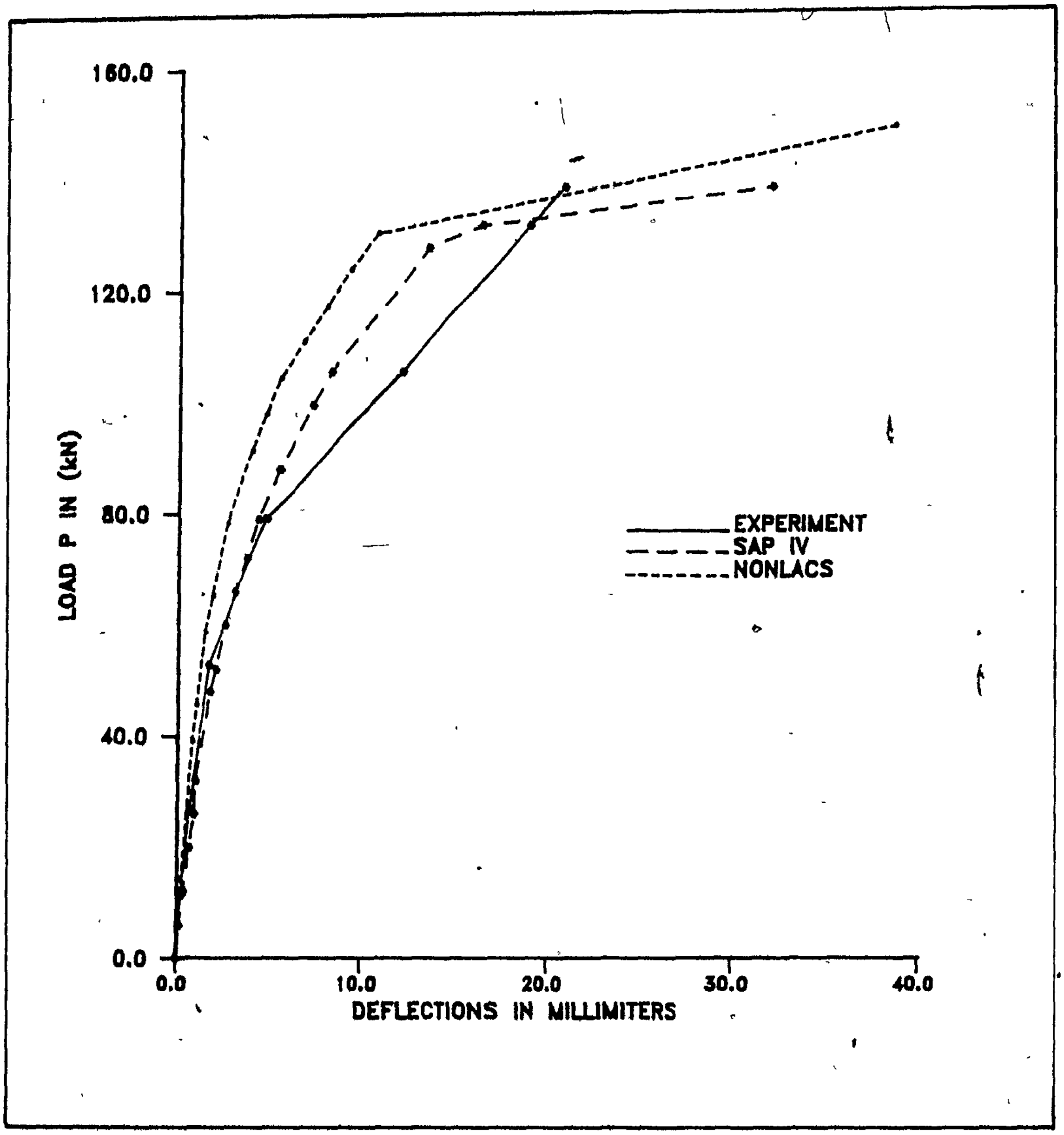

Figure 6.13 COMPARISON OF LOAD-DEFLECTION CURVES.

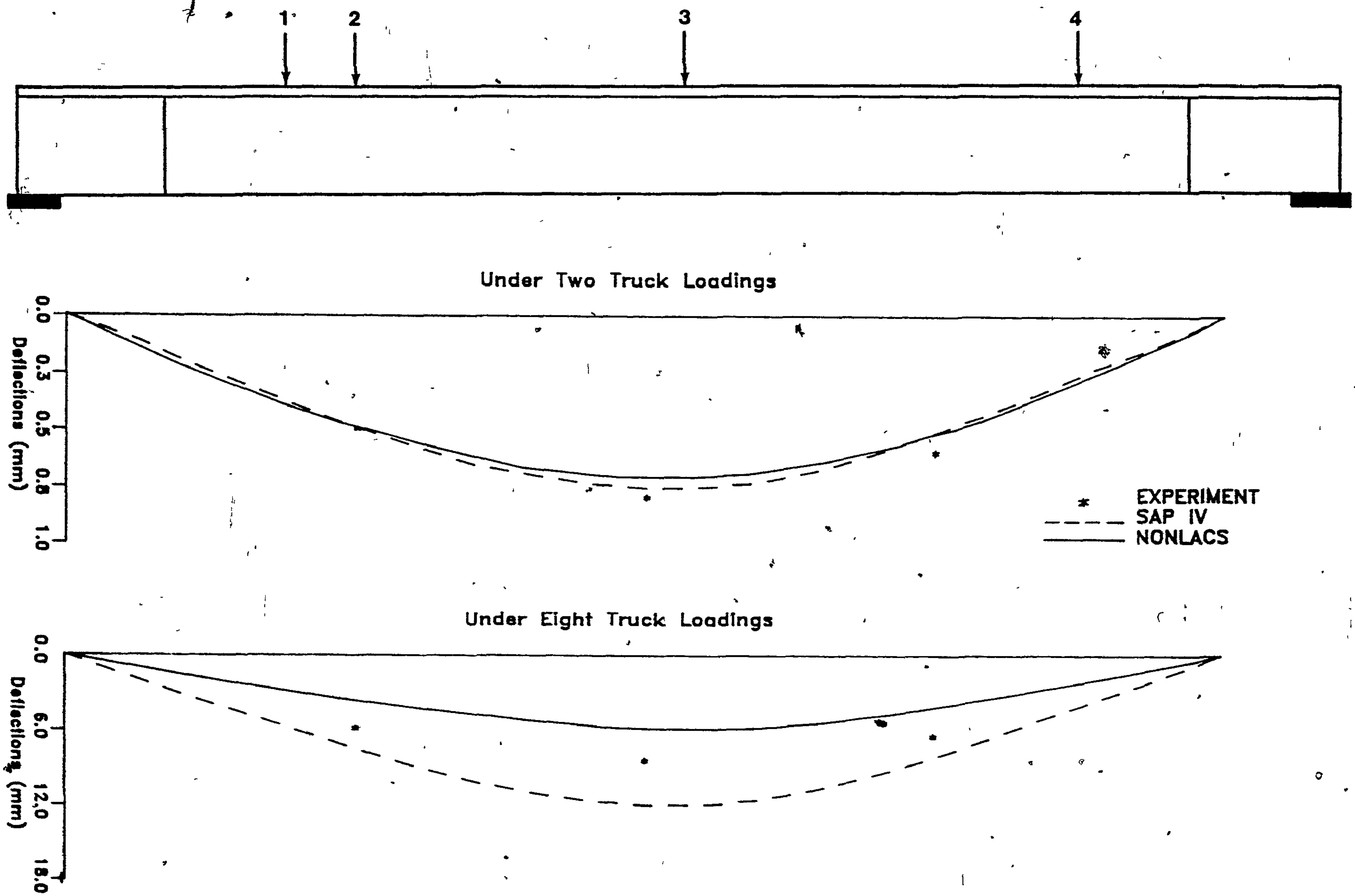

Figure 6.14 VERTICAL DEFLECTIONS ALONG THE SPAN

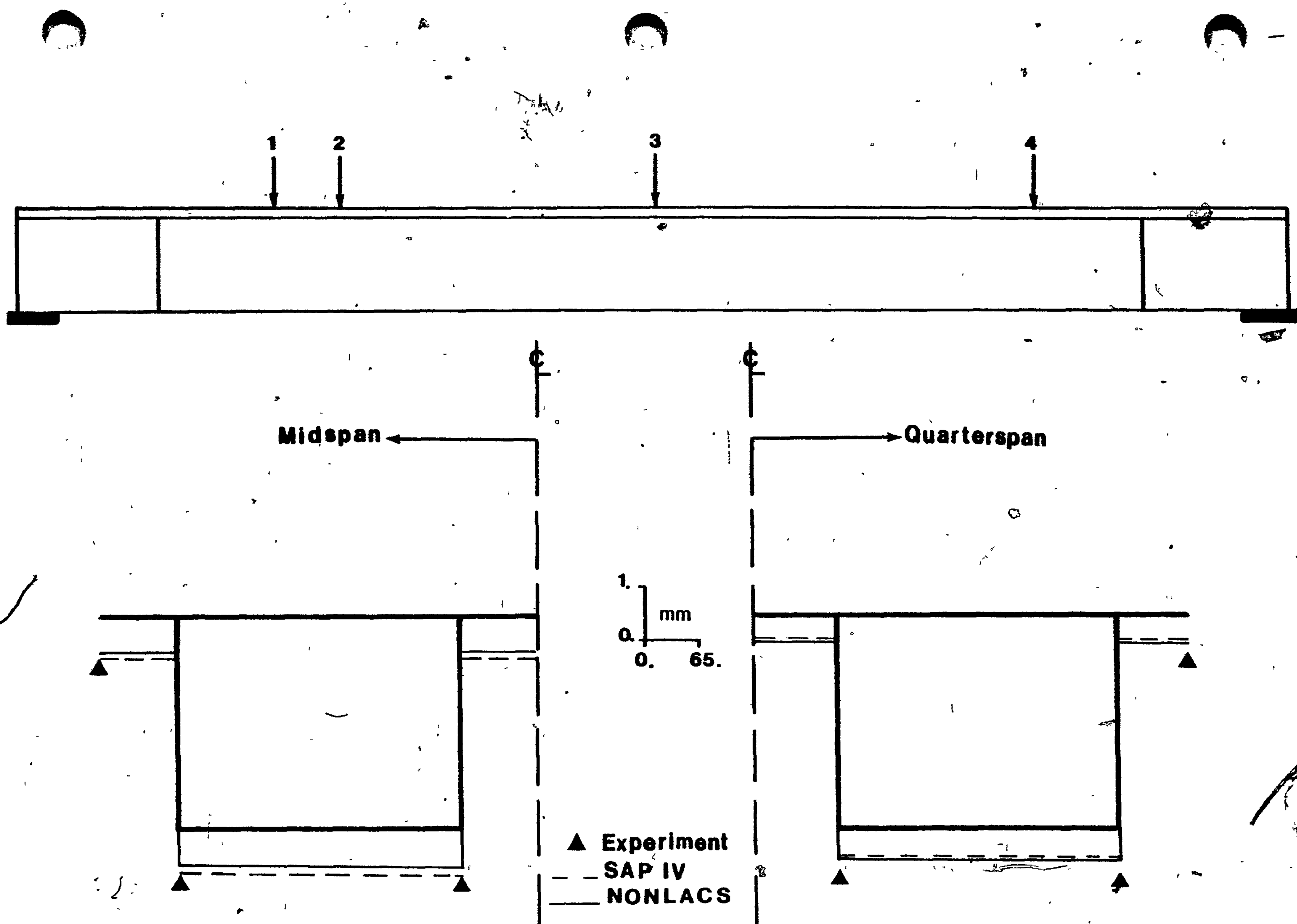

Figure 6.15 COMPARISON OF VERTICAL DEFLECTIONS OF THE BRIDGE MODEL (TWO TRUCK LOADINGS)

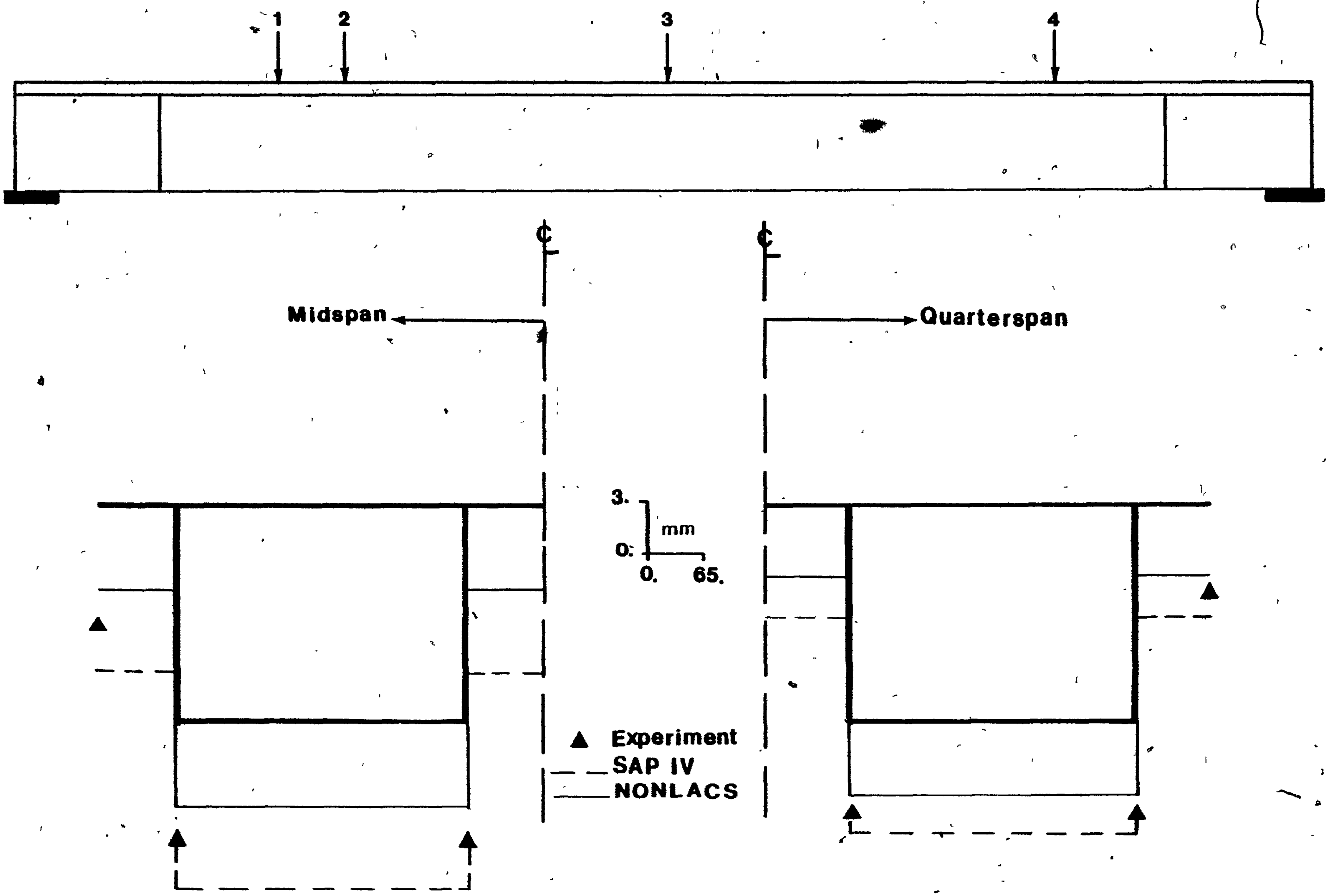

Figure 6.16 COMPARISON OF VERTICAL DEFLECTIONS OF THE BRIDGE MODEL (EIGHT TRUCK LOADINGS)

program and the experimental results.

For all the cases considered, the analytical response and the behaviour of the box-girder bridge both in the linear and the nonlinear ranges as predicted by the NONLACS computer program, show resonable agreement compared with the experimental results obtained from the bridge model tests while the SAP IV program results for deflections were lower by about 48 %.

6.2.2.2 STRESSES

This part consists of the determination of the concrete stresses, and the strains in the prestressing wires under different loading cases and the comparison of the experimental and analytical results. The variation of the longitudinal concrete strains in the top and bottom slab at midspan and 1/4 span is presented. The variation of the transverse stresses under two and eight truck loadings is also reported.

It was difficult to obtain accurate measurements of concrete strains because of the presence of microcracks. It was almost impossible to detect a microcrack in the concrete, which if it is near the location of the electrical strain gauge, can effect the strain measurement significantly, even if the variation of temperature and humidity in the laboratory is controlled well. Therefore, in comparing the experimental and the analytical values, the concrete strains should be interpreted with due caution.

6.2.2.2.1 STRAINS IN THE PRESTRESSING WIRES

Load-steel strain curves for the different loading cases for strain gauge No 2, No 7 and No 10 are shown in Figures 6.17, 6.18 and 6.19, respectively. These prestressing steel strains were recorded during each static test. The strain in the wires was 9000 microstrains (strain gauge No.2) at a load value of 132.0 kN corresponding to 5.0 times two truck loads. It was also noted that the prestressing wires behaved linearly up to an applied load of 79.80 kN (3 times the two truck loads). Under loads corresponding to 8 and 9.1 truck loads, corresponding to load values of 105.60 kN and 120.20 kN, respectively, the strain in the prestressing wire was equal to 10200 microstrains and 11500 microstrains, respectively, which indicated that the wires were still in their preyielding range. The prestressing wires yielded under a load equal to 128.0 kN (9.7 truck loads).

Comparison of load-prestressing wire strain curves for strain gauge numbers 3 and 6 are shown in Figures 6.20 a) and 6.20 b), respectively.

The experimental and prestressing wire strains calculated using modified SAP IV and NONLACS program were

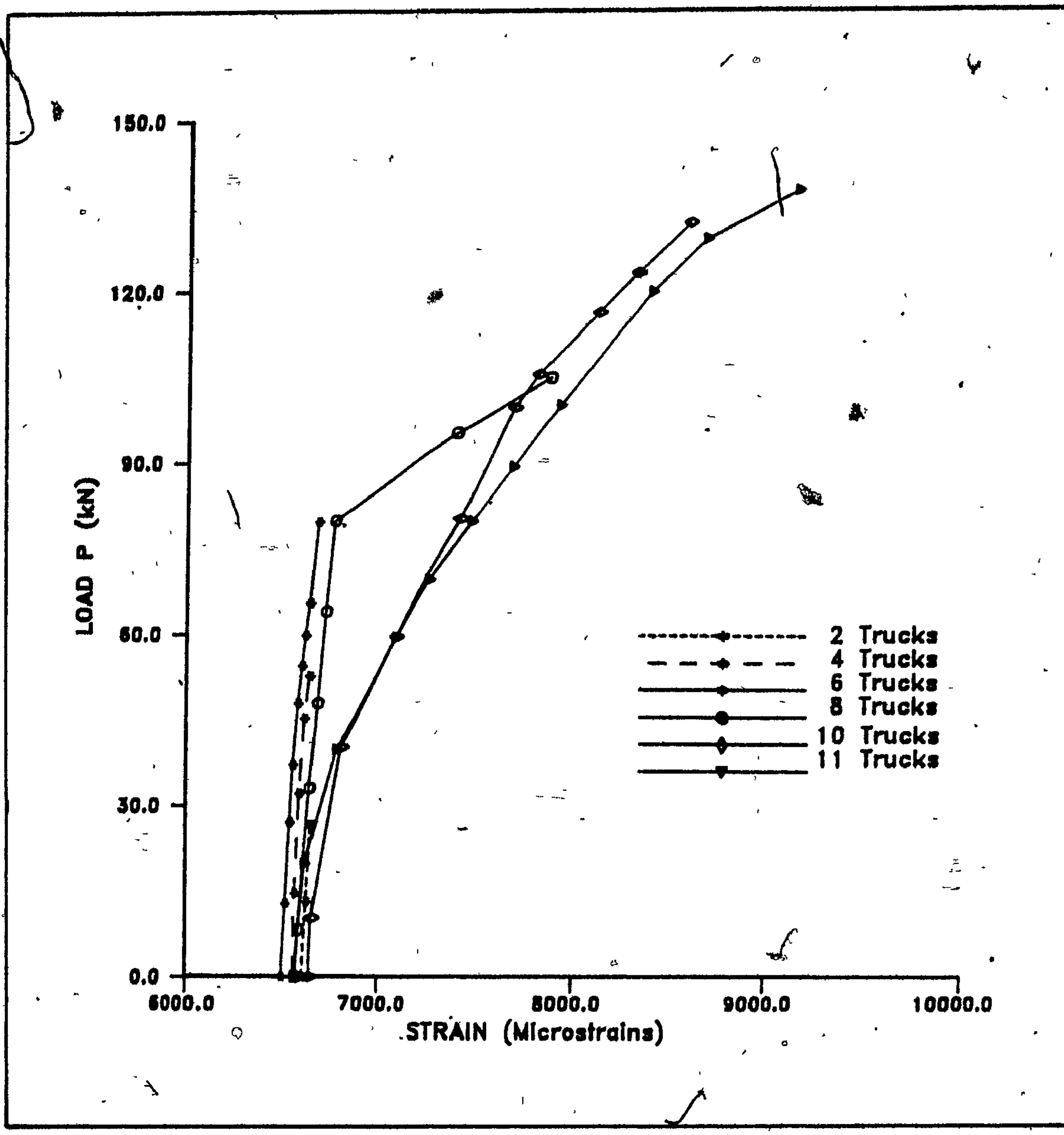

Figure 6.17 LOAD-PRESTRESSING WIRE STRAIN CURVES.
STRAIN GAUGE No.2

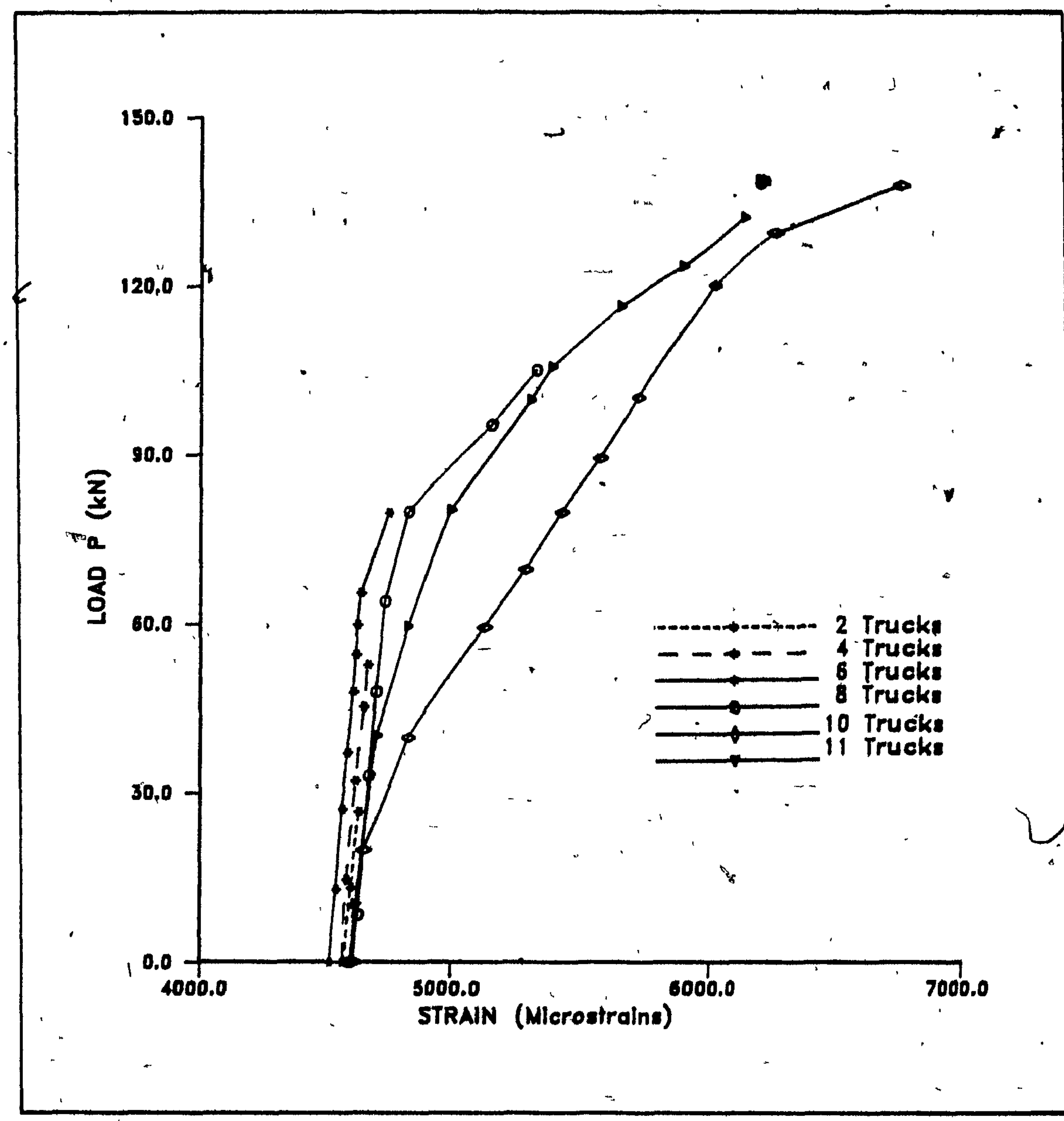

Figure 6.18 LOAD-PRESTRESSING WIRE STRAIN CURVES.
STRAIN GAUGE No.7

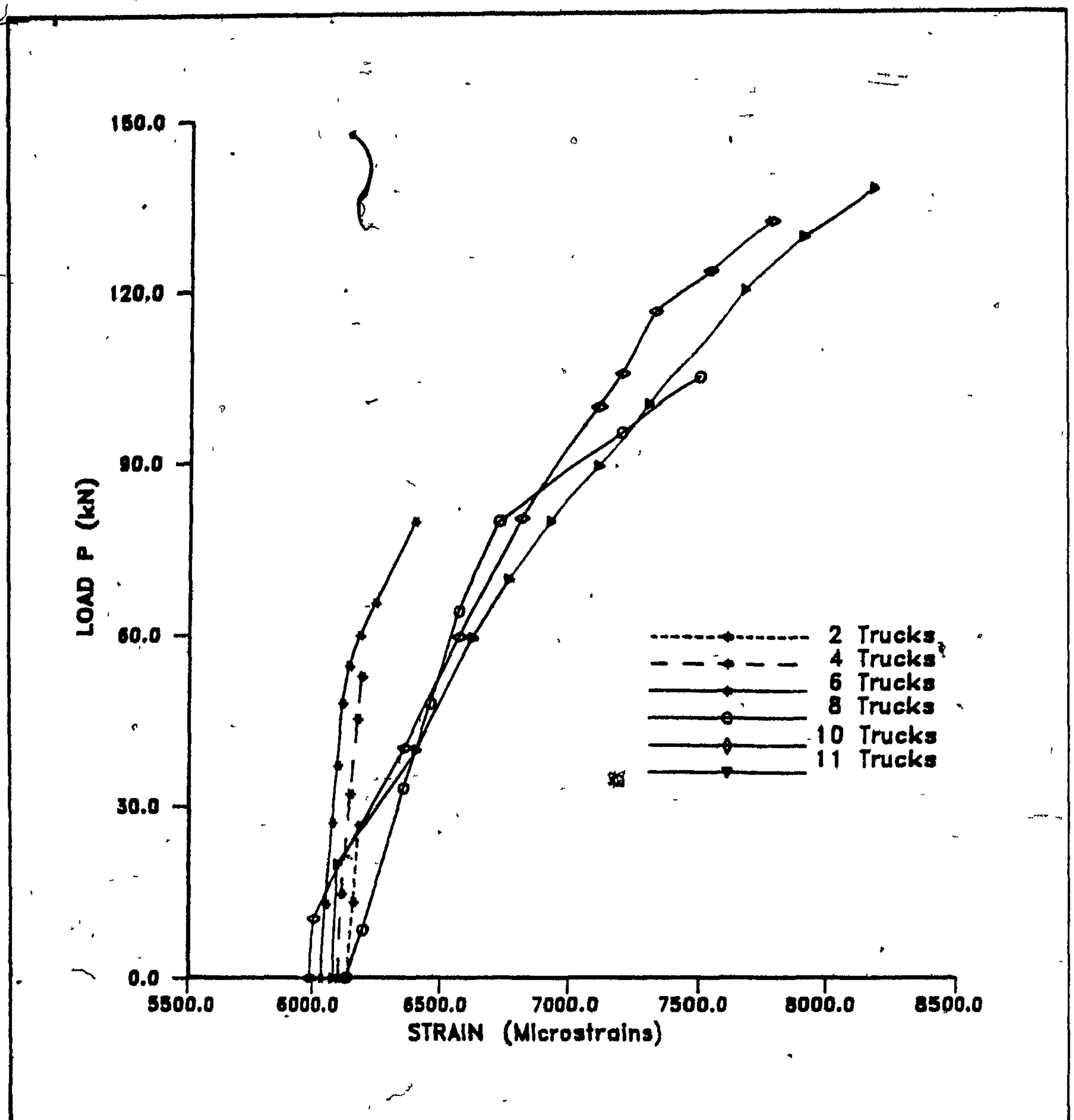

Figure 6.19 LOAD-PRESTRESSING WIRE STRAIN CURVES.
STRAIN GAUGE No.10

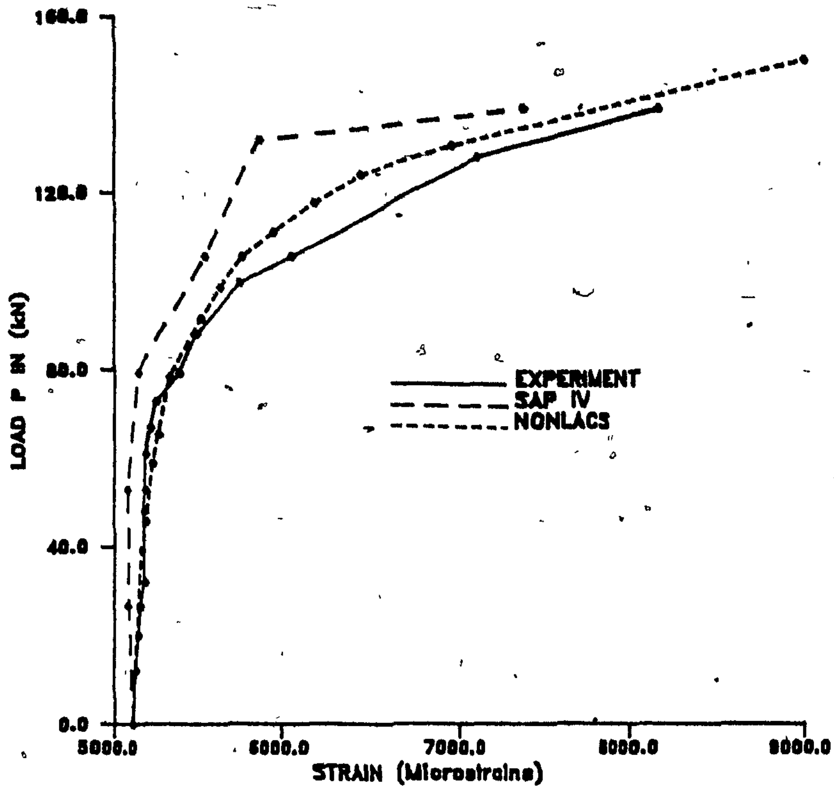

a) WIRE No 1.

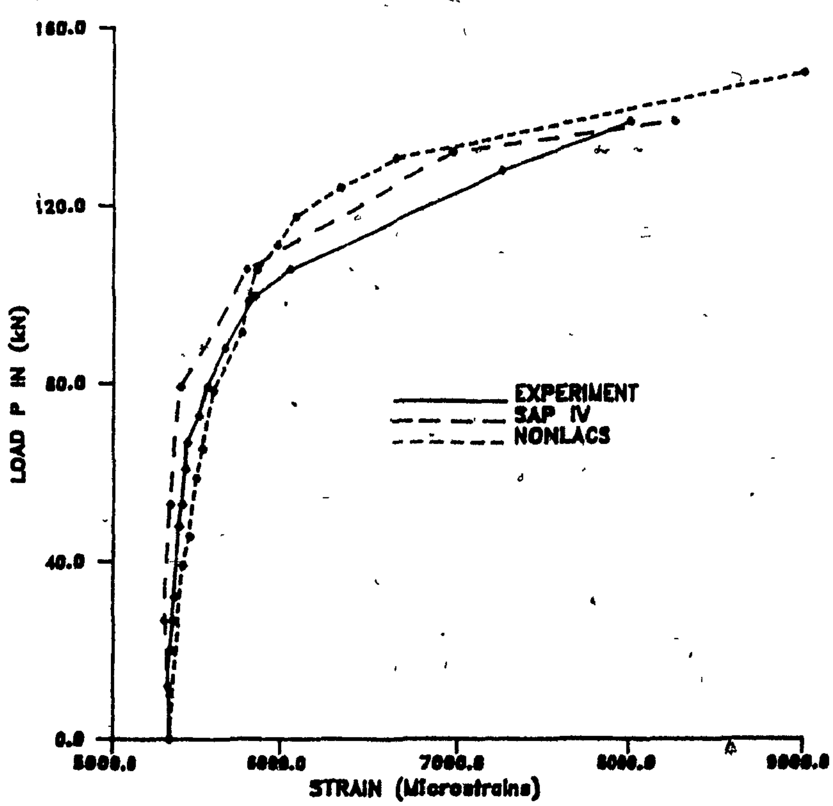

b) WIRE No 3.

Figure 6.20 COMPARISON OF THE LOAD-PRESTRESSING WIRE STRAIN CURVES.

linear up to a load value of 79.80 kN (6 truck loads).Large strains were obtained under 8 truck loads; the prestressing wires yielded under a load corresponding to 9.7 truck loads. These results are shown in Figures 6.17 through 6.19. The results computed using the NONLACS program showed a sudden variation in the strains of the prestressing wires which is basically due to the bilinear stress-strain curve used for the prestressing wire in this model. As shown in Figure 6.20, the SAP IV program gives smaller strains in the prestressing wires. This is due to the fact that the truss element used in the analytical model to simulate the prestressing wires was not fully bonded.

6.2.2.2.2 STRESSES IN THE CONCRETE

Figures 6.21 and 6.22 show the variation of the concrete stresses in the top slab at midspan and quarterspan under two and eight truck loadings, respectively.

The variation of the longitudinal concrete strains at different locations through the bridge span in the top slab with increasing load are shown in Figures 6.23 and 6.24, respectively. During all of the loading stages, the stresses at the top fiber of the cross-section were compressive.

For comparison, the concrete stresses in the top slab at midspan and quaterspan sections obtained from the

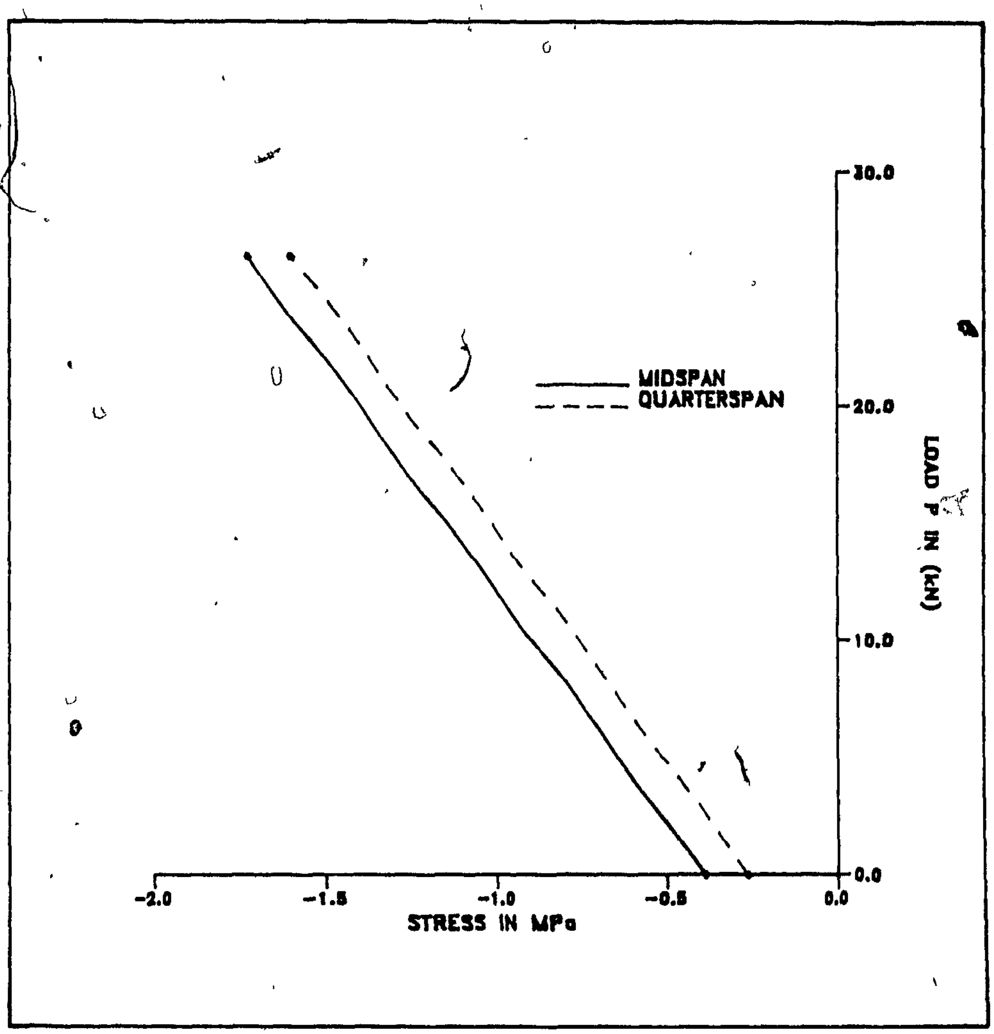

Figure 6.21 VARIATION OF THE CONCRETE STRESSES IN THE TOP SLAB UNDER TWO TRUCK LOADINGS.

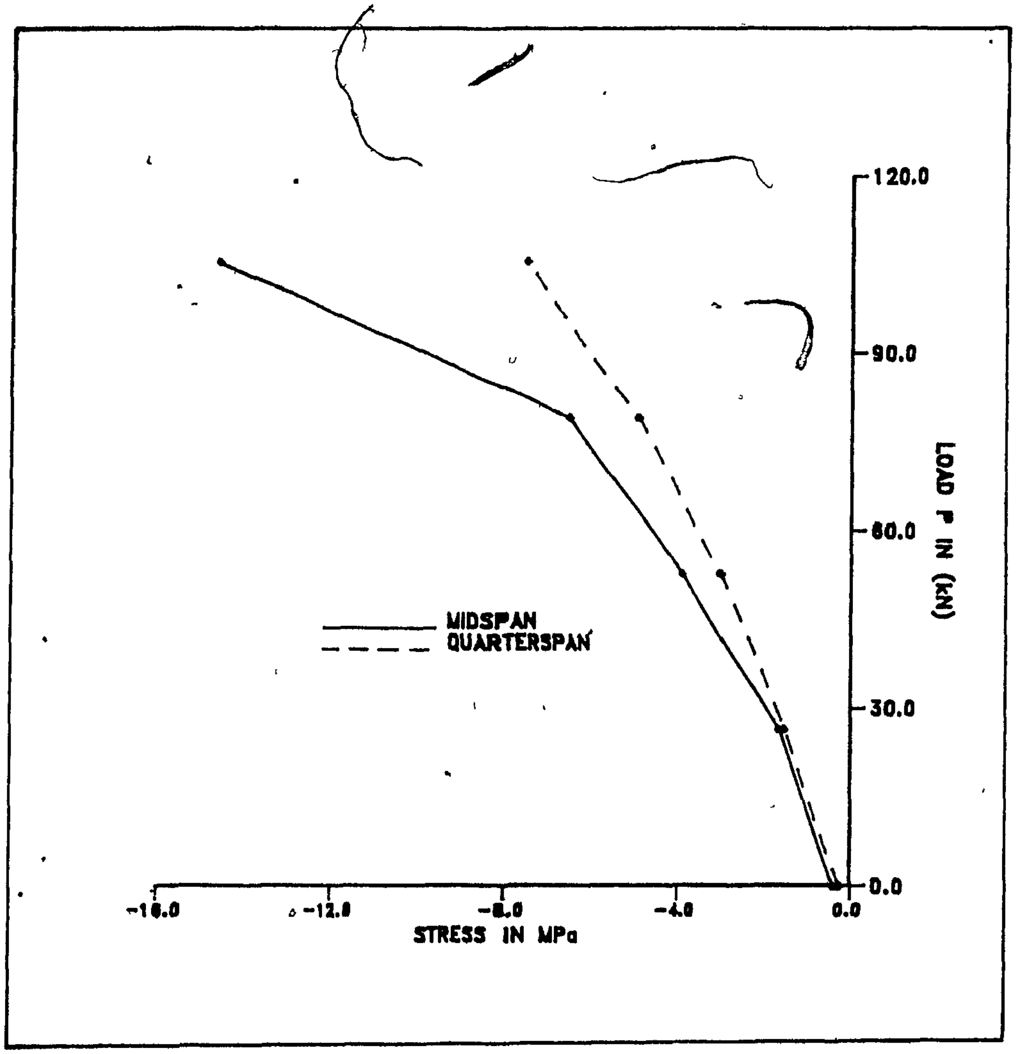

Figure 6.22 VARIATION OF THE CONCRETE STRESSES IN THE TOP SLAB UNDER EIGHT TRUCK LOADINGS.

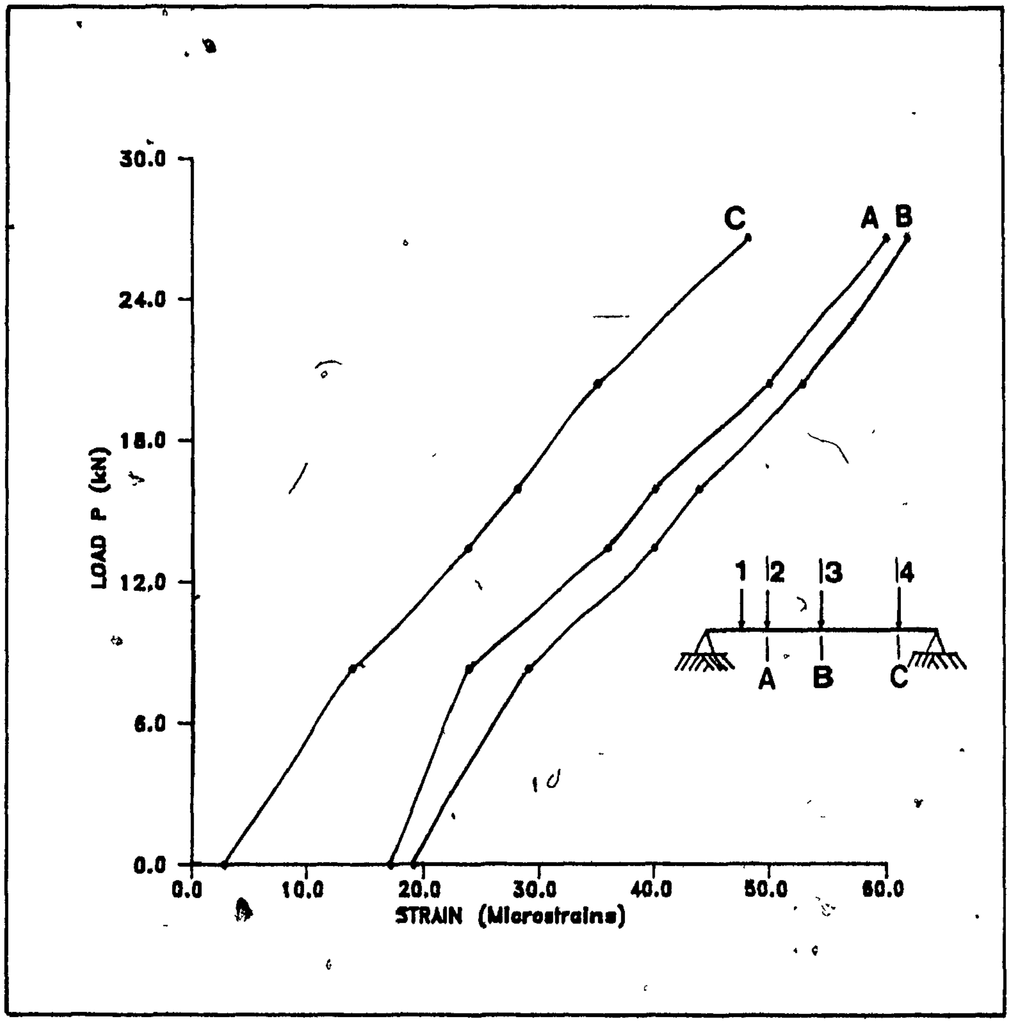

Figure 6.23 LONGITUDINAL CONCRETE STRAINS IN THE TOP SLAB UNDER TWO TRUCK LOADINGS.

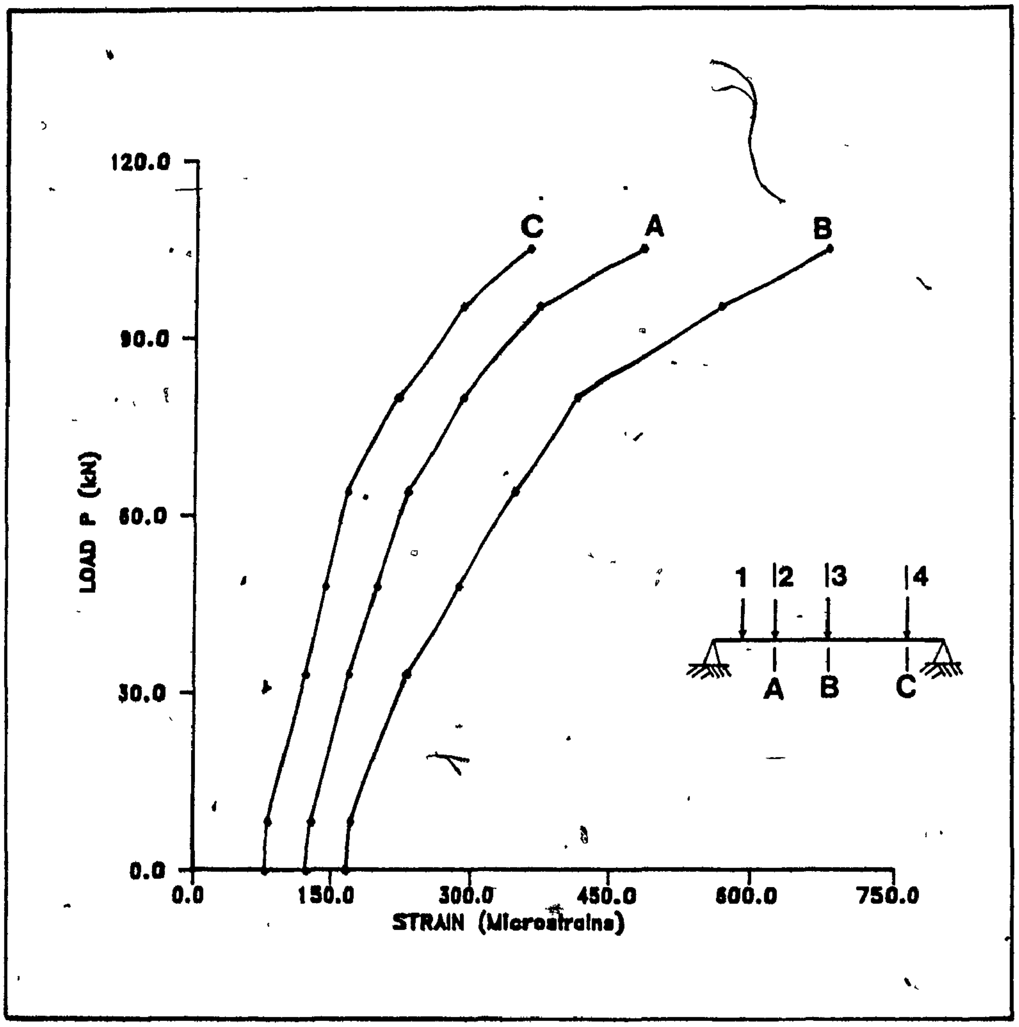

Figure 6.24 LONGITUDINAL CONCRETE STRAINS IN THE TOP SLAB UNDER EIGHT TRUCK LOADINGS.

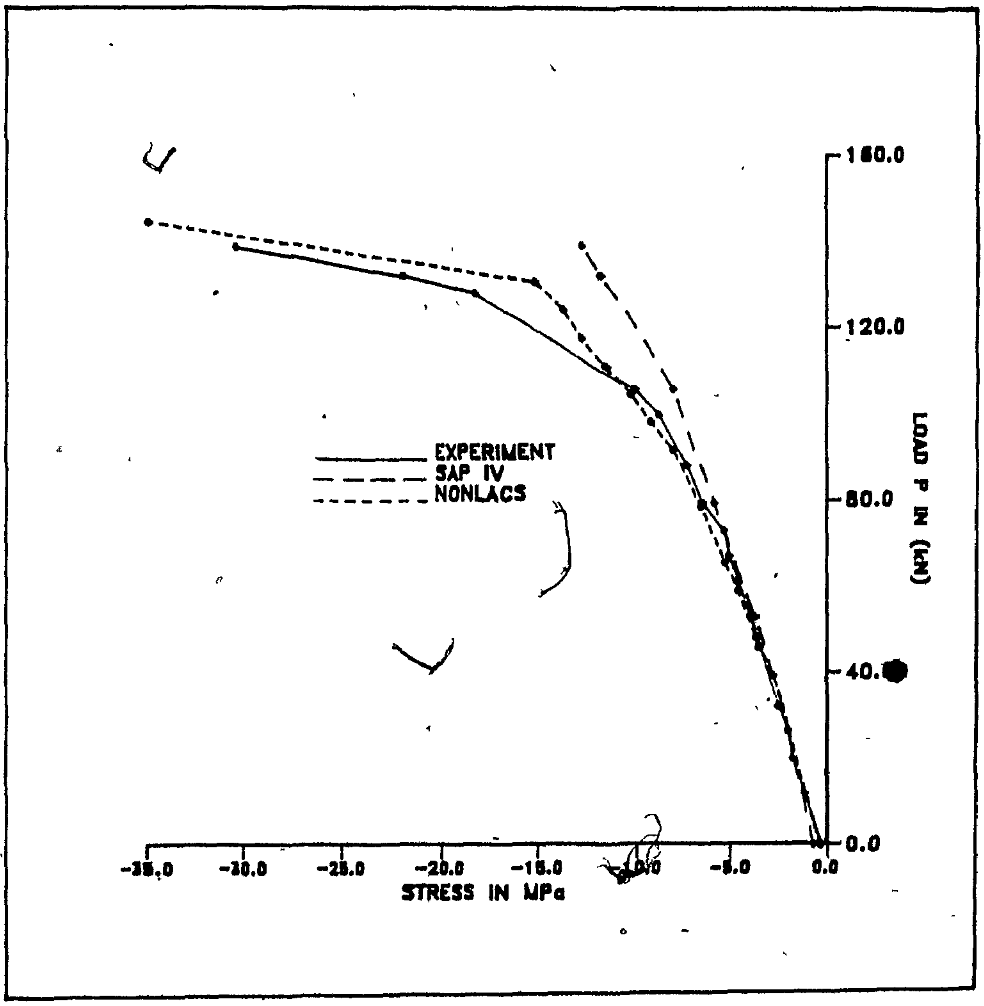

Figure 6.25 COMPARISON OF THE CONCRETE STRESSES IN THE TOP SLAB AT MIDSPAN.

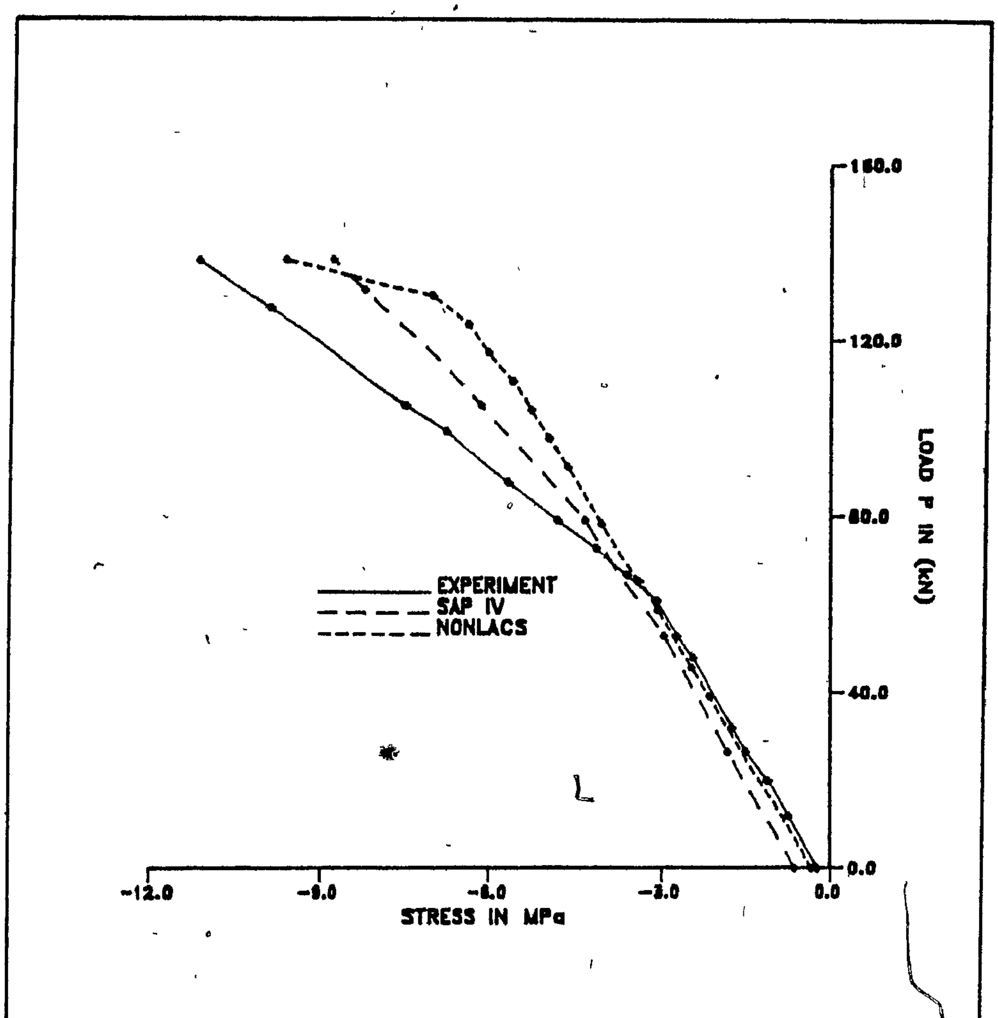

Figure 6.26 COMPARISON OF THE CONCRETE STRESSES IN THE TOP SLAB AT QUARTERSPAN.

experimental and both finite element program are shown in Figures 6.25 and 6.26, respectively. The load-stress curves show a good agreement between the experimental and the analytical values at midspan up to a load value of 105.60 kN (8 truck loads) and up to a load value equal to 79.80 kN (6 truck loads) at quarterspan. The difference was approximately 5 % at midspan and 10 % at quarterspan. Beyond a total load of 8 truck loads on the bridge, a difference of about 17 % was noted in the experimental and computed values of the concrete stresses at midspan. A similar difference was observed for the concrete stresses at quarterspan beyond a total load of 6 truck on the bridge.

Longitudinal concrete strains in the bottom slab were also recorded during each flexural test. Figures 6.27 and 6.28 show the variation of longitudinal concrete strains in the bottom slab at midspan and at quarterspan, respectively. During the testing process, the concrete strains in the bottom fiber of the cross-section were tensile.

The distribution of transverse stresses could not be obtained from the experiment. This is due to the lack of strain measurements at specific points. Figures 6.29 through 6.32 show the distribution of transverse stresses obtained from the analytical model (NONLACS) under two, four, six and eight truck loads, respectively. The transverse stresses were about 10 % to 20 % of the longitudinal stresses under the same loading at the same locations .

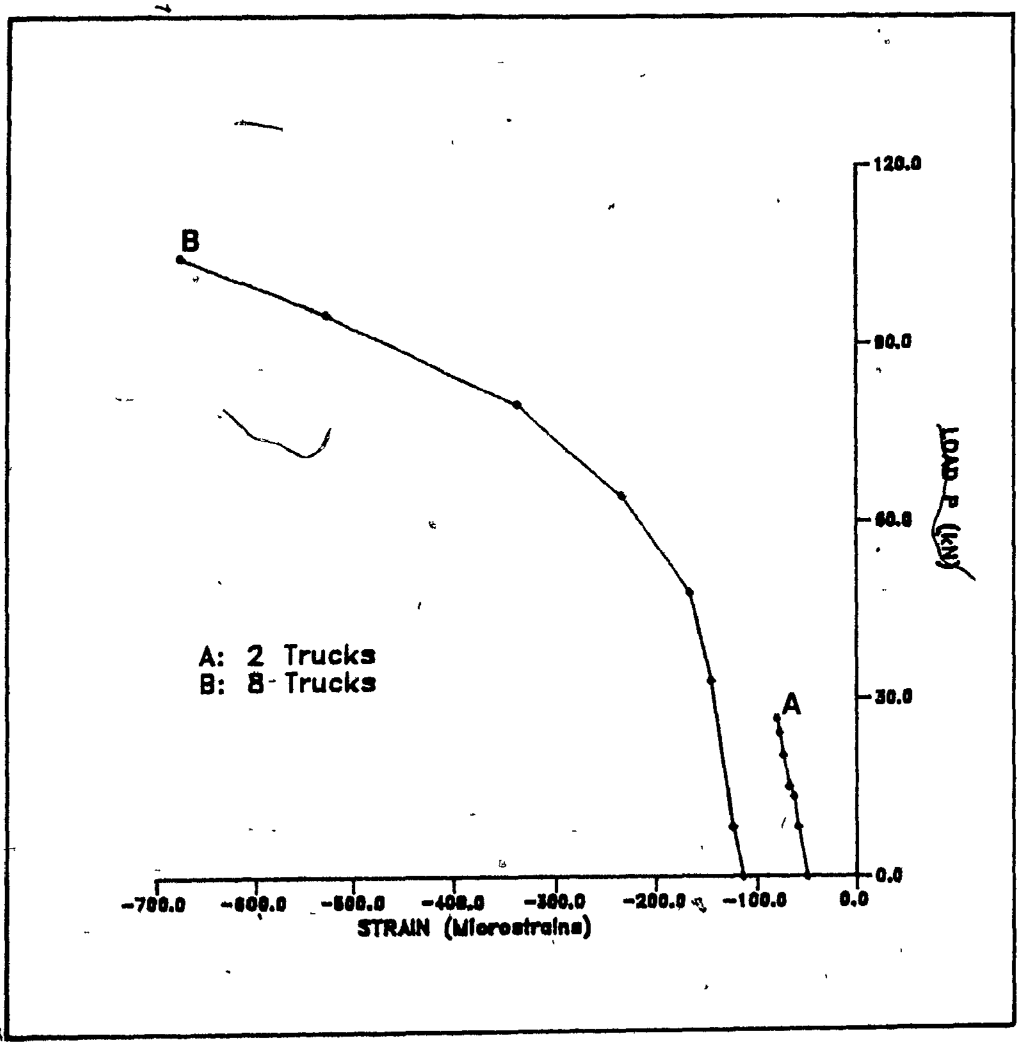

Figure 6.27 LONGITUDINAL CONCRETE STRAINS IN BOTTOM SLAB AT MIDSPAN.

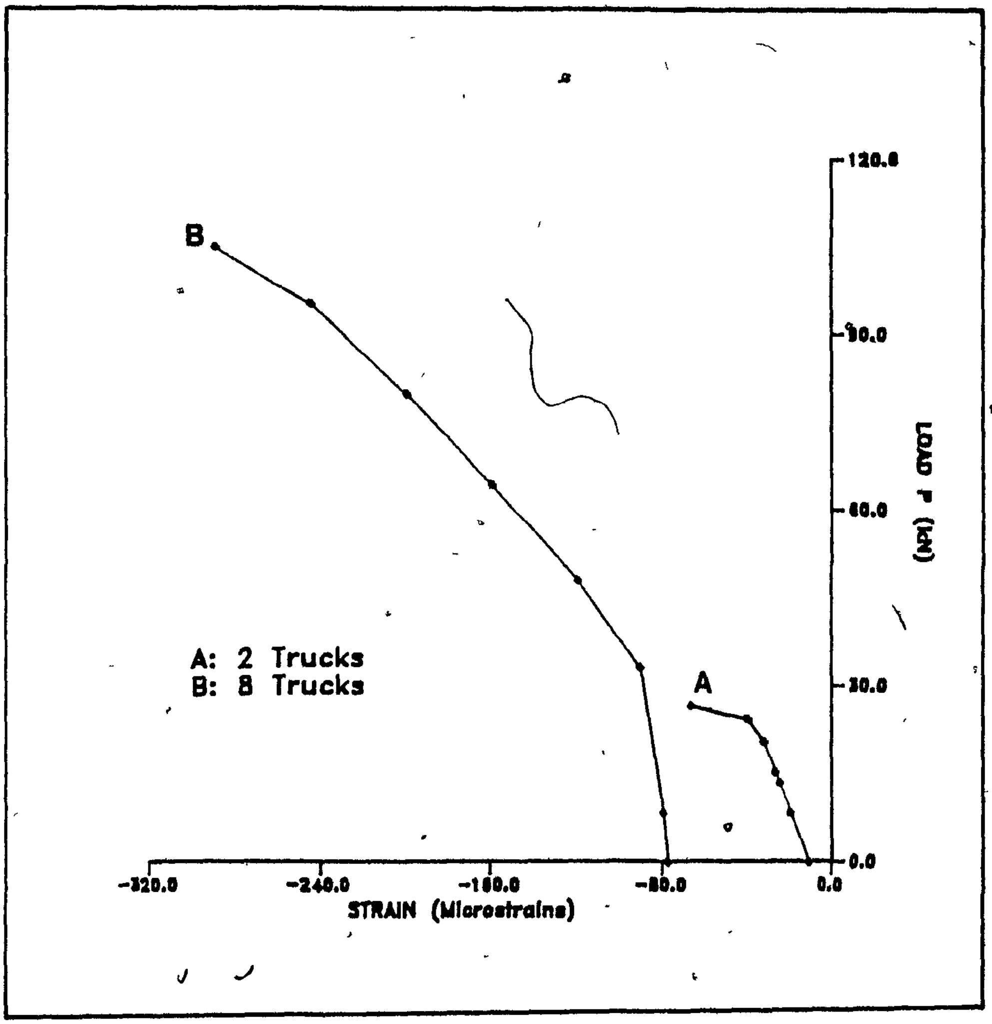

Figure 6.28 LONGITUDINAL CONCRETE STRAINS IN THE BOTTOM SLAB AT QUARTERSPAN.

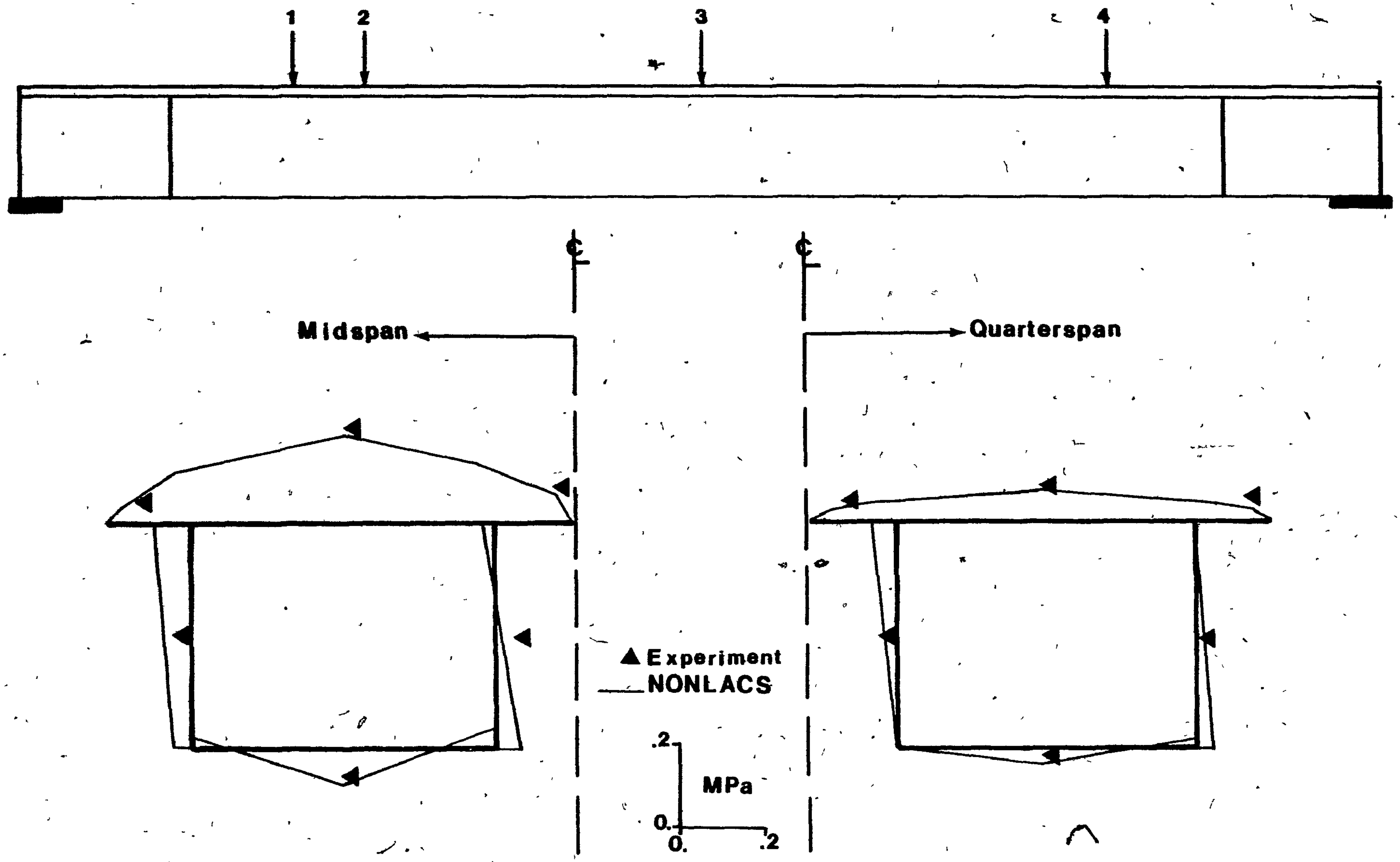

Figure 6.29 TRANSVERSE CONCRETE STRESSES UNDER 2 TRUCK LOADS

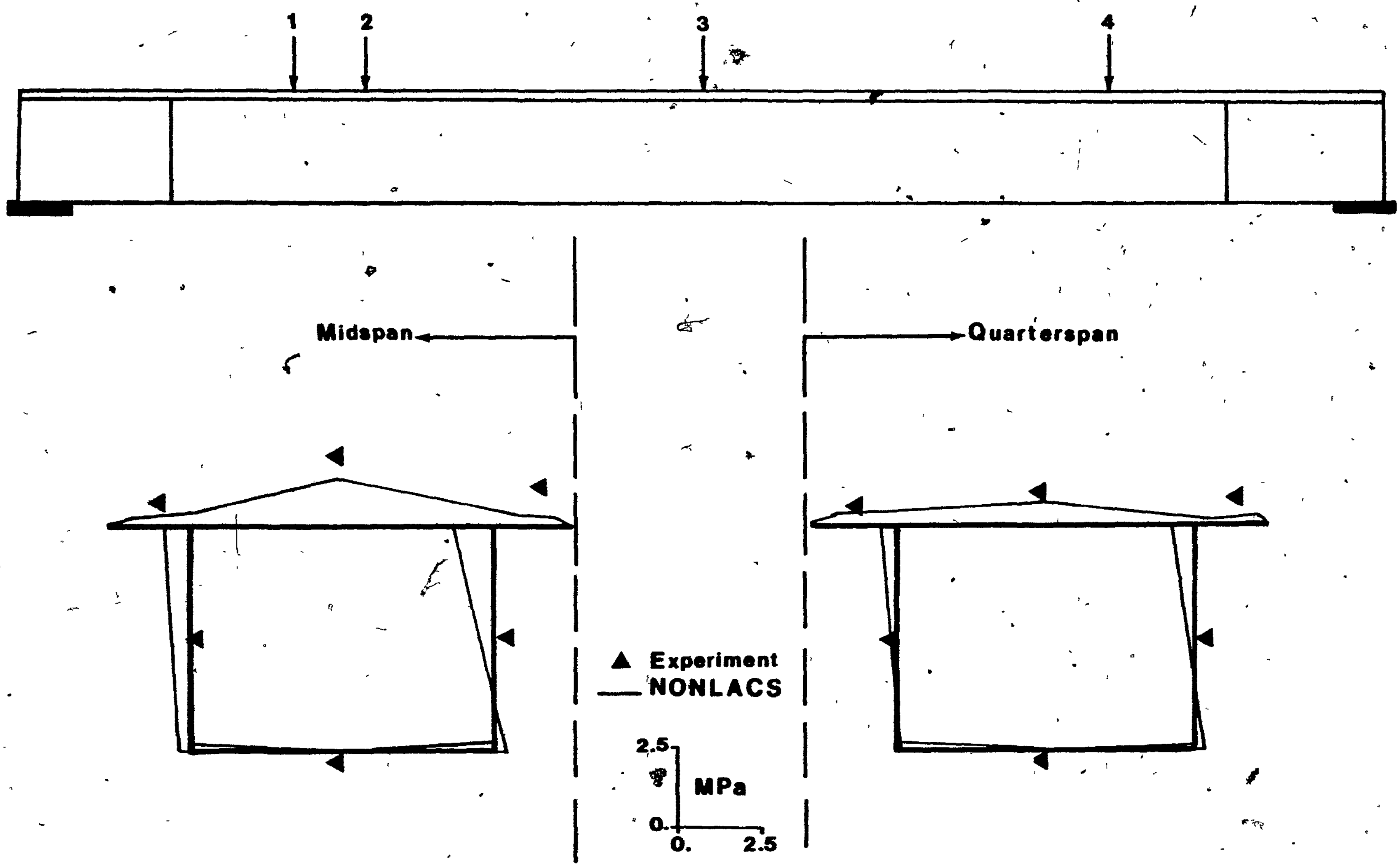

Figure 6.30 TRANSVERSE CONCRETE STRESSES UNDER 4 TRUCK LOADS

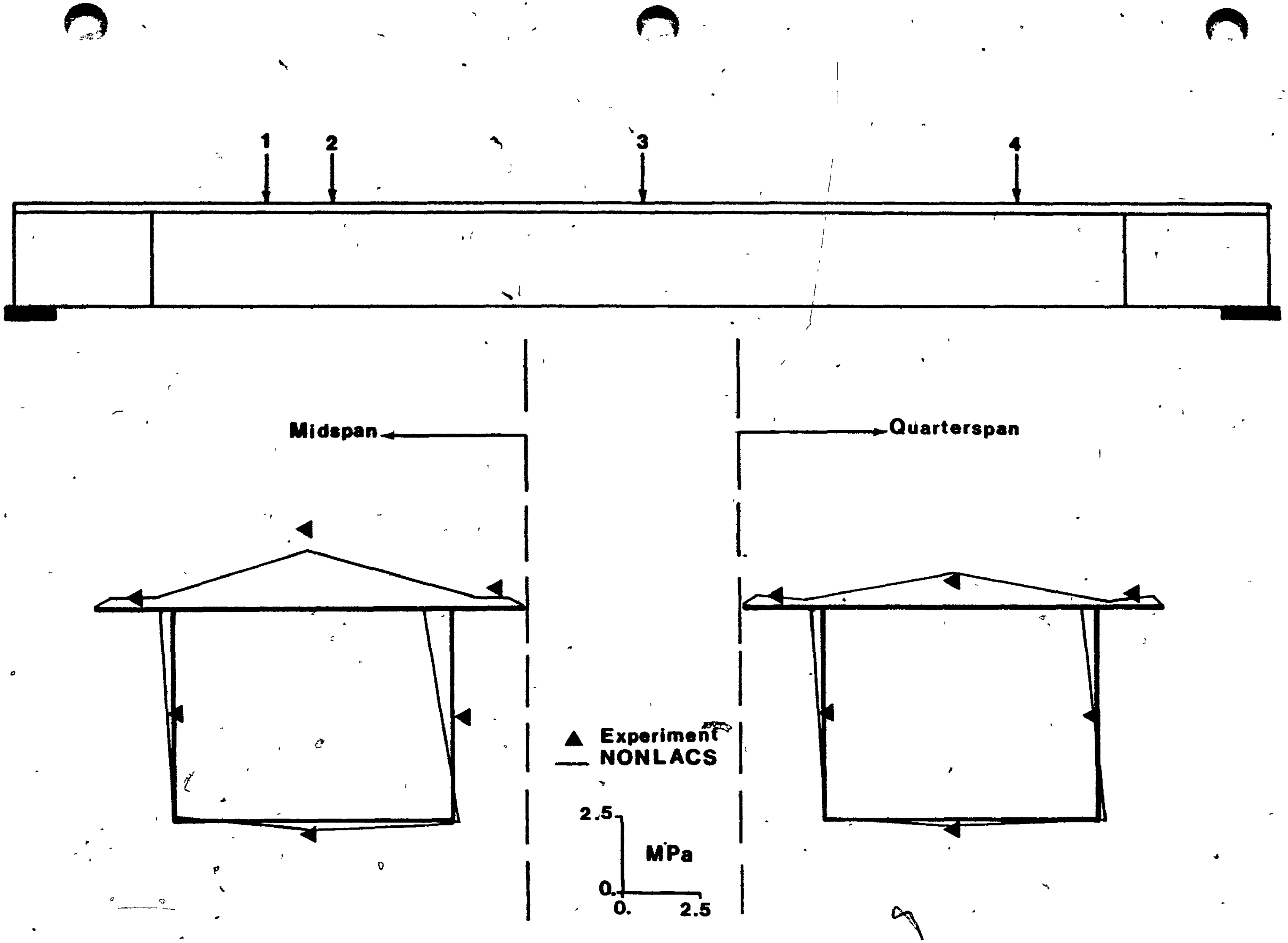

Figure 6.31 TRANSVERSE CONCRETE STRESSES UNDER 6 TRUCK LOADS

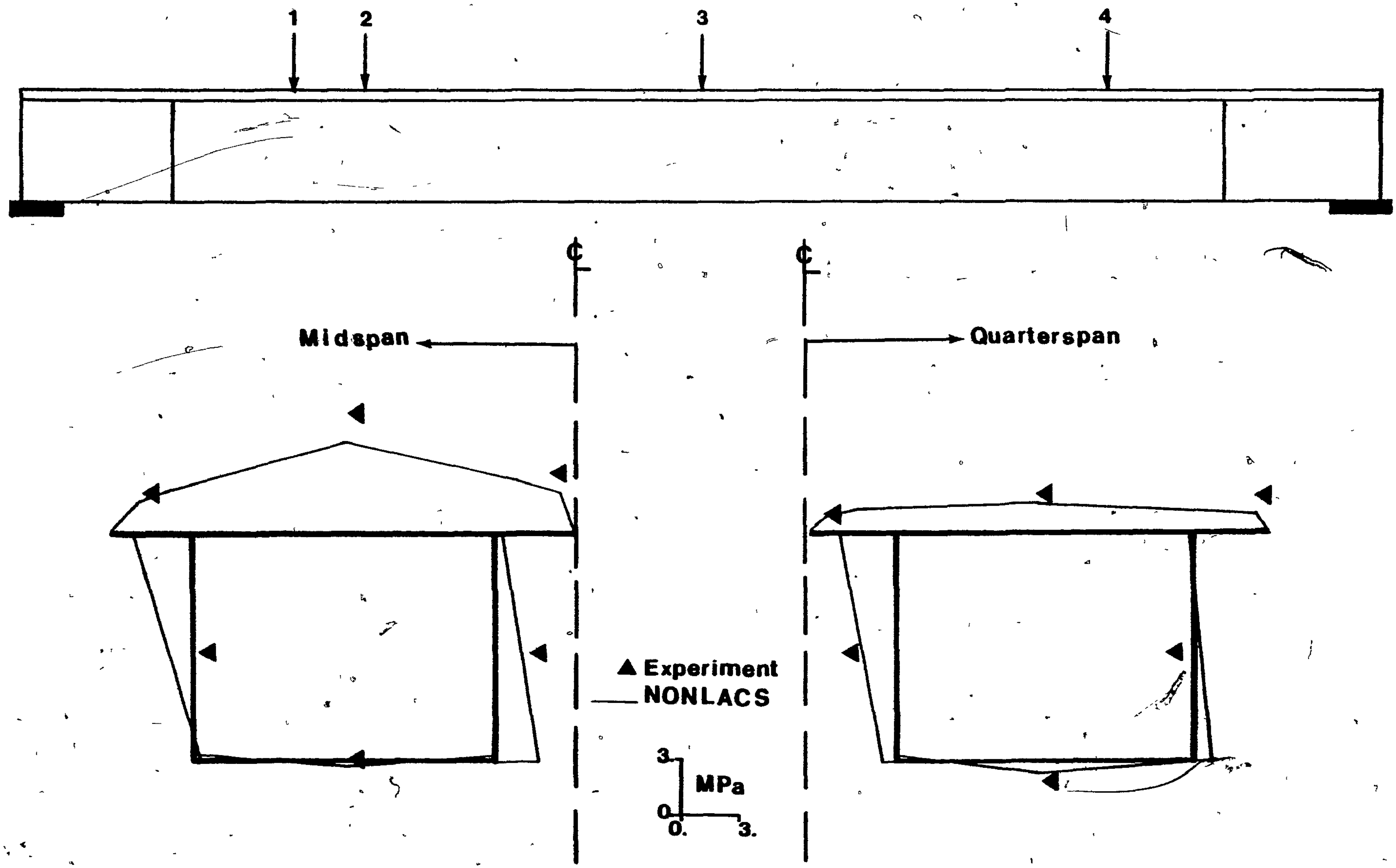

Figure 6.32 TRANSVERSE CONCRETE STRESSES UNDER 8 TRUCK LOADS

The distribution of the longitudinal and transverse stresses in the top slab was not uniform but symmetrical about the centerline of the bridge model. This confirms the ability of box section to distribute the load in the transverse direction. Also, the materials and geometrical properties were consistent for the entire structure.

6.2.2.3 DEVELOPMENT OF CRACKS

The first crack was observed at a total load of 48.0 kN (1.8 times two truck loads) and appeared as a tension crack in the web near the midspan. Two more cracks appeared at each side of the middle crack at a load value of 52.8 kN (2 times two truck loads). After this loading stage, when the load was released, the cracks were not visible on the surface of the webs, showing good bond between the prestressing steel and the concrete. Figure 6.33 shows the propagation of cracks after four truck loads for girder 1 and girder 2.

More cracks appeared in the webs and bottom slabs when the load was applied again up to a load value of 79.20 kN (3 times the two truck loads). The flexural cracks became wider and propagated up to about three quarters of the depth of the webs, and along the entire width of the

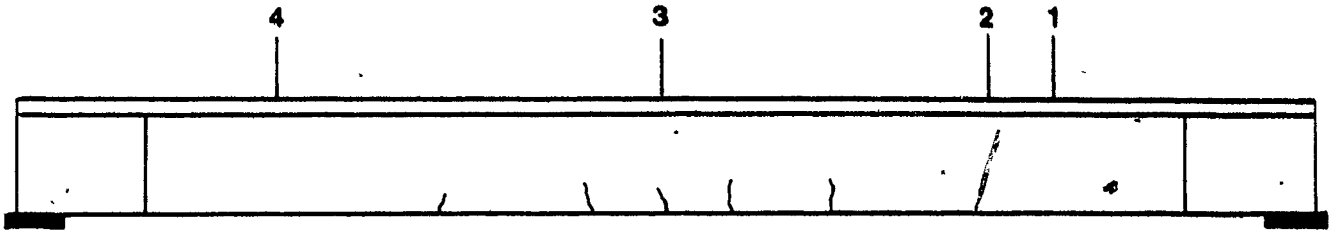

a. 4 Truck Loads

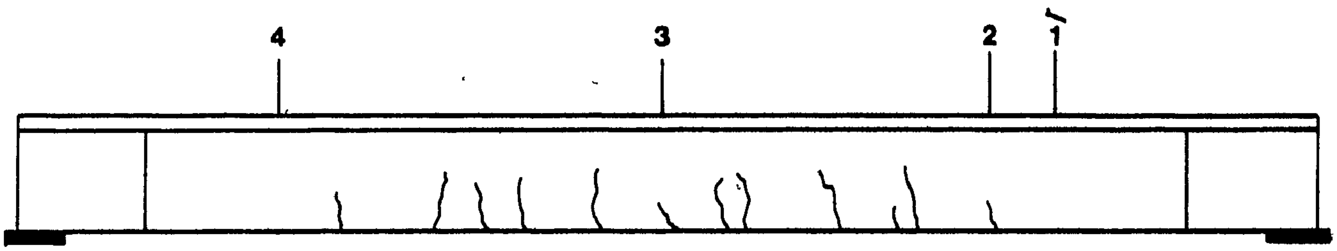

b. 6 Truck Loads

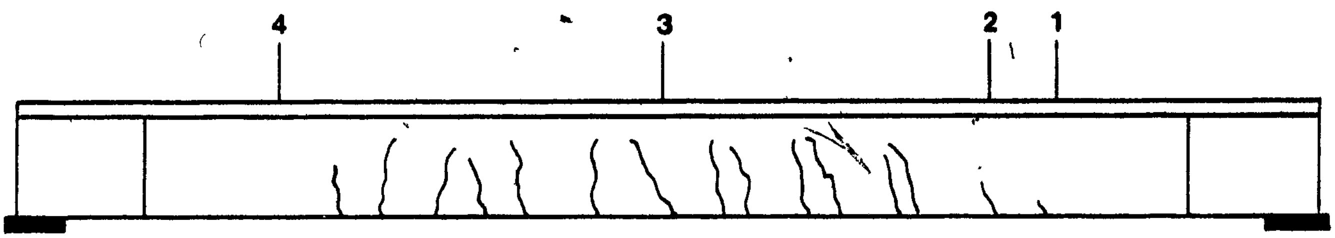

c. 8 Truck Loads

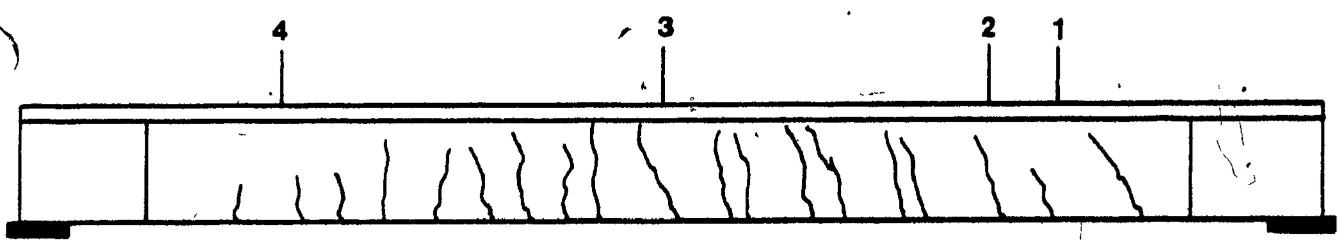

d. 10 Truck Loads

Figure 6.33 PROPAGATION OF CRACKS.

bottom slabs at a load value of 105.60 kN (4 times the two truck loads). At an applied load of 132.00 kN (5 times the two truck loads), shear cracks appeared near the end blocks but wide flexural crack developed near the midspan. All cracks propagated along the total depth of the webs and the total width of the bottom slabs. At this stage, a large crack appeared along the entire width of the top slab at midspan which was accompanied by a loud noise due to fracture of two prestressing wires. At this stage, the structure was near failure. Propagation of cracks after 4,6,8 and 10 truck loads are shown in Appendix B.

6.2.2.4 FAILURE TEST

After 10 truck loads were applied, the bridge model had almost failed. At this stage, the flexural cracks at midspan widened considerably, and more prestressing wires fractured resulting in loud noises due to release of energy, and a flexural failure was expected. In order to determine the mode of failure, the structure was loaded under a flexural truck load up to a load value of 139.0 kN (10.5 times the truck load) and the model bridge failed in flexure as expected. The box girder bridge model showed a significant reserve of strength.

6.3 DYNAMIC TESTS

After each static test corresponding to an applied total load equal to 0, 2, 4, 6, 8 and 10 times the truck load, both flexural and torsional free vibration tests were performed. The different displacement readings were obtained from 9 L.V.D.T's (Figure 4.17). Some of the data obtained are shown in this thesis in Figures 6.34 through 6.57.

During the bridge free vibration tests, there was almost no perceptible motion at the supports.

6.3.1 FLEXURAL VIBRATION TESTS

A mass of 230 kg was suspended by a 1.75 mm diameter mild steel wire from the horizontal 25 mm rod, used for harping the prestressing wires, at the bridge centre (at midspan and at the centre of the transverse direction). All of the L.V.D.T's were calibrated prior the test and readings were taken before cutting the wire. Then, the wire was severed by a pair of pliers to set the bridge model into free vibrations. The response of the L.V.D.T's was recorded using the MINC computer. This flexural vibration test was conducted after the appropriate static test described in Section 4.2.2.

6.3.1.1 NATURAL FREQUENCIES OF VIBRATION

Figures 6.34 through 6.45 show the data obtained during the flexural free vibration tests performed on the structure after each static test corresponding to a load equal to 0, 2, 4, 6, 8 and 10 times the OHBD Code model truck load. Nine L.V.D.T's were used to determine the natural frequency of vibrations of the bridge model for each test. The locations of these L.V.D.T's are shown in Figure 4.8. The average value of the natural frequencies of vibration obtained from the response of the L.V.D.T's was taken as the natural frequency of vibration of the bridge model corresponding to each loading stage. The natural frequency values given by the L.V.D.T's were quite close and the difference was less than 1.5 %. The results are summarized in Table 6.3 along with the corresponding analytical values obtained using the SAP IV program.

For the first four tests, corresponding to no live load and live load equal to 2, 4, and 6 truck loads, there was a small change in the fundamental natural frequency of vibration from 15.61 Hz to 13.54 Hz. However, the dynamic response test conducted for 8 and 10 times the truck load after the appearance of the flexural cracks at the midspan of the bridge model, showed a large decrease in the fundamental natural frequency of vibration. The value recorded at that stage was 11.95 Hz. At this level of load

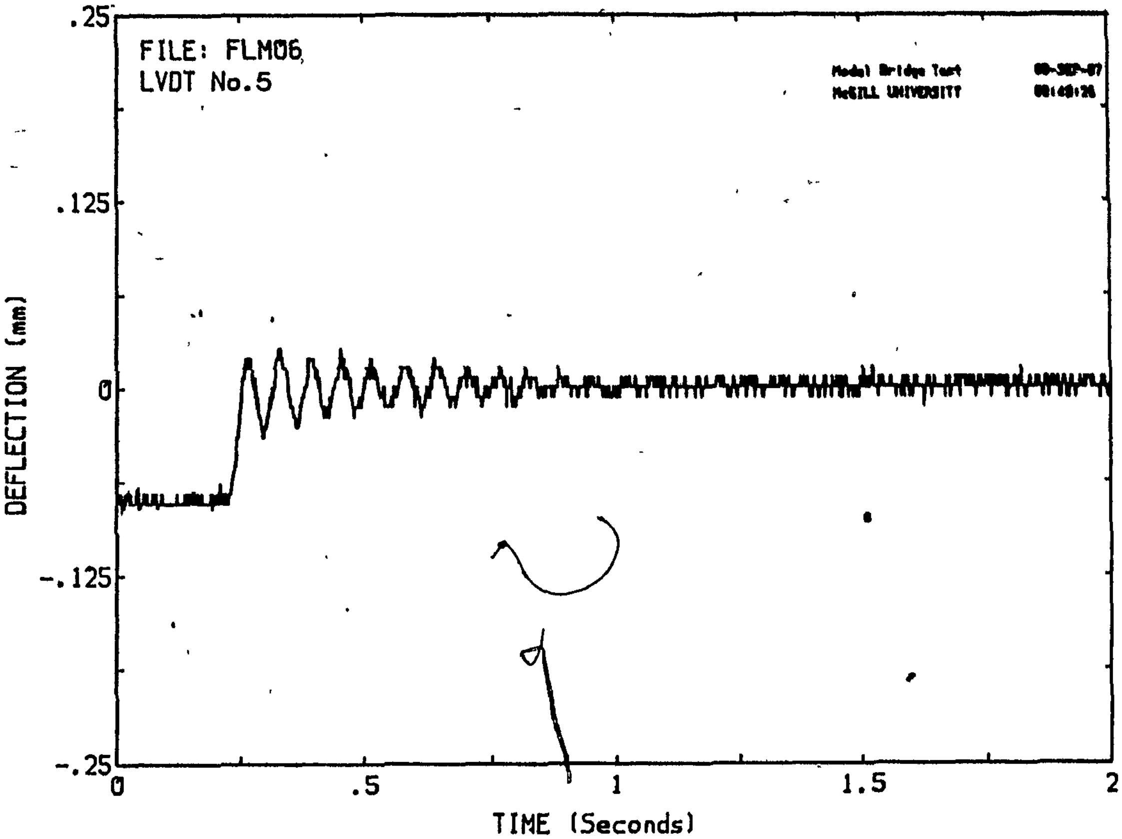

Figure 6.34 FLEXURAL TEST (UNCRACKED BRIDGE). L.V.D.T No.5.

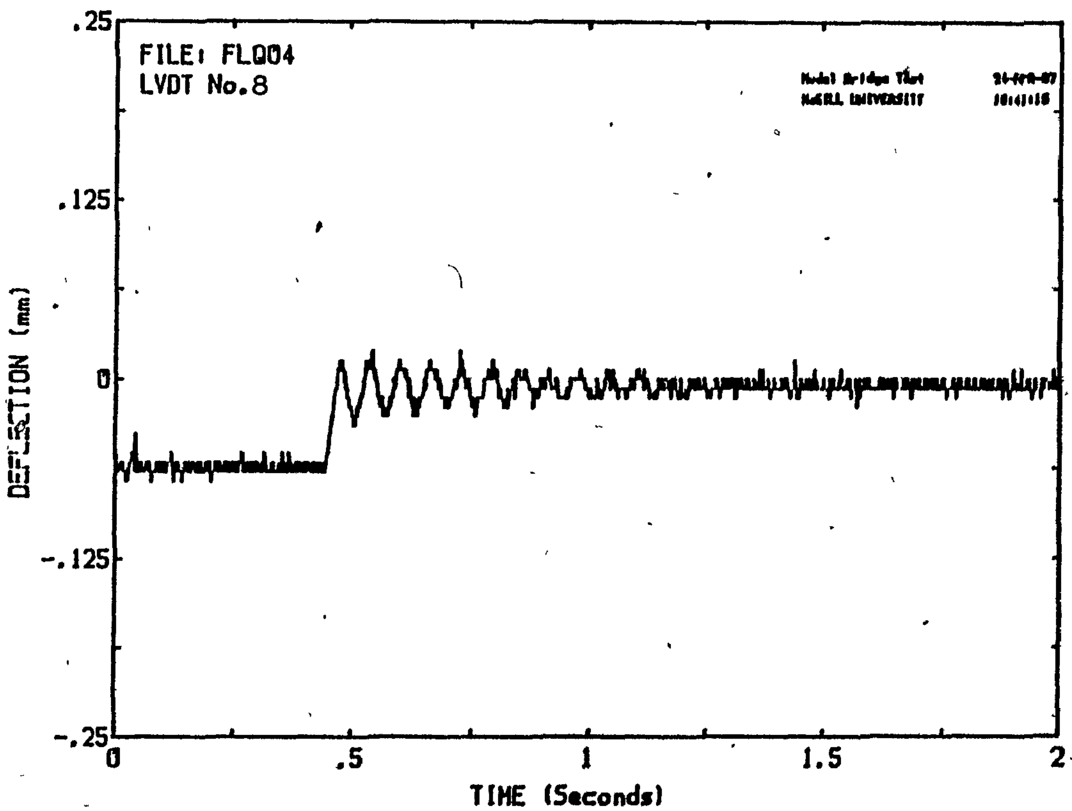

Figure 6.35 FLEXURAL TEST (UNCRACKED BRIDGE). L.V.D.T No.8.

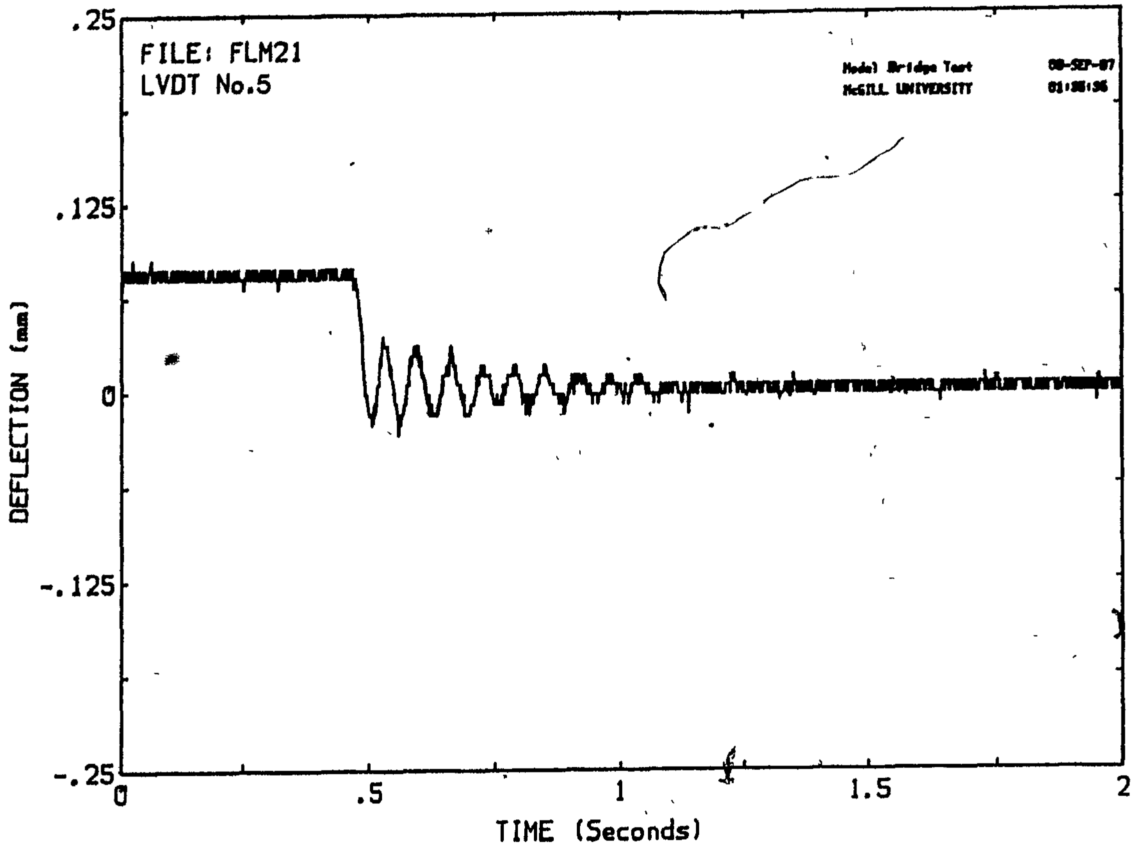

Figure 6.36 FLEXURAL TEST WITH 2 TRUCK LOADS. L.V.D.T No.5.

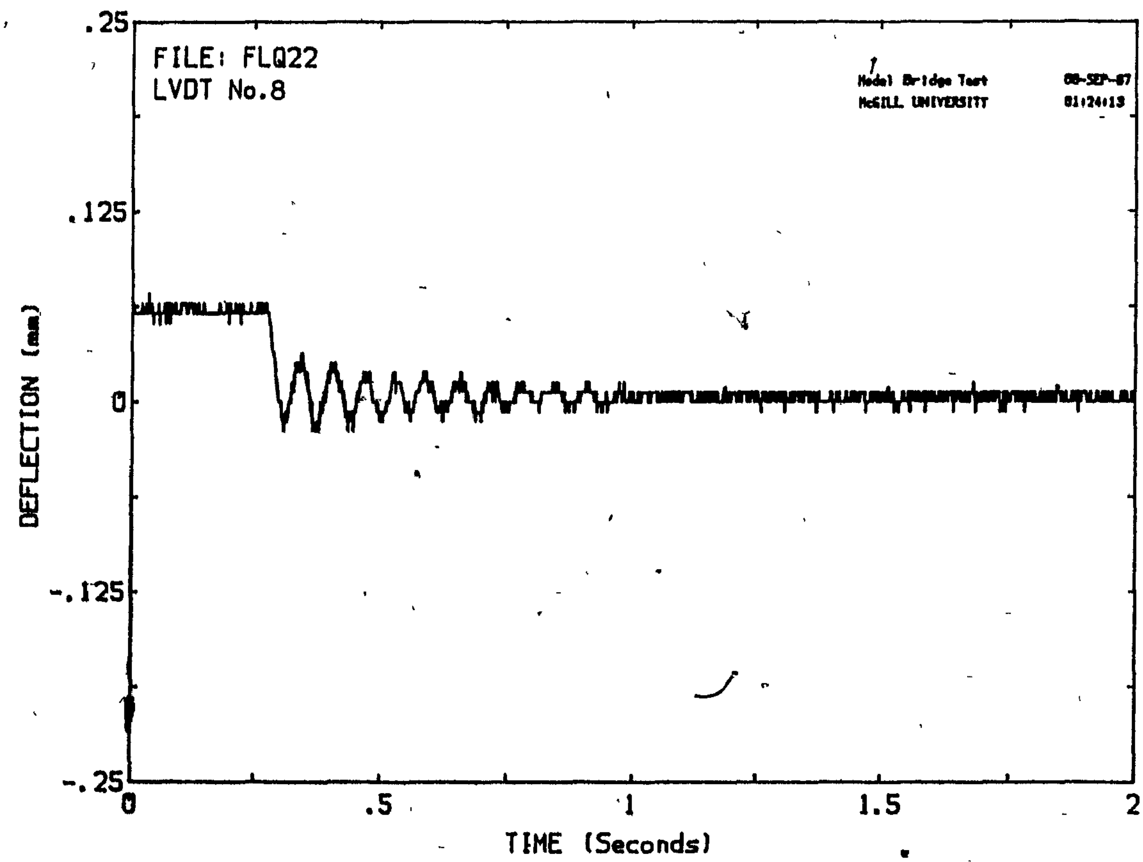

Figure 6.37 FLEXURAL TEST WITH 2 TRUCK LOADS. L.V.D.T No.8.

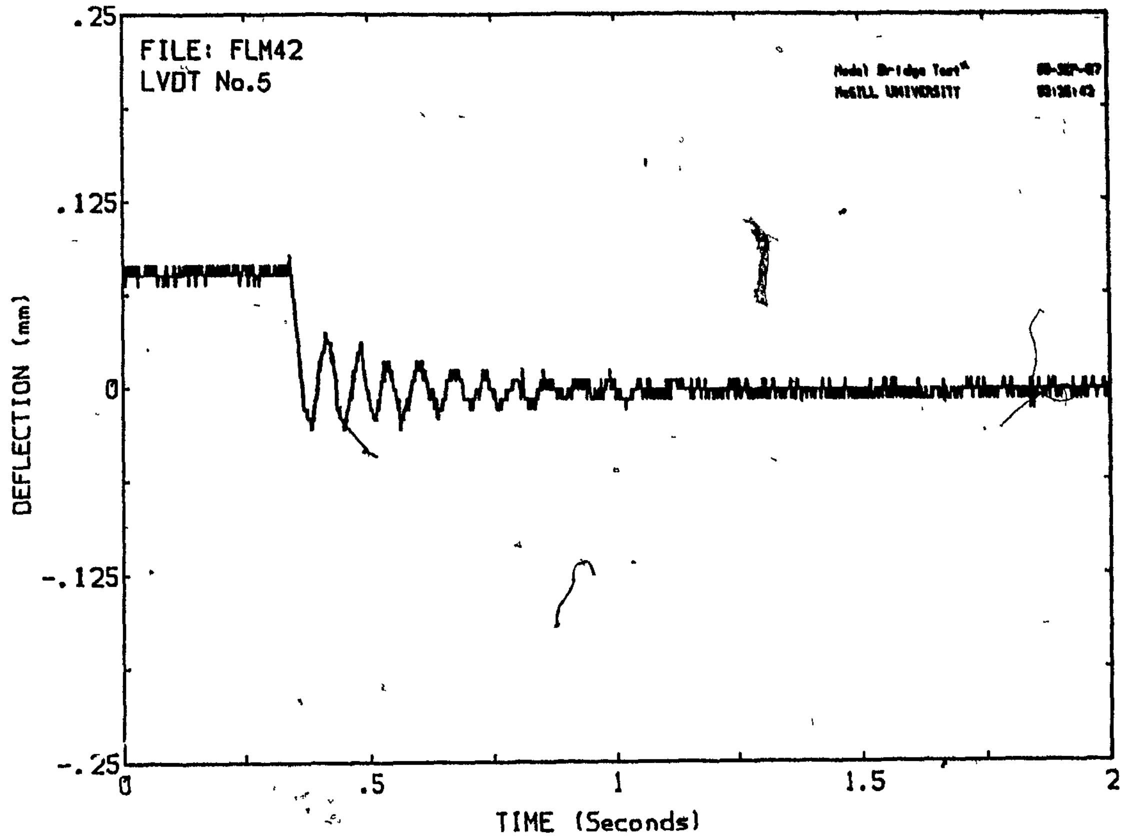

Figure 6.38 FLEXURAL TEST WITH 4 TRUCK LOADS. L.V.D.T No.5.

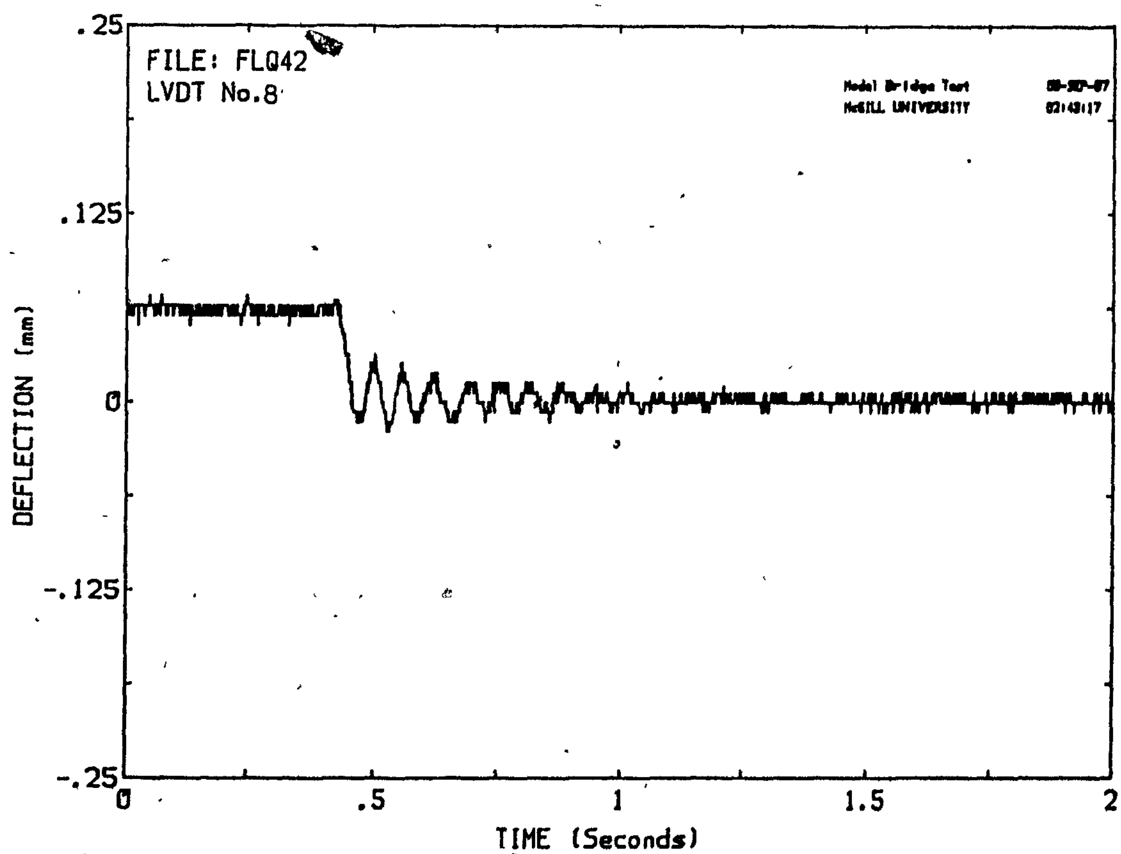

Figure 6.39 FLEXURAL TEST WITH 4 TRUCK LOADS. L.V.D.T No.8.

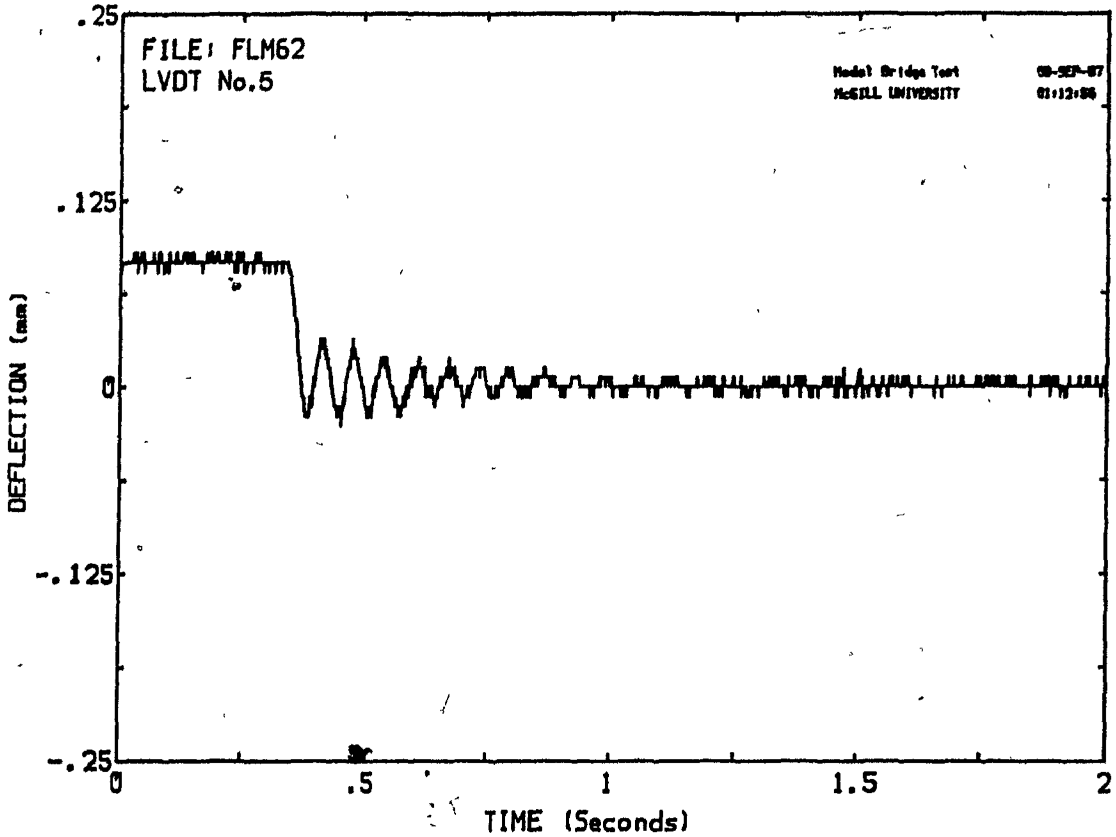

Figure 6.40 FLEXURAL TEST WITH 6 TRUCK LOADS. L.V.D.T No.5.

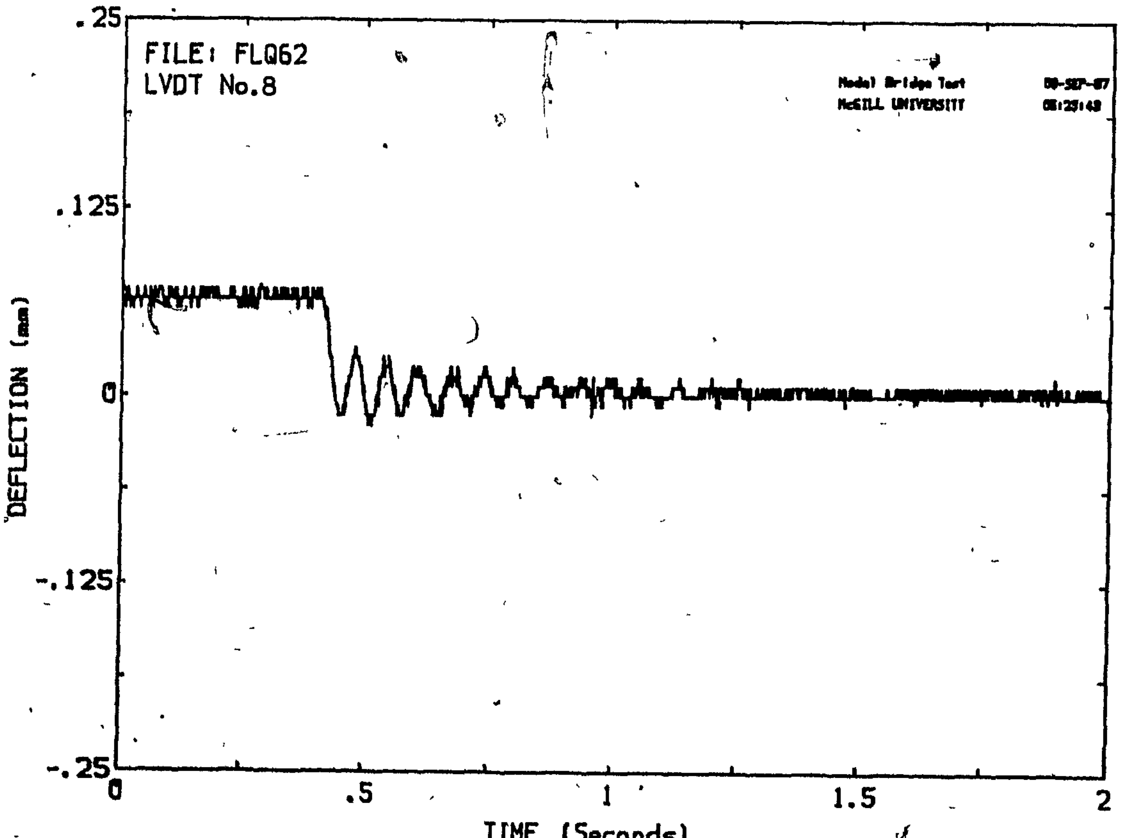

Figure 6.41 FLEXURAL TEST WITH 6 TRUCK LOADS. L.V.D.T No.8.

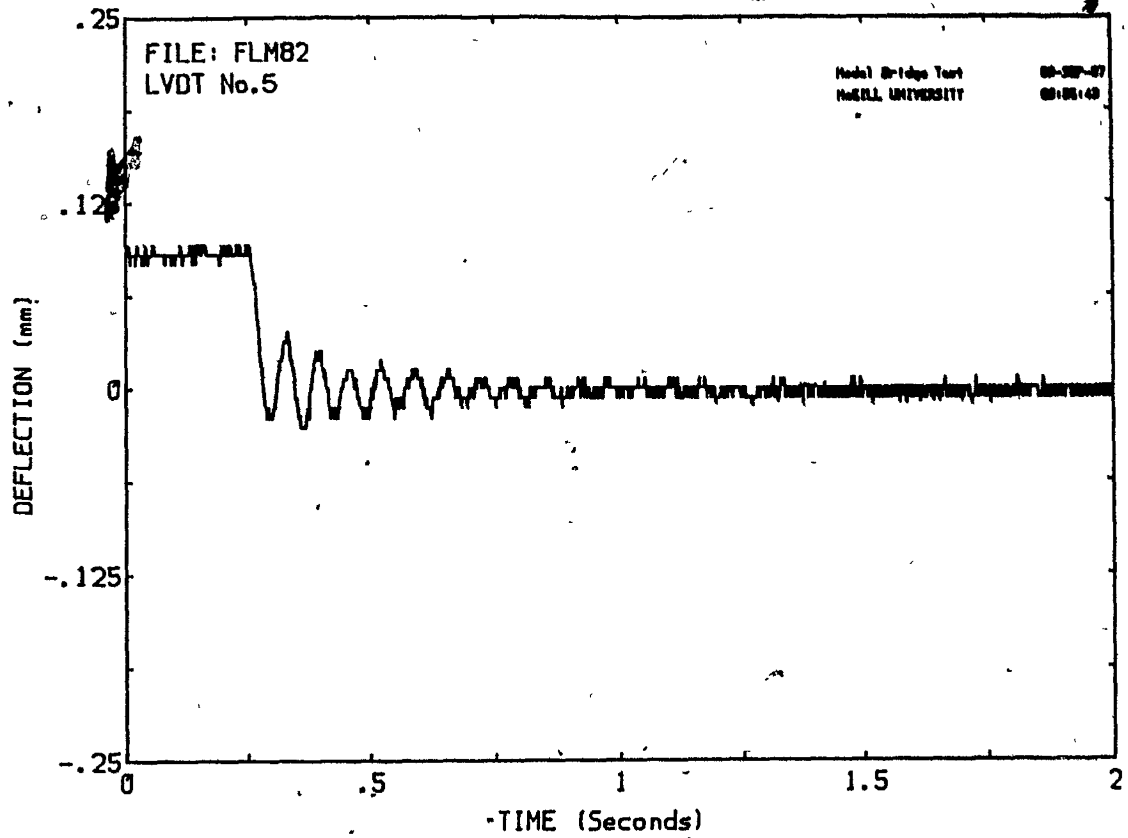

Figure 6.42 FLEXURAL TEST WITH 8 TRUCK LOADS. L.V.D.T No.5.

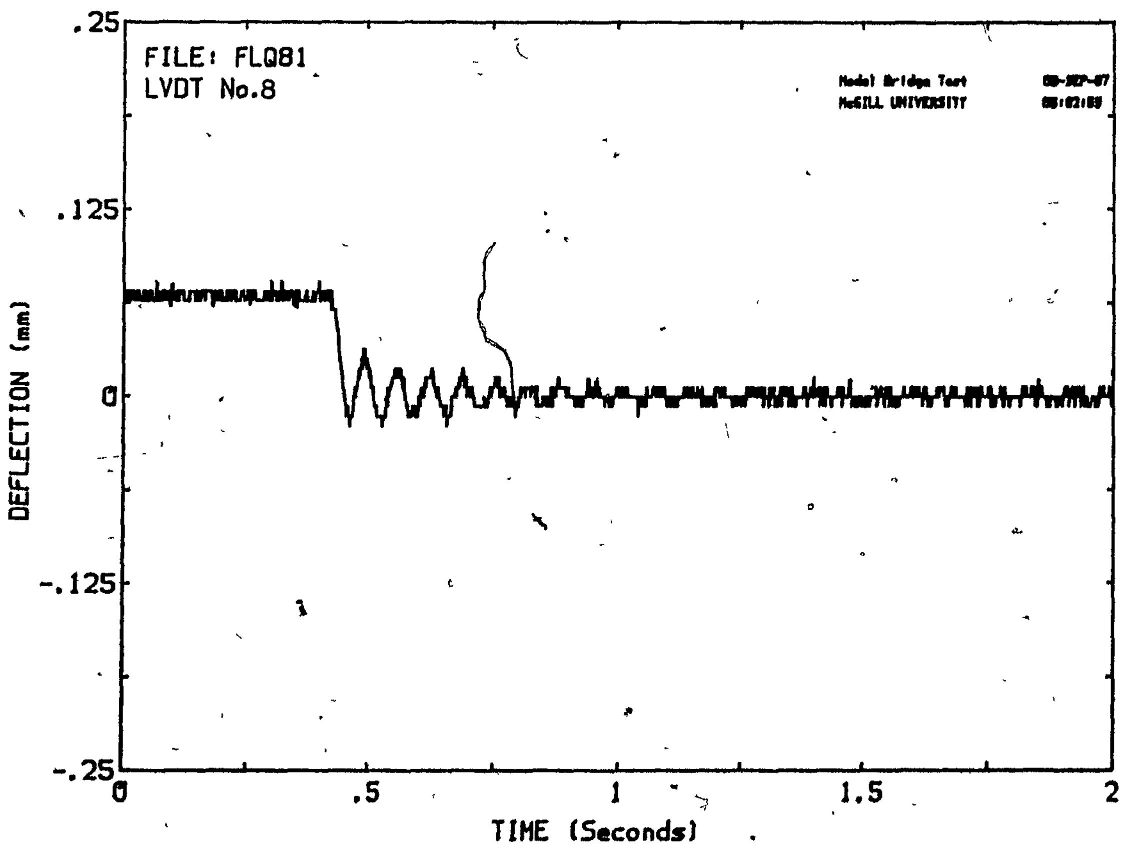

Figure 6.43 FLEXURAL TEST WITH 8 TRUCK LOADS. L.V.D.T No.8.

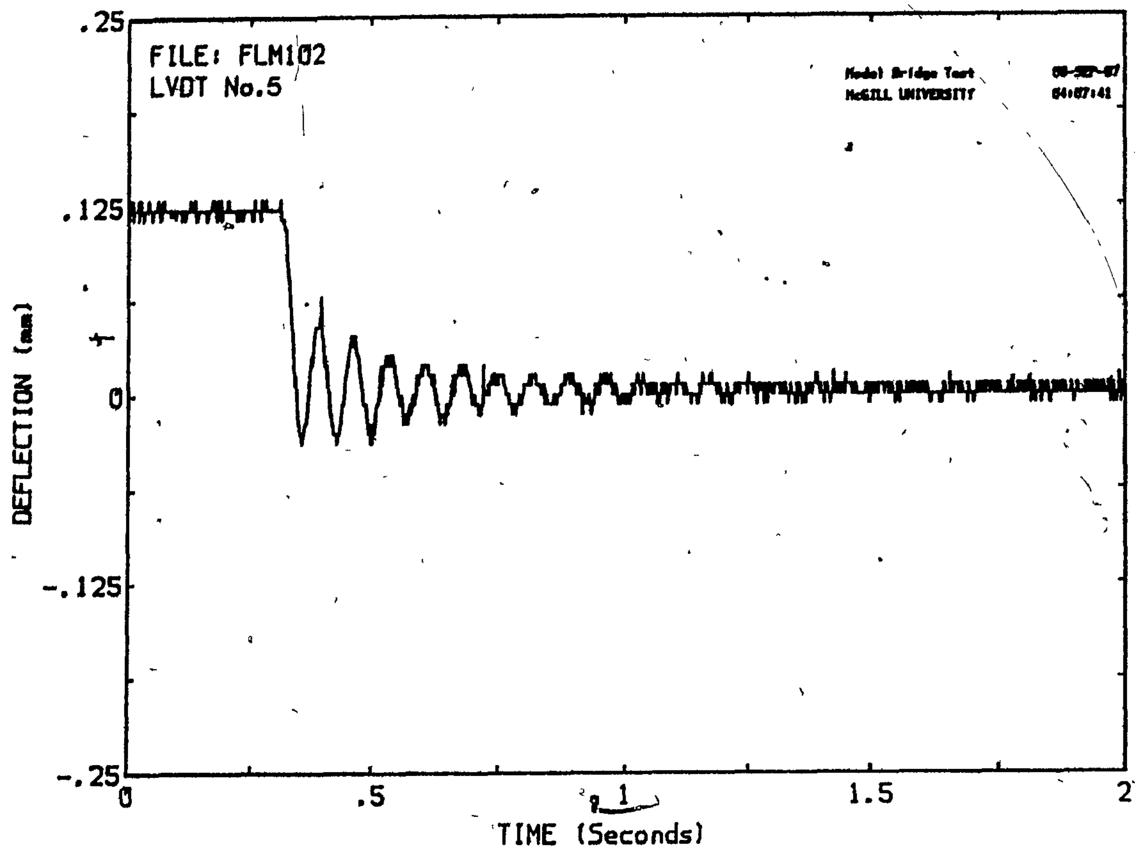

Figure 6.44 FLEXURAL TEST WITH 10 TRUCK LOADS. L.V.D.T No.5.

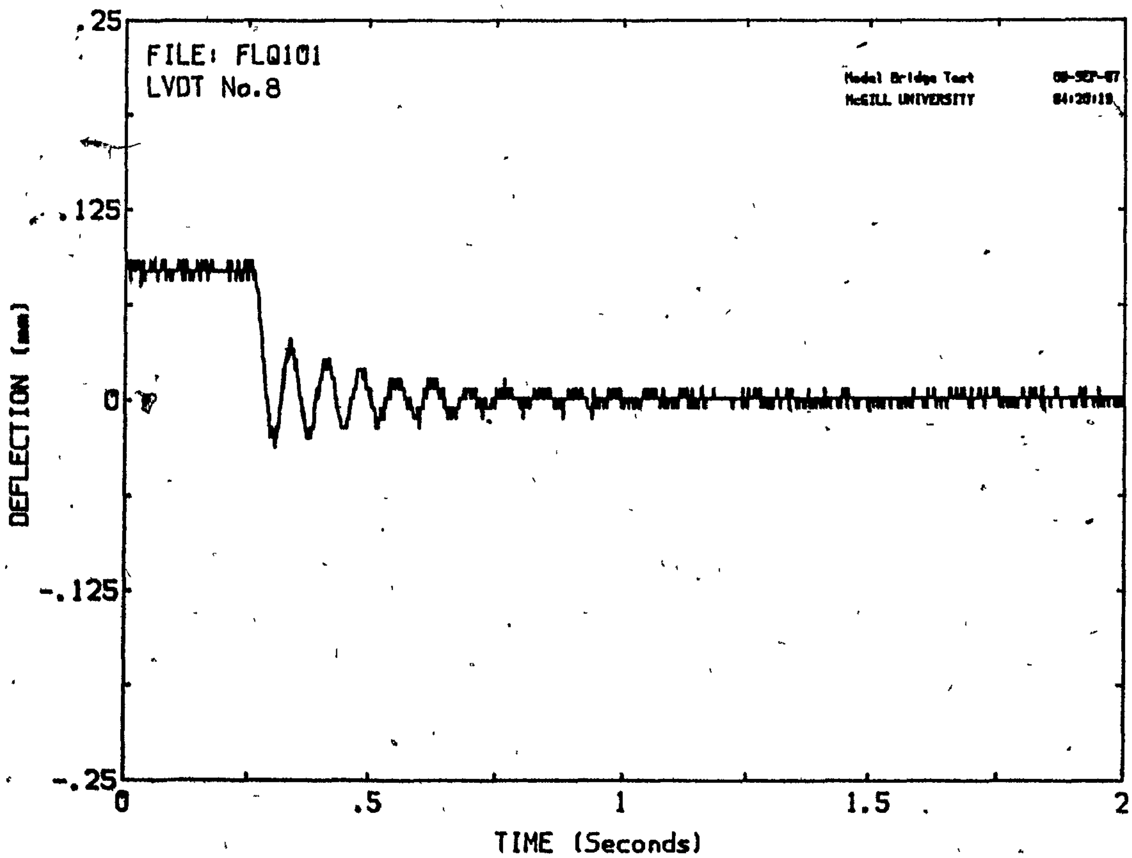

Figure 6.45 FLEXURAL TEST WITH 10 TRUCK LOADS. L.V.D.T No.8.

stage, the structure was severely cracked and the prestressing wires had yielded. The observed mode of vibration was flexural. Also, it was noted that, during all of the tests, the vibrations got damped after a short interval of about 2 seconds. The SAP IV program was used to calculate the first 6 modes of vibrations at different levels of damage. Table 6.3 shows the first experimental natural frequency of vibration with the corresponding analytical values given by the SAP IV program at different levels of loadings. These values were ploted and shown in Fig.6.46. Good agreement was found between experimental and analytical results.

NUMBER OF TRUCKS	EXPERIMENTAL NATURAL FREQUENCY (Hz)	ANALYTICAL NATURAL FREQUENCY (Hz)	DIFFERENCE (%)
0	15.61	15.49	.70
2	15.61	15.49	.70
4	14.50	14.89	2.4
6	13.54	12.82	5.3
8	12.69	11.30	10.95
10	11.95	9.69	18.91

TABLE 6.3 NATURAL FREQUENCY OF VIBRATION (FLEXURE TESTS).

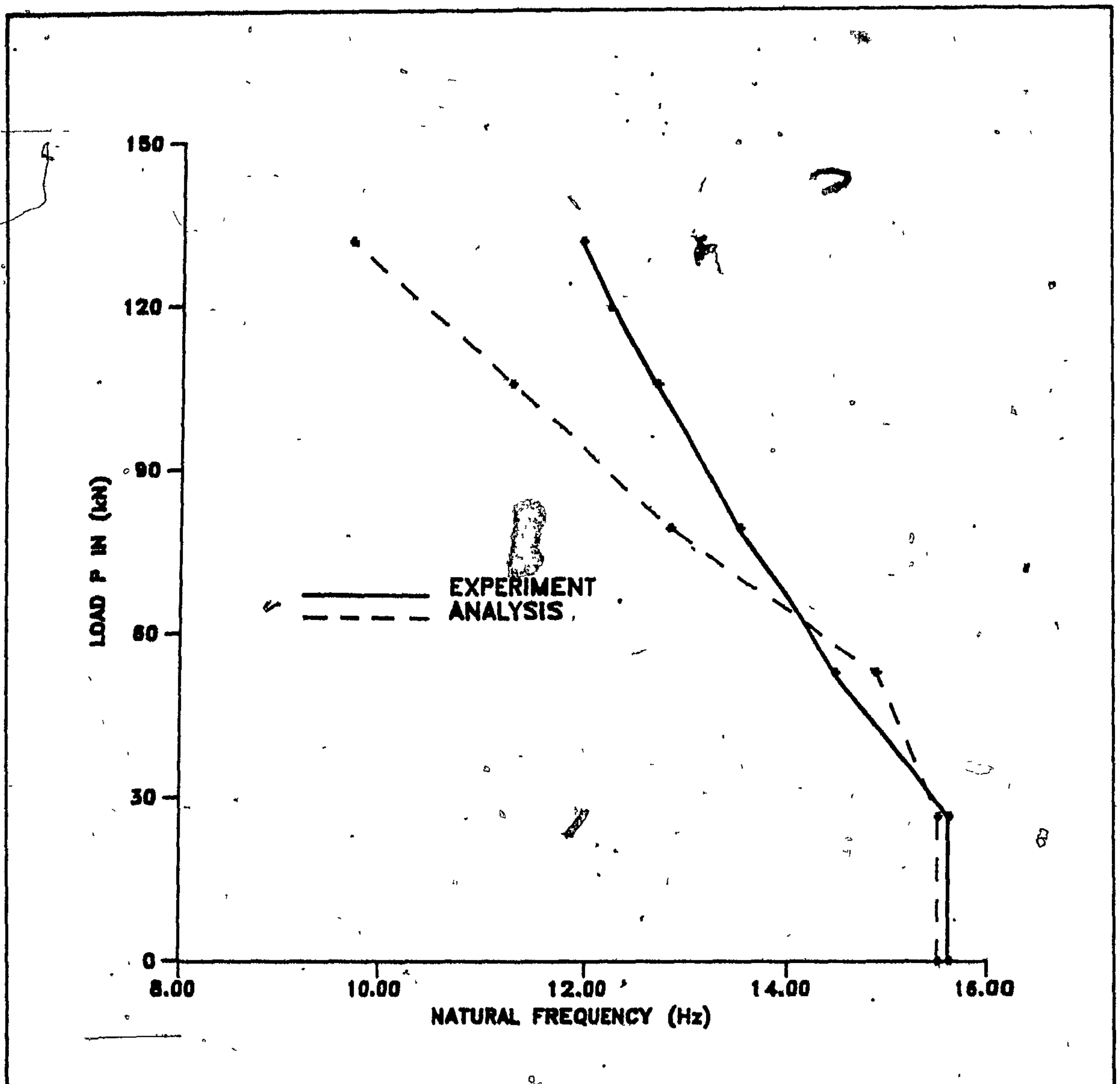

Figure 6.46 VARIATION OF THE NATURAL FREQUENCY AT DIFFERENT LEVELS OF DAMAGE

6.3.1.2 DAMPING RATIO

6.3.1.2.1 EVALUATION OF THE DAMPING RATIO

The damping ratio can be evaluated by using the simplest and most frequently used experimental method which consists of measurement of the decay of free vibrations. When a system is set into free vibrations, the damping ratio can be determined from the ratio of the two displacement amplitudes, U_n and U_{n+m}, measured at an interval of m cycles. The damping ratio is given by the equation :

$$\zeta = \frac{\delta_m}{2.\pi.m\ [\ \omega/\omega_D\ ]} \tag{6.1}$$

where $\delta_m = \ln\left(\frac{U_n}{U_{n+m}}\right)$ represents the logarithmic decrement, and ω and ω_D are the undamped and damped frequencies, respectively.

In most practical structures, the values of ω and ω_D normally differ by about 2 %. A negligible error is introduced in the value of the damping ratio ζ by assuming $\omega = \omega_D$ to simplify the calculations. With this approximation, equation (6.1) then becomes:

$$\zeta = \frac{\delta_m}{2.\pi.m} \tag{6.2}$$

6.3.1.2.2 EXPERIMENTAL DAMPING RATIO

The damping ratio of the bridge model at different load levels was calculated using the above method and the data obtained from the 9 L.V.D.T's. The average damping ratio for the uncracked bridge worked out to be 2.20 %.

At a load level corresponding to 8 times the truck loads, the damping ratio was equal to 5.9 %. At this stage, the structure was severely cracked and the prestressing wires had yielded but without the loss of all the prestressing.

Newmark and Hall [27] estimated that the damping ratio, for a prestressed structure, is normally between 2 and 3 per cent at working load level, not exceeding half the yield level load, between 5 and 7 per cent at or just below yield point without complete loss in prestress and between 7 and 10 per cent at yielding point with no prestress left. The experimental damping ratios at different levels of damage are summarized in Table 6.4 and are comparable with the corresponding damping ratio values suggested by Newmark and Hall. The variation of the damping ratio is shown in Fig.6.47.

LEVEL OF DAMAGE	DAMPING RATIO (%)
UNCRACKED	2.20
AFTER 2 TRUCKS	3.70
AFTER 4 TRUCKS	4.70
AFTER 6 TRUCKS	5.00
AFTER 8 TRUCKS	5.91
AFTER 10 TRUCKS	7.64

TABLE 6.4 VARIATION OF THE DAMPING RATIO AT DIFFERENT LEVELS OF DAMAGE.

6.3.1.3 VARIATION OF THE FLEXURAL RIGIDITY

The flexural rigidity of the bridge model was determined using the simple beam theory, along which considers the bridge as a beam with a uniformly distributed mass along the length and assumes that the flexural rigidity EI is constant along the span at any loading condition. In this case, the frequency of the first mode of vibration of

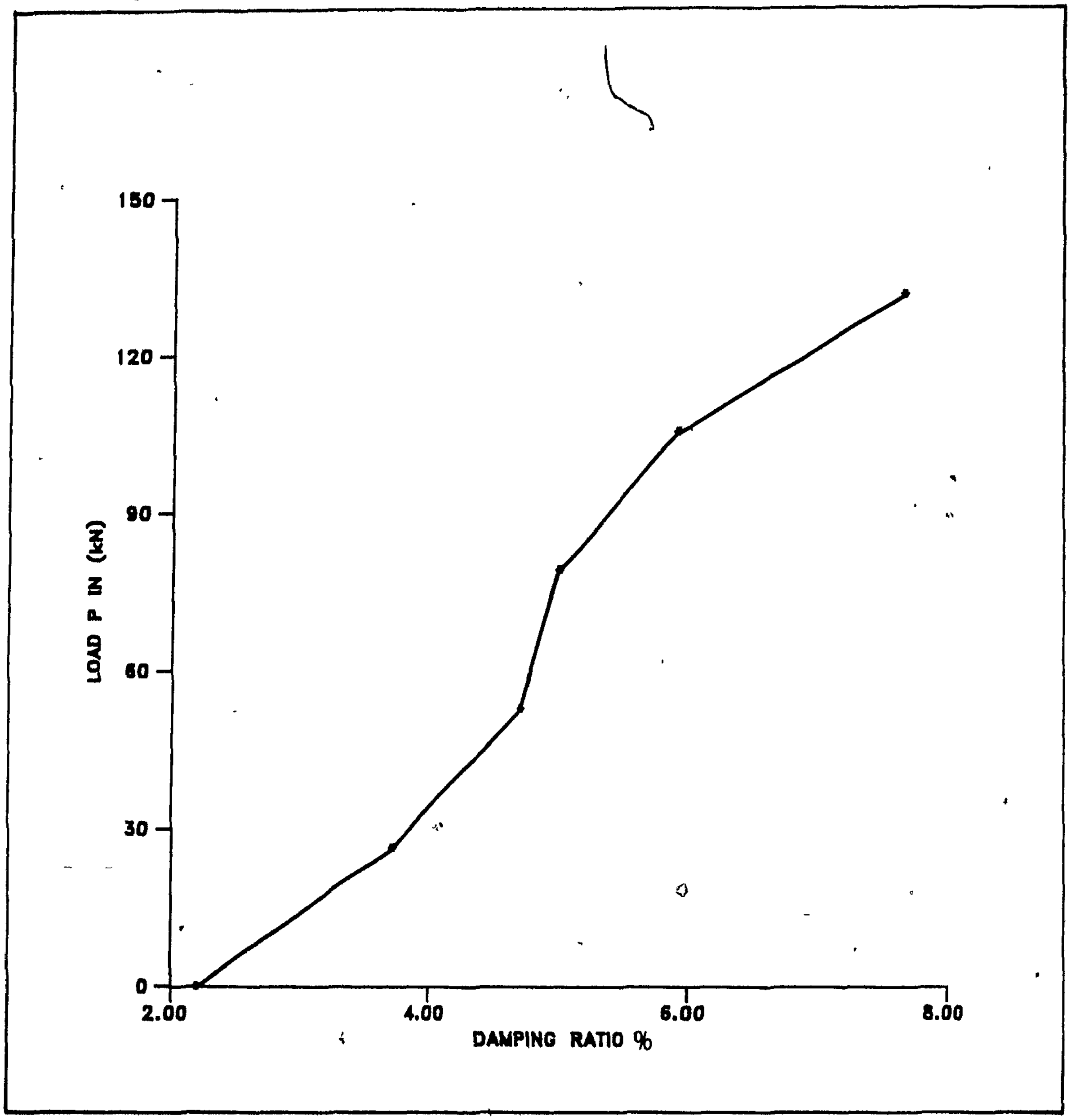

Figure 6.47 VARIATION OF THE DAMPING RATIO AT DIFFERENT LEVELS OF LOADS

the bridge is given by:

$$\omega_1^2 = \pi^4 \frac{EI}{m.L^4} \tag{6.3}$$

where L is the span length

and m is the uniformly distributed mass.

Using equation (6.3), the variation of the flexural rigidity has been calculated and tabulated in Table 6.5. These results are shown in Fig.6.48. Good agreement was found between the calculated and the experimental flexural rigidity of the bridge model.

6.3.2 TORSIONAL VIBRATION TESTS

A mass of 230 kg was suspended at midspan by a mild steel wire of 1.75 mm diameter at an eccentricity of 560 mm from the centerline of the bridge. By cutting the wire, the bridge was set into free vibrations, which got damped rapidly. A combination of flexural and torsional deformations was observed as the mode of vibration. Some of the data obtained from the responses of the 9 L.V.D.T's are shown in Figures 6.49 to Figure 6.60.

6.3.2.1 NATURAL FREQUENCIES OF VIBRATIONS

The torsion tests performed on the uncracked bridge set it into free vibrations are shown in Figures 6.49 and

NUMBER OF TRUCK	EXPERIMENTAL NATURAL FREQUENCY (rad/sec)	FLEXURAL RIGIDITY	EXPERIMENTAL FLEXURAL RIGIDITY
0	98.11	EI	EI
2	98.11	EI	0.90 EI
4	91.10	0.86 EI	0.76 EI
6	85.03	0.75 EI	0.65 EI
8	79.72	0.66 EI	0.57 EI
10	75.07	0.59 EI	0.33 EI

TABLE 6.5 VARIATION OF THE FLEXURAL RIGIDITY WITH THE LEVEL OF DAMAGE

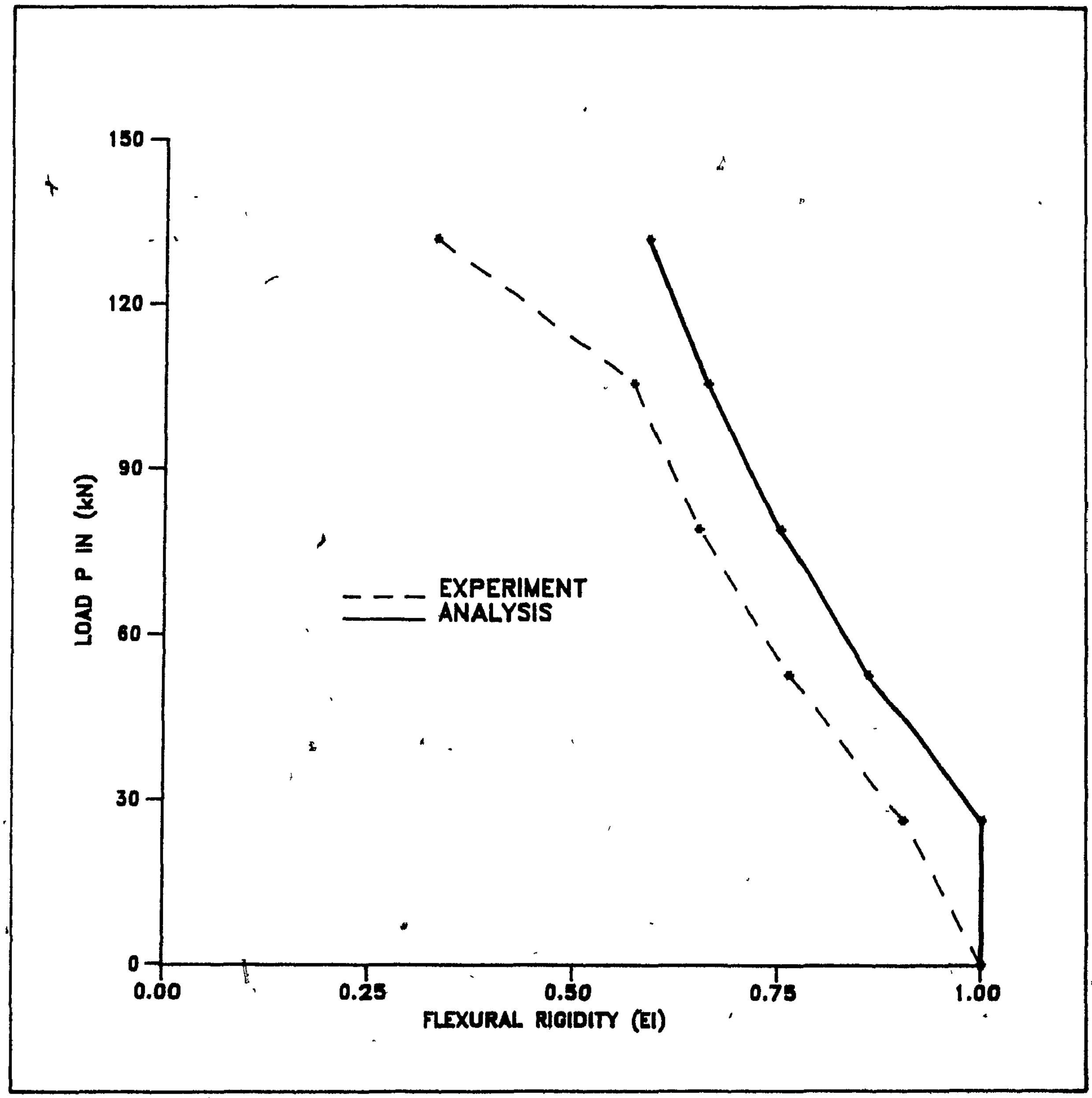

Figure 6.48 VARIATION OF THE FLEXURAL RIGIDITY WITH THE LEVEL OF DAMAGE

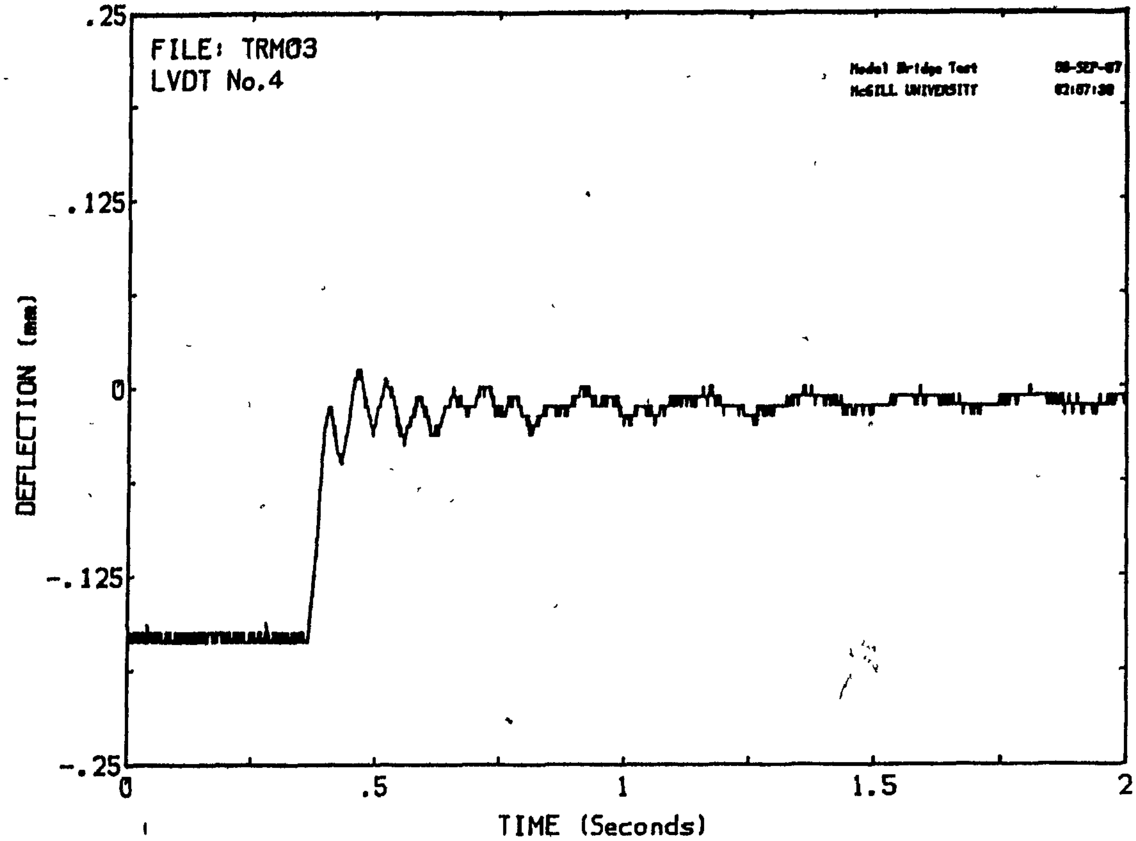

Figure 6.46 TORSIONAL TEST (UNCRACKED BRIDGE). L.V.D.T No.4.

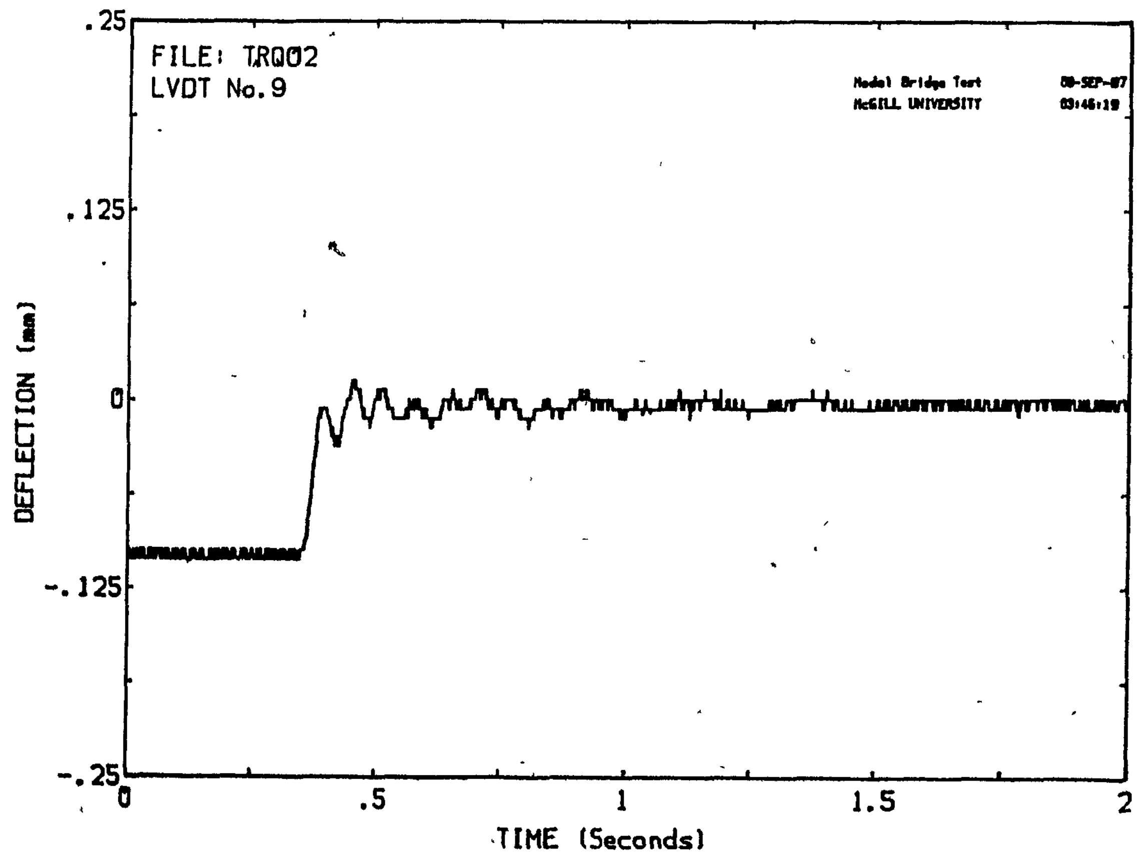

Figure 6.47 TORSIONAL TEST (UNCRACKED BRIDGE). L.V.D.T No.9.

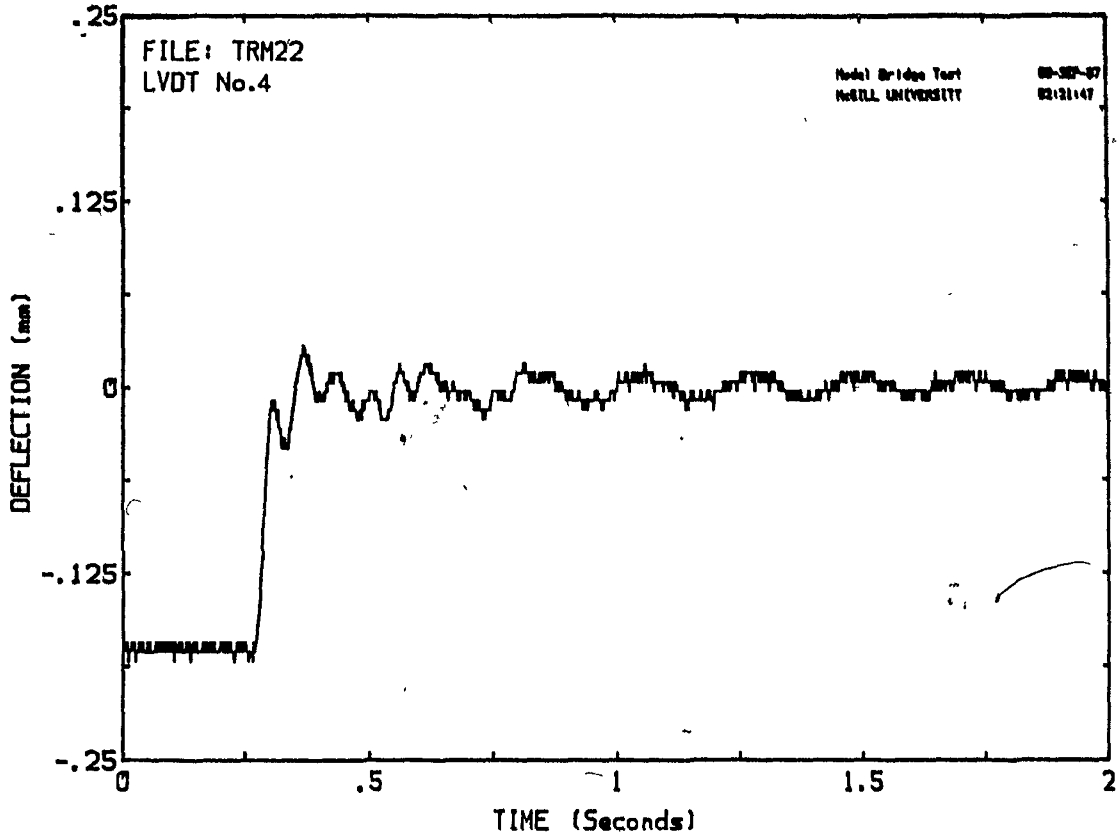

Figure 6.48 TORSIONAL TEST WITH 2 TRUCK LOADS. L.V.D.T No.4.

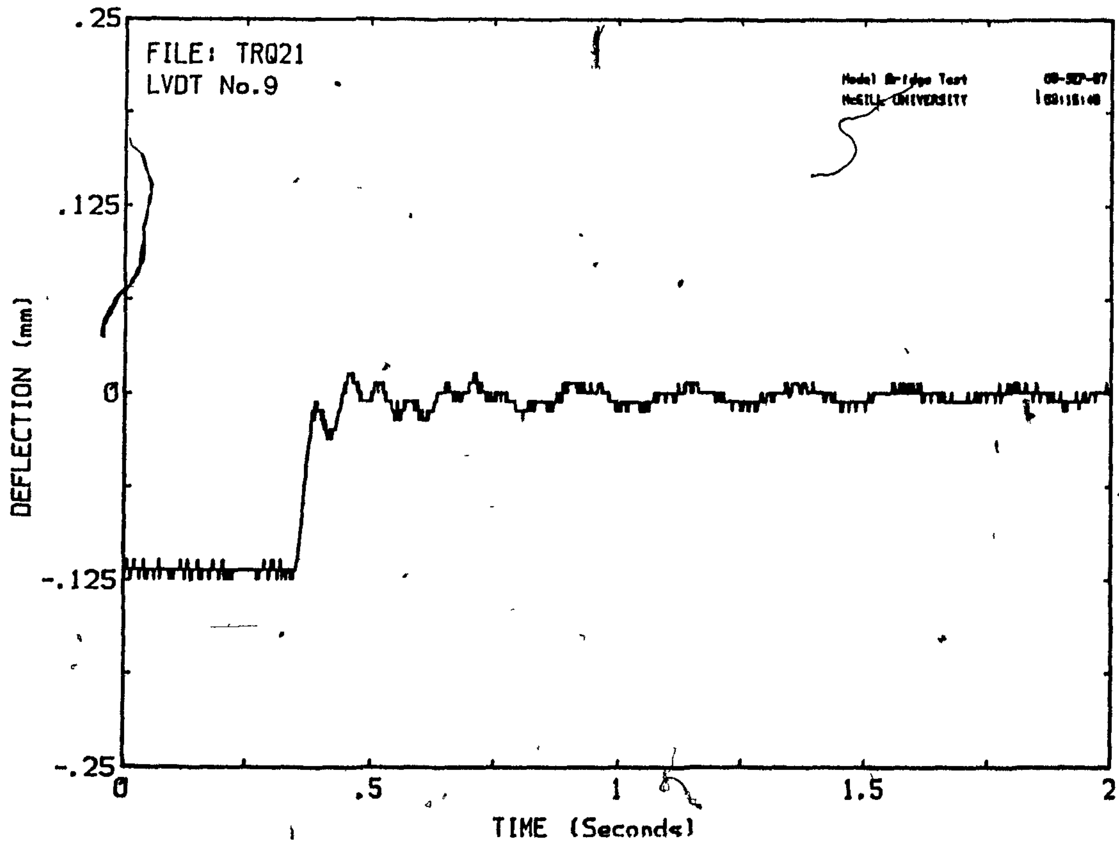

Figure 6.49 TORSIONAL TEST WITH 2 TRUCK LOADS. L.V.D.T No.9.

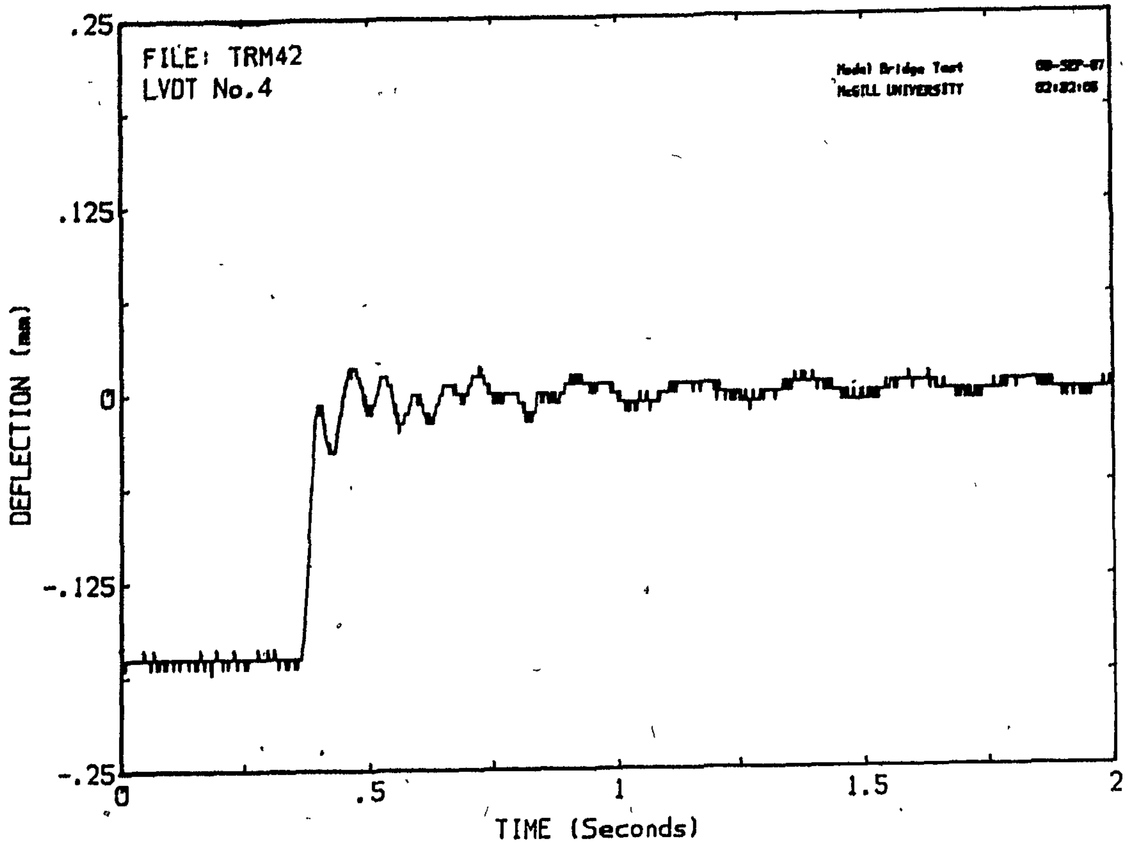

Figure 6.50 TORSIONAL TEST WITH 4 TRUCK LOADS. L.V.D.T No.4.

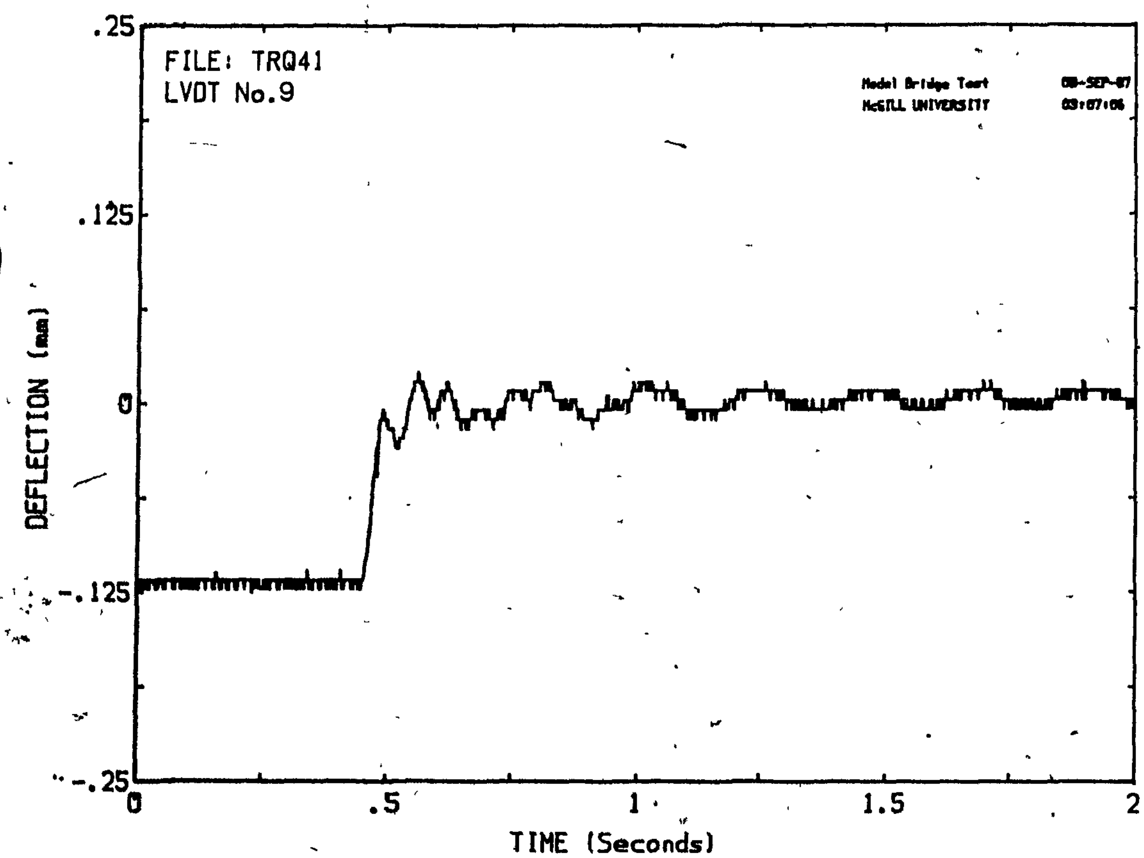

Figure 6.51 TORSIONAL TEST WITH 4 TRUCK LOADS. L.V.D.T No.9.

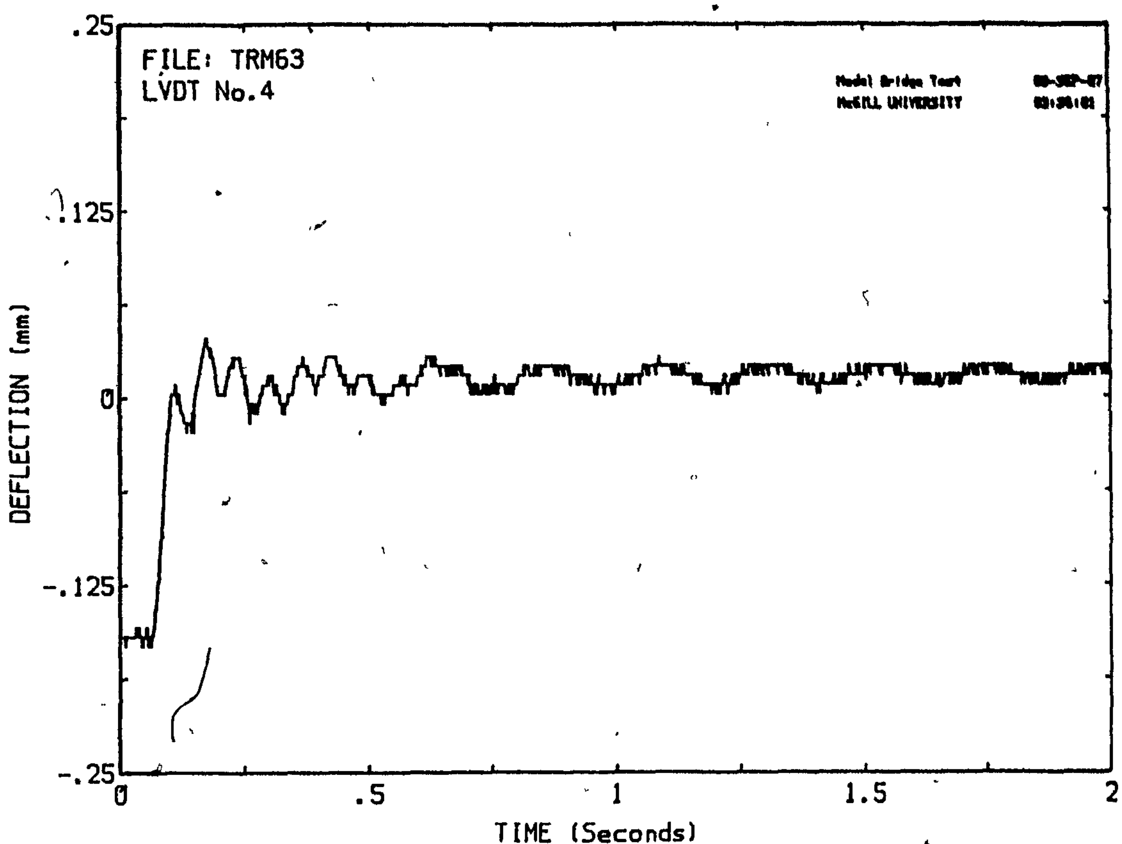

Figure 6.52 TORSIONAL TEST WITH 6 TRUCK LOADS. L.V.D.T No.4

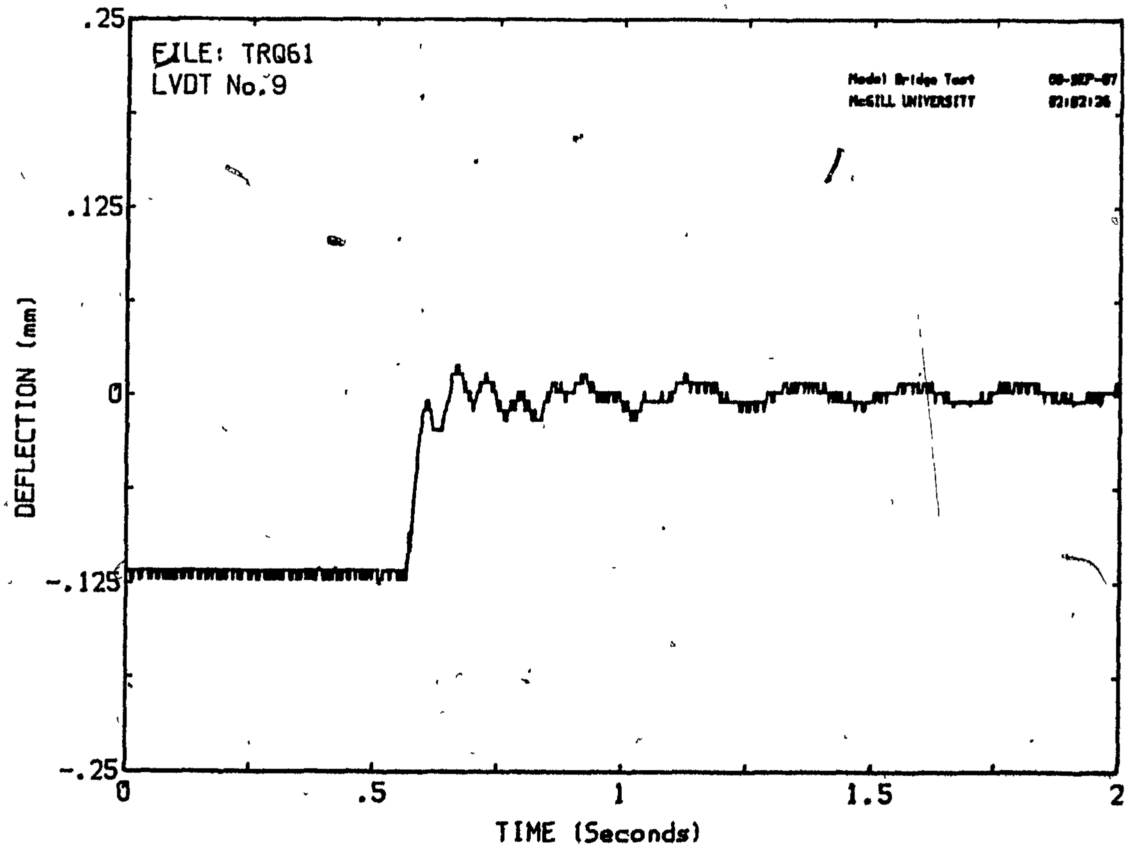

Figure 6.53 TORSIONAL TEST WITH 6 TRUCK LOADS. L.V.D.T No.9.

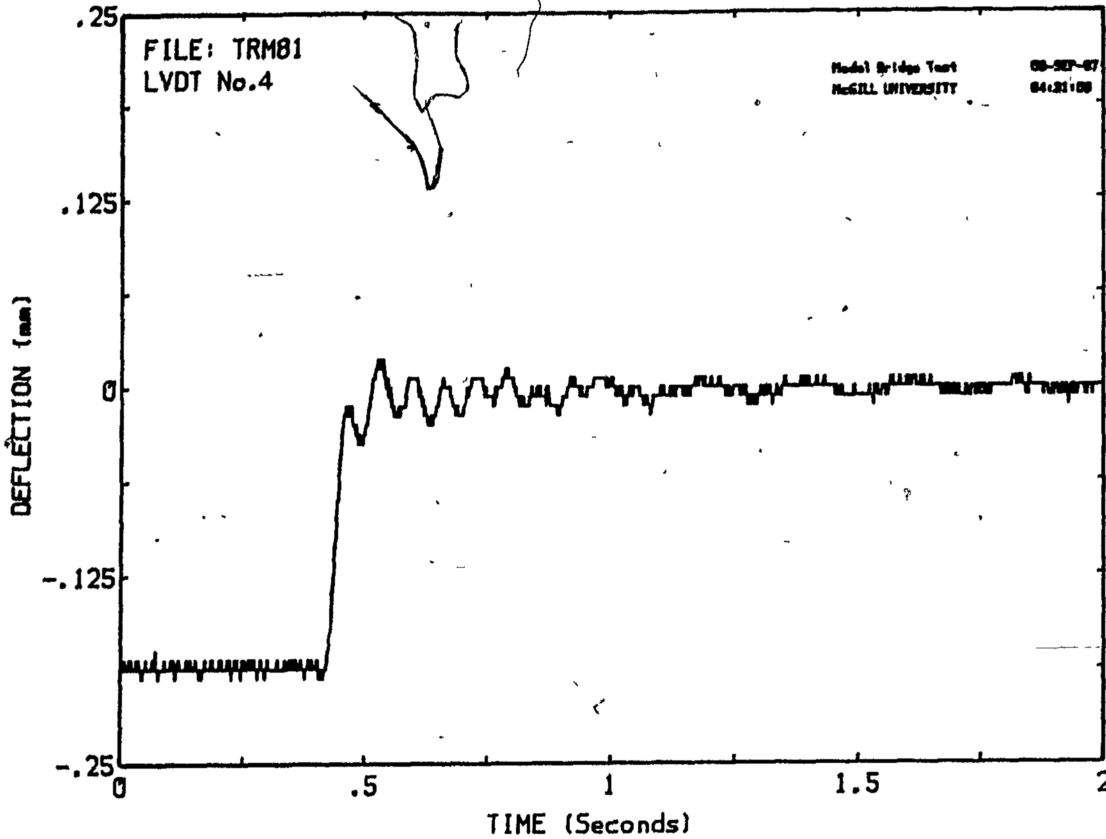

Figure 6.54 TORSIONAL TEST WITH 8 TRUCK LOADS. L.V.D.T No.4.

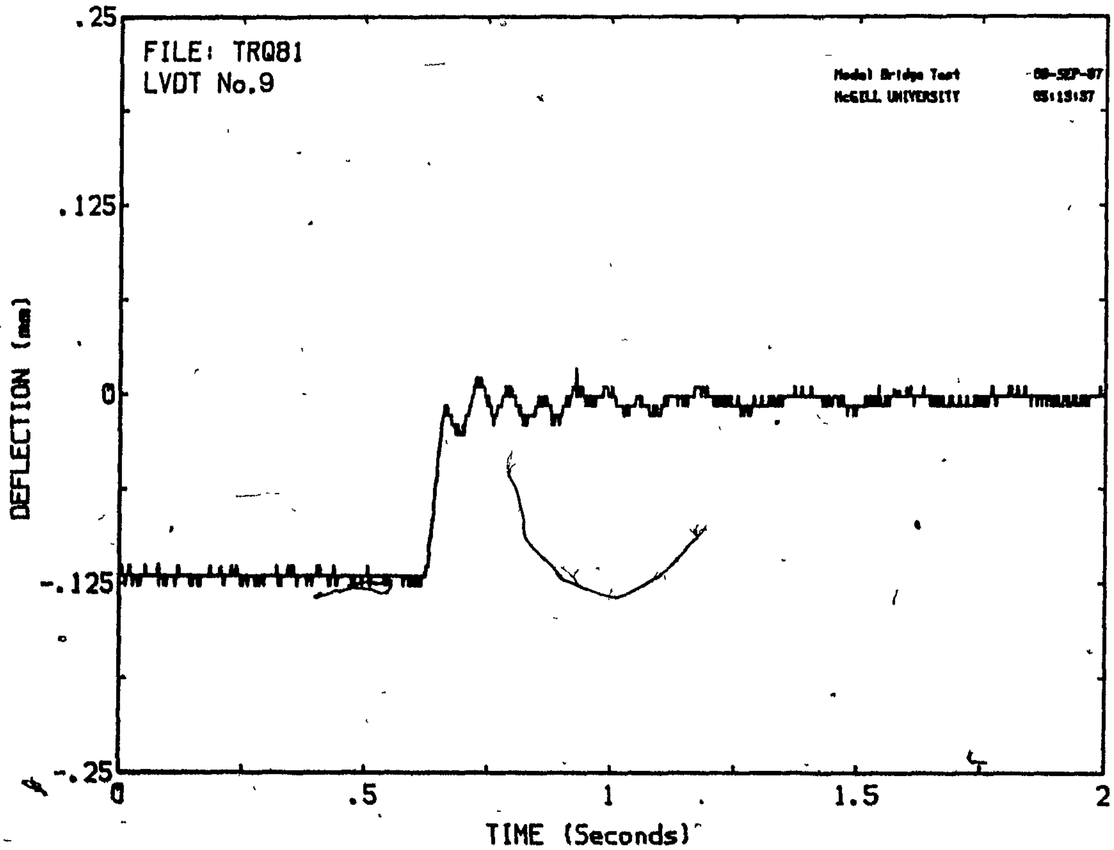

Figure 6.55 TORSIONAL TEST WITH 8 TRUCK LOADS. L.V.D.T No.9.

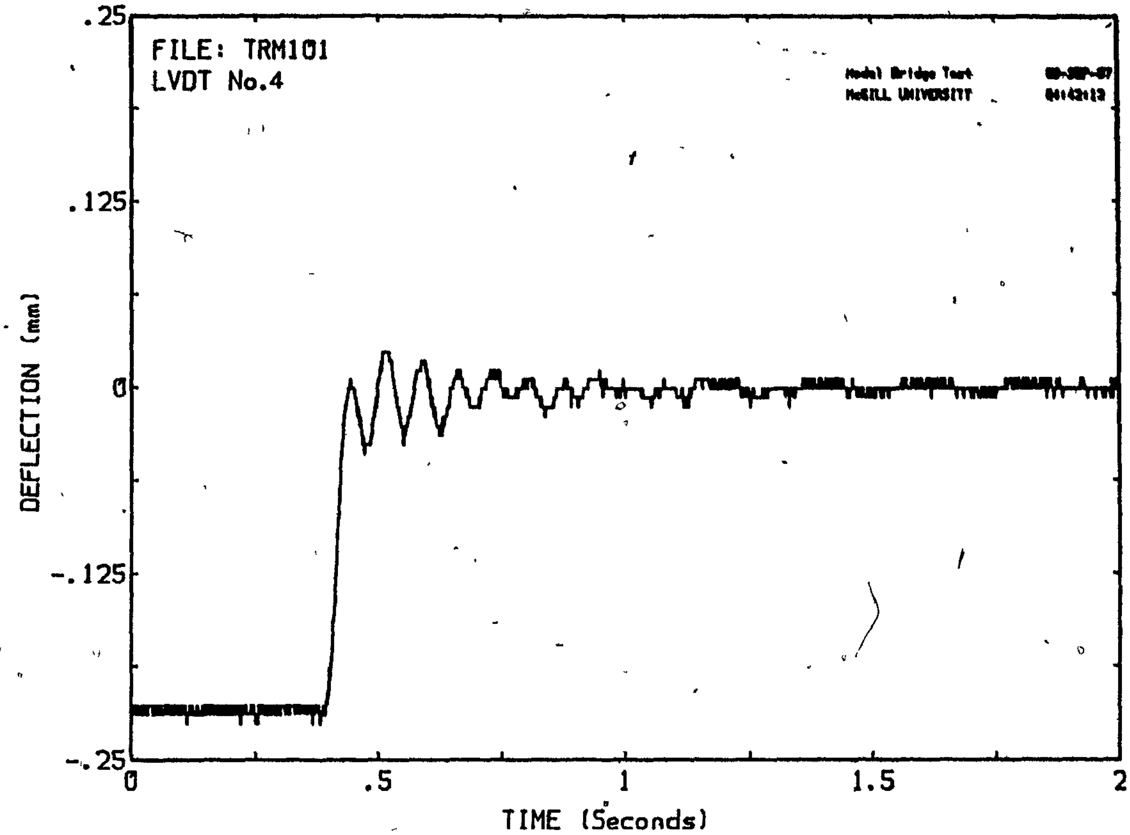

Figure 6.56 TORSIONAL TEST WITH 10 TRUCK LOADS. L.V.D.T No.4.

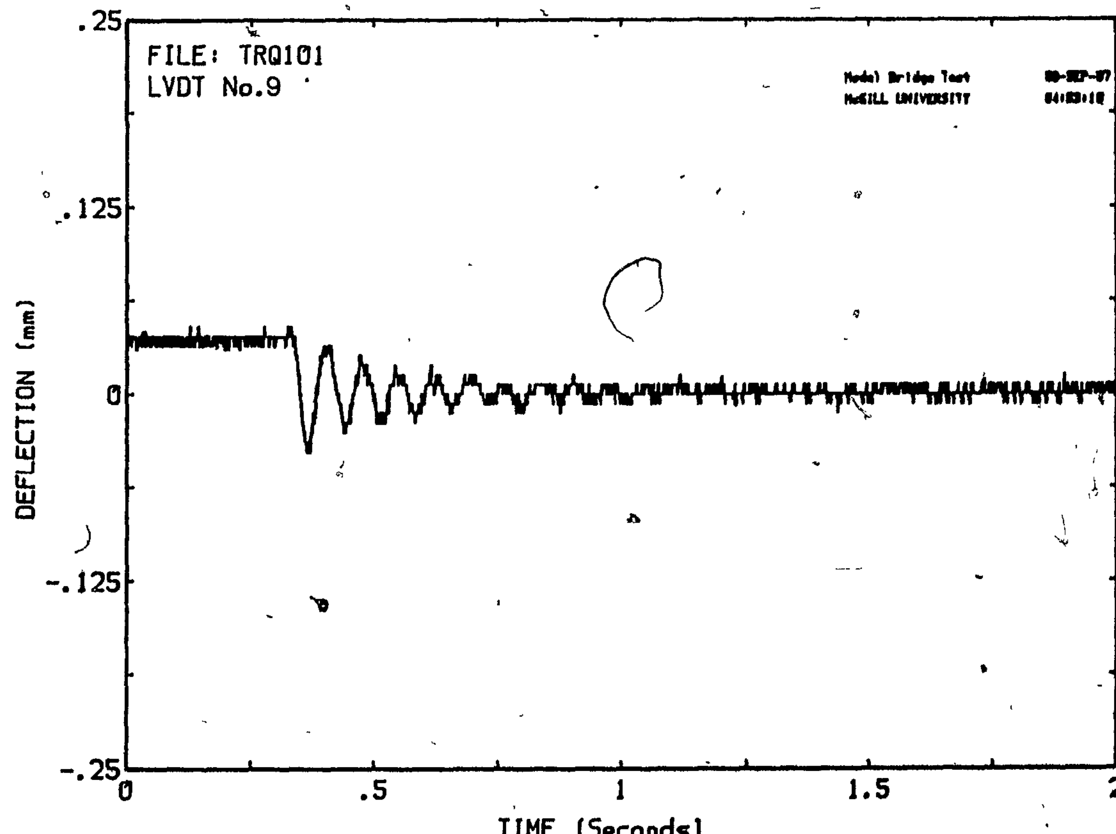

Figure 6.57 TORSIONAL TEST WITH 10 TRUCK LOADS. L.V.D.T No.9.

6.50. This data was used to derive two distinct natural frequencies of vibration as follow:

. Flexural natural frequency equal to 16.95 Hz.

. Torsional natural frequency equal to 3.52 Hz.

All of the flexural natural frequencies of vibration of the bridge model corresponding to the loading case of 2, 4, 6, 8 and 10 times the truck loads are summarized in Table 6.6.

During all of the torsion tests performed on the bridge model, it was observed that the flexural response was more dominant.

LEVEL OF DAMAGE	EXPERIMENTAL NATURAL FREQUENCY OF VIBRATION (Hz)
UNCRACKED	16.05
2	15.95
4	14.72
6	13.92
8	13.13
10	12.19

TABLE 6.6 NATURAL FREQUENCIES OF VIBRATION.

CHAPTER 7

CONCLUSIONS AND SUGGESTED AREAS FOR FURTHER RESEARCH

The results of this experimental-analytical study of the structural behaviour of the two-cell, prestressed concrete box girder bridge can be summarized as follows:

1. The model bridge studied was quite stiff. It behaved linearly up to approximately 1.8 times the service loads corresponding to 2 times the Ontario Highway Bridge Design Code model truck load and showed no signs of cracking. The deflection at the service load level corresponding to 2 truck loads at midspan was very small and the deflection/span ratio was approximately 1/4400.

2. The bridge model was able to resist an ultimate load equal to 10 times the truck load showing clearly the significant reserve strength of the prestressed concrete box girder bridge.

3. The flexural stiffness of the bridge model decreased with an increase in the applied load due to the formation and propagation of cracks and inelasticity of the concrete. When flexural cracks appeared at midspan, the prestressing steel was highly strained and the flexural stiffness of the structure decreased by approximately 30 %. The structure failed in flexure as expected.

4. The longitudinal and transverse stress distibution at the top and bottom slab were not uniform but symmetrical about the centerline of the structure showing the ability of the box girder section to distribute the applied truck load in the transverse direction.

5. Under the symmetrical truck loading, for the cases of 2, 4, 6, 8 and 10 trucks, the transverse stresses at midspan and quarterspan sections were about 10 % to 20 % of the longitudinal stress at the same locations.

6. Reasonable agreement was found between the first flexural natural frequencies of vibration observed in the physical and the computed model at different levels of damage. Under eight and ten truck loads, the natural frequency of vibration was observed to decrease by about 20 %. The structure had then severely cracked and the prestressing steel had yielded.

7. The experimental results obtained from tests performed on the box girder bridge model proved that the physical model is an adequate tool to predict the linear and nonlinear static and dynamic responses of reinforced and prestressed concrete box girder bridges.

8. The quasi-nonlinear finite element analysis using the SAP IV program which was conducted by incorporating the experimental data on the number, orientation and width of cracks in developing the stiffness matrix on each element, worked out to be an adequate, inexpensive method to study the behaviour of the prestressed concrete box girder bridge

under static and dynamic loadings at higher load levels.

9. Good agreement was found between the static responses of the analytical model using the NONLACS program and the physical model at every load level. At the working load level, the difference between the results was approximately 5 % to 10 % and at higher level (8 truck loads) about 15 % to 25 %. Under the symmetrical truck loading, the NONLACS program proved to be an adequate nonlinear method for the investigation of the static responses of reinforced and prestressed concrete box girder bridges at higher load levels.

10. The box girder bridge model had shown a good reserve of strength (10 times the truck load); the design codes appear to be a little conservative.

SUGGESTED AREAS FOR FURTHER RESEARCH

The experimental-analytical investigation conducted on a 1:7 scale direct model generated useful results for the nonlinear static and dynamic responses of a simply supported, two- cell, prestressed concrete box girder bridge. The data obtained from tests performed on this physical model should impove the understanding of the nonlinear response of a box section bridge and the variation of the dynamic characteristics of the structure, such as the damping ratio and the fundamental natural frequency, at different levels of damage which are relatively new in the field.

Experimental research using small scale direct models is strongly recommended to develop more data on the nonlinear dynamic response of multi-cell box girder bridges.

The use of improved finite element analysis programs such as the NONLACS program which takes into account all of the material properties, shrinkage and creep effects, can be useful for the study of the nonlinear response of box section bridges.

REFERENCES

1. American Association of State and Highway Transportation Officials (AASHTO), "Standard Specifications for Highway Bridges", 12th Edition, AASHTO, Washington, 1977.

2. American Concrete Institute, ACI 318-1971, "Building Code Requirements for Reinforced Concrete", Detroit, Michigan, 1971.

3. Bathe, K.J., Wilson, E.L and Peterson, F.E., "SAP IV- A Structural Analysis Program for Static and Dynamic Response of Linear Systems ", Earthaquake Engineering Research Center, Report No. EERC 73-11, University of California, Berkeley, April 1974.

4. Billing, J.R., "Dynamic Loading and Testing of Bridges in Ontario, 1980", Proceedings of International Conference on Short and Medium Span Bridges, Toronto, August 1982, pp. 125-139.

5. Campbell, T.I. and Batchelor, B.de V., " Load Testing of Model Two-Span Continuous Prestressed Concrete Trapezoidal Bridge Girder", Journal of Prestressed Concrete Institude, Vol.22, November-December 1977, pp. 62-79.

6. Canadian Institute of Steel Construction, " Handbook of Steel Construction", CISC, Fourth Edition. Willowdale, Ontario, 1985.

7. Cheung, M.S, Gardner, N.J. and Ng, S.F. , " Load Distribution Characteristics of Slab-on-Girder Bridges at Ultimate", Proceedings of the Second International Conference on Short and Medium Span Bridges, Vol. 2, Ottawa, August 1986, pp.461-485.

8. Canadian Standard Association, "Code for the Design of Concrete Structures for Buildings, CAN3-A23.3-M84", Canadian Standards Association, Rexdale, Ontario, 1984.

9. Canadian Standard Association, "Design of Highway Bridges, Standard CAN3-S6-M78", Canadian Standards Association, Toronto, 1978.

10. Conrad, P., Heins, M., and Sahin, M.A., "Natural Frequency of Curved Box Girder Bridges", ASCE, Journal of the Structural Division, Vol.105, ST-12, December 1979, pp. 2591-2600.

11. Clough, R.W. and Penzien, J.,"Dynamics of Structures", McGraw-Hill Book Company, New York, 1975.

12. Cordoba, R.A., " Behaviour of Open Web Precast Bridge Girder- Experimental Study ", M. Eng. Thesis, Department of Civil Engineering and Applied Mechanics, McGill University, Montreal, August 1974.

13. Coutie, M.G., Davies, G. and Wyatt, M.J., "Shear Lag Effects in Box Girder Bridges of Varying Depth ", Proceedings of Second International Conference on Short and Medium Span Bridges, Volume 2, Ottawa, August 1986, pp. 399-413.

14. Cussens, A.R., and Pama, R.P., "Bridge Deck Analysis", John Wiley & Sons Ltd., Bristol, England, 1975.

15. Fam, A.R., "Static and Free Vibration Analysis of Curved Box Bridges" Ph.D. Thesis, Department of Civil Engineering and Applied Mechanics, McGill University, Montreal, March 1973.

16. Ferdjani, O.," Behaviour of a One-Cell Prestressed Concrete Box Girder Bridge - Analytical Study", M.Eng. Thesis, Department of Civil Engineering and Applied Mechanics, McGill University, Montreal, March 1987.

17. Ghoneim, G.A.M. and Ghali, A., "Nonlinear Analysis of Concrete Structures", Canadian Journal of Civil Engineering, Vol.9, No.3, September 1982, pp. 489-501.

18. Hadj-Arab, A.,"Behaviour of a One-Cell Prestressed Concrete Box Girder Bridge-Experimental Study", M.Eng. Thesis, Department of Civil Engineering and Applied Mechanics, McGill University, Montreal, March 1987.

19. Huang, T., "Vibration of Bridges", Shock and Vibration Digest, Volume 8, No.3, Abstracts 1-948, March 1976, pp. 61-76.

20. Inomata, S., "Japanese Practice in Seismic Design of Prestressed Bridges" , Journal of Prestressed Concrete Institute, Vol.17, No.4, July-August 1972, pp.76-85.

21. Khaled, A., "Behaviour of a Two-Cell Prestressed Conrete Box Girder Bridge-Analytical Study", M.Eng. Thesis, Department of Civil Engineering and Applied Mechanics, McGill University, Montreal, January 1988.

22. Maisel, B.I., "Review of Literature Related to the Analysis and Design of Thin-Walled Beams", Technical Report No.42 Cement and Concrete Association, London, July 1970

23. Maisel, B.I., Rowe, R.E. and Swan, R.A., " Concrete Box-Girder Bridges ", The Structural Engineer, London, Vol.51, No.10, October 1973, pp. 363-376.

24. Mirza, M.S., (Editor), "Structural Concrete Models." (Materials, Instrumentation, Correlation) --A State - of - the - Art Report, Department of Civil Engineering and Applied Mechanics, McGill University, Montreal, 1972, pp. 232.

25. Mirza, M.S., Manatakos, C.K., Murali, R.D., Igwemezie, J.O., Wyzykowski, J., "An Analytical - Experimental Study of the Behaviour of a Composite Concrete Deck - Steel Box Girder Bridge", Report Prepared for Public Works Canada, Department of Civil Engineering and Applied Mechanics, McGill University, Montreal, March 1985.

26. Mirza, M.S, "Bond in Reinforced Concrete Models", Proceedings of the Institute of Structural Engineers (Building Research Establishment, Seminar on Reinforced and Prestressed Micro-Concrete Models, Garston, England, May 1978.

27. Newmark, N.M., Hall, W.J.,"Earthquake Spectra and Design", Earthquake Engineering Research Institute, Pasadena, California, March 1982.

28. Norris, C.H., Hanson, R.J., Holly, M.J., Biggs, J.M., Namyek, S., Minami, J.K., "Structural Design for Dynamic Loads.", McGraw-Hill Book Company, New York, 1959.

29. Ontario Ministry of Transportation and Communication, "1983 Ontario Highway Bridge Design Code and Commentary", Highway Engineering Division, Ontario Ministry of Transportation and Communications, Toronto, 1983.

30. Pang, C.L., "Reliability of Models in the Analysis of Prestressed Concrete Beams in Flexure", M.Eng. Thesis, McGill University, Montreal, April 1965.

31. Perry, S.H., Pinkney, M.W. and Waldron, P., "Construction and Testing to Failure of a Model Prestressed Concrete Elevated Road Junction ", Proceedings of theInternational Conference on Short and Medium Span Bridges, Toronto, August 1982, pp. 341- 355.

32. Nofal, M., "Load-Distribution in Slab Girder Bridge at Ultimate Load", M.Eng. Thesis being finalized at Department of Civil Engineering at Carleton University.

33. Sabnis, G.M., Harris, H.G., White, R.N., Mirza, M.S., "Structural Modeling and Experimental Techniques",

Prentice-Hall, Englewood Cliffs, New Jersey, 1983, 585 pp.

34. Scordelis, A.C., " Analysis of Simply Supported Box Girder Bridges ", Structural Engineering and Structural Mechanics, Report No. SESM-66-17, University of California, Berkeley, October 1966.

35. Scordelis, A.C., Bouwkamp, J.G. and Wasti, S.T., "Study of AASHTO Loadings on a Concrete Box Girder Bridge Model", Highway Research Record, No.428, July 1973, pp.22-31.

36. Scordelis, A.C., Bouwkamp, J.G. and Wasti, S.T.,"Structural Response of Concrete Box Girder Bridge", ASCE, Journal of the Structural Division, Vol.99, No.ST 7-12, October 1973, pp.2031-2048.

37. Seible, F. and Scordelis, A.C., "Non-Linear Behaviour and Failure Analysis of Multi-Cell RC Box Girder Bridges", Proceedings of the International Conference on Short and Medium Span Bridges,Toronto, August 1982, pp. 391-405.

38. Soliman, M.I., "Behaviour and Analysis of a Reinforced Concrete Box Girder Bridge", Ph.D. Thesis, Department of Civil Engineering and Applied Mechanics, McGill University, Montreal, March 1979.

39. Spiller, R.M., Kromolicki, R.E., and Danglidis, M.I., "Lateral Forces Due to Longitudinal Prestressing of Concrete Box Spine-Beam Bridges with Inclined Webs," The Structural Engineer, London, Vol. 63A, No.2, February 1985, pp. 54-57.

40. Tabba, M.M., "Free Vibrations of Curved Box Girder Bridges", M.Eng. Thesis, Department of Civil Engineering and Applied Mechanics, McGill University, Montreal, July 1972.

41. Tschanz, T., "Behaviour of Open Web Precast Bridge Girder - Analytical Study", M.Eng. Thesis, Department of Civil Engineering and Applied Mechanics, McGill University, Montreal, August 1974.

APPENDIX A

REQUIERED COMPENSATING DEAD WEIGHT

For true modeling, the similitude analysis requires that the density of the model concrete must be 7.0 times the density of the prototype concrete (see Table 2.2).

Density of prototype concrete	$= 2403\ kg/m^3$
Density of model concrete	$= 2290\ kg/m^3$
Total weight of the model bridge	$= \rho_m . A_m . L_m$
	$= 2290 \times 90384E{-}6 \times 3.53$
	$= 731\ kg$
Required density of the model for true modeling	$= 7.0 \times 2403$
	$= 16821\ kg/m^3$
Total weight of the model bridge as required for true modeling	$= 16821 \times 90384E{-}6 \times 3.5$
	$= 5368\ kg$
Additional dead weight required for true modeling of the prototype bridge	$= 4637\ kg$

The required compensating weight was divided in two parts:

(a) 1029 kg of steel plates were placed on the end blocks and 980 kg of steel billets were distributed uniformly inside the boxes.

(b) 2628 kg of concrete blocks were placed on the top slab.

8 concrete blocks of each of the following types are used:

Type A : 240 mm x 280 mm x 460 mm Size

Weight = 2403 x .24 x .28 x .46 x 8

= 594 kg

Type B : 200 mm x 420 mm x 500 mm Size

Weight = 2403 x .2 x .42 x .5 x 8

= 770 kg

Type C : 200 mm x 320 mm x 500 mm Size

Weight = 2403 x .2 x .32 x .5 x 8

= 620 kg

Type D : 170 mm x 200 mm x 340 mm Size

Weight = 2403 x .17 x .2 x .34 x8

= 225 kg

Type E : 240 mm x 340 mm x 260 mm Size

Weight = 2403 x .24 x .34 x .26 x 8

= 408 kg

APPENDIX B

PROPAGATION OF CRACKS

The detection of cracks was conducted manually after each loading case. The cracks were traced and are shown in Figures B.1, B.2, B.3 and B.4 after each load step corresponding to six, eight and ten truck loads respectively.

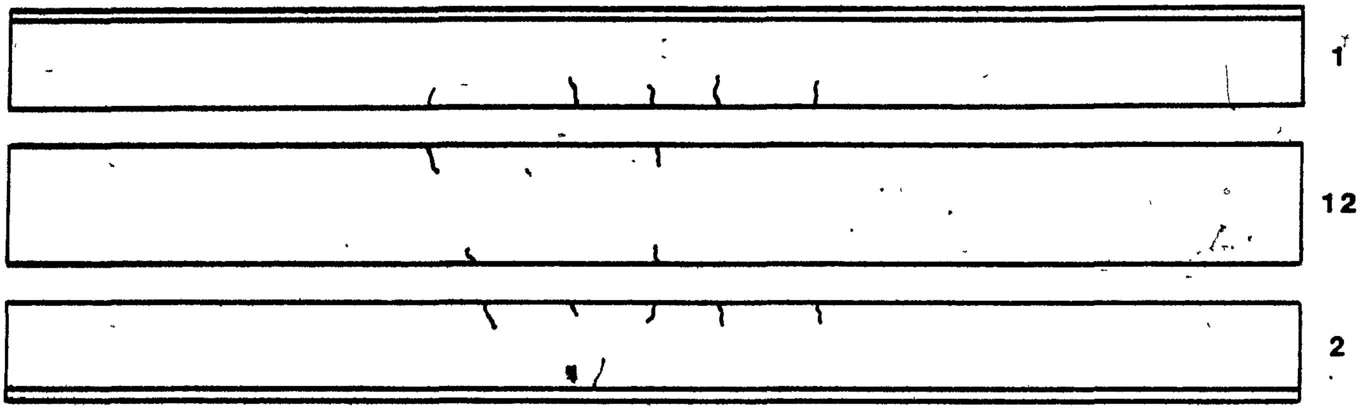

a. Girder 1

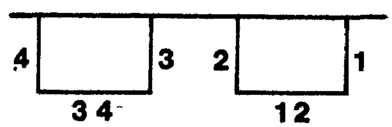

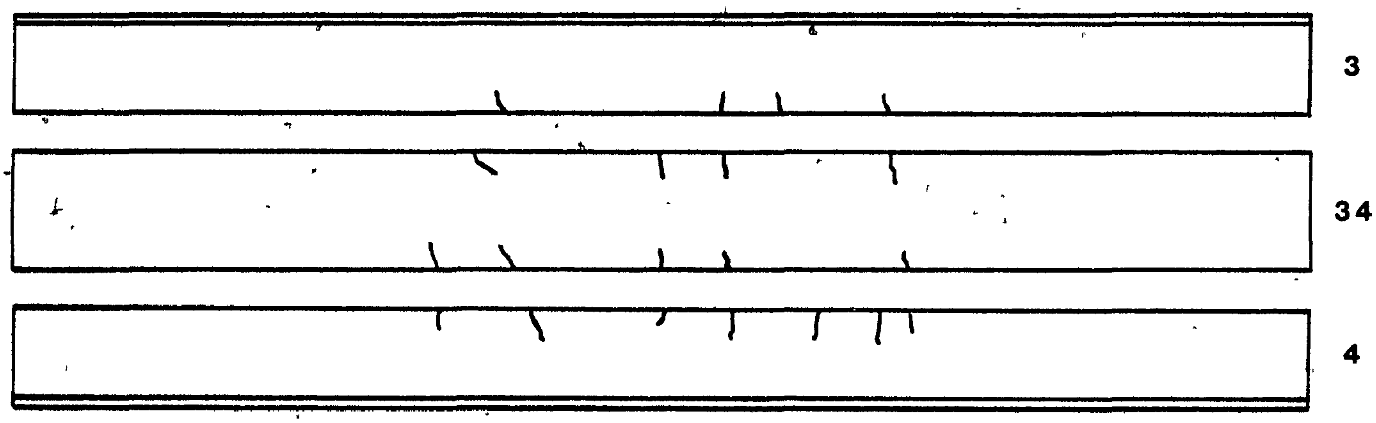

b. Girder 2

Figure B.1 PROPAGATION OF CRACKS AFTER FOUR TRUCK LOADS.

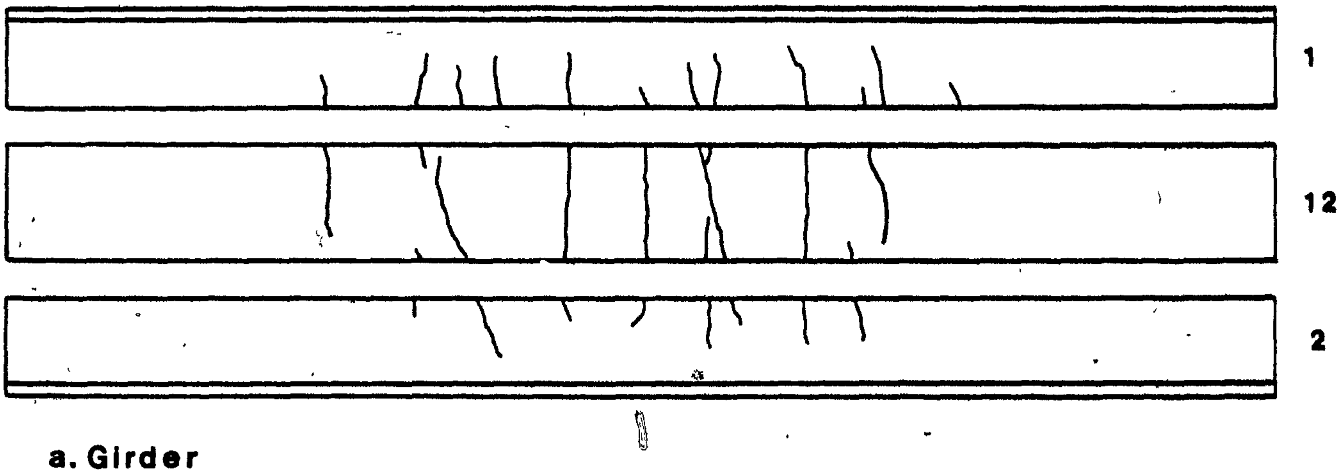

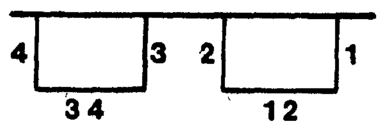

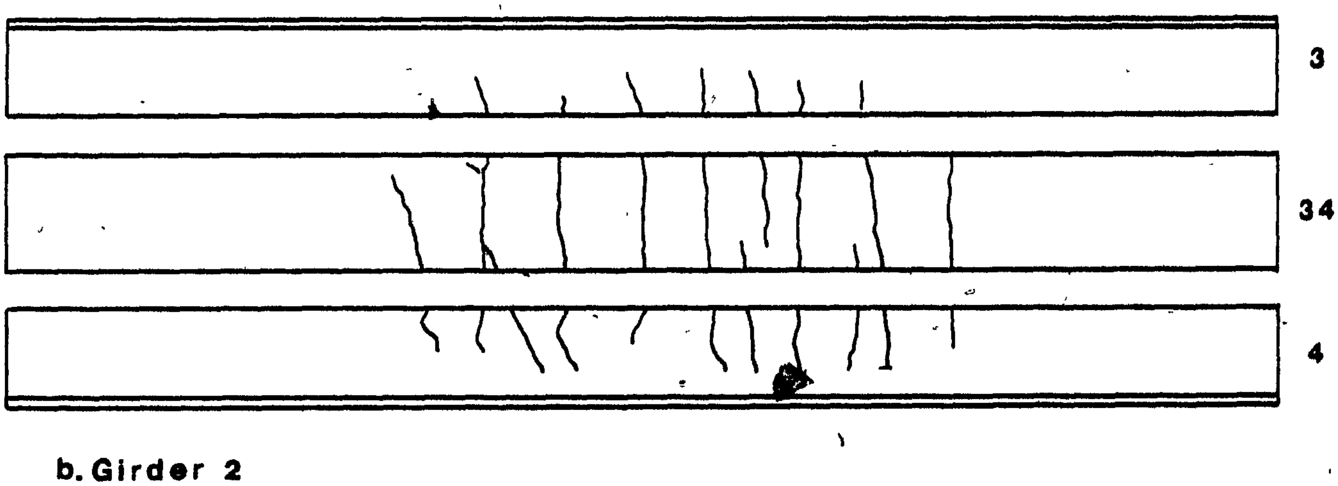

Figure B.2 PROPAGATION OF CRACKS AFTER SIX TRUCK LOADS.

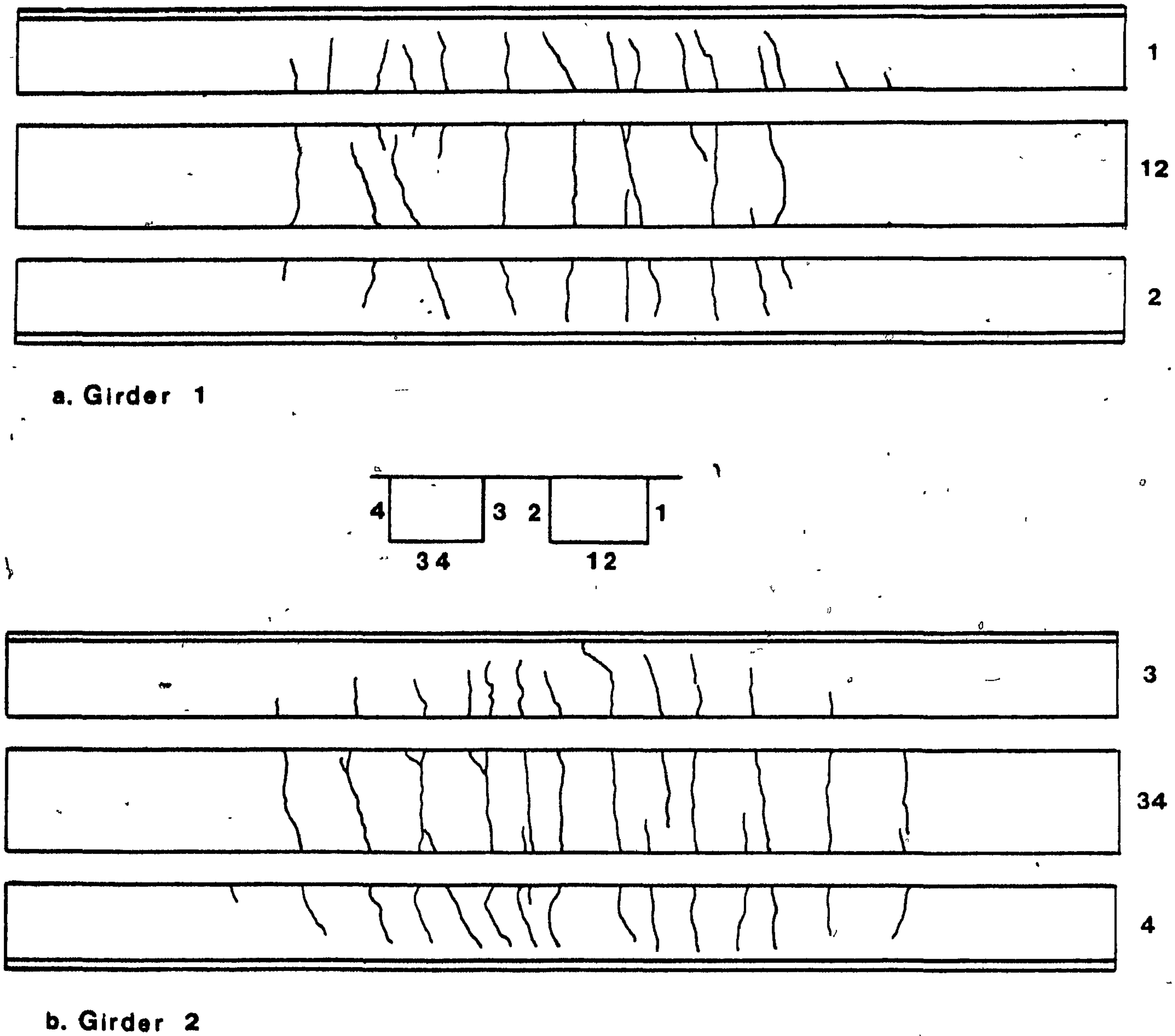

Figure B.3 PROPAGATION OF CRACKS AFTER EIGHT TRUCK LOADS.

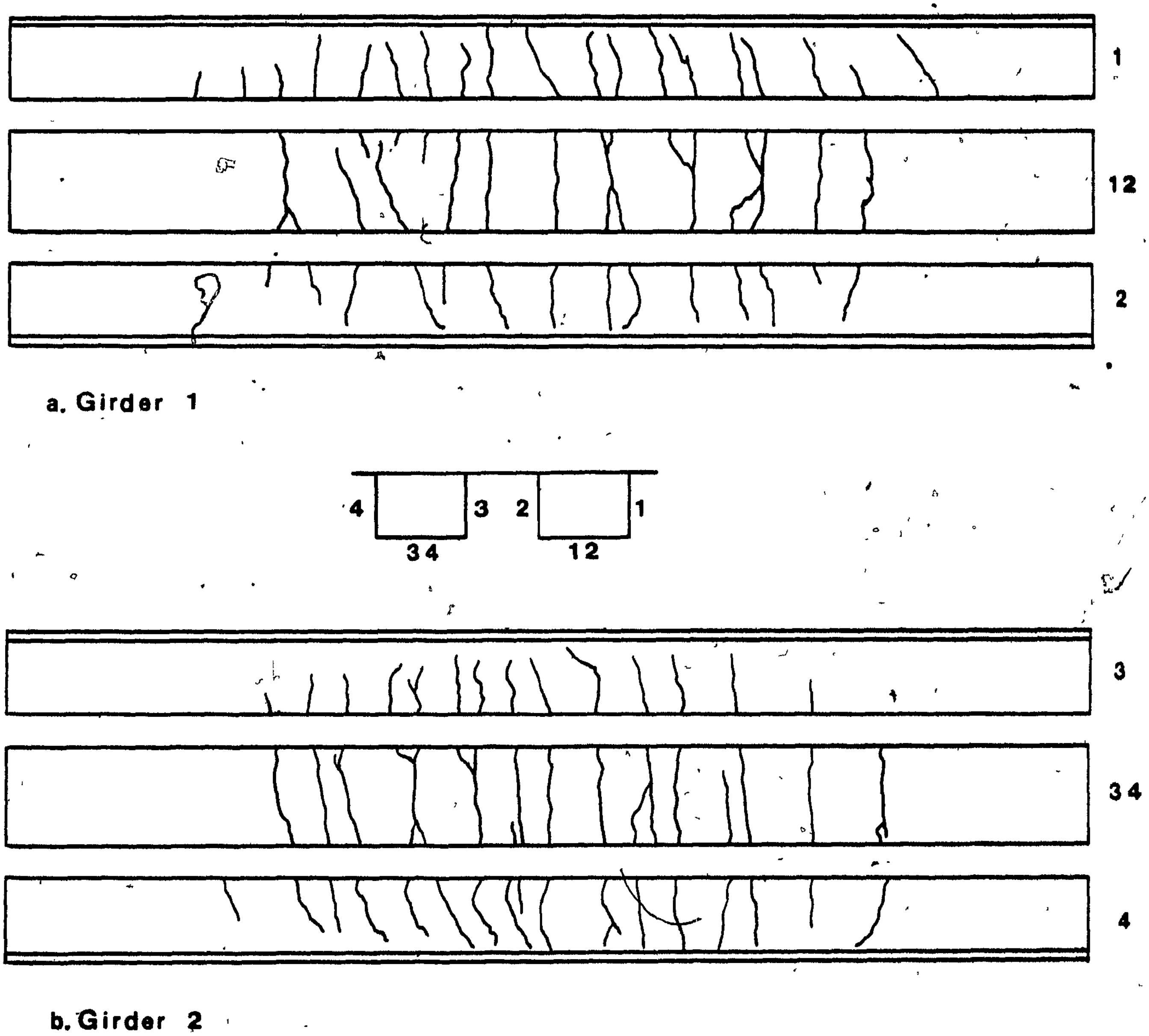

Figure B.4 PROPAGATION OF CRACKS AFTER TEN TRUCK LOADS.